Evolution of antifungal drug resistance of the human-pathogenic fungus *Candida albicans*

Evolution der Antimykotikaresistenz
im humanpathogenen Pilz *Candida albicans*

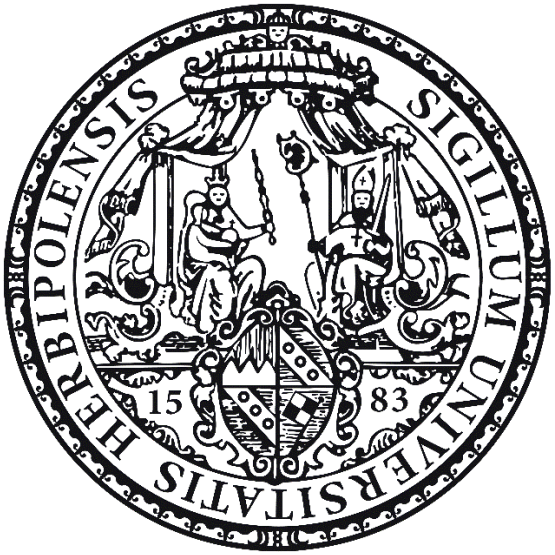

Doctoral thesis for a doctoral degree

at the Graduate School of Life Sciences

Julius-Maximilians-Universität Würzburg

Section Infection and Immunity

Submitted by

Christina Popp

born in Kitzingen, Germany

Würzburg, 2021

Submitted on:

……..

Office stamp

Members of the Thesis Committee:

Chairperson: Prof. Dr. Thomas Dandekar

Primary Supervisor: Prof. Dr. Joachim Morschhäuser

Supervisor (Second): PD Dr. Wilma Ziebuhr

Supervisor (Third): Prof. Dr. Frank Ebel

Date of Public Defense: ……

Date of receipt of Certificate: …….

Danksagung

Ich möchte mich an dieser Stelle bei den nachstehenden Personen bedanken, ohne deren Unterstützung die Anfertigung meiner Dissertation nicht möglich gewesen wäre.

Ganz besonders möchte ich meinem Doktorvater Prof. Dr. Joachim Morschhäuser danken, der mich seit vielen Jahren fördert und unterstützt. Für meine Promotion hat er hat mir faszinierende Themen gegeben und mir die Teilnahme an vielen internationalen Konferenzen ermöglicht, auf denen ich mich mit Experten auf verschiedensten Gebieten austauschen konnte. Ich möchte außerdem hervorheben, dass seine Tür immer für mich offenstand und ich jederzeit mit Fragen, Problemen und zur Diskussion meiner Ergebnisse zu ihm kommen konnte.

Ich möchte mich auch bei den Mitgliedern meines Promotionskomitees PD Dr. Wilma Ziebuhr und Prof. Dr. Frank Ebel für die wissenschaftlichen Diskussionen, die Erstellung der Gutachten und für das stets offene Ohr bedanken.

Darüber hinaus möchte ich mich bei unseren Kooperationspartnern PD Dr. Knut Ohlsen, Dr. Tobias Hertlein und Liane Dreher für die *in vivo* Experimente und die tolle Arbeitsatmosphäre bedanken.

Mein Dank gilt auch den ehemaligen und aktuellen Mitgliedern der AG Morschhäuser Ines Krüger, Sabrina Schneider, Sonja Schwanfelder und den Studierenden Natalie Pluta, Nico Alexander Liebig und Viola Schmitt für die Unterstützung bei u.a. Southern Blots und Mating Experimenten und die vielen fröhlichen Momente. Ebenfalls Austin, Christoph, Irene und Nico möchte ich für die wissenschaftliche Diskussionen und mentale Unterstützung danken. Außerdem möchte ich mich bei Benjamin, Bernardo, Christa, Julia, Michael, Sabrina Schubert, Selene, Tina und Rebecca für eine tolle Zeit im und außerhalb des Labors bedanken.

Ich schätze sehr, Teil des Instituts für Molekulare Infektionsbiologie (IMIB) unter der Leitung von Prof. Dr. Jörg Vogel gewesen zu sein, wodurch ich die Möglichkeit hatte u.a. großartige Wissenschaftler kennenzulernen. Mein besonderer Dank gilt Dr. Charlotte Wermser, Dr. Clivia Lisowski, Dr. Christian Perez und seiner Gruppe, Hilde Merkert, Josef Heger, Lara Kricks, Lisa Pfeuffer, Dr. Rabea Wagner, Dr. Sonja Schönfelder und Dr. Susanne Bury. Darüber hinaus möchte ich bei den mit dem IMIB-assoziierten Wissenschaftlern Dr. Jasmin Lother und Dr. Jorge Amich bedanken. Ich danke der Graduate School of Life Sciences (GSLS) für die exzellente Forschungs- und Bildungsumgebung und die Vermittlung des Mentors Dr. Tassilo Krug von Nidda, der mich in vielerlei Hinsicht unterstützt. Besonderer Dank gilt Dr. Gabriele Blum-Oehler, die stets ein offenes Ohr für mich hatte.

Ich möchte meinem Sohn Aaron und meinem Partner Tobias für alle unvergesslichen und wunderbaren Momente danken und für die Geduld, die sie mir gegenüber entgegenbringen. Außerdem möchte ich Tobias für sein stets offenes Ohr und alle wissenschafltichen Diskussionen danken.

Für die mentale Unterstützung während allen Hochs und Tiefs möchte ich allen meinen Freunden danken. Vor allem Anne, Jasmin und Susi sind und waren mir eine große Stütze.

Abschließender Dank gilt meiner wundervollen Familie (Popp, Hertlein und Amslinger). Besonders bedanken möchte ich mich für die Betreuung von Aaron während der SARS-CoV-2 Pandemie und immer dann wenn es brennt.

-

Für Aaron

Table of Contents

Summary

Infections with the opportunistic yeast *Candida albicans* are frequently treated with the first-line drug fluconazole, which inhibits ergosterol biosynthesis. An alarming problem in clinics is the development of resistances against this azole, especially during long-term treatment of patients. Well-known resistance mechanisms include mutations in the zinc cluster transcription factors (ZnTFs) Mrr1 and Tac1, which cause an overexpression of efflux pump genes, and Upc2, which results in an overexpression of the drug target. *C. albicans* strains with such gain-of-function mutations (GOF) have an increased drug resistance conferring a selective advantage in the presence of the drug. It was previously shown that this advantage comes with a fitness defect in the absence of the drug. This was observed in different conditions and is presumably caused by a deregulated gene expression.

One aim of the present study was to examine whether *C. albicans* can overcome the costs of drug resistance by further evolution. Therefore, the relative fitness of clinical isolates with one or a combination of different resistance mutations in Mrr1, Tac1 and/or Upc2 was analyzed in competition with the matched fluconazole-susceptible partner. Most fluconazole-resistant isolates had a decreased fitness in competition with their susceptible partner *in vitro* in rich medium. In contrast, three fluconazole-resistant strains with Mrr1 resistance mutations did not show a fitness defect in competition with their susceptible partner. In addition, the fitness of four selected clinical isolate pairs was examined *in vivo* in mouse models of gastrointestinal colonization (GI) and disseminated infection (IV). In the GI model all four fluconazole-resistant strains were outcompeted by their respective susceptible partner. In contrast, in the IV model only one out of four fluconazole-resistant isolates did show a slight fitness defect in competition with its susceptible partner during infection of the kidneys. It can be stated, that in the present work the *in vitro* fitness did not reflect the *in vivo* fitness and that the overall fitness was dependent on the tested conditions. In conclusion, *C. albicans* cannot easily overcome the costs of drug resistance caused by a deregulated gene expression.

In addition to GOFs in Mrr1, Tac1 and Upc2, resistance mutations in the drug target Erg11 are a further key fluconazole resistance mechanism of *C. albicans*. Clinical isolates often harbor several resistance mechanisms, as the fluconazole resistance level is further increased in strains with a combination of different resistance mutations. In this regard, the question arises of how strains with multiple resistance mechanisms evolve. One possibility is that strains acquire mutations successively. In the present study it was examined whether highly drug-resistant *C. albicans* strains with multiple resistance mechanisms can evolve by parasexual recombination as another possibility. In a clonal population, cells with individually acquired resistance mutations could combine these advantageous

traits by mating. Thereupon selection could act on the mating progeny resulting in even better adapted derivatives.

Therefore, strains heterozygous for a resistance mutation and the mating type locus (*MTL*) were grown in the presence of fluconazole. Derivatives were isolated, which had become homozygous for the resistance mutation and at the same time for the *MTL*. This loss of heterozygosity was accompanied by increased drug resistance. In general, strains which are homozygous for one of both *MTL* configurations (*MTL***a** and *MTL*α) can switch to the opaque phenotype, which is the mating-competent form of the yeast, and mate with cells of the opposite *MTL*. In the following, *MTL***a** and *MTL*α homozygous strains in the opaque phenotype were mated in all possible combinations. The resulting mating products with combined genetic material from both parents did not show an increased drug resistance. Selected products of each mating cross were passaged with stepwise increasing concentrations of fluconazole. The isolated progeny showed high levels of drug resistance and loss of wild-type alleles of resistance-associated genes. In conclusion, selective pressure caused by fluconazole exposure selects for resistance mutations and at the same time induces genomic rearrangements, resulting in mating competence. Therefore, in a clonal population, cells with individually acquired resistance mutations can mate with each other and generate mating products with combined genetic backgrounds. Selection can act on these mating products and highly drug-resistant und thus highly adapted derivatives can evolve as a result.

In summary, the present study contributes to the current understanding of the evolution of antifungal drug resistance by elucidating the effect of resistance mutations on the fitness of the strains in the absence of the drug selection pressure and investigates how highly drug-resistant strains could evolve within a mammalian host.

Zusammenfassung

Infektionen mit dem opportunistischen Hefepilz *Candida albicans* werden häufig mit dem First-Line-Medikament Fluconazol behandelt, welches die Ergosterol-Biosynthese hemmt. Ein besorgniserregendes Problem in der Klinik, insbesondere bei der Langzeitbehandlung von Patienten, ist die Entwicklung von Resistenzen gegen dieses Azol. Zu den bekannten Resistenzmechanismen gehören Resistenzmutationen in den Zink-Cluster-Transkriptionsfaktoren (ZnTFs) Mrr1 und Tac1, die eine Überexpression von Effluxpumpen-Genen bewirken und Resistenzmutationen in Upc2, die zu einer Überexpression des Wirkstofftargets führen. *C. albicans* Stämme mit solchen Gain-of-Function-Mutationen (GOF) weisen eine erhöhte Medikamentenresistenz auf, was einen selektiven Vorteil in Gegenwart des Medikaments bedeutet. Es wurde zuvor gezeigt, dass dieser Vorteil mit einem Fitnessdefekt in Abwesenheit des Medikaments einhergeht. Dies wurde in verschiedenen Bedingungen nachgewiesen und wird vermutlich durch eine deregulierte Genexpression verursacht.

Ein Ziel der vorliegenden Studie war es zu untersuchen, ob *C. albicans* die Kosten der Medikamentenresistenz durch Evolution kompensieren kann. Daher wurde die relative Fitness von klinischen Isolaten mit einer oder einer Kombination verschiedener Resistenzmutationen in Mrr1, Tac1 und/oder Upc2 im Wettbewerb mit dem zugehörigen Fluconazol-sensitiven Partner analysiert. Die meisten Fluconazol-resistenten Isolate hatten eine verminderte Fitness im Wettbewerb mit ihrem sensitiven Partner *in vitro* in vollwertigem Medium. Dennoch zeigten drei Fluconazol-resistente Stämme mit Mrr1-Resistenzmutationen keinen Fitnessdefekt im Wettbewerb mit ihrem jeweiligen Partner. Zusätzlich wurde die Fitness von vier ausgewählten klinischen Isolat-Paaren *in vivo* in Mausmodellen für gastrointestinale Kolonisation (GI) und disseminierte Infektion (IV) untersucht. Im GI-Modell wurden alle vier Fluconazol-resistenten Stämme von ihren sensitiven Partnern überwachsen. Im Gegensatz dazu zeigte im IV-Modell nur einer der vier Fluconazol-resistenten Isolate einen leichten Fitnessdefekt im Wettbewerb mit dem jeweiligen Fluconazol-sensitiven Partner während der Infektion der Nieren. Es kann festgestellt werden, dass in der vorliegenden Arbeit die *in vitro*-Fitness nicht die *in vivo*-Fitness widerspiegelt und dass die Gesamtfitness von den getesteten Bedingungen abhängig ist. Zusammenfassend lässt sich sagen, dass *C. albicans* die Kosten der Medikamentenresistenz, die durch eine deregulierte Genexpression verursacht werden, nur schwer überwinden kann.

Neben GOFs in Mrr1, Tac1 und Upc2 sind Resistenzmutationen im Wirkstofftarget Erg11 ein wichtiger Resistenzmechanismus von *C. albicans*. Klinische Isolate weißen oft mehrere Resistenzmechanismen auf, da die Kombination verschiedener Resistenzmutationen die Fluconazol-Resistenz potenziert. In diesem Zusammenhang stellt sich die Frage, wie sich Stämme mit mehreren Resistenzmechanismen

entwickeln. Eine Möglichkeit ist, dass Stämme Mutationen sequenziell erwerben. In der vorliegenden Studie wurde untersucht, ob als weitere Möglichkeit hochresistente *C. albicans* Stämme mit multiplen Resistenzmechanismen durch parasexuelle Rekombination evolvieren können. In einer klonalen Population könnten Zellen mit individuell erworbenen Resistenzmutationen diese vorteilhaften Eigenschaften durch Paarung kombinieren. Daraufhin könnte Selektionsdruck auf die Matingprodukte wirken und so die Entstehung von besser angepassten Derivaten begünstigen.

Daher wurden Resistenzmutation und Mating Type Locus (*MTL*) heterozygote Stämme in Gegenwart von Fluconazol kultiviert. So konnten Derivate isoliert werden, die homozygot für die Resistenzmutation und gleichzeitig für den *MTL* geworden waren. Dieser Verlust der Heterozygotie ging mit einer erhöhten Medikamentenresistenz einher. Generell können Stämme, die homozygot für eine der beiden *MTL*-Konfigurationen (*MTL***a** und *MTL*α) sind, in den opaque Phänotyp wechseln, der die paarungskompetente Form der Hefe darstellt, und sich mit Zellen des gegensätzlichen *MTL* paaren. Im Folgenden wurden *MTL***a** und *MTL*α homozygote Stämme im opaque Phänotyp in allen möglichen Kombinationen verpaart. Die resultierenden Matingprodukte mit kombiniertem genetischem Material beider Elternteile wiesen keine erhöhte Medikamentenresistenz auf. Ausgewählte Paarungsprodukte jeder Kreuzung wurden mit stufenweise ansteigenden Konzentrationen von Fluconazol passagiert. Die isolierten Nachkommen zeigten ein hohes Maß an Medikamentenresistenz und den Verlust von Wildtyp-Allelen der resistenzassoziierten Gene. Zusammenfassend lässt sich sagen, dass der selektive Druck, der durch die Fluconazol-Exposition verursacht wird, für Resistenzmutationen selektiert und gleichzeitig genomische Umlagerungen induziert, die eine Paarung ermöglichen. Daher können sich in einer klonalen Population Zellen mit individuell erworbenen Resistenzmutationen miteinander paaren und Matingprodukte mit kombiniertem genetischem Hintergrund generieren. Auf diese Matingprodukte kann die Selektion wirken, woraufhin sich hochresistente und damit stark an ihre Umwelt angepasste Derivate entwickeln können.

Zusammenfassend trägt die vorliegende Studie zum aktuellen Verständnis der Evolution der Antimykotika-Resistenz bei, indem sie den Effekt von Resistenzmutationen auf die Fitness der Stämme in Abwesenheit des Medikamenten-Selektionsdrucks untersucht und aufklärt, wie sich hochgradig resistente Stämme in einem Säugetierwirt entwickeln könnten.

1. Introduction

The kingdom Fungi encompasses about five million species, including approximately 300 fungal species which can cause human disease [1]. Infections can range from superficial to life-threatening invasive infections. Most people will be challenged by superficial fungal infections at least once during their lifetime. In general, therapy of these superficial infections is uncomplicated. Of concern are the widely underestimated life-threatening invasive fungal infections from which millions of patients suffer worldwide and which require challenging diagnostics and treatment [2].

Around 1.7 billion people worldwide suffer from superficial infections of skin and nails prevalently caused by dermatophytes [3]. Mucosal infections of the genital tract and oral tract are frequently diagnosed. Around 50 to 75% of women in their childbearing years develop vulvovaginal infections at least once and approximately 75 million women suffer from recurrent infection cycles [4]. Roughly 10 million oral thrush infections and 2 million cases of esophageal fungal infections are reported each year in parts of the world with constrained health care and are linked to HIV infections [5]. The most common cause of superficial infections are different species of *Candida* and in general, *Candida* spp. are the second leading cause of fungal infections worldwide [2].

Although invasive fungal infections are less frequent than superficial infections, they are an alarming problem. Even though different antifungal drugs are obtainable, invasive infections have a high mortality rate of around one and a half million people per year [2]. The ten most common invasive fungal diseases cause as many deaths as malaria or tuberculosis [2]. *Cryptococcus*, *Candida*, *Aspergillus* and *Pneumocystis* are the four genera that cause 90% of fungal-related deaths [2]. Estimated numbers based on available data suggest mortality rates of patients infected with *Aspergillus fumigatus* (Aspergillosis) to be 30 to 95%, with *Candida albicans* (Candidiasis) 46 to 75% and with *Cryptococcus neoformans* (Cryptococcosis) 20 to 70% worldwide [2]. Furthermore, Brown *et al.* [2] suggests that the true burden of fungal infections is underestimated due to factors like misdiagnosis and too few studies in certain parts of the world.

Life-threatening invasive mycoses are most often caused by *Candida* species in patients with severe immunosuppression or those who have undergone invasive clinical procedures or experienced severe trauma followed by a long stay in intensive care units [2]. Due to nosocomial (hospital-acquired) infections, fungal infections have become a major challenge in clinics [6] and the outcome for underlying diseases can be altered by invasive mycoses [1]. For example, data from the US shows *Candida* species as the fourth major cause of nosocomial bloodstream infections with high mortality rates of up to 50% [7-9].

Clinically important are at least 30 members of the *Candida* species [10]. Among those are *C. albicans*, *C. glabrata*, *C. tropicalis*, *C. parapsilosis*, *C. dubliniensis* and *C. auris*. *C. auris* is of growing concern in healthcare as it is multi-drug resistant and often misdiagnosed. Between 2015 and 2018 reported incidents rose by 318% [11]. Nevertheless, among the different *Candida* species, *Candida albicans* is most frequently recovered. A large proportion of cases of oral and systemic candidiasis [12-14] and community-onset and nosocomial candidemias are caused by *C. albicans* [15].

1.1. The organism *Candida albicans*

Hippocrates had already described the symptoms of candidiasis, or thrush, by around 400 B.C. Nevertheless, it wasn't until 1846 that the oral lesions caused by thrush were connected with *C. albicans* [16]. Due to its wide range of morphologies, the taxonomic classification has been critically discussed. In 1923 Berkhout [17] provided a reclassification scheme describing the fungus as *Candida albicans*. The term *Candida* derives from *toga candida*, which is Latin for white robe and was worn by applicants for public offices. The word *Albicans* is Latin as well and means white, describing the white colonies of the yeast which grow on solid agar.

The organism *Candida albicans* is diploid and belongs to the phylum Ascomycota. It is one of approximately 200 members of the genus *Candida*, the largest genus of medically important yeasts. Furthermore, it is part of the CTG clade which is defined by its genetic code deviation. These yeasts translate the CTG codon as serine instead of the universal leucine [18-22]. *Candida* species were described as yeasts which can form pseudohyphae or true hyphae, but which are imperfect or asexual [23]. Nevertheless, an unusual parasexual mating cycle has been discovered in *C. albicans* (see chapter 1.4). For mating to be possible, the cells need to switch from the sterile white phenotype to the mating-competent opaque phenotype [24, 25]. The smooth and spherical white cells grow white dome-shaped colonies. In contrast, the pimpled and elongated opaque cells give rise to dark and flat colonies [26, 27]. Further morphology types include chlamydospores, which are thick-walled and have spore-like shapes [28], and the gray phenotype, which is described in chapter 1.3.3. In addition, Pande *et al.* [29] found that a proportion of *C. albicans* cells which were passaged through the mouse gut switched to the so-called GUT (gastrointestinally induced transition) phenotype, a specialized commensal cell type. This fascinating phenotypic plasticity of *C. albicans* contributes profoundly to the ability to colonize and infect almost every part of the human body [30].

As a harmless commensal, *C. albicans* colonizes the oral cavity, skin, gastrointestinal tract and reproductive tract of a vast part of the human population. Recent data suggests that *C. albicans* is not an obligate mammalian commensal, but that it may also colonize environmental reservoir(s) [31, 32].

Only under particular conditions, like immunosuppression, misbalance of the microflora and damage of tissue barriers, *C. albicans* causes infections, that can range from superficial skin to life-threatening systemic infections. Most infections are endogenous and arise from strains of the microflora of the patient [33-35]. In addition to the microbial flora and host factors, a wide range of virulence factors and fitness attributes of the fungus are involved during the transition from a harmless commensal to an aggressive pathogen. Virulence factors include adhesins and invasion factors, the morphological transition between yeast and hyphal forms, biofilm formation, secreted hydrolases and phenotypic switching [36]. Fitness attributes include metabolic flexibility, acquisition of nutrients, adaption to a fluctuating environmental pH and stress response systems [36]. In general, *C. albicans* has become a key model organism to study the molecular biology of fungal pathogenesis.

1.2. Treatment of infections with *Candida albicans*

In general, the discovery and development of drugs is challenging. The global market for antifungal drugs was worth $14.6 billion in 2019 and it is estimated to grow to $17.6 billion by 2024 [37]. Different classes of antifungal drugs are available for the treatment of fungal infections, which target different cellular processes. There are both fungistatic agents which act by inhibiting growth and fungicides which act by killing the pathogens. Among these are azoles, polyenes, allylamines, morpholines, echinocandins and 5-Flucytosine (5FC) [11].

The most commonly used class of antimycotics for treatment and prevention of infections with *Candida* are the fungistatic **azoles** [11]. For example, in sub-Saharan Africa azoles are the preferred drug against mycoses for HIV/AIDS patients due to their accessibility, low cost and oral formulation [2, 38]. Azoles are grouped into imidazoles (azole ring with two nitrogens) and triazoles (azole ring with three nitrogens). An important member of the triazoles is the commonly used first-line drug fluconazole [11], which is preferred due to its safety profile and usability as both oral and intravenous formulations [39]. Azoles target the ergosterol biosynthesis, which is catalyzed by twenty-five different enzymes in *C. albicans* [11]. Ergosterol is analogous to the mammalian cholesterol, which are both the major sterols of the respective plasma membrane [40]. Specifically, azoles bind the enzyme Erg11, a 14α-demethylase, which in turn causes a depletion of ergosterol in the fungal plasma membrane, the accumulation of the toxic sterol 14,24-dimethylcholesta-8,24(28)-dien-3ß,6α-diol (DMCDD), which is otherwise not produced, and results in permeabilization of the plasma membrane, leading to growth arrest [41]. In addition, azoles cause increased reactive oxygen species (ROS) levels [42].

Another class of antimycotics is the fungicidal **polyenes**, which includes amphotericin B. This drug binds to ergosterol in the plasma membrane, which results in pore formation [43]. Thereupon, monovalent

ions (K+, Na+, H+, Cl-) rapidly flow out of the cells, leading to cell death. Amphotericin B is mainly used to treat *Candida* infections in cases in which the yeast has developed a resistance against another drug or in cases in which the relevant niche is not bioavailable to other drugs [11].

Further classes of antifungals include **allylamines** and **morpholines**, which are used to treat various fungal infections, including those caused by *Candida* spp. Both classes act against members of the ergosterol biosynthesis pathway. Allylamines target Erg1, a squalene epoxidase, and morpholines target the ergosterol biosynthetic enzyme C-14 sterol reductase Erg24 [44].

Echinocandins, a mostly fungicidal class of antifungals, include caspofungin, micafungin and anidulafungin. These drugs inhibit the fungal cell wall synthesis by targeting the ß-1,3-D-glucan synthase, which is encoded by *FKS1* [45, 46]. This enzyme utilizes uridine diphosphate glucose (UDP-glucose) to synthesize ß-1,3-D-glucan [47]. Targeting the ß-1,3-D-glucan synthase results in osmotic instability and cell death [48, 49]. In contrast, mammalian cells do not have a cell wall and thus echinocandins cause only low toxicity in humans and are therefore commonly used [50]. In general, patients who were previously medicated with azoles and patients with moderate to severe disease are treated with these drugs [51].

One of the oldest classes of antifungals is the base analog **5-Flucytosine** (5FC), which acts against the nucleic acid biosynthesis. 5FC affects protein translation in the fungal cells. After uptake by a specific transporter into the fungal cell, it is metabolized via the intermediate 5-Fluorouracil (5FU) to 5-Fluorouridine triphosphate (5UTP), which incorporates into the RNA as an alternative for uridine triphosphate (UTP). Another mode of action is the inhibition of thymidylate synthase, which results in the inhibition of DNA biosynthesis and cell division. This takes place by the metabolization of 5FC to 5-Fluorodeoxyuridine monophosphate (5FdUMP) [52].

Despite treatment with antifungal drugs, **mortality rates** associated with invasive mycoses remain high. The main reason for this is the absence of early and directed antifungal therapy due to missing rapid diagnostic tests [53]. Diagnosis of the most prevalent invasive Candidiasis is still performed by examination of routine fungal blood cultures, urine tissue and body fluids [11]. Limitations of this technique are low sensitivity and high false-positive rates caused by contamination during the procedure [11]. Further challenges include limits in the route of administration, bioavailability in the targeted tissues and the spectrum of activity and toxicity of the antimycotic drugs [53]. Drug interactions can have further adverse effects. For example triazoles can interact with corticosteroids and statins among other drugs, restricting the range of drug administration [53]. It should also be mentioned that biofilm formation of the fungus on the surface of medical equipment is a major problem, since biofilms are intrinsically resistant to antifungal drugs and to azoles in particular [54].

A concerning problem is **antifungal drug resistance** among *Candida* spp., which can in the worst case lead to therapeutic failure [53]. In naive *C. albicans* strains azole resistance is relatively rare. The CLSI (Clinical and Laboratory Standards Institute) has determined a MIC (minimal inhibitory concentration) of ≥ 8mg/L as the clinical breakpoint for fluconazole resistance of *C. albicans*, which was reached in 3.5% of all analyzed samples in several studies [55-60]. In the report of antibiotic resistance threat published in 2019, the US Center of Disease Control and Prevention (CDC) described more than 34,000 cases and 1,700 deaths per year caused by drug-resistant *Candida* species. For example, long-term treatment and prophylaxis with azoles like fluconazole, the drug of choice for prophylaxis and treatment of *Candida* infections, can lead to a resistance development of this pathogenic yeast. This leads to reduced efficiency of drug treatment and may even result in treatment failure. Resistances against azoles were observed in *C. albicans* strains of patients suffering from an HIV infection and less frequently in patients with other systemic immunodeficiencies [61-76]. In particular after prolonged or repeated therapy cycles in patients with AIDS who were infected several times with oropharyngeal candidiasis, *C. albicans* has been described to develop resistance to this antimycotic drug [76].

1.3. Evolution of antifungal drug resistance

Organisms acquire the ability to survive and outcompete competitors in changing environments by evolutionary adaption, such as in the ancient and ubiquitous evolution of drug resistance [77, 78]. This process takes place either gradually or suddenly and can be observed at multiple levels.

Reversible adaption mechanisms such as the adjustment of gene expression and cellular activities are important on the **species level** [79]. For example, the capacity of proliferation in the presence of antimicrobials without acquiring specific adaptive mutations is often described as tolerance [46, 80, 81].

Changes in the genome play an important role at the **population level**, especially when hostile changes in the environment are of prolonged duration [79]. Derivatives with such acquired selective advantage will dominate the population under selective pressure. The reduction of inhibitory effects of drugs is termed resistance and is mainly developed during antimicrobial therapy against pathogenic microorganisms [79]. Furthermore, the frequency of acquisition of drug resistance differs depending on the antifungal class [79]. For example, resistance to polyenes is very rare, since resistance goes hand in hand with increased sensitivity to host-relevant stresses like neutrophil killing, oxidative stress and temperatures reached during a fever [82]. Azole resistance develops more frequently since this drug is fungistatic and puts the surviving cells of a population under strong selective pressure [81, 83].

1.3.1. Mechanisms of fluconazole resistance

C. albicans has developed various mechanisms of antifungal drug resistance to survive and reproduce even in the presence of azoles.

A prominent mechanism of fluconazole resistance is **resistance mutations in the fluconazole target Erg11**, which can lead to a decreased drug binding affinity [84-86]. A drug target structure in which changes can take place are interaction regions such as the H-bond interaction of the haem group of Erg11 with the azole ring. In the ligand-binding pocket, azoles and the ergosterol precursor compete with each other and steric hinderance changes can also emerge at this position [54]. In general, different mutations can cause different levels of azole resistance [54]. Data on a recent study by Warrilow *et al.* [87] suggest that Erg11 amino acid substitutions may affect azole resistance not only by changing the binding affinity to azoles. Interestingly, the baseline catalytic turnover of Erg11 proteins with different amino acid substitutions varied between the single *C. albicans* proteins expressed by *Escherichia coli*. In *in vitro* experiments, the amino acid substitutions contributed significantly to the azole resistance, even though some variants had a weak binding affinity to azoles.

One critically discussed resistance mechanism against fluconazole is the reduction of the toxic effects of the drug by **defective *ERG3***, which encodes a $\Delta^{5,6}$-desaturase. As described in chapter 1.2, azoles like fluconazole inhibit the 14α-demethylase Erg11, leading to the conversion of the precursor molecule lanosterol to the toxic sterol DMCDD, which is normally not produced [88]. Loss-of-function mutations in *ERG3* can impede the production and accumulation of the growth-inhibiting sterol DMCDD, thus leading to increased drug resistance [89, 90].

In addition, an **upregulated *ERG11* expression** often plays a role in the development of fluconazole resistance. In ergosterol shortage conditions, the zinc cluster transcription factor (ZnTF) Upc2 (sterole uptake control), which is an important regulator of ergosterol biosynthesis genes, is induced [91, 92]. Activating mutations in Upc2, which lead to a constitutive activity of this ZnTF, cause this kind of overexpression of *ERG11* [93-96]. In addition to *ERG11, s*everal ergosterol biosynthesis genes are coordinately up-regulated by *UPC2* in fluconazole-resistant strains, which was revealed by genome-wide gene expression profiling. 202 promoters were described to be bound to Upc2 in ChIP-microarray location analysis. These promoters regulate the expression of ergosterol biosynthesis genes and in addition, transcription factors and the efflux pump genes *CDR1* and *MDR1.* Therefore, *UPC2* is not only a regulator in sterol biosynthesis [93, 97, 98].

A key mechanism driving fluconazole resistance is the reduction of the intracellular drug concentration to a level that is too low for sufficient drug target inhibition. In an energy-dependent manner fluconazole is actively transported to the extracellular space by **efflux systems**. The ABC (ATP-binding

cassette) transporters Cdr1 and Cdr2 (*Candida* drug resistance), which are powered by adenosine triphosphate (ATP), play an important role in fluconazole resistance. Furthermore, the major facilitator pump Mdr1 (multidrug resistance), which is energized by the proton gradient across the membrane, confers fluconazole resistance [99]. In addition to antifungal drugs, these membrane transport proteins, which are localized in the cytoplasmic membrane, pump out toxic substances (xenobiotics) and endogenous metabolites [99]. Under standard growth conditions, Cdr1 is significantly expressed, in contrast to Cdr2 and Mdr1. Cdr1 expression levels are further increased in in the presence of fluconazole. Furthermore, *C. albicans* strains with a Cdr1 deletion are fluconazole hypersusceptible indicating that this membrane transport protein is necessary for basal drug tolerance [100, 101]. In contrast, deletion of *CDR2* and *MDR1* does not influence drug susceptibility, and expression of both transporters is weak during standard growth conditions with or without fluconazole [71, 100, 102]. By the overexpression of genes encoding such efflux pumps, the drug efflux is potentiated. The overexpression of the efflux pumps *CDR1*/*CDR2* and *MDR1* is caused by the Zn(II)-Cys(6) transcription factors Tac1 (transcriptional activator of *CDR* genes) and Mrr1, respectively, with activating mutations. These **hyperactive transcription factors** do not only upregulate the expression of these efflux pumps, but also of additional target genes that contribute to fluconazole resistance [97, 98, 103-114]. Multiple GOFs in these ZnTFs have been described to date [104-107, 109-111, 114]. It should be noted that in addition to the increased transcription caused by hyperactive Tac1, an increased mRNA stability could contribute to the constitutive high expression of *CDR1* and *CDR2*. This increased mRNA stability has been connected to loss-of-heterozygosity (LOH) for the poly(A) polymerase1 allele and mRNA hyperadenylation [115, 116].

Apart from *MRR1*, *TAC1* and *UPC2*, **other ZnTFs** may also play a role in fluconazole resistance. Schillig *et al*. [101] identified, with the help of a library of artificially activated ZnTfs, Mrr2 to be presumably involved in azole resistance since it also activates the *CDR1* promoter. Indeed, in 2015 a first clinical isolate was identified with a putative *MRR2* GOF, which caused increased *CDR1* expression [117]. In a recent study *MRR2* mutations of clinical isolates did not cause an increased *CDR1* expression and drug resistance in the genetic background of a fluconazole-susceptible wild-type strain [118]. Only artificially activated Mrr2 caused an increased fluconazole resistance and *CDR1* expression [118]. Concluding whether further ZnTFs are involved in clinical azole resistance is still under investigation.

Many clinical *C. albicans* isolates exhibit a **combination of resistance mechanisms** resulting in high levels of drug resistance and therapy failure [62, 73, 75, 119, 120]. Sasse *et al.* [121] showed that the stepwise acquisition of resistance mutations in *ERG11*, *MRR1*, *TAC1* and *UPC2* has additive effects. The authors of this study demonstrated this by introducing the hyperactive alleles in all possible combinations in a wild-type *C. albicans* strain. The same study showed that strains which are

homozygous for a resistance mutation are more fluconazole-resistant than strains which are heterozygous for the same hyperactive allele in *ERG11*, *MRR1*, *TAC1* and *UPC2*. Indeed, fluconazole-resistant clinical isolates are often homozygous for hyperactive allele(s) [62, 73, 94, 104, 107, 109, 110, 120, 122]. In clinical isolates, local or broader recombination events involving extended regions of the chromosome are responsible for this **loss-of-heterozygosity** (LOH) [104, 109, 110]. Also, whole-chromosome loss and duplication can be responsible for the LOH, as it was observed in particular in fluconazole-resistant strains passaged *in vitro* in fluconazole-selective conditions [104, 110]. Interestingly, during stressful conditions, like for example fluconazole exposition, the LOH frequency is increased [123]. This observations suggest that fluconazole selects for resistance mutations and in addition promotes fluconazole resistance by causing genome rearrangements [124].

In addition, **aneuploidy** is involved in azole resistance. In a study by Ford *et al.* [125] clinical isolates from patients treated with azoles showed an increasing ratio of aneuploidy over the course of time. Amplification of whole chromosomes or chromosomal parts can be a common way to gain resistance to fluconazole. The mechanism behind this is that the copy number of genes involved in drug resistance increases and thereby so does the expression of the respective genes, such as *ERG11* [126, 127]. Also, the expression of other genes of the ergosterol biosynthesis pathway [125] and efflux pumps [126, 127] can be affected by aneuploidies. Isochromosomes have been described as an important example, which contain two copies of the left arm of chromosome 5. At the two inverted repeat regions, which are flanking the centromere, recombination takes place [126]. *ERG11* and *TAC1* are located on the left arm of chromosome 5 and therefore strains with such isochromosomes have elevated numbers of these resistance-associated genes. In line with this observation, the expression of *ERG11* and hyperactive *TAC1* is increased in such strains, contributing to drug resistance [109, 127]. Interestingly, isochromosome 5 formation frequently is accompanied by a recombination event causing a LOH. Like this, strains can become homozygous for *ERG11* and *TAC1* resistance mutations, which in turn can result in increased drug resistance [109]. Without selection pressure, the unstable aneuploidies are frequently lost, leading to a decrease in drug resistance [66, 109, 126, 128]. Evolution of drug resistance may be promoted by the amplification of chromosomal regions or whole chromosomes, even if they are transient. As already mentioned, for example, the probability for LOH of hyperactive alleles involved in drug resistance can be increased [125]. It is possible that aneuploidy is an intermediate state on the way to reaching drug resistance, since it is often observed during the development of drug resistance [129]. The hypothesis that aneuploidy may promote adaption by generating genetic diversity is supported by the finding that strains acquired transient aneuploidies before acquiring major adaption of drug resistance [125, 129]. As previously stated, fluconazole exposure itself increases the likelihood of the development of drug resistance since it induces chromosome segregation defects, resulting in aneuploidies (see also chapter 1.3.3) [130].

Although mechanisms of drug resistance in *C. albicans* are extensively studied, many **questions** remain unsolved. Up-to-date azole importer(s) are unknown and novel mechanisms of azole resistance are currently being researched. For example, Gao *et al.* [131] recently showed that the alteration of sphingolipid synthesis resulted in fluconazole resistance, conferred by *FEN1* and *FEN12* deletion. This could be a natural resistance mechanism since these composition changes are comparable to changes in wild-type cells induced by fluconazole.

1.3.2. Effect of fluconazole resistance on the fitness

Whether cells with newly acquired resistance mechanisms dominate or persist in a population or are outcompeted by others also depends, among other factors, on the impact of these mechanisms on the fitness of the organism in different environments [132]. The resistance mutations often alter key cellular functions, which can impair the fitness of the cells. For example, by loss-of-function mutations in *ERG3* the sterol composition of the cellular membranes is affected and the hyperactive ZnTFs *MRR1*, *TAC1* and *UPC2* cause a deregulated gene expression [90, 124, 133]. Also increased levels of efflux pump activity could affect the fitness since necessary nutrients , along with the drug, are pumped out of the cell.

The effect of different resistance mutations on the fitness *in vitro* and *in vivo* was studied by different groups. For example, strains with loss of function of the $\Delta^{5,6}$-desaturase encoded by *ERG3* exhibited a lower virulence in a mouse model of disseminated candidiasis. These strains had lost the activity of this important enzyme by nonsense mutations or gene deletion [90, 133]. Another study by Vale-Silva *et al*. [134] did not observe a decreased virulence of clinical isolates with an inactivating mutation in *ERG3*. In contrast, in the background of a wild-type strain the same mutation resulted in a decreased virulence, indicating that the clinical isolate could have compensated the costs of drug resistance by further mechanisms. Sasse *et al.* [121] analyzed the fitness of isogenic strains with resistance mutations in the zinc cluster transcription factors *MRR1*, *TAC1* and *UPC2* in all possible combinations. These strains exhibited a mild but significant fitness defect in optimal growth conditions *in vitro* in the absence of the drug, which was potentiated when several resistance mutations were present in the same strain. Furthermore, *in vivo* experiments in a mouse model of gastrointestinal infection strains harboring all three constitutively active zinc cluster transcription factors showed a severe fitness defect. The authors hypothesize that the fitness defect could be caused by a waste of energy and a limitation of the adaptive flexibility caused by the deregulated gene expression. In minimal medium, single mutants did not show a significant fitness defect. The fitness defect was only obvious when a combination of mutations was present. The observation that GOFs come with a cost dependent on the

environment is also supported by the study of Lohberger *et al*. [106]. Both studies are discussed in detail in chapter 3.1. In addition, strains with a resistance mutation in *ERG11* (G464S amino acid substitution) were not found to exhibit a significant fitness defect [121]. This mutation causes a decreased enzyme activity and drug binding and is present in many fluconazole-resistant clinical isolates [84]. Nevertheless, other *ERG11* resistance mutations might affect the fitness.

In general, drug resistance is not always costly under non-selective conditions. Although aneuploidies are usually transient and not well tolerated by the cells, cells with an isochromosome 5 L did not show a fitness defect under non-selective conditions. These strains, generated during fluconazole exposure *in vitro* showed an increased fitness in comparison to the parental strain [135].

In addition, reversible fluconazole resistance was observed for strains which were obtained after serial passaging in the presence of different fluconazole concentrations *in vitro*. After propagation of the strains in the absence of the drug, they lost the fluconazole resistance [136]. It is likely that in the individual populations the resistant cells were outcompeted by the susceptible cells in the absence of the drug selection pressure, indicating that drug resistance comes with a cost [124]. In contrast, Huang *et al.* [137] found that fluconazole-resistant isolates that evolved *in vitro* did not exhibit a decreased fitness under non-selective conditions and as a matter of fact some even showed an increased fitness. It could be that adaptation to the growth medium was at least partly responsible for the observation that the fluconazole-resistant strain showed an increased fitness in competition with the parental-susceptible strain under non-selective conditions. It should be noted that neither in the study by Calvet *et al.* [136], nor in the study by Huang *et al.* [137] were the resistance mutations identified. Angiolella *et al.* [138] exposed a vaginal isolate to stepwise increasing concentrations of fluconazole and isolated a fluconazole-resistant derivative. This strain had an increased virulence in a mouse model of disseminated candidiasis, although it had no opportunity to adapt to this environment beforehand. In contrast, in a rat model of vaginal candidiasis it did not show an altered virulence. This isolate overexpressed the efflux pumps *MDR1*, *CDR1* and *CDR2*, suggesting that resistance-mutations in *MRR1* and *TAC1* could be responsible for the increased drug resistance [124, 138]. In comparison to the parental strain, its fluconazole-resistant derivative also had an increased adherence, formation of hyphae and biofilms and ability to invade [138]. These virulence factors might be changed due to alterations in the genome caused by incubation in the presence of fluconazole, since it had not been described that GOFs in *MRR1* and *TAC1* are responsible for such changes [124].

Furthermore, studies which compared the fitness of drug resistant strains with a *MRR1* or *TAC1* GOF with their matched susceptible isolates revealed that the drug-resistant strains exhibited a decreased fitness in a mouse model of disseminated or oral candidiasis [139, 140]. Other studies found no fitness defect of fluconazole-resistant strains in competition with the matched fluconazole-susceptible strains

in different environments [141]. Interestingly, clinical isolate series with different resistance mechanisms first had a decreased fitness and later recovered fitness, while the reduction of the costs of fitness proceeded over the time [125]. Also fluconazole-resistant strains isolated *in vitro* were found to eliminate fitness costs of drug resistance by further evolution [142].

Altogether these studies suggest that *C. albicans* may compensate the costs of drug resistance caused by resistance mutations and genomic rearrangements through further evolution and that fitness costs are dependent on the environmental conditions [124].

1.3.3. The highly flexible genome of *Candida albicans*

C. albicans exhibits a remarkable genomic plasticity displayed by several possible changes in karyotype [126, 135, 143-146]. Alterations can be comprised of a single nucleotide exchange up to several chromosome rearrangements. This genomic plasticity plays an important role by generating genetic diversity, which is important for adaptation to varying and stressful environments. This includes the colonization of diverse host niches and the adaptation to selection pressures like exposure to antifungal drugs [104, 123, 125, 126, 147-152].

In general, the **genome of *C. albicans*** consists of eight chromosomes, specifically chromosome 1-7 and chromosome R. Furthermore, the major proportion of *C. albicans* isolates is found to be diploid [125, 147, 153]. According to the CGD homepage, retrieved on October 12th, 2020, the haploid genome size of the reference strain SC5314 consists of 15,473,750bp including the mitochondrial genome [154]. As of this date, a total of 6,198 protein open reading frames (ORFs) have been predicted, 27.89% are verified, 2.44% are dubious and 69.67% uncharacterized. Some of the mechanisms by which the genome of *C. albicans* can be altered are discussed in the following.

Genomic variation can be caused by **point mutations**. Such base substitutions are well tolerated and arise with a high frequency (see chapter 3.2) [147, 155-157]. Point mutations in resistance-associated genes such as *ERG11*, *MRR1*, *TAC1* and *UPC2* can cause an increased drug resistance as described in chapter 1.3.1. Approximately every 200 genes, a heterozygous single nucleotide polymorphism (SNP) generates a premature stop codon in the reference strain SC5314 [158]. This finding suggests functional heterozygosity for several genes [159]. In addition, approximately half of the open reading frames (ORFs) were found to have non-synonymous SNPs [158]. RNA expression was found to be modulated by allelic-specific phenomena [157]. Such tuning of gene expression was also demonstrated by Staib *et al.* [160]. Pentameric repeats in the promoters of *SAP2* had an divergent effect on the expression of the respective allele. In addition to differences in the RNA expression, translation can

also be affected. About 4% of all *C. albicans* alleles were found with varying translation [161]. Therefore, phenotypic trajectories can be a result of transcriptional and translational tuning caused by heterozygous alleles.

It should be noted that the **distribution of point mutations** is not random, since an accumulation was observed particularly in intergenic and repetitive genome regions [156], probably because at least in gene-poor repetitive regions and intergenic regions the likelihood for deleterious effects of such base substitutions is lower. In genes encoding cell surface proteins with repetitive regions like the *ALS* adhesins, an increased number of base substitutions was found. This could be reasoned by changes in function regarding the host-pathogen interaction [162, 163]. Also, selection against the accumulation of non-synonymous base substitutions was observed throughout short-term evolution [156]. An even distribution of non-synonymous mutations and a widely varying distribution of synonymous mutations coupled with the chromosomal position was observed over long-term evolution [147].

In comparison to other fungi, *C. albicans* has substantial potential of genetic variation due to a greater number of **protein-encoding genes with short-repeats**, which can be altered by contraction or extension [164, 165]. Wilkins *et al.* [165] found synonymous mutations in some genes which reduced the probability of varying the number of repeats by recombination. Furthermore, this study suggests that for a certain strain background or host niche, tandem repeats are adjusted to an optimum by selection.

The genome of *C. albicans* has a **high degree of heterozygosity**. Butler *et al.* [155] counted 43,665 heterozygous positions in SC5314. Nevertheless, different clinical isolates show a widely varying degree of heterozygosity [147, 153, 166]. LOH can be caused by events comprising short- or long-range genomic regions or loss/truncation of chromosomes [159]. On the one hand, LOH for recessive alleles can result in deleterious or lethal effects for the cells [167]. This is presumably the cause for a low fitness of haploid *C. albicans* cells, which maintained the poor fitness despite auto-diploidization [143]. On the other hand, LOH can lead to enhanced genetic diversity. Stress exposure, like antifungal drugs, oxidative stress, and high temperatures, as well as the infection of the mammalian host enhances the rates of LOH [123, 156, 168-170]. LOH plays an important role in regard of phenotypic changes like increased drug resistance (see chapter 1.3.1) and is an important prerequisite for white-to-opaque switching and thus for mating (see chapter 1.4). Another example is the gray phenotypic state discovered in a subset of clinical isolates by Tao *et al.* [171]. Some clinical isolates are functional heterozygous at the *EFG1* locus. Thereby, one allele contains mutations disrupting the ORF. By LOH (or by de novo mutation) strains can become homozygous for the afunctional *EFG1* allele and thereupon white cells can transition to the gray state [172]. Several studies found that these *efg1* null mutants have an increased fitness in the murine gastrointestinal model and therefore LOH at the *EFG1* locus is

an important mechanism of adaptation *in vivo* [29, 159, 172-174]. A study by Sitterle *et al.* [175] , which examined oral *C. albicans* strains isolated from healthy individuals, described genetic within-host diversity that was caused to a large extent by LOH. Strains isolated from a single host exhibited many short-tract LOH events (95% with at least <3kb) and less frequent large-tract LOH events comprising hundreds of thousands of SNPs. On average 106-254 LOH events among the strains from a single healthy host were found, indicating that LOH is an important driver of genetic diversity in *C. albicans*.

LOH for large chromosomal parts or whole chromosomes have been addressed by several studies [123, 156, 176, 177]. Break-induced replication (BIR) and mitotic crossover can be causes for LOH events affecting long-range segments comprising regions from the recombination site to the end of the chromosome arm [147, 156, 178]. Wang *et al.* [166] found by sequencing *C. albicans* strains, that the degree of LOH decreased from the telomere towards the centromere. *C. albicans* encodes hundreds of long repeat sequences and a recent study by Todd *et al.* [179] found that a wide range of long-range LOH (and all segmental aneuploidies) happened at these positions. Such LOH events and segmental amplification deletions and inversions could be induced by the repair of DNA double-strand breaks at these repeats [179]. Furthermore, LOH of whole chromosomes can be caused by chromosome loss and reduplication of the remaining chromosome. In clinical isolates this happens rarely in comparison to segmental LOH [147, 153].

LOH for short regions comprising less than 5kb is caused by gene conversion or double crossovers and is little studied [180]. In a study by Ene *et al.* [156] local LOH rose at similar rates as point mutations. Therefore, heterozygosity levels are kept steady when LOH covering large chromosomal segments are excluded. Most LOH events comprised only 1-2 heterozygous positions and small genomic regions, on average affecting 368 bp. The rate of short-tract LOH decreased from telomeres to centromeres, but in general, LOH tracts occurred across the whole genome of clinical isolates [166]. At repetitive regions, at telomeres and in genes with repetitive elements, like the *ALS* genes, LOH events affecting short regions are observed more frequently [156]. In addition, during microevolution, large-scale LOH was observed relatively seldom in comparison to short-tract LOH [156, 167].

Different **stable ploidy states** (number of sets of chromosomes) in addition to the diploid state were observed in *C. albicans* varying from haploid to tetraploid as illustrated in the schematic overview in Figure 1 [143, 181]. For a long time, *C. albicans* was not considered to exhibit a haploid state due to the presence of recessive lethal alleles, which have been evidenced in the wild-type SC5314 [167, 182]. Nevertheless, Hickman *et al.* [143] uncovered viable haploid SC5314 cells. In the diploid state *C. albicans* accumulates deleterious recessive mutations, which were eliminated in the haploid state. Such haploid cells had a decreased fitness and virulence. Autodiploidization was observed frequently, by which homozygous diploid strains emerged. These strains had a decreased fitness in comparison to

heterozygous diploid cells, indicating that the fitness defect is caused by LOH and not by the ploidy state. Furthermore, these strains had the ability to switch to the opaque phenotype and mate [143]. The yeast can undergo ploidy shifts by the parasexual cell cycle (see also chapter 1.4) as well as asexual mechanisms. For example, by opposite-sex mating of *MTL***a** homozygous cells with *MTL*α homozygous cells in the mating-competent opaque phenotype, cells can double their ploidy to tetraploid [25]. By chromosome loss, whole chromosomes are lost randomly and the overall ploidy can change from tetraploid to diploid [181, 183, 184]. In a mouse model of disseminated candidiasis, tetraploid cells gradually lost ploidy over the course of time [185]. Furthermore, tetraploid mating progeny was observed to reach a near-tetraploid, triploid, diploid, or transient haploid state [143]. During this process of ploidy change, phenotypic heterogeneity is generated by the formation of genetically diverse progeny and to some extent by the production of a variation of transient aneuploid states [184, 186].

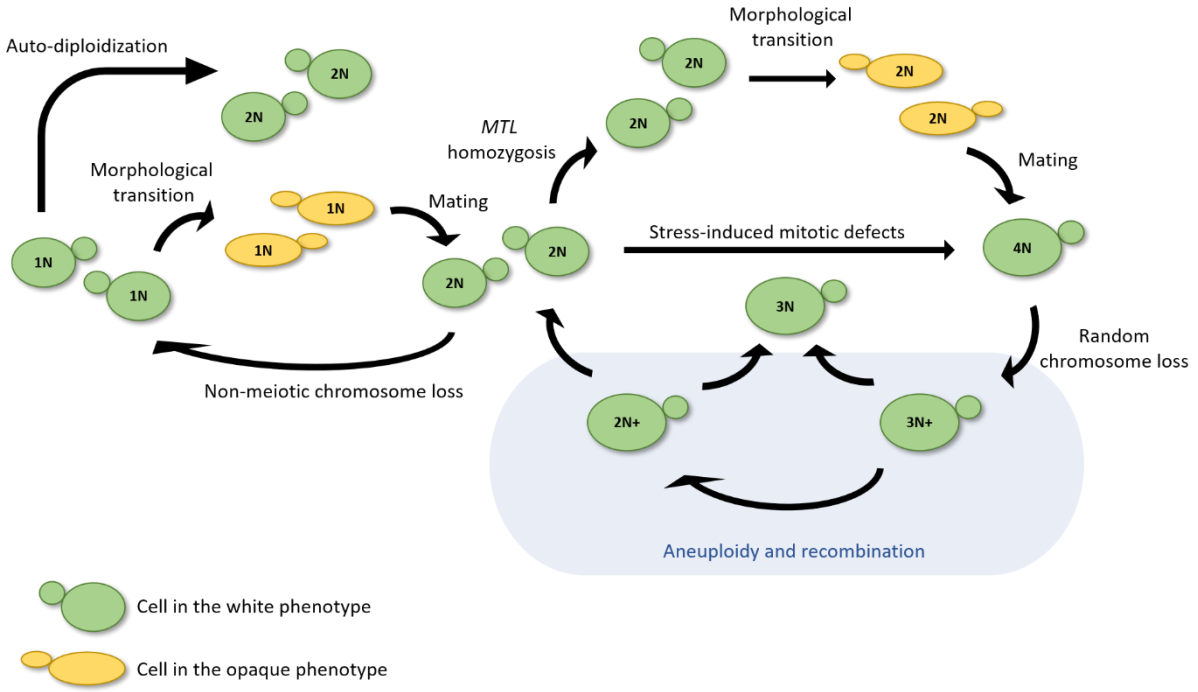

Figure 1: Schematic overview of ploidy transitions in *C. albicans*. Indicated are euploid states (1N, 2N, 3N and 4N) and aneuploid intermediates (2N+ and 3N+) and their connections by arrows [130, 143, 146, 181, 183]. Mating requires a morphological transition of *MTL* homozygous cells to the mating-competent opaque phenotype (yellow cells) [24, 25]. Opaque cells with opposing *MTL* configuration (*MTL***a** and *MTL*α) can mate with each other to form diploid or tetraploid progeny with combined genetic background [24, 26, 143, 187]. Tetraploid cells can undergo a chromosome loss and reach the diploid state via the aneuploid states [184]. During this random process, LOH of various parts of the genome and recombination of homolog chromosomes takes place in a higher frequency than in diploid cells [181, 184]. With permission adapted from Dr. Meleah A. Hickman [188, 189].

Aneuploidy can develop within a single cell division and can be caused by chromosome nondisjunction during mitosis [129]. This state is defined as a modification in the number of chromosomes with one or more additional or missing chromosomes (modification of the multiplicity of the whole chromosome set is termed ploidy). Furthermore, it is an often unstable intermediate state, since no whole sets of chromosomes are lost during the reduction of ploidy (e.g. from tetraploid to diploid), but single

chromosomes are acquired or lost sequentially [146, 183]. Tetraploids and aneuploids will reach a particular ploidy state with a reproducible probability. Individual cells resolve that ploidy state via different paths [181]. However in general, cells will shift back to the euploid state. This was observed especially during the growth of cells in laboratory standard conditions [129]. *In vitro* aneuploid cells were generated in the presence of azoles, low nitrogen and certain sugars [135, 144, 145, 181, 190]. Interestingly, *C. albicans* tolerates aneuploidy very well [129]. This stands in contrast to eukaryotes where aneuploidy is connected to a decreased fitness. In *C. albicans* aneuploidy can come with advantages under certain conditions [126, 142, 147]. For example, isochromosome 5 formation (supernumerary chromosome) in the presence of azoles is connected to increased drug resistance [126, 142, 147]. Furthermore, different studies recovered strains from the mammalian host with supernumerary chromosomes [148, 152, 156].

In different studies, varying **frequencies of aneuploidies** were described. A proportion of 9.9% aneuploid (segmental and whole chromosomal) strains were found in 182 sequenced strains [153]. Another study found aneuploidies in 38% (8/21) of sequenced clinical isolates [147]. Reasons for these varying observations may be a different exposure of the strains to antifungal drugs or other environmental stresses, which were described to select for aneuploidies [125, 126, 156, 191]. Interestingly, Selmecki *et al.* [126] identified in approximately 50% of the isolated azole-resistant *C. albicans* strains at least one aneuploid chromosome. Harrison *et al.* [130] found that a transient increase in ploidy can be caused by the exposure to antifungal drugs. Cells with a ploidy level of up to 16N were isolated after treatment with fluconazole [130]. So-called trimeras with several nuclei composed of connected mother, daughter and granddaughter cells were generated due to an impaired coordination of cell division and subsequent DNA replication [130]. The following mitotic collapse generated 4N cells with additional spindles and aneuploid ploidy occurred via chromosome mis-segregation [130]. These findings suggest that genetic variation and change of phenotypes and thereby survival can be enhanced rapidly by aneuploidy as an answer, even if imprecise, to severe and abrupt stress exposure. Furthermore, this ploidy state can be reversible, as by chromosome loss, and endoreduplication strains can reverse to a stable ploidy state [129, 135, 180].

Presumably by changing gene expression that aligns with the relative copy number of genes, aneuploidy-associated phenotypes develop. In most, but not all cases, RNA expression levels aligned with **gene dosage in aneuploid strains**. Nevertheless, some genes compensated the gene dosage and showed expression at the disomic level [192]. Fitness costs were described for nearly every observed aneuploidy. It is hypothesized that these costs are caused by an uneven stoichiometry of various compounds of large complexes in aneuploid cells, since in most cases the copy number of the genes correlates with the expression of the protein [129]. Aneuploidy might be lost after a stable solution

with a lower cost in a certain stress condition is developed, such as a point mutation or LOH as described in chapter 1.3.1 [129]. It should be noted that aneuploidy itself is not necessarily adaptive. A major part of aneuploidy in yeast isolates does not increase drug resistance and in addition was observed to come with a fitness cost. Nevertheless, this fitness cost was not extraordinarily strong in some natural yeast isolates when the stress conditions weakened [193, 194].

1.4. The parasexual life cycle - an important element of evolution

Sex is an important way to generate diversity, which may be especially important to adapt to stressful or fluctuating environments [195, 196]. A meiotic program of ploidy reduction has not been described in *C. albicans* and for a long time this organism was regarded as an asexual yeast [168, 197]. Nevertheless, a parasexual cell cycle exists in *C. albicans* [198, 199]. Cells in the opaque phenotype can mate with each other and form mating progeny with the genetic material of both parents [25]. The offspring randomly loses DNA content and thereby generates diversity [181, 184, 186, 200]. This process is described in greater detail in the following.

An important prerequisite for mating is the morphological transition from the sterile white to the mating-competent opaque phenotype. Cells need to be homozygous for the **mating-type locus** (*MTL*) for this switch to occur [24, 26]. The *MTL* is located on chromosome 5 and has the *MTL***a** and *MTL*α idiomorphs [201]. Most clinical *C. albicans* strains (~97%) are heterozygous for the *MTL*, although some isolates are *MTL***a** or *MTL*α homozygous [24, 25]. The *MTL* locus consists of four transcription factors that control cell identity and mating, which are **a**1 and **a**2 encoded by the *MTL***a** locus and α1 and α2 encoded by the *MTL*α locus. In addition, the *MTL* encodes *PIK*, *PAP* and *OBP*, which are nonsex genes [201]. In *MTL***a**/α cells, the heterodimer **a**1/α2 binds to the promotor of the master regulator *WOR1* and thereby inhibits its transcription and, at the same time, the switch to the opaque phenotype by this epigenetic mechanism [25, 202-204]. Nevertheless, under certain prerequisites, *MTL* heterozygous strains can switch to the opaque phenotype as well, although opaque *MTL***a**/α strains remain mating-incompetent. Such prerequisites are loss-of-function mutations in specific genes (e.g. *HBR1*) or the presence of specific physiologically relevant environmental signals (e.g. increased CO_2 levels) [205].

In *MTL* heterozygous cells, white-to-opaque switching is regulated by the **master regulator Wor1** [202-204]. By LOH, as described in chapter 1.3.3, cells can become homozygous for the *MTL*. Such strains encode only **a**1 or α2, therefore the suppression of the *WOR1* transcription is relieved and the cells can switch to the opaque phenotype [24-26, 202]. *MTL* homozygous cells in the white state have a low expression of *WOR1*. White-to-opaque switching happens in single cells, when the Wor1 level reaches a threshold by a stochastic gain of Wor1 [206]. By binding to its promotor, Wor1 activates its own

expression. Transient ectopic Wor1 expression is enough to reach Wor1 levels needed for white-to-opaque switching and maintenance of the opaque state [206]. The decline of Wor1 levels in the cell leads to a destabilization of the opaque phenotype and a switch back to the white state. Furthermore, white-opaque switching is stochastic and both phenotypes are heritable, which results in this bistable expression of *WOR1* [30].

In addition, **expression control of *WOR1*** is facilitated by an interaction network of repression and activation including the described positive autoregulation by Wor1 itself. Additional regulatory components of *WOR1* are the transcription factors Czf1, Efg1 and Wor2 [206]. Also Ahr1 and Wor3 play a role [207]. Efg1 expression shifts the balance to the white phenotype and Wor1 expression to the opaque phenotype [207]. Regulation of *EFG1* and *WOR1* is complex and takes place by an alternative interacting regulatory network in the white and opaque state. In the white state Czf1 and Ahr1 control Efg1 and in the opaque state Ahr1, Efg1, Czf1, Wor2 and Wor3 control Wor1 [207]. Interestingly, the highly complex process of switching regulation is not only mediated by transcription factors, but also by further factors like histone and DNA modifications altering the chromatin structure [208].

MTL homozygous cells can **switch** (all-or-none) reversibly between the white and opaque phenotypes and this transition is affected by different environmental signals, for example CO_2 levels, anaerobic conditions, sugar source, temperature, and oxidative stress [26, 27, 209-216]. Presumably switching takes place in certain host niches [30]. For example on the skin of mice, switching towards the opaque phenotype was observed at 31.5°C [217]. Cell morphology is heritable for many generations and under standard laboratory conditions the switching rate between the single cell types is around once every 10^4 generations [26, 218].

Between the **white and opaque morphologies** expression of about 16% of the genome is different and therefore cells show strongly varying phenotypes and functional characteristics [27, 219-221]. White cells are round-to-oval-shaped and opaque cells bean-shaped or elongated. On solid agar, cells in the white phenotype grow hemispherical white colonies and cells in the opaque phenotype flat gray colonies [30]. Each state reacts differently to distinct environments as can be demonstrated in the example of filamentation. White cells filament for example in the presence of serum and opaque cells filament for example in phosphate limitation conditions [222]. In addition, under standard laboratory growth conditions white cells are stable at 37°C, whereas the majority of the opaque cells switch to the white phase at this temperature [27]. In anerobic environments and conditions with increased carbon dioxide levels or N-acetylglucosamine or nutrient limitation, cells are steady in the opaque phenotype at 37°C [209-212, 214, 223, 224]. Furthermore, in different environments the cell types show differences in the fitness as a consequence of variation in metabolism [225]. In the host the

efficiency to colonize special niches differs between the two morphologies. For example opaque cells cause more efficient cutaneous infection and white cells disseminated infection [226]. In addition, white and opaque cells interact differently with the immune system. For example, in contrast to opaque cells, white cells secrete a specific polymorphonuclear leukocyte (PMNs) chemoattractant [227]. This phenomenon could lead to an invisibility of opaque cells for PMNs and hence could prevent phagocytosis of mating-competent cells. Sasse *et al.* [228] incubated white and opaque cells with human PMNs and only white cells were engulfed by these cells of primary host defense. Also phagocytic cells of the mouse and *Drosophila* favored cells in the white phenotype over cells in the opaque phenotype [229].

For mating to occur, the production of the **mating pheromones a and α**, encoded by *MF**a**1* and *MFα1*, respectively, is important [230-233]. *MFα1* is constitutively expressed in high levels by *MTL*α homozygous opaque cells and not by white cells [232]. Thereby a pheromone precursor peptide is generated, which is posttranslationally modified by the protease Kex2 and the dipeptidyl aminopeptidase A Ste13. Consequently, mature α pheromones are produced, two identical tridecapeptides and one tetradecapeptide, which are able to induce mating response [232-238]. Under standard laboratory conditions only low *MF**a**1* expression by *MTL***a** homozygous cells was described [231]. Nevertheless, *MTL***a** homozygous white and opaque cells express *MF**a**1* and *MFα1* in high levels in the presence of α-pheromone [230, 239]. The expression of *MF**a**1* produces a precursor peptide as well, which is thought to be posttranslationally modified like the **a**-pheromone of the yeast *Saccharomyces cerevisiae* [231, 240, 241]. Presumably by the Ste24 and Axl1 proteases the **a** pheromone precursor peptide is processed, followed by the modification with Ram1 and Ram2 (prenyl-group-adding enzymes), Rce1 (prenyl-dependent protease) and Ste14 (cysteine-carboxy methyltransferase) [231, 240]. The resulting prenylated tetradecapeptide is the mature **a**-pheromone and is exported by the ABC transporter Hst6 [231, 241, 242].

The aspartyl protease Bar1 degrades the α pheromone, a process which is termed **barrier activity** [243]. By impeding pheromone hyperstimulation and abolishing cell cycle arrest, heterothallic (opposite-sex) mating is facilitated [243]. In addition, homothallic (same-sex) mating is inhibited by impeding auto-pheromone stimulation. This auto-pheromone stimulation happens when opaque *MTL***a** homozygous cells secrete α pheromone, which binds to the α pheromone receptor Ste2 on the same cell which in turn causes self-activation for mating [230]. Nevertheless, homothallic mating of unisexual opaque cells by this autocrine pathway is possible in specific strain backgrounds (e.g. deleted *BAR1*) and environments reflecting niches in the human host (e.g. glucose starvation and oxidative stress) [230, 244].

The MAPK (Mitogen-Activated Protein Kinase) signaling pathway **transduces pheromone signals** and changes gene expression in opaque cells [245, 246]. Several genes are upregulated by the transcription factor Cph1, which mediates pheromone response in opaque cell. These include genes regulating adhesion, virulence, MAPK signaling, karyogamy, cell fusion and filamentation [187, 232, 238, 239, 247]. The α-pheromone receptor *STE2* is upregulated in opaque *MTL***a** homozygous cells and Ste2 localizes at the tip of the growing mating projections [187, 232, 239, 247, 248].

These **mating** projections elongate towards the highest pheromone concentration gradient and can grow up to several cell diameters [187, 249]. It is assumed that in the host chemotropism of the mating projections may bridge long distances [208]. A conjugation bridge is formed after fusion of the two mating projections (= conjugation tubes), which leads to the fusion of the two nuclei generating a tetraploid nucleus [187]. For several cell divisions the structure remains stable and generates mating progeny, which is tetraploid [23, 187]. It is worth noting that the phenotype of the conjugation tubes is similar to the phenotype of hyphae, but without septa [187, 247]. By heterothallic mating of *MTL***a** and *MTL*α cells, tetraploid mating progeny (*MTL***a**/α) arise, which have been observed to have a decreased virulence and are less competitive in comparison to diploid cells in a mouse model of disseminated candidiasis [185]. The resulting mating products of heterothallic mating are heterozygous for the *MTL* [23, 183, 199]. Mating may happen more often in specific host niches like in certain nutrient-limited conditions and in recently discovered sexual biofilms formed by *MTL* homozygous cells [205, 238]. In addition, a study by Bennett *et al*. [238] suggests a connection between the nutrient-sensing (e.g. cAMP-PKA) and pheromone (e.g. MAPK) signaling pathways. Initiated by specific environmental signals, tetraploid mating progeny loses randomly chromosomes, which is a non-meiotic parasexual process [23, 183]. In this process Spo11 is involved, which is part of meiosis in other fungi [184]. As described in chapter 1.3.3, by this process of ploidy reduction, genetically diverse progeny and transient aneuploid states are formed and thereby phenotypic heterogeneity is generated [184, 186]. Diversity is not only the outcome of cells with varying ploidy/aneuploidy, but also of vast recombination between the chromosome homologs during this process and of the homolog composition in the single cells (e.g. descendants AA or BB and parental strain AB) [181, 184, 200].

Mating comes with significant **costs**. Sex needs energy [250-252] and an advantageous combination of alleles can be disturbed [251, 253]. Therefore, especially as a short-term reproduction strategy, asexual reproduction is preferred [250, 254]. While asexual reproduction preserves well-adapted genotypes, parasex can lead to a rapid evolution in alternating environments by newly combined alleles. In this way detrimental mutations can be removed from the population and beneficial alleles can be combined [181, 183, 184, 255, 256]. This ability may be relevant for the colonization of various niches in the mammalian host as a pathogen and as a commensal [23] and may play an important role in the

development of drug resistance. Furthermore, through sex, organisms can keep pace with coevolving pathogens, a phenomenon which is described by the red queen hypothesis [257-259]. This hypothesis is based on the proclamation of the Red Queen in *Through the Looking Glass*: “Now, here, you see, it takes all the running you can do, to keep in the same place.” [260].

1.5. Aim of the work

Infections by the opportunistic fungus *C. albicans* are a growing problem in clinics and are often treated with the azole fluconazole [11]. Especially during long-term infection, the yeast can develop resistances against this antimycotic drug [76]. Different *C. albicans* strains can develop various strategies to cope with the stress induced by drug exposure. Well-known fluconazole resistance mechanisms include mutations in *MRR1*, *TAC1* and *UPC2* [261-263]. It has been shown that such gain-of-function mutations (GOFs) not only come with an increased fluconazole resistance level, but can also cause a fitness defect under non-selective conditions in isogenic strains [121]. Although some studies suggest that *C. albicans* can compensate for the fitness defect by further evolution [125, 141], this observation is still not sufficiently substantiated. Therefore, one aim of this work was to investigate the fitness of clinical isolates with one or a combination of different resistance mutations to reveal whether they overcame the fitness defect caused by the hyperactive transcription factors through compensatory mutations.

In contrast to resistance mutations in *MRR1*, *TAC1* and *UPC2*, Sasse *et al.* [121] described that a resistance mutation (G464S) in the drug target *ERG11* did not have a negative effect on the competitive fitness of *C. albicans* under the tested conditions in isogenic strains. Nonetheless, resistance mutations in *ERG11* are an important part of the development of fluconazole resistance in addition to GOFs in *MRR1*, *TAC1* and *UPC2* [62, 73, 264, 265]. Clinical isolates often harbor several resistance mechanisms, as the fluconazole resistance level is further increased in strains with a combination of different resistance mutations [62, 73, 75, 104, 119, 121, 264, 266]. In this regard, resistance mutations can be acquired successively [124]. Since *C. albicans* is a diploid yeast, mutations will occur in one allele first. Strains with a homozygous resistance mutation have a higher resistance level than strains which are heterozygous for the same resistance mutation [121]. By LOH strains can become homozygous for an existing resistance mutation and indeed, most clinical isolates are homozygous for resistance mutation(s) [121]. By genomic rearrangements during which LOH takes place, several loci and chromosomes can be affected [148, 267, 268] and importantly, the frequency of LOH is increased during stress conditions like fluconazole exposure [123, 130]. The LOH for an existing resistance mutation can be accompanied by the LOH of the *MTL* (mating type locus) [109-111, 269]. Interestingly, strains which are homozygous for the *MTL* can switch into the opaque phenotype which is the mating-

competent form of the yeast [24, 25]. Therefore, in the present study it was examined whether strains of a clonal population with individually acquired resistance mutations can become homozygous for a resistance mutation and at the same time for the *MTL.* Hence, such strains would have acquired the ability to mate with each other and could generate mating products with combined genetic background on which selection can act. In the following the question arises of whether mating progeny, which is highly drug resistant due to the combination of different resistance mechanisms, evolves in the presence of fluconazole.

2. Results

2.1. Fitness of clinical *Candida albicans* isolates with resistance mutations in *MRR1*, *TAC1* and *UPC2*

C. albicans infections are often treated with the fungistatic azole fluconazole [11]. Different drug resistance mechanisms allow the yeast to survive the exposure to this drug. Among the most important mechanisms are resistance mutations in the zinc cluster transcription factors *MRR1*, *TAC1* and *UPC2*. While gain-of-function mutations (GOFs) in Mrr1 and Tac1 result in overexpression of the multidrug efflux pumps *MDR1* and *CDR1*/*CDR2*, respectively, GOFs in Upc2 confer overexpression of the drug target *ERG11* [93-96, 98, 103-114]. On one hand, these resistance mutations cause a selective advantage in the presence of fluconazole. On the other hand, the mutations confer a fitness defect in the absence of the drug. The deregulated gene expression caused by the constitutively active transcription factors squanders energy and impedes adaptation. It is conceivable that *C. albicans* can overcome the cost of drug resistance through further evolution by compensatory mutations, a question that was examined in the first part of this study.

2.1.1. Identification of resistance mutations in *MRR1*, *TAC1* and/or *UPC2* of fluconazole-resistant clinical strains

To address the issue of whether fluconazole-resistant clinical *C. albicans* strains can overcome the costs of drug resistance through further evolution, matched sets of fluconazole-susceptible and fluconazole-resistant clinical isolates were examined. In all cases, the fluconazole-sensitive strain was recovered from a patient at an early timepoint, and the fluconazole-resistant partner was isolated from the same patient at a later stage of infection. Previous studies have verified, via fingerprint methods and sequencing, that the two partners are related (for references see Table 17).

Ten clinical isolate pairs were chosen for competition assays (Table 1). Fluconazole resistance levels of the strains were determined by MIC assays. For all pairs, the resistance level of the resistant strain was at least two MIC values higher than that of the respective sensitive strain (Table 1). Previous studies have identified GOF mutations in *MRR1*, *TAC1* and/or *UPC2* as a reason for drug resistance in most of the fluconazole-resistant isolates used here. Some strains have been found to exhibit phenotypes that suggest further, previously unknown mutations within these genes. F5 has been shown to overexpress *ERG11* [62], which is often caused by resistance mutations in *UPC2* [95]. Therefore, *UPC2* of F2 and F5 was sequenced in this study (chapter 4.2.5.1) and indeed, the fluconazole-resistant isolate F5 had acquired a homozygous G1942A substitution in *UPC2* corresponding with a G648S amino acid change.

This GOF mutation has been previously described for other strains and is known to increase drug resistance and cause an overexpression of *ERG11* [95]. Similarly, TW17 has been described to overexpress *MDR1* [75]. Since resistance mutations in *MRR1* are known to cause *MDR1* overexpression in fluconazole-resistant strains [104, 107, 108, 270], *MRR1* of the TW series isolates TW1, TW2, TW3 and TW17 was sequenced in this study (chapter 4.2.5.1). TW2 had acquired a heterozygous G2839A exchange, while TW3 and TW17 were already homozygous for this G947S GOF mutation, explaining increased *MDR1* expression levels, as described by White *et al.* [75].

Table 1: Resistance level and resistance mutations of the selected clinical isolate pairs. Adapted from [266].

Strain name[(a)]	**$MIC_{fluconazole}$ [µg/ml]**	**Resistance mutations**		
		MRR1	***TAC1***	***UPC2***
1442	0.5	-/-		
2271	16	*MRR1*^{Q350L}/*MRR1*^{Q350L}		
1490	1	-/-		
1587	4	*MRR1*^{N803D}/*MRR1*^{N803D}		
5833	1	-/-		
6692	64	*MRR1*^{K335N}/*MRR1*^{T360I}		
B3	1	-/-		
B4	32	*MRR1*^{G878E}/*MRR1*^{G878E}		
DSY294 (C43)	1		-/-	
DSY296 (C56)	128		*TAC1*^{N977D}/*TAC1*^{N977D}	
DSY2285 (26)	1	-/-		
DSY2286 (91)	16	*MRR1*^{T896I}/*MRR1*^{T896I}		
F2	8	-/-		-/-
F5	128	*MRR1*^{P683S}/*MRR1*^{P683S}		*UPC2*^{G648S}/*UPC2*^{G648S}
G2	1	-/-		
G5	128	*MRR1*^{G997V}/*MRR1*^{G997V}		
Gu4	4		-/-	
Gu5	>256		*TAC1*^{G980E}/*TAC1*^{G980E}	
TW1 (#1)	1	-/-	-/-	-/-
TW17 (#17)	>256	*MRR1*^{G947S}/*MRR1*$^{G947S(b)}$	*TAC1*^{A736V}/*TAC1*$^{\Delta 962-969}$	*UPC2/UPC2*^{A643V}

[(a)] Strain names used in previous studies are indicated in parentheses.

[(b)] The G947S amino acid exchange was previously described as the G963S mutation [106]. In the SC5314 reference sequence, this mutation correlates with the G947S exchange, since Mrr1 of TW17 has 5 tandem repeats of the NPQS sequence from position 165 to 168. In the present study this was validated by sequencing.

2.1.2. Labeling of clinical isolates with *RFP*

It was necessary to be able to distinguish strains in a competition experiment. Therefore, *RFP* (red fluorescent protein)-labeling of the isolates was chosen as a method of differentation. This allows for an identification of the strains by colony color, since *RFP*-labeled isolates grow red colonies and unlabeled strains white colonies on YPD agar plates. A set of *RFP*-labeled strains had already been constructed in previous studies (for references see Table 17). Nevertheless, the fluconazole-susceptible strains F2 and TW1 and the fluconazole-resistant partners F5 and TW17, respectively, had to be marked with *RFP*. The plasmid pADH1R1A, which contains *RFP* under the control of the constitutively active *ADH1* promotor, was digested with the restriction enzymes ApaI and SacII (Figure

2). The resulting insert was used to construct two independent transformants of F2, F5, TW1 and TW17. The separately generated strains were named with the suffixes -A and -B. Accordingly, the strains were termed F2ADH1R1A and -B, F5ADH1R1A and -B, TW1ADH1R1A and -B and TW17ADH1R1A and -B. Correct integration of the cassette into the *ADH1* locus was verified by Southern blotting. For this purpose, chromosomal DNA was digested with the restriction enzyme EcoRI. An *ADH1* promotor region probe (amplified with the primers Prom.ADH1.fwd and Prom.ADH1.rev) and an *ADH1* probe (amplified with the primers Adh1.term1 and Adh1.term2) were used. Red fluorescence of labeled strains was verified at the microscope and the fluconazole resistance level of the constructed strains was determined by MIC assays, which in all cases did not vary from the resistance level of the unlabeled parental strains.

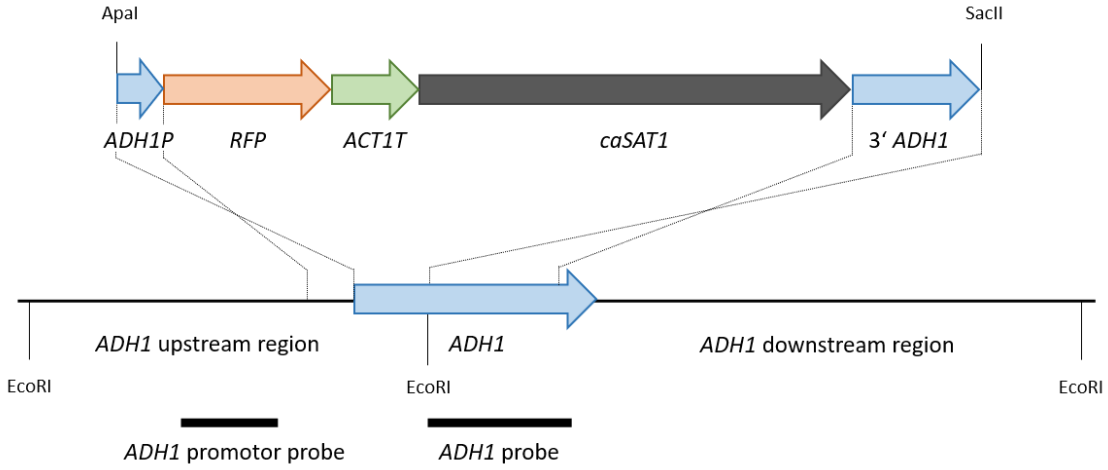

Figure 2: Schematic drawing illustrating the integration of *RFP* into the *ADH1* locus of selected clinical isolates. The ApaI-SacII fragment from pADH1R1A was used to transform F2, F5, TW1 and TW17. The blue arrows indicate sequences of *ADH1*. *RFP* is pictured as the orange arrow, the *ACT1* transcription termination sequence as the green arrow and the *caSAT1* selection marker as the gray arrow. EcoRI sites in *ADH1* and its flanking regions are shown and sites of homologous recombination during transformation are indicated by lines. Adapted from [271].

2.1.3. Competitive fitness of fluconazole-resistant clinical isolates *in vitro*

To examine the competitive fitness of clinical isolates with resistance mutations in *MRR1*, *TAC1* and/or *UPC2*, competition experiments were conducted under non-selective conditions *in vitro*. In order to distinguish between the pairs of competing strains, one member expressed *RFP*, which allowed it to be visually differentiated from the other. The fluconazole-sensitive clinical isolate was mixed separately with the two independently constructed *RFP*-labeled resistant partners in approximately equal proportions. *Vice versa*, the fluconazole-resistant strain was mixed separately with both independently generated *RFP*-labeled fluconazole-sensitive partners. Thus, it was ensured that the genetic manipulation and the ectopic *RFP* expression did not influence the results of the experiments.

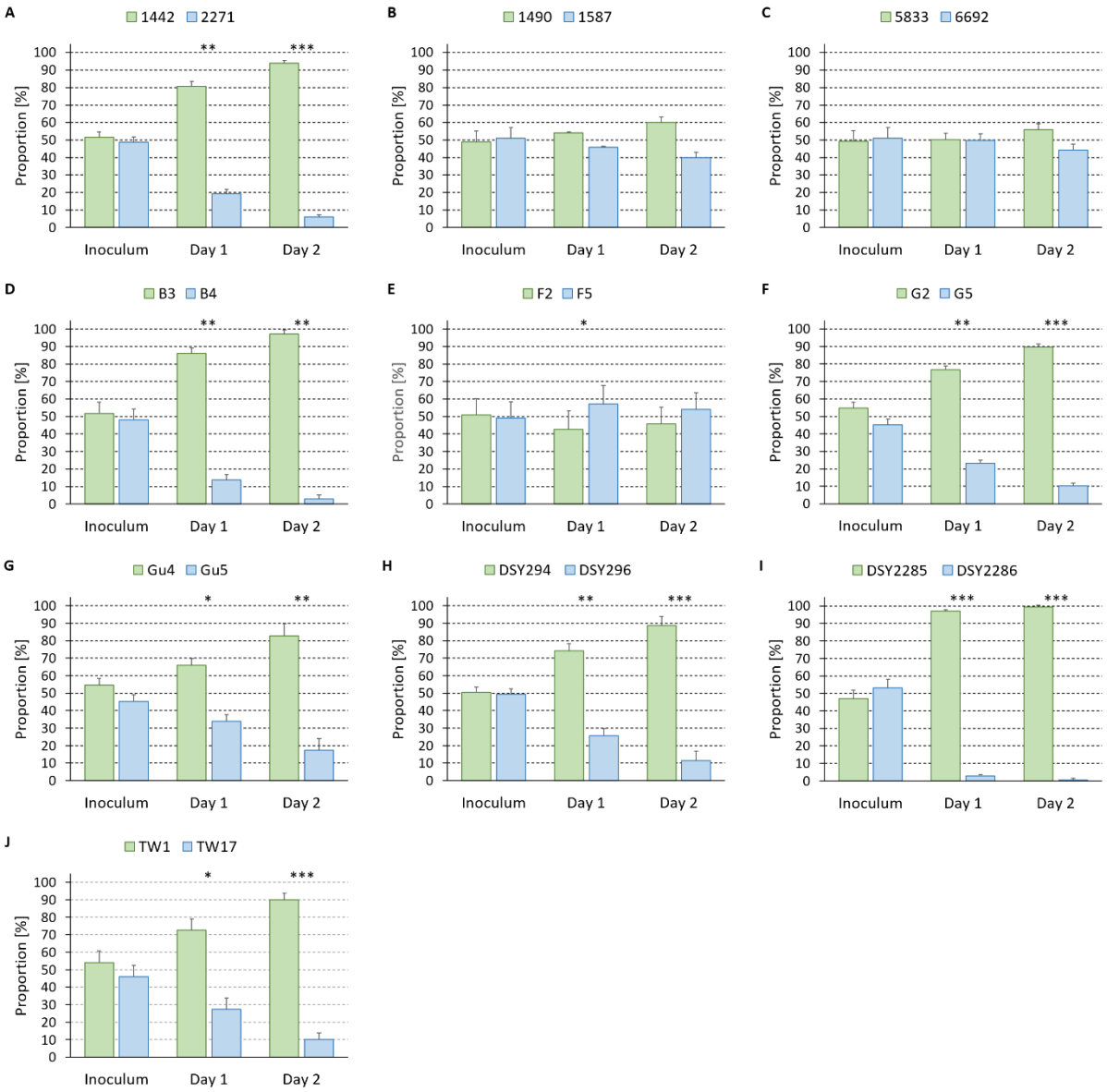

Figure 3: Relative proportion of fluconazole-susceptible isolates (green bars) in relation to the respective fluconazole-resistant partner (blue bars) in the inoculum and after 24h and 48h of co-culture under non-selective conditions (YPD-medium, 30°C). Means of four co-cultures are shown, except for strain pair F2/F5, which was tested four times (16 co-cultures). Proportions of (A) 1442/2271 (*MRR1*^{Q350L}/*MRR1*^{Q350L}), (B) 1490/1587 (*MRR1*^{N803D}/*MRR1*^{N803D}), (C) 5833/6692 (*MRR1*^{K335N}/*MRR1*^{T360I}), (D) B3/B4 (*MRR1*^{G878E}/*MRR1*^{G878E}), (E) F2/F5 (*MRR1*^{P683S}/*MRR1*^{P683S}; *UPC2*^{G648S}/*UPC2*^{G648S}), (F) G2/G5 (*MRR1*^{G997V}/*MRR1*^{G997V}), (G) Gu4/Gu5 (*TAC1*^{G980E}/*TAC1*^{G980E}), (H) DSY294/DSY296 (*TAC1*^{N977D}/*TAC1*^{N977D}), (I) DSY2285/DSY2286 (*MRR1*^{T896I}/*MRR1*^{T896I}) and (J) TW1/TW17 (*MRR1*^{G947S}/*MRR1*^{G947S}; *TAC1*^{A736V}/*TAC1*$^{\Delta962-969}$; *UPC2*/*UPC2*^{A643V}) are given. Furthermore, standard deviations are shown, and statistically significant differences are indicated by asterisks. A significant difference is indicated by * (p-value between 0.01 to 0.05), a very significant difference by ** (p-value between 0.001 to 0.01) and an extremely significant difference by *** (p-value between 0.0001 to 0.001). In case not otherwise specified, no significant difference was measured (p-value ≥ 0.05). Adapted from [266].

The mixtures were grown for two days in YPD medium, which enables a fast growth. After 24h of growth, the cultures were diluted in fresh YPD medium. In the starting culture and after 24h and 48h of growth in the co-culture, the proportions of the strains were monitored by plating of appropriate dilutions and counting red (*RFP*-labeled strain) and white (unlabeled strain) colonies. As an additional control to show that all *RFP*-labeled strains grew red colonies and all unlabeled strains white colonies, each strain was grown separately, in parallel, and treated the same as the co-cultures. Indeed, all

labeled strains grew only red colonies and all unlabeled strains only white colonies. Results of competition assays with the strain pairs 1442/2271, 1490/1587, 5833/6692, B3/B4, 1490/1587, DSY291/DSY292, DSY294/DSY296, DSY2285/DSY2286, G2/G5 and Gu4/Gu5 have previously been described [271].

Out of 10 isolate pairs, seven fluconazole-resistant strains showed a significant fitness defect in comparison to the fluconazole-susceptible partner after 24h of co-culture, which was even more obvious after 48h of growth (Figure 3). These include the strains G5, B4, 2271 and DSY2286, which have a GOF in *MRR1*, Gu5 and DSY296 with a *TAC1* resistance mutation and TW17, which acquired GOFs in *MRR1*, *TAC1* and *UPC2* (Table 1). It is likely that the hyperactivity of the zinc cluster transcription factors caused the fitness defect, but other genomic alterations cannot be excluded. Interestingly, the three isolates 1587, 6692 and F5 did not show a fitness defect in comparison to the fluconazole-susceptible partner. All three strains acquired a resistance mutation in *MRR1* and F5 in addition to a GOF in *UPC2.* These strains could have compensated for the fitness defect caused by the hyperactive zinc cluster transcription factor *MRR1* through further evolution. Another possibility is that the specific *MRR1* resistance mutations of 1587, 6692 and F5 do not cause a fitness defect.

2.1.4. Fitness effects of *MRR1* resistance mutations in an isogenic strain background

The fluconazole-resistant clinical isolates which were chosen for the present study have a variety of different *MRR1* resistance mutations (Table 1). Sasse *et al.* [121] showed that the P683S mutation, found also in isolate F5, causes a mild fitness defect in the genetic background of the SC5314 wild-type strain under non-selective conditions. Nevertheless, different GOFs could have a different effect on the fitness of the strains. Of special interest were the amino acid exchanges N803D (isolate 1587), K335N (isolate 6692) and T360I (isolate 6692) since the clinical isolates 1587 and 6692 did not show a fitness defect in competition with their fluconazole-susceptible partner (see Figure 3).

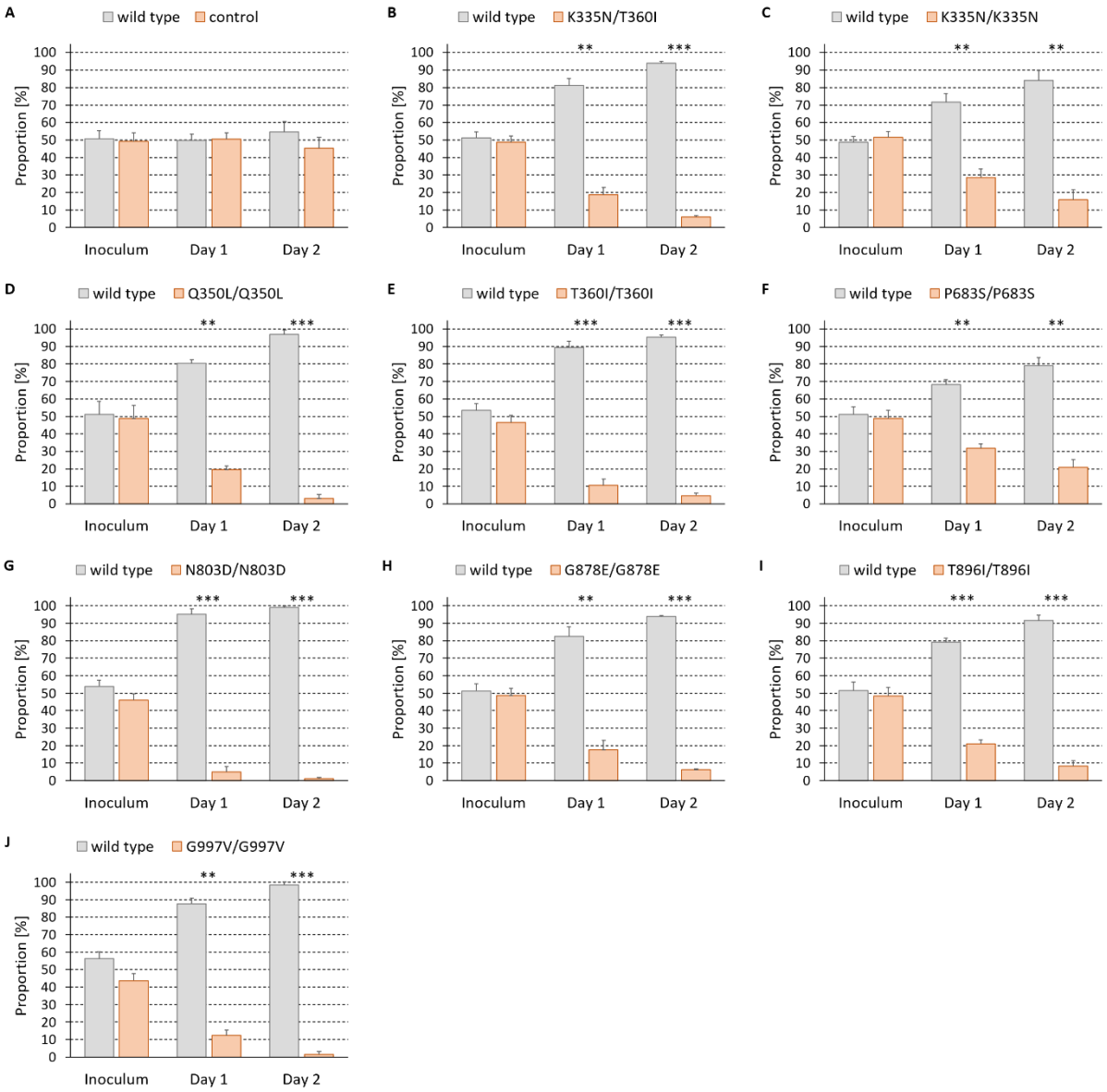

Figure 4: Relative proportion of isogenic strains with *MRR1* resistance mutations (orange bars) in competition with the *RFP*-labeled wild-type strain (SCADH1R1A, gray bars) in the inoculum and after 24h and 48h of co-culture under non-selective conditions (YPD-medium, 30°C). Means of four co-cultures are shown, except for the control strains (A), which were tested six times (twelve co-cultures). Proportions of the *RFP*-labeled wild-type strain (SCADH1R1A) mixed with (A) SCMRR1R24A and -B (wild-type *MRR1*), (B) SCMRR1R982A and -B (*MRR1*^{K335N}/*MRR1*^{T360I}), (C) SCMRR1R94A and -B (*MRR1*^{K335N}/*MRR1* ^{K335N}), (D) SCMRR1R64A and -B (*MRR1*^{Q350L}/*MRR1*^{Q350L}), (E) SCMRR1R84A and -B (*MRR1*^{T360I}/*MRR1*^{T360I}), (F) SCMRR1R34A and -B (*MRR1*^{P683S}/*MRR1*^{P683S}), (G) SCMRR1R74A and -B (*MRR1*^{N803D}/*MRR1*^{N803D}), (H) SCMRR1R54A and -B (*MRR1*^{G878E}/*MRR1*^{G878E}), (I) SCMRR1R104A and -B (*MRR1*^{T896I}/*MRR1*^{T896I}) and (J) SCMRR1R44A and -B (*MRR1*^{G997V}/*MRR1*^{G997V}) are given. Furthermore, standard deviations are shown, and statistically significant differences are indicated by asterisks. A significant difference is indicated by * (p-value between 0.01 to 0.05), a very significant difference by ** (p-value between 0.001 to 0.01) and an extremely significant difference by *** (p-value < 0.001). In case not otherwise specified, no significant difference was measured (p-value ≥ 0.05). Adapted from [266].

To verify that the *MRR1* resistance mutations cause a fitness defect in an isogenic strain background, they were introduced into the wild-type strain SC5314 (for references see Table 18). Both endogenous *MRR1* alleles were replaced by alleles with resistance mutations found in the clinical isolates. These strains were mixed with the *RFP*-labeled parental strain (SCADH1R1A) and competition experiments were performed under non-selective conditions in rich medium as previously described (chapter 2.1.3). The *RFP*-labeled wild-type (SCADH1R1A) was in all cases mixed twice with two independently

constructed strains in roughly equal proportions. As a control to show that the genetic manipulation did not affect the fitness of the strains, the *RFP*-labeled wild-type (SCADH1R1A) was also tested in combination with the SC5314 strain in which both endogenous wild-type *MRR1* alleles were exchanged by the wild-type *MRR1* with the *SAT1*-flipper cassette strategy (SCMRR1R24A and -B) as it was done for the other strains. These strains did not show an altered fitness in comparison with the *RFP*-labeled wild-type strain (Figure 4A), showing that the strategy of genetic manipulation does not affect the fitness of the strains. Note that the *SAT1*-flipper cassette has been previously described [98, 272, 273].

Indeed, all tested *MRR1* resistance mutations caused a significant fitness defect in the isogenic strain background in the absence of the drug (Figure 4). As described in chapter 2.1.3, 1587 (*MRR1*^{N803D}/*MRR1*^{N803D}), 6692 (*MRR1*^{K335N}/*MRR1*^{T360I}) and F5 (*MRR1*^{P683S}/*MRR1*^{P683S}; *UPC2*^{G648S}/*UPC2*^{G648S}) did not show a significant fitness defect in competition with their fluconazole-susceptible partner. Nevertheless, the respective *MRR1* GOFs showed a significant fitness defect in the SC5314 strain background. Also strains harboring only a homozygous K335N or T360I mutation were outcompeted by the wild-type. These findings suggest that the effect of the resistance mutation on the fitness strongly depends on the strain background.

2.1.5. Introduction of *MRR1* GOFs in fluconazole-susceptible clinical isolates

An interesting question was how the strains 1587, 6692 and F5 were able to overcome the apparent fitness costs of their respective *MRR1* mutations. Two scenarios were hypothesized. One possibility was that the strains acquired a compensatory mutation after the resistance mutation appeared. Another possibility was that the *MRR1* mutations did not cause a fitness defect in the genetic background of the clinical isolates due to previous adaptations to the environment, which enabled the strains to tolerate hyperactive Mrr1. To determine which hypothesis is correct, an experiment was set up to establish whether the *MRR1* resistance mutations of F5 and 6692 cause a fitness defect in the genetic background of the respective fluconazole-susceptible clinical isolate. For this purpose, the P683S substitution (isolate F5) was introduced into F2, and K335N and T360I (isolate 6692) into 5583 by using the recyclable *SAT1*-flipper cassette.

The SacI-ApaI-digested pMRR1R3 plasmid containing the P683S substitution was used to transform F2 two times independently. Furthermore, the SacI-ApaI-digested pMRR1R8 with the T360I substitution was taken to transform 5833 two times independently. Correct integration of the insert was verified by Southern blots of NsiI-digested chromosomal DNA with the *MRR1* specific probes 3'MRR1 (PCR primers for probe amplification: ZCF36-6 and ZCF36-7) and 5'MRR1 (PCR primers for probe

amplification: ZCF36-1 and ZCF36-47), or MRR1-GOF (PCR primers for probe amplification: ZCF36-1 and ZCF36-2). Resulting strains were named F2MRR1R31A and -B and 5833MRR1R81A and -B.

All plasmids used (pMRR1R3, pMRR1R8 and pMRR1R9) contain the *MRR1* coding region (Figure 5A) and differed from each other in the *MRR1* resistance mutation. Due to the long homologous *MRR1* region (only one base exchange in comparison to the wild-type *MRR1* of F2 and 5833), the actual crossover event during transformation could have also happened downstream of the GOF of interest. Therefore, sequencing of the transformants was essential to confirm that they not only harbored the *SAT1*-flipper cassette, but also the respective resistance mutation. *MRR1* of the transformants was reamplified by PCR, followed by sequencing. Primers used for this purpose are listed in Table 2.

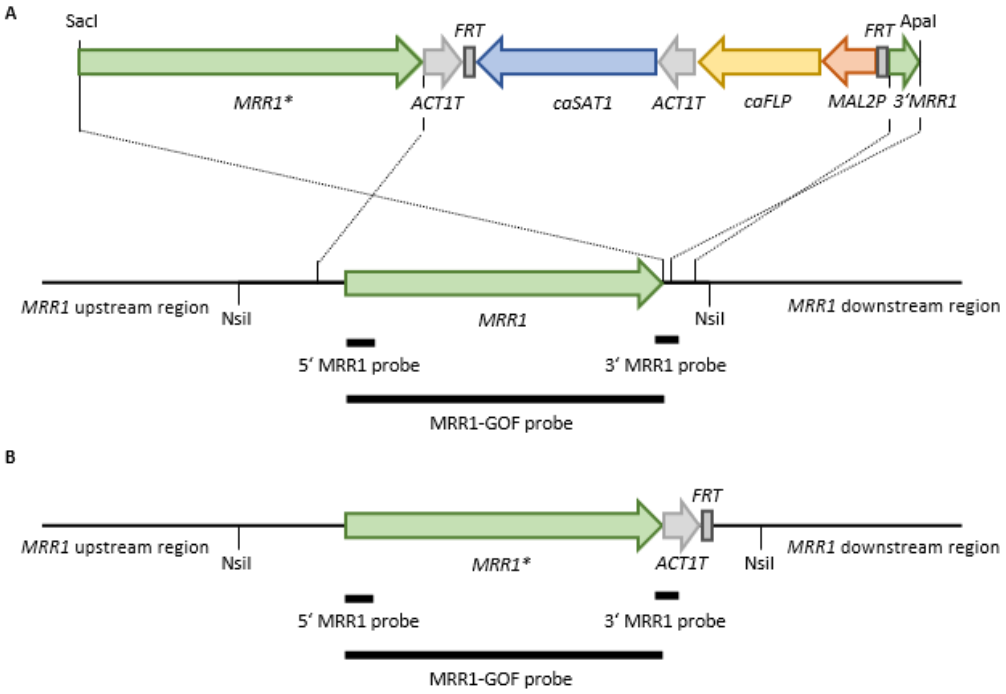

Figure 5: Schematic drawing illustrating the integration of *MRR1* sequences with a resistance mutation into a wild-type *MRR1* allele and the transformed locus after recycling of the *SAT1*-flipper cassette. (A) The SacI-ApaI fragment from pMRR1R3 and pMRR1R8 and pMRR1R9 was used to transform F2 and 5833, respectively. *MRR1* is indicated by a green arrow and hyperactive *MRR1* alleles are highlighted by an asterisk. The site-specific recombinase *caFLP* is pictured as a yellow arrow and the *MAL2* promotor *(MAL2P*) as a red arrow. Also shown are *FRT* sites in dark gray, the *ACT1* transcription termination sequence by the light gray arrow and the *caSAT1* selection marker by the blue arrow. Shown are NsiI sites in the flanking regions of *MRR1*, and sites of homologous recombination during transformation are indicated by lines. (B) *MRR1** locus after successful recycling of the *SAT1*-flipper cassette.

Correct clones were cultivated in the presence of maltose to induce the recycling of the *SAT1* flipper cassette by induction of the *FLP* expression. This gene encoding for the Flp recombinase is under the control of the maltose-induced *MAL2* promotor in the *SAT1* flipper cassette (Figure 5A). Afterwards, the genome by site-specific recombination by the Flp recombinase takes place at the Flp-recognition target (*FRT*) sites. Correct recycling of the *SAT1* flipper cassette was validated by Southern hybridization of NsiI-digested chromosomal DNA with the *MRR1* specific probes 3'MRR1 and 5'MRR1,

or MRR1-GOF (Figure 5B). Resulting strains were termed F2MRR1R32A and -B and 5833MRR1R82A and -B.

Table 2: Primers used for PCR amplification and subsequent sequencing of the constructed strains.

Strain name	PCR primers	Sequencing primers
F2MRR1R31	Act18 and ZCF36seq2	ZCF36-66
F2MRR1R33	ZCF36-8 and ZCF36seq2	
5833MRR1R81	Act18 and ZCF36seq7	ZCF36-61
5833MRR1R981	ZCF36-8 and ZCF36seq7	ZCF36-52

Thereafter, the second endogenous *MRR1* allele of the strains was replaced. F2MRR1R32A and -B were transformed with the SacI-ApaI-digested pMRR1R3 plasmid containing the P683S substitution. 5833MRR1R82A and -B were transformed with the SacI-ApaI-digested pMRR1R9, which has the K335N substitution. Verification of the clones was performed by Southern hybridization and sequencing, as described above. Resulting strains were named F2MRR1R33A and -B and 5833MRR1R891A and -B. The *SAT1*-flipper of the strains was recycled as previously described and final strains were termed F2MRR1R34A and -B and 5833MRR1R892A and -B. These strains were used for competition experiments (chapter 2.1.6.). In addition, the resistance level of the constructed strains was determined (Table 3). Fluconazole resistance was already increased when the *MRR1* GOF was present in one allele. F2MRR1R34A and -B with the homozygous *MRR1* substitution P683S reached a resistance level of 64µg/ml. Nevertheless, 5833MRR1R892A and -B showed a lower resistance level than 6692, although it has the same two hyperactive *MRR1* alleles (*MRR1*^{K335N}/*MRR1*^{T360I}). It is possible that other unknown resistance mechanisms are responsible for the increased resistance level of 6692.

Table 3: Minimal inhibitory concentrations (MICs) of clinical isolate derivatives and their respective resistance mutation(s).

Strain name	MIC [µg/ml]	Parent	Resistance mutations
5833	1	-	-
5833MRR1R81A and -B	4	5833	*MRR1*/*MRR1*^{T360I}
5833MRR1R82A	4	5833MRR1R81A	*MRR1*/*MRR1*^{T360I}
5833MRR1R82B	4	5833MRR1R81B	*MRR1*/*MRR1*^{T360I}
5833MRR1R891A	16	5833MRR1R82A	*MRR1*^{K335N}/*MRR1*^{T360I}
5833MRR1R891B	16	5833MRR1R82B	*MRR1*^{K335N}/*MRR1*^{T360I}
5833MRR1R892A	16	5833MRR1R891A	*MRR1*^{K335N}/*MRR1*^{T360I}
5833MRR1R892B	16	5833MRR1R891B	*MRR1*^{K335N}/*MRR1*^{T360I}
6692	64	-	*MRR1*^{K335N}/*MRR1*^{T360I}
F2	8	-	-
F2MRR1R31A and -B	16	F2	*MRR1*/*MRR1*^{P683S}
F2MRR1R32A	16	F2MRR1R31A	*MRR1*/*MRR1*^{P683S}
F2MRR1R32A	16	F2MRR1R31B	*MRR1*/*MRR1*^{P683S}
F2MRR1R33A	64	F2MRR1R32A	*MRR1*^{P683S}/*MRR1*^{P683S}
F2MRR1R33B	64	F2MRR1R32B	*MRR1*^{P683S}/*MRR1*^{P683S}
F2MRR1R34A	64	F2MRR1R33A	*MRR1*^{P683S}/*MRR1*^{P683S}
F2MRR1R34B	64	F2MRR1R33B	*MRR1*^{P683S}/*MRR1*^{P683S}
F5	128	-	*MRR1*^{P683S}/*MRR1*^{P683S}; *UPC2*^{G648S}/*UPC2*^{G648S}

2.1.6. Fitness effects of *MRR1* resistance mutations in clinical strains

Competition experiments were conducted to test whether the clinical isolates 6692 and F5 compensated for the costs of hyperactive Mrr1, or whether the *MRR1* resistance mutations did not cause a fitness defect in the genetic background of the clinical isolates. The *RFP*-labeled fluconazole-susceptible clinical isolates 5833 and F2 were mixed in a 1:1 ratio with their respective derivatives in which the *MRR1* resistance mutation of the matched fluconazole-resistant clinical isolates had been introduced (6692 and F5, see chapter 2.1.5). For every strain, both independently constructed strains were tested with the two independently constructed strains of the respective derivative. Therefore, results of 4 co-cultures in rich medium (YPD) under non-selective conditions are shown in Figure 6.

Strains with *MRR1* GOFs (P683S/P683S and K335N/T360I) in the genetic background of the fluconazole-susceptible clinical isolates did not show a significant fitness defect in comparison to the fluconazole-susceptible clinical isolates. This finding supports the hypothesis that hyperactive Mrr1 did not cause a fitness defect in the genetic background of the fluconazole-resistant clinical isolates, since these strains acquired adaptations to the environment which bypassed the fitness defect usually caused by *MRR1* resistance mutations.

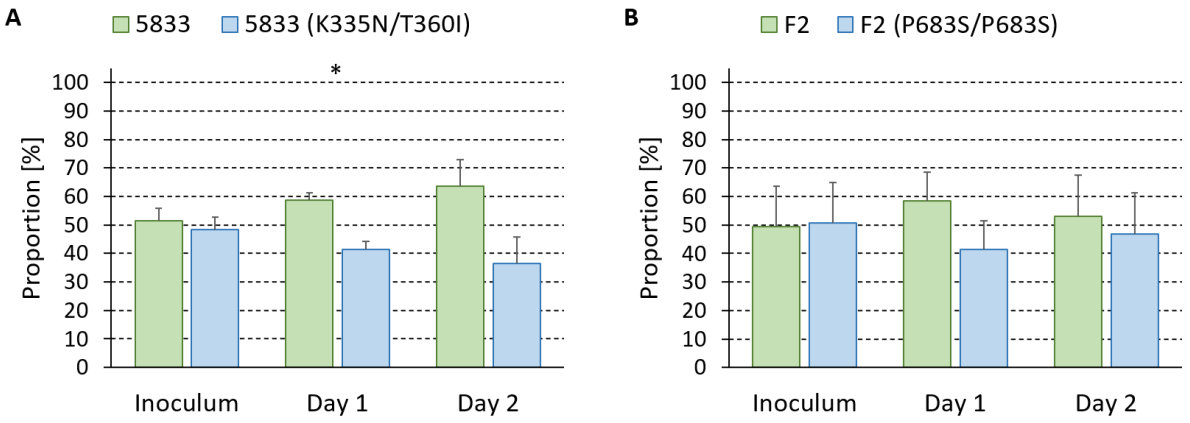

Figure 6: Relative proportion of fluconazole-susceptible isolates (green bars) in relation to the respective derivative with *MRR1* resistance mutations (blue bars) in the inoculum and after 24h and 48h of co-culture under non-selective conditions (YPD-medium, 30°C). Means of four co-cultures are shown. Proportions of (A) 5833/5833 (*MRR1*^{K335N}/*MRR1*^{T360I}) and (B) F2/F2 (*MRR1*^{P683S}/*MRR1*^{P683S}) are given. In addition, deviations are shown, and statistically significant differences are indicated by asterisks. A significant difference is indicated by * (p-value between 0.01 to 0.05) and unless otherwise specified, no significant difference was measured (p-value ≥ 0.05). Adapted from [266].

2.1.7. Competitive fitness of fluconazole-resistant clinical isolates *in vivo*

Fitness effects measured *in vitro* in rich medium (optimal growth conditions) do not necessarily reflect the fitness of the strains in a mammalian host. In addition, a study by Sasse *et al.* [121] showed that a constructed strain with resistance mutations in the three zinc cluster transcription factors Mrr1, Tac1 and Upc2 had a decreased fitness under non-selective conditions in a mouse model of gastrointestinal colonization. It was found that a single of these hyperactive transcription factors alone was not sufficient to decrease the *in vivo* fitness significantly, although the fitness defect was evident *in vitro*. Therefore, similar *in vivo* competition experiments in a mouse model of gastrointestinal colonization were conducted in the present study with the sets of clinical isolates. Additionally, the fitness of the strains was examined in an infection model of disseminated candidiasis.

For these experiments, two strain pairs with fluconazole-resistant clinical isolates which overcame the costs of drug resistance in YPD medium (5833/6692 and F2/F5) were chosen. Furthermore, two strain pairs were tested, of which the fluconazole-resistant clinical isolates showed a significant fitness defect *in vitro* (B3/B4 and TW1/TW17). The fluconazole-susceptible clinical isolate was mixed with the *RFP*-labeled fluconazole-resistant matched partner in a 1:1 ratio. Accordingly, the fluconazole-resistant strain was grown in competition with the *RFP*-labeled fluconazole-susceptible strain. The unlabeled isolate was tested in all cases with each of the two independently constructed labeled partners. In total, four mixtures were tested for each of the four clinical isolate pairs.

For the mouse model of gastrointestinal colonization (GI), at least three mice per mixture were fed with the yeast suspension. Thereafter, feces were collected for seven days after infection. Surprisingly, all fluconazole-resistant strains were outcompeted by their susceptible partner (Figure 7). 6692 and F5, which did not show a fitness defect *in vitro*, showed a strong fitness defect in competition with the susceptible partner during colonization of the gastrointestinal tract. TW17, which was outcompeted by its partner in YPD medium, showed a slight, but significant fitness defect (day 7) *in vivo* in the GI model. These findings suggest that the *in vitro* fitness does not predict the fitness of the strains *in vivo* during colonization of the gastrointestinal tract of the mice.

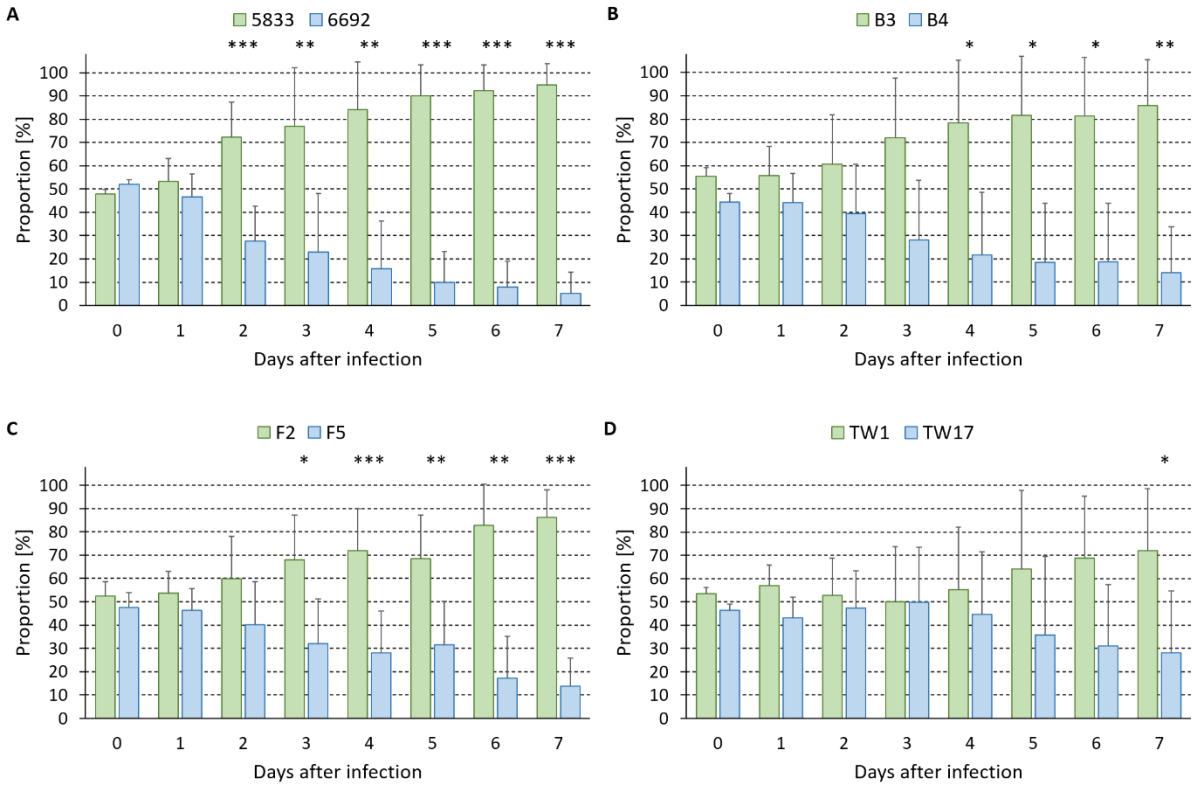

Figure 7: Competitive fitness of clinical isolates *in vivo* in a mouse model of gastrointestinal colonization. (A-D) Fluconazole-susceptible clinical isolates (green bars) were mixed with two independently constructed *RFP*-labeled fluconazole-resistant partners (blue bars). *Vice versa*, fluconazole-resistant strains (blue bars) were mixed with the two independently constructed *RFP*-labeled fluconazole-susceptible strains (green bars). Therefore, four mixtures were tested per matched strain pair. Three mice per mixture were infected (four mice for the strain combinations 5833/6692ADH1R1A and TW1/TW17ADH1R1A). Mean proportions of (A) 5833/6692 (*MRR1*^{K335N}/*MRR1*^{T360I}), (B) B3/B4 (*MRR1*^{G878E}/*MRR1*^{G878E}), (C) F2/F5 (*MRR1*^{P683S}/*MRR1*^{P683S}; *UPC2*^{G648S}/*UPC2*^{G648S}) and (D) TW1/TW17 (*MRR1*^{G947S}/*MRR1*^{G947S}; *TAC1*^{A736V}/*TAC1*$^{\Delta 962\text{-}969}$; *UPC2*/*UPC2*^{A643V}) are given. Three mice were infected with each of the four mixtures and mean proportions are given. Furthermore, standard deviations are shown, and statistically significant differences are indicated by asterisks. A significant difference is indicated by * (p-value between 0.01 to 0.05), a very significant difference by ** (p-value between 0.001 to 0.01) and an extremely significant difference by *** (p-value between 0.0001 to 0.001). Unless otherwise specified, no significant difference was measured (p-value ≥ 0.05). Adapted from [266].

In the human body, *C. albicans* not only colonizes the gastrointestinal tract, but also other niches [31]. Therefore, another mouse model, one of disseminated candidiasis, was chosen for further studies. For this, mice were infected by injection of the aforementioned mixtures into the lateral tail vein. Six days after infection, kidneys were collected and proportions of the strains were determined. F5 and TW17 showed no fitness defect in competition with the respective fluconazole-susceptible partner. B4 was able to compete with its susceptible partner, although it showed a tendential fitness defect. Only 6692 was outcompeted by 5833. These findings show that the effect of the resistance mutations on the fitness strongly depends on the environment and the fitness defect can be observed only in certain host niches.

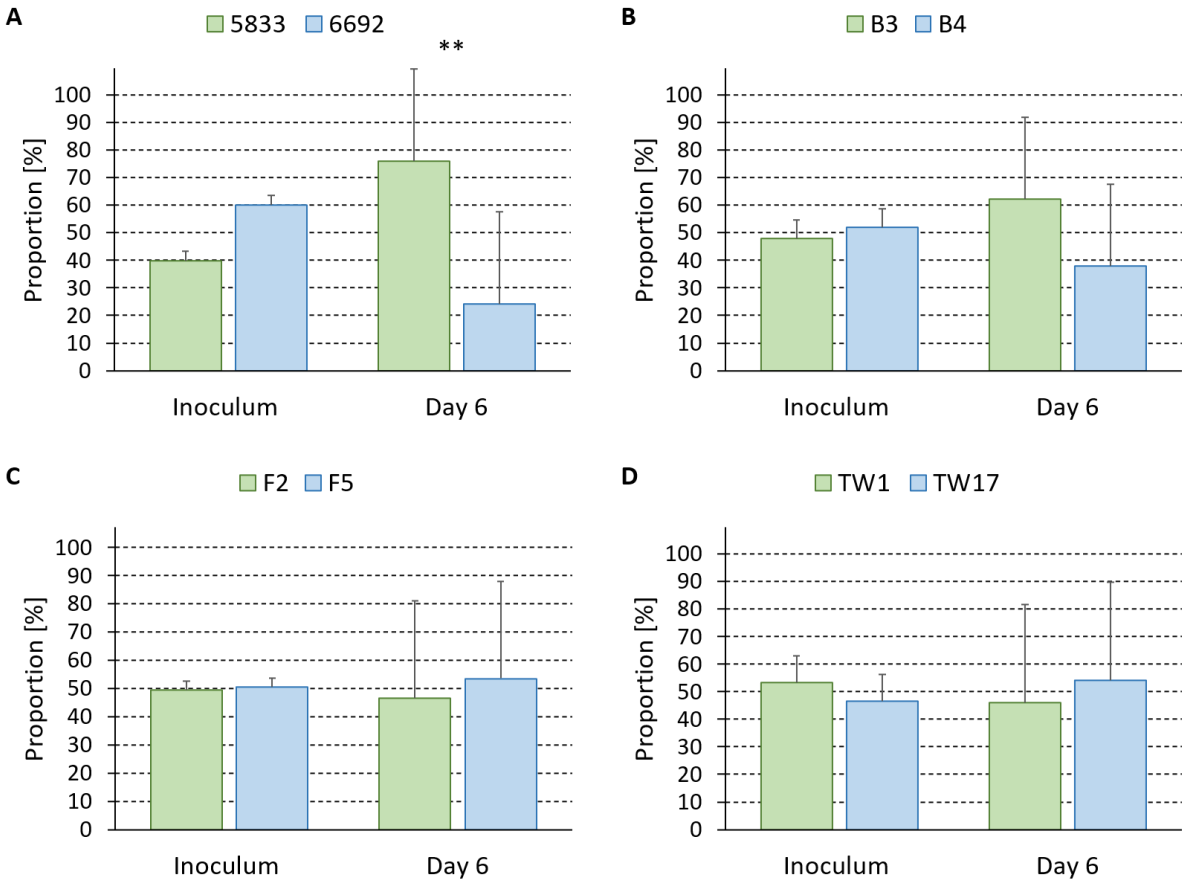

Figure 8: Competitive fitness of clinical isolates *in vivo* in a mouse model of intravenous infection. Fluconazole-susceptible clinical isolates (green bars) were mixed with two independently constructed *RFP*-labeled fluconazole-resistant partners (blue bars). *Vice versa*, fluconazole-resistant strains (blue bars) were mixed with the two independently constructed *RFP*-labeled fluconazole-susceptible strains (green bars). Therefore, four mixtures were tested per matched strain pair. Three mice per mixture were infected (five mice for the strain combination B3/B4ADH1R1B). Mean proportions of (A) 5833/6692 (*MRR1*^{K335N}/*MRR1*^{T360I}), (B) B3/B4 (*MRR1*^{G878E}/*MRR1*^{G878E}), (C) F2/F5 (*MRR1*^{P683S}/*MRR1*^{P683S}; *UPC2*^{G648S}/*UPC2*^{G648S}) and (D) TW1/TW17 (*MRR1*^{G947S}/*MRR1*^{G947S}; *TAC1*^{A736V}/*TAC1*$^{\Delta 962\text{-}969}$; *UPC2*/*UPC2*^{A643V}) are given. Furthermore, standard deviations are shown, and statistically significant differences are indicated by asterisks. A very significant difference is indicated by ** (p-value between 0.001 to 0.01). Unless otherwise specified, no significant difference was measured (p-value ≥ 0.05). Adapted from [266].

2.2. Evolution of highly drug-resistant *C. albicans* strains by mating

Although hyperactive *MRR1*, *TAC1* and *UPC2* alleles cause a fitness defect in certain host niches (chapter 2.1.7), they also confer a selective advantage in the presence of the antimycotic drug fluconazole [121, 266]. GOFs (gain-of-function mutations) in Mrr1 and Tac1 lead to a constitutive overexpression of the efflux pumps *MDR1* and *CDR1*/*CDR2*, respectively, increasing drug resistance [104-107, 109-112, 114, 266]. In addition, hyperactive Upc2 causes an overexpression of the drug target *ERG11* [93-96, 266]. Another well-known resistance mechanism is resistance mutations in *ERG11* itself, which encodes a sterol 14α-demethylase, reducing efficiency of drug binding [62, 73, 264, 265]. The resistance mutations in *ERG11*, *MRR1*, *TAC1* and *UPC2* affect the resistance level of a strain to different degrees. Furthermore, the combination of mechanisms in one strain potentiates drug

resistance [121, 266]. Interestingly, patients are often infected with highly drug resistant strains with a combination of different resistance mechanisms [62, 73, 75, 104, 119, 121, 264, 266]. This begs the question of how these highly drug resistant strains with a combination of different resistance mechanisms evolve.

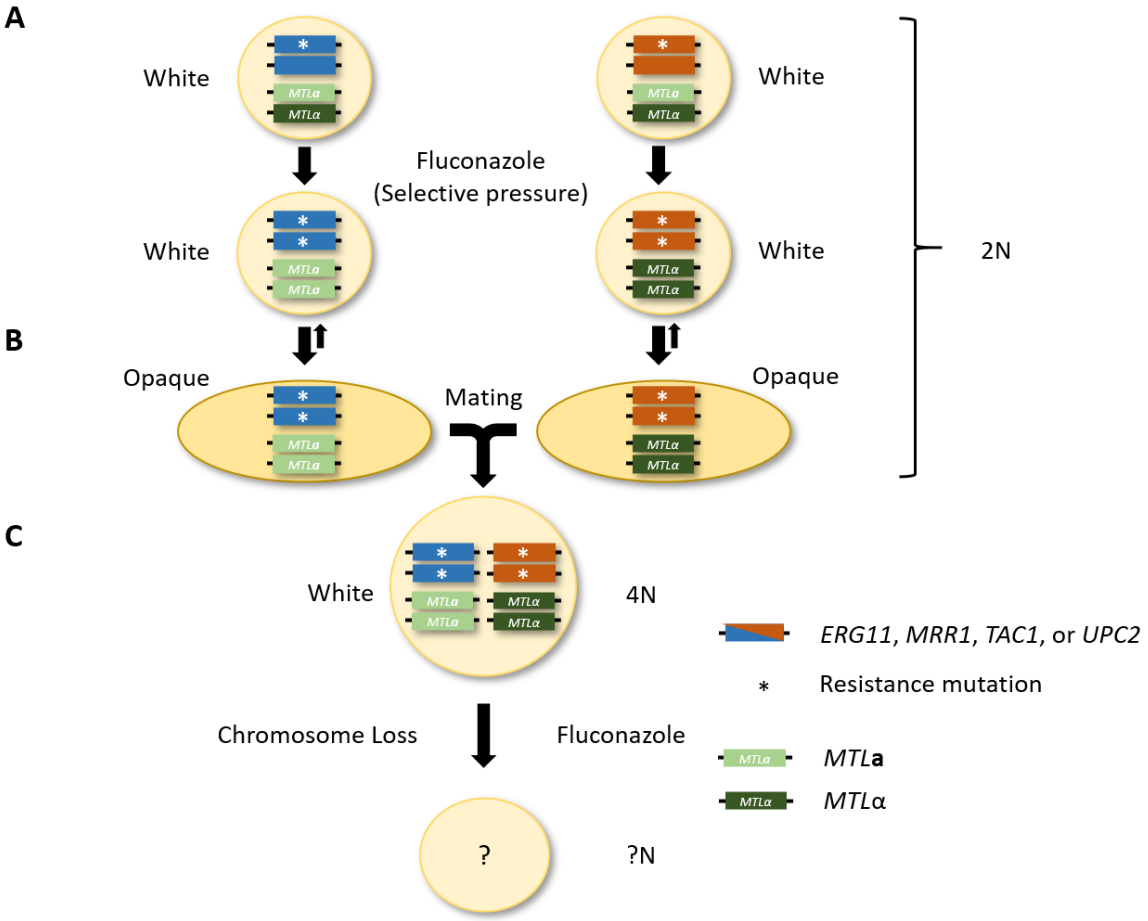

Figure 9: Hypothesis of the evolution of highly drug resistant strains by parasexual recombination after acquiring fluconazole-induced mating competence. The two *MTL* configurations are indicated by a light green (*MTL***a**) and a dark green (*MTL*α) bar. Alleles of the resistance-associated genes *ERG11*, *MRR1*, *TAC1* and *UPC2* are indicated by blue or red bars, and a resistance mutation by an asterisk. (A) Strains in the white phenotype with a heterozygous resistance mutation in one of the resistance-associated genes and a heterozygous *MTL* locus could become homozygous for both loci under fluconazole pressure. (B) These strains could switch into the mating-competent opaque phenotype and mate with cells with the opposite *MTL* idiomorph, which are homozygous for a different resistance-associated gene. (C) The resulting mating products would have acquired the genetic material of both mating partners and therefore exhibit wild-type and hyperactive alleles of the resistance-associated genes and alleles of both types of the *MTL* locus. These mating products could randomly lose DNA content in the presence of fluconazole and form highly drug resistant progeny by reassorting their genomes in an advantageous way.

In this study, one hypothesis examined was whether strains in a clonal population can combine individually-acquired resistance mechanisms by parasexual recombination following the acquisition of drug-induced mating competence, as illustrated in Figure 9. In particular, in the presence of fluconazole selection pressure, strains which are heterozygous for a resistance mutation in *ERG11*, *MRR1*, *TAC1* or *UPC2* could become homozygous for the respective resistance mutation and at the same time for the mating type locus (*MTL*, Figure 9A). The likelihood of this occurring may be increased,

since it is known that strains with a homozygous resistance mutation in these genes have a higher resistance level than strains which are heterozygous for the same resistance mutation [121]. In addition, genomic recombination causing the loss-of-heterozygosity (LOH) at a resistance-associated locus can affect the *MTL* locus as well, resulting in a homozygosity at both loci [267, 268]. Interestingly, *C. albicans* strains which are homozygous for the *MTL* locus can switch reversibly into the mating-competent opaque phenotype [24, 25]. It is conceivable that opaque cells homozygous for both the *MTL* and a particular resistance mutation could mate with each other and thereby generate recombinant mating progeny with a combination of different resistance mechanisms on which selection can act (Figure 9B). In general, mating products can reduce DNA content in a non-meiotic way and reach a diploid, or near-diploid ploidy state, thereby generating diversity [181, 183, 184, 186, 200]. An interesting aspect is whether highly drug resistant strains and thus highly adapted strains can arise by the propagation of the mating progeny with combined resistance mechanisms in the presence of fluconazole (Figure 9C).

2.2.1. Loss of heterozygosity in strains with heterozygous resistance mutations and *MTL* locus stimulated by fluconazole

To isolate strains with a loss of heterozygosity (LOH) for a resistance mutation in *ERG11*, *MRR1*, *TAC1* or *UPC2* and at the same time a LOH for the mating type locus (Figure 9A), a set of eight isogenic strains with heterozygous GOFs were passaged in the presence of fluconazole. Two independently constructed derivatives (named with the suffixes -A and -B) of the wild-type strain SC5314 (*MTL*-heterozygous) with a heterozygous *ERG11*^{G464S}, *MRR1*^{P683S}, *TAC1*^{G980E} or *UPC2*^{G648D} allele were chosen. These strains were selected since the effect of the respective resistance mutation on the resistance level and fitness is well-studied (chapter 2.1) [121, 266].

The chosen strain SCERG11R32A has an *ERG11*^{G464S} allele, which is located on chromosome 5B as well as the *MTL*α allele (Figure 10). Accordingly, strain SCERG11R32B encodes the *ERG11*^{G464S} allele, which is linked to the *MTL***a** on chromosome 5A. SCMRR1R32A and -B harbor a *MRR1*^{P683S} allele on chromosome 3. In SC5314 this chromosome is largely homozygous, which impedes differentiation of the two wild-type *MRR1* alleles. SCTAC1R32A encodes the *TAC1*^{G980E} allele and the *MTL*α on the left arm of chromosome 5B and SCTAC1R32B the *TAC1*^{G980E} allele and the *MTL***a** on the homologous chromosome 5A. The independently constructed strains SCUPC2R12A and -B contain the *UPC2*^{G648D} allele on chromosome 1.

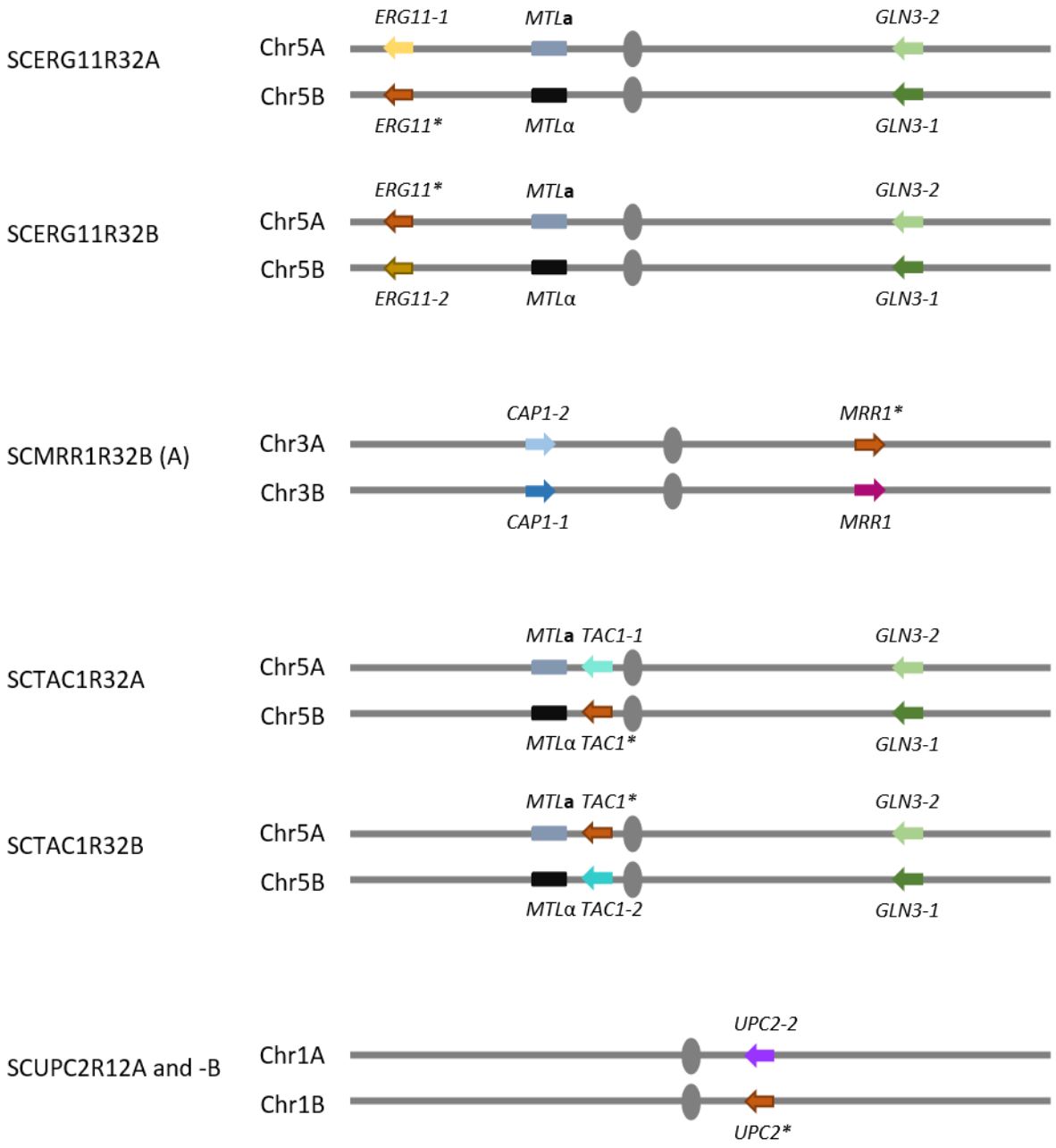

Figure 10: Schematic drawing (not to scale) illustrating the location of resistance-associated genes, the *MTL* locus and polymorphism markers of strains selected for microevolution experiments. Relative positions of wild-type *ERG11*, *MRR1*, *TAC1* and *UPC2* alleles (colored arrows) on the chromosomes (gray lines) with the centromeres (gray ovals) are shown. Hyperactive alleles are indicated by an asterisk, and the two idiomorphs of the *MTL* are pictured (*MTL***a** by gray bars and *MTL*α by black bars). Furthermore, the polymorphism markers *GLN3* (green arrows) and *CAP1* (blue arrows) are pictured. Chromosome 3 of SC5314 is largely homozygous for the right arm. Therefore, it was not possible to distinguish the two *MRR1* wild-type alleles. The linkage of the mutated *MRR1* allele with the *CAP1-2* allele of SCMRR1R32B was concluded after LOH in homozygous progeny (chapter 2.2.1.2). Adapted from [266].

2.2.1.1. Isolation and characterization of *TAC1** and *MTL* homozygous strains

First, a method was established to distinguish strains with a homozygous resistance mutation from strains with a heterozygous resistance mutation. Strains with a homozygous G980E substitution in *TAC1* were differentiated from heterozygous strains by colony size on YPD agar containing fluconazole. While *TAC1*^{G980E} homozygous strains grow in large colonies, *TAC1*^{G980E} heterozygous strains form small colonies on this agar (Figure 11) [271].

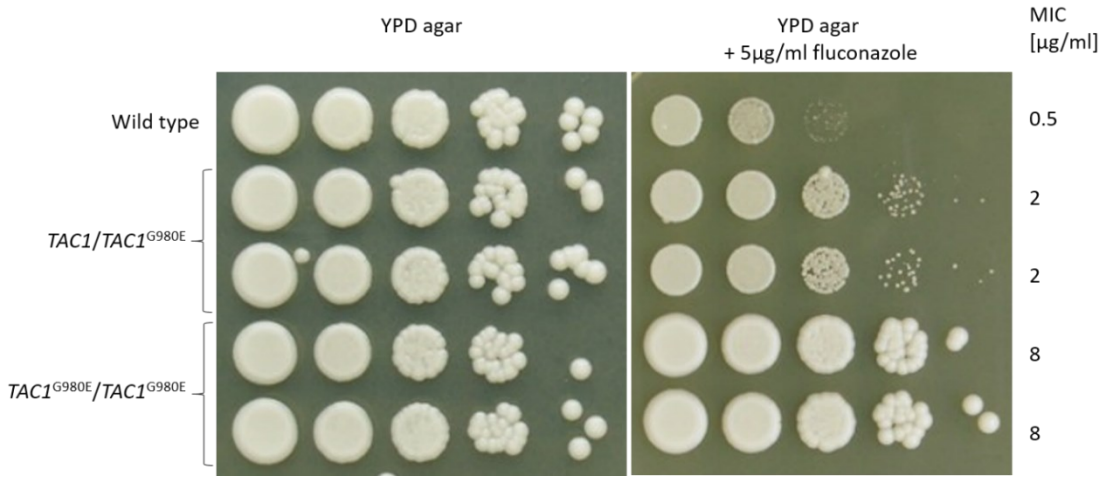

Figure 11: Growth of *TAC1* GOF heterozygous and homozygous strains on YPD agar containing fluconazole. Dilutions of the wild-type strain (SC5314) and the two independently constructed *TAC1*^{G980E} heterozygous (SCTAC1R32A and -B) and homozygous (SCTAC1R34A and -B) strains were plated on YPD agar with and without 5µg/ml fluconazole. Furthermore, MICs of the strains were determined. Adapted from [271].

To select for strains which had become homozygous for *TAC1*^{G980E}, the two independently constructed *TAC1*^{G980E} heterozygous strains (SCTAC1R32A and -B) were cultivated in the presence of 5µg/ml fluconazole for several passages (chapter 4.2.4.1). An appropriate dilution of each passage (growth for one day) was plated for single colonies on YPD agar plates containing 5µg/ml fluconazole. Already after passage two large colonies grew on the agar plates. Twelve colonies were picked and the *TAC1* locus was analyzed by a preliminary PCR analysis [271], followed by Southern hybridization (Figure 12). Seven of the analyzed mutants were homozygous for the *TAC1*^{G980E} allele. This implies that the LOH for the hyperactive *TAC1* allele was the main reason for the increased fluconazole resistance level (better growth on fluconazole-containing agar plates). Accordingly, these mutants had an increased fluconazole resistance level of 8µg/ml, correlating with the MIC of genetically engineered strains with a homozygous *TAC1*^{G980E} allele (SCTAC1R34A and -B). In comparison, the *TAC1*^{G980E} heterozygous parental strains have a MIC of 2µg/ml (Table 4, Figure 13).

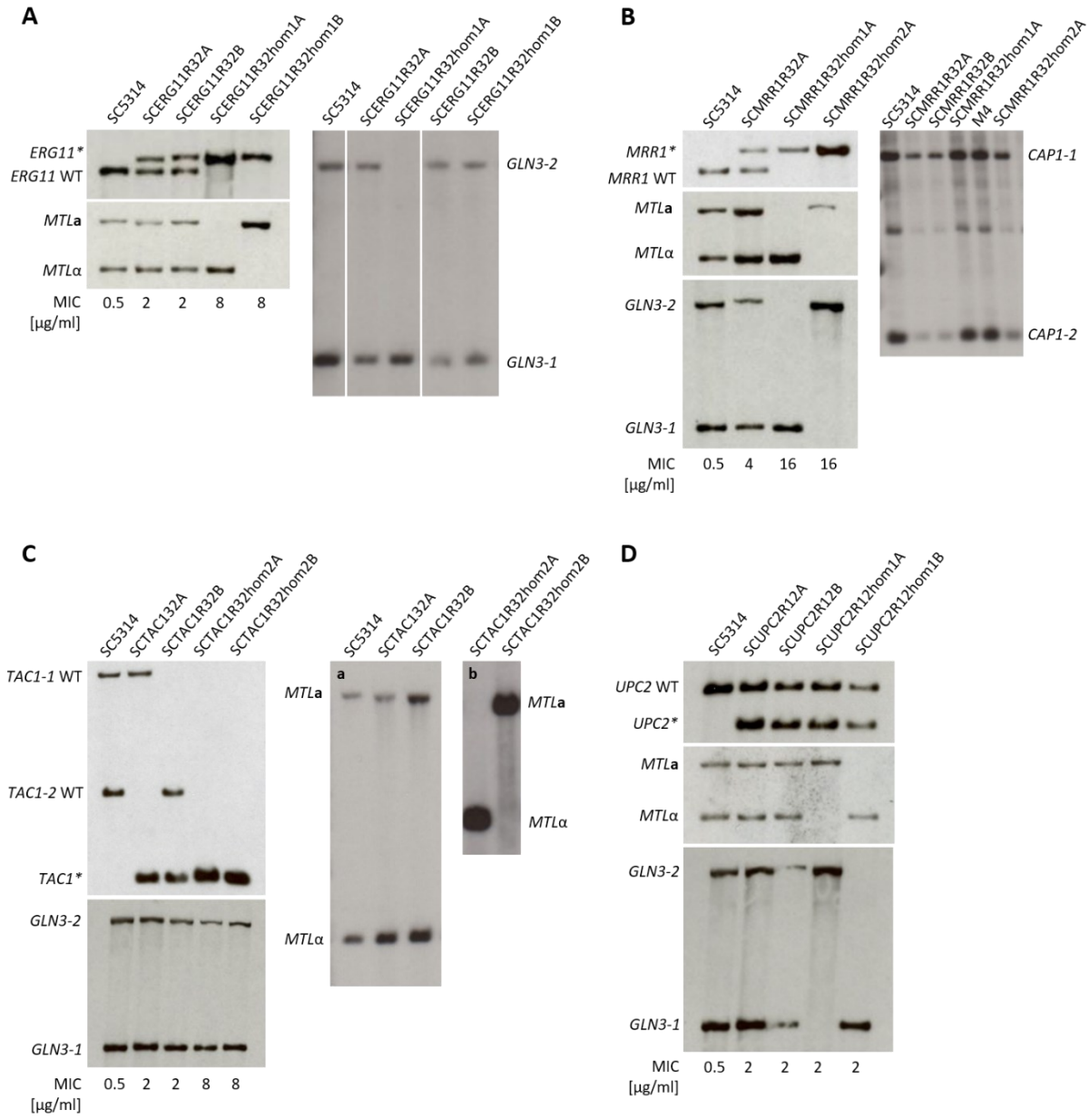

Figure 12: Genetic analysis of resistance-associated genes, the *MTL* locus and restriction site polymorphism markers of selected strains passaged in the presence of fluconazole. Selected strains with a fluconazole-induced LOH for a resistance mutation in (A) *ERG11* (SCERG11R32hom1A and SCERG11R32hom1B), (B) *MRR1* (SCMRR1R32hom1A and SCERG11R32hom2A), (C) *TAC1* (SCTAC1R32hom2A and SCTAC1R32hom2B), or (D) *UPC2* (SCUPC2R12hom1A and SCUPC2R12hom1B). Their respective parental strains and the wild-type strain SC5314 were analyzed by Southern hybridization. Restriction enzymes and probes used and a schematic showing the expected fragment sizes after hybridization are given in chapter 4.2.5.2 (Table 22, Figure 30, Figure 31). (a) Note that during the beginning of this study the restriction enzyme XhoI was used to analyze the *MTL* locus, (b) but was later replaced by EcoRI. The *MRR1* locus was analyzed with NsiI. (A, B, D) Southern blots of the *MTL* locus shown here were conducted with EcoRI-digested chromosomal DNA and the 5'MTL probe. (C, a) Southern blots of the *MTL* locus of the wild-type reference strain SC5314 and the parental strains SCTAC1R32A and -B were done with XhoI-digested DNA and the 5'MTL probe. (C, b) SCTAC1R32hom2A and SCTAC1R32hom2B were analyzed with EcoRI-digested DNA and the 3'MTL probe. In some cases, different genomic DNA preparations were used for the blots. Signal intensities are caused by uneven DNA concentrations. MICs of the strains are indicated for comparison. Experiments were conducted with the help of Ines Krüger and Sonja Schwanfelder. Parts published by Popp *et al.* [274].

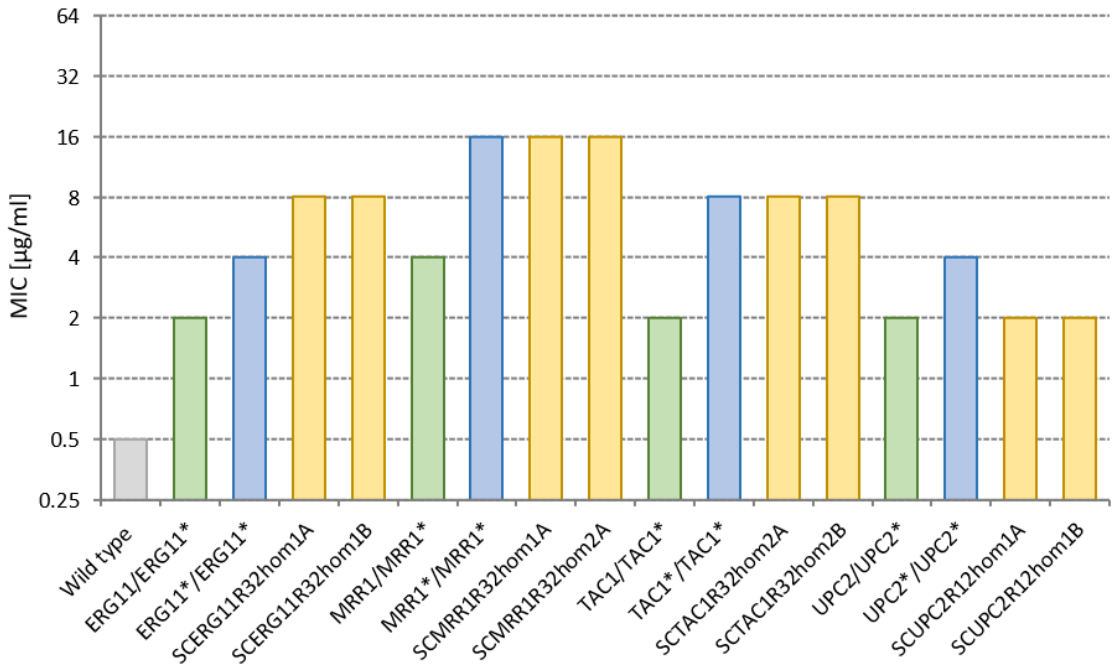

Figure 13: Overview of the fluconazole resistance level of selected fluconazole-induced *MTL* homozygous strains in comparison to the respective parental strains and controls. Hyperactive alleles of resistance-associated genes are indicated by an asterisk. MICs of the wild-type strain SC5314 (gray bar) and of the isolated fluconazole-induced *MTL* homozygous strains (yellow bars) SCERG11R32hom1A (*ERG11*^{G464S}/*ERG11*^{G464S}), SCERG11R32hom1B (*ERG11*^{G464S}/*ERG11*^{G464S}), SCMRR1R32hom1A (*MRR1*^{P683S}/*MRR1*^{P683S}), SCMRR1R32hom2A (*MRR1*^{P683S}/*MRR1*^{P683S}), SCTAC1R32hom2A (*TAC1*^{G980E}/*TAC1*^{G980E}), SCTAC1R32hom2B (*TAC1*^{G980E}/*TAC1*^{G980E}), SCUPC2R12hom1B (*UPC2*/*UPC2*^{G648D}) and SCUPC2R12hom1A (*UPC2*/*UPC2*^{G648D}) are shown. Furthermore, data for the genetically engineered resistance mutation heterozygous parental strains (green bars) and genetically engineered resistance mutation homozygous strains (blue bars) are given. The following strains were examined: SCERG11R32A and B (*ERG11*/*ERG11*^{G464S}), SCERG11R34A and B (*ERG11*^{G464S}/*ERG11*^{G464S}), SCMRR1R32A and B (*MRR1*/*MRR1*^{P683S}), SCMRR1R34A and B (*MRR1*^{P683S}/*MRR1*^{P683S}), SCTAC1R32A and B (*TAC1*/*TAC1*^{G980E}), SCTAC1R34A and B (*TAC1*^{G980E}/*TAC1*^{G980E}), SCUPC2R12A and B (*UPC2*/*UPC2*^{G648D}) and SCUPC2R14A and B (*UPC2* ^{G648D} /*UPC2*^{G648D}). Please note that the MICs of the two independently constructed resistance mutation heterozygous and homozygous strains are indicated by one single green or blue bar, respectively.

In addition, all seven *TAC1*^{G980E} homozygous isolates were homozygous for the *MTL* locus as well (Figure 12). The three derivatives of SCTAC1R32A were homozygous for *MTL*α and the 4 derivatives of SCTAC1R32B were homozygous for *MTL***a**. This is not surprising, since the mutated *TAC1* allele of the parental strain SCTAC1R32A lies on chromosome 5B in close linkage to the *MTL*α allele, and the mutated *TAC1* of SCTAC1R32B is located on chromosome 5A along with the *MTL***a** (Figure 10). Therefore, during the LOH event for the *TAC1* resistance mutation, the linked *MTL* locus was also affected. Furthermore, by analyzing the restriction site polymorphism marker *GLN3*, possible LOH events on the right arm of chromosome 5 were examined. All three derivatives of SCTAC1R32A and one derivative of SCTAC1R32B were still heterozygous for the *GLN3* locus, indicating a local genomic rearrangement. Three derivatives of SCTAC1R32B were homozygous for *GLN3-2*, suggesting the loss of a whole chromosome, since *GLN3-2* and *TAC1*^{G980E} are both located on Chr5A in the parental strain SCTAC1R32B. However, it cannot be excluded that a combination of several events lead to the LOH of the three loci.

Table 4: *TAC1*^{G980E} and *MTL* homozygous derivatives isolated after passaging in the presence of fluconazole and their parental strains. Strains selected for mating experiments are highlighted in bold font.

Strain name[(a)]	Parent	MIC [µg/ml]	*TAC1* resistance mutation	*MTL* configuration	*GLN3*	Fluconazole passages
SC5314	-	0.5	-/-	*MTL***a** /*MTL*α	*GLN3-1*/ *GLN3-2*	-
SCTAC1R32A and -B	SC5314	2	-/*TAC1*^{G980E}	*MTL***a** /*MTL*α	*GLN3-1*/ *GLN3-2*	-
SCTAC1R32hom1A (A1)	SCTAC1R32A	8	*TAC1*^{G980E}/*TAC1*^{G980E}	*MTL*α/*MTL*α	*GLN3-1*/ *GLN3-2*	2x5µg/ml
SCTAC1R32hom2A (A2)	SCTAC1R32A	8	*TAC1*^{G980E}/*TAC1*^{G980E}	*MTL*α/*MTL*α	*GLN3-1*/ *GLN3-2*	2x5µg/ml
SCTAC1R32hom3A (A5)	SCTAC1R32A	8	*TAC1*^{G980E}/*TAC1*^{G980E}	*MTL*α/*MTL*α	*GLN3-1*/ *GLN3-2*	2x5µg/ml
SCTAC1R32hom1B (B2)	SCTAC1R32B	8	*TAC1*^{G980E}/*TAC1*^{G980E}	*MTL***a**/*MTL***a**	*GLN3-2*/ *GLN3-2*	2x5µg/ml
SCTAC1R32hom2B (B3)	SCTAC1R32B	8	*TAC1*^{G980E}/*TAC1*^{G980E}	*MTL***a**/*MTL***a**	*GLN3-1*/ *GLN3-2*	2x5µg/ml
SCTAC1R32hom3B (B4)	SCTAC1R32B	8	*TAC1*^{G980E}/*TAC1*^{G980E}	*MTL***a**/*MTL***a**	*GLN3-2*/ *GLN3-2*	2x5µg/ml
SCTAC1R32hom4B (B6)	SCTAC1R32B	8	*TAC1*^{G980E}/*TAC1*^{G980E}	*MTL***a**/*MTL***a**	*GLN3-2*/ *GLN3-2*	2x5µg/ml

[(a)] Originally used strain names are indicated in parentheses. Please note that initially randomly picked strains of all experiments were consecutively numbered. Subsequently, selected *MTL* homozygous strains were systematically renamed.

Next, white-to-opaque switching competence was examined, since cells in the mating-competent opaque phase were needed for mating experiments (mating experiments described in chapter 2.2.2.1). White phase cells of each of the seven fluconazole-induced *MTL* homozygous strains were spread for single colonies on two Lee's agar plates with phloxine B, which selectively stains opaque colonies pink [218]. One plate was incubated under room conditions for several days to determine spontaneous switching rates. The other plate was incubated for two days at a high CO_2 concentration (18% CO_2) to induce white-to-opaque switching, as described by Huang *et al.* [211], followed by an incubation for several days under room conditions. The experiment was conducted at least three times independently for each strain. As controls, *MTL* hemizygous derivatives of the wild-type SC5314 (SCMTLaM2A with deleted *MTL***a** and SCMTLαM2A with deleted *MTL*α) and WO-1 (*MTL*α homozygous) were examined. WO-1 was selected, because it is a model strain to analyze white-to-opaque switching and the strain itself was named after this morphological transition [26].

All seven fluconazole-induced *MTL* homozygous strains were switching-competent, since after the switching induction with high CO_2 concentrations, at least 89.9% of the colonies on the Lee's agar plates with phloxine B grew in the opaque or white-opaque mixed phenotype. In addition, mean spontaneous switching rates under room conditions did not exceed 1.2% of the colonies (Appendix A1). Data on the strains SCTAC1R32hom2A and SCTAC1R32hom2B are shown in Figure 14.

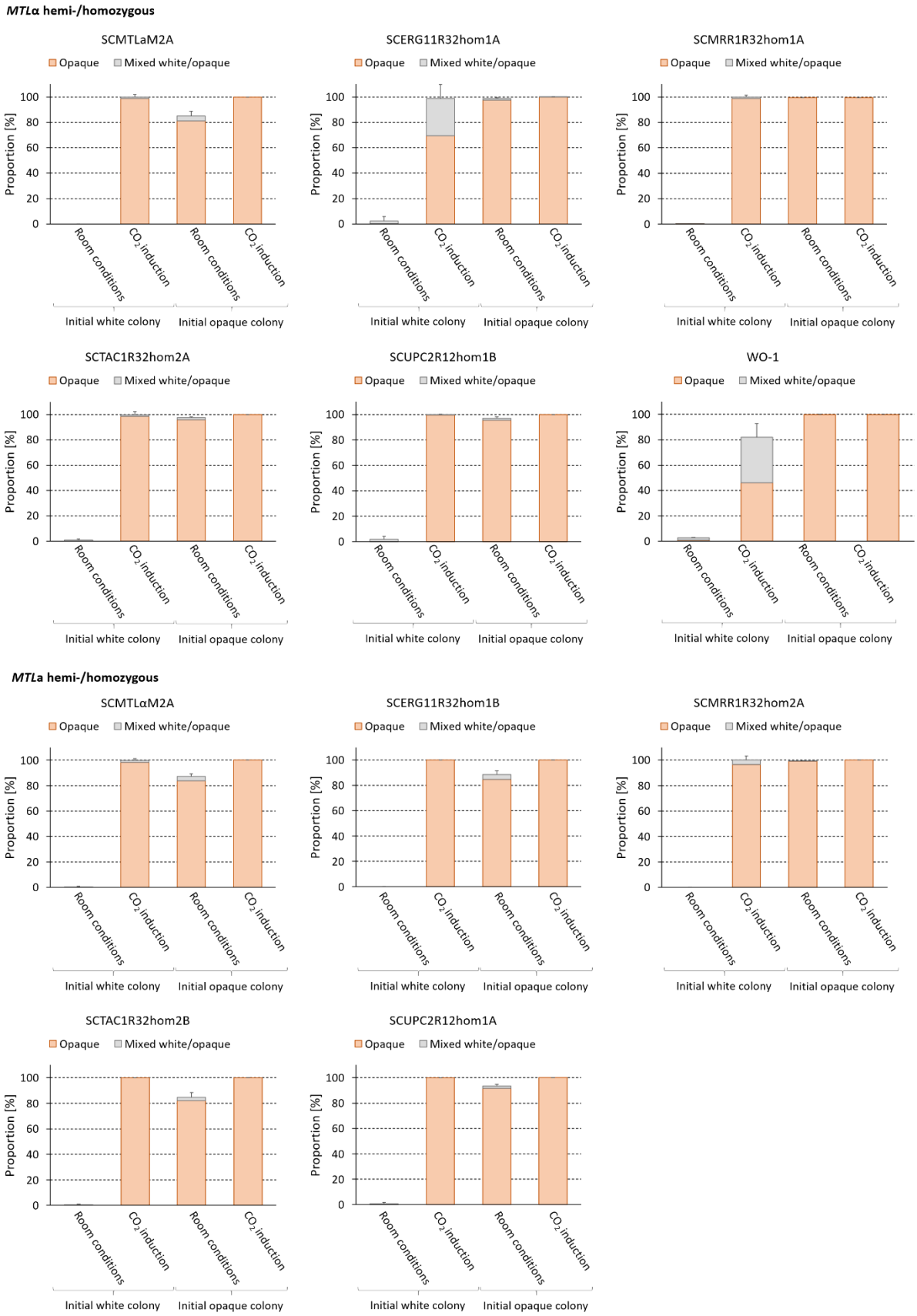

Figure 14: White-to-opaque switching competence and stability of the opaque phenotype of selected *MTL* homozygous isolates derived after incubation in the presence of fluconazole. White and opaque cells were spread on Lee's agar plates with phloxine B and incubated for several days under room conditions, or at high CO_2 concentrations, followed by an incubation under room conditions. Afterwards, opaque, white-opaque mixed and white colonies on the plates were counted. Mean proportions of opaque and mixed colonies of at least three independent experiments and standard deviations are

shown. Data on the selected *MTL*α homo-/hemizygous strains SCERG11R32hom1A (*ERG11*^{G464S}/*ERG11*^{G464S}), SCMRR1R32hom1A (*MRR1*^{P683S}/*MRR1*^{P683S}), SCTAC1R32hom2A (*TAC1*^{G980E}/*TAC1*^{G980E}), SCUPC2R12hom1B (*UPC2*/*UPC2*^{G648D}) and the controls WO-1 and SCMTLaM2A are given. Furthermore, data on the selected *MTL***a** homo-/hemizygous strains SCERG11R32hom1B (*ERG11*^{G464S}/*ERG11*^{G464S}), SCMRR1R32hom2A (*MRR1*^{P683S}/*MRR1*^{P683S}), SCTAC1R32hom2B (*TAC1*^{G980E}/*TAC1*^{G980E}), SCUPC2R12hom1A (*UPC2*/*UPC2*^{G648D}) and the control SCMTLαM2A are shown. Exact numbers of all analyzed controls and fluconazole-induced *MTL* homozygous strains are listed in Appendix A1 and Appendix A2.

In addition, the stability of the cells in the opaque phenotype was tested. For this, opaque phase cells of each of the fluconazole-induced *MTL* homozygous strains and the controls SCMTLaM2A, SCMTLαM2A and WO-1 were spread for single colonies on two Lee's agar plates with phloxine B. One plate was incubated under room conditions for several days to examine spontaneous switching rates to the white phenotype. The other plate was incubated for two days at a high CO_2 concentration (18% CO_2) and at 25°C, followed by an incubation for several days under room conditions. At least three independent experiments per strain were conducted. All strains grew stably in the opaque phenotype (Appendix A2). A minimum of 84.7% (SCTAC1R32hom2B) of the colonies of the fluconazole-induced *MTL* homozygous strains remained in the opaque and mixed phenotype even without applying a high CO_2 concertation. Data on the strains SCTAC1R32hom2A and SCTAC1R32hom2B are shown in Figure 14.

Furthermore, pictures of white and opaque colonies and cells were taken (of at least 3 experiments), which were grown on Lee's agar plates with phloxine B in two different conditions (18% CO_2 and 25°C, or room conditions). In general, white and opaque colonies appear smooth, white cells are small and round and opaque cells are larger and elongated. This can be observed in Figure 15 for the control strain WO-1. Filamentation was observed in opaque colonies of all seven fluconazole-induced *MTL* homozygous isolates with homozygous *TAC1** alleles. Pictures of SCTAC1R32hom2A and SCTAC1R32hom2B colonies and cells are shown in Figure 15. This suggests that genomic rearrangements causing the LOH for the *TAC1* and *MTL* locus affected loci relevant for filamentation of white and/or opaque cells. However, the *MTL* hemizygous control strains SCMTLaM2A and SCMTLαM2A also showed a slight filamentation under the tested conditions (Figure 15). Therefore, another reason for the observed filamentation could be the chosen agar composition. Lee's agar contains amino acids such as proline, which have been described to induce hyphal morphogenesis in *C. albicans* [275].

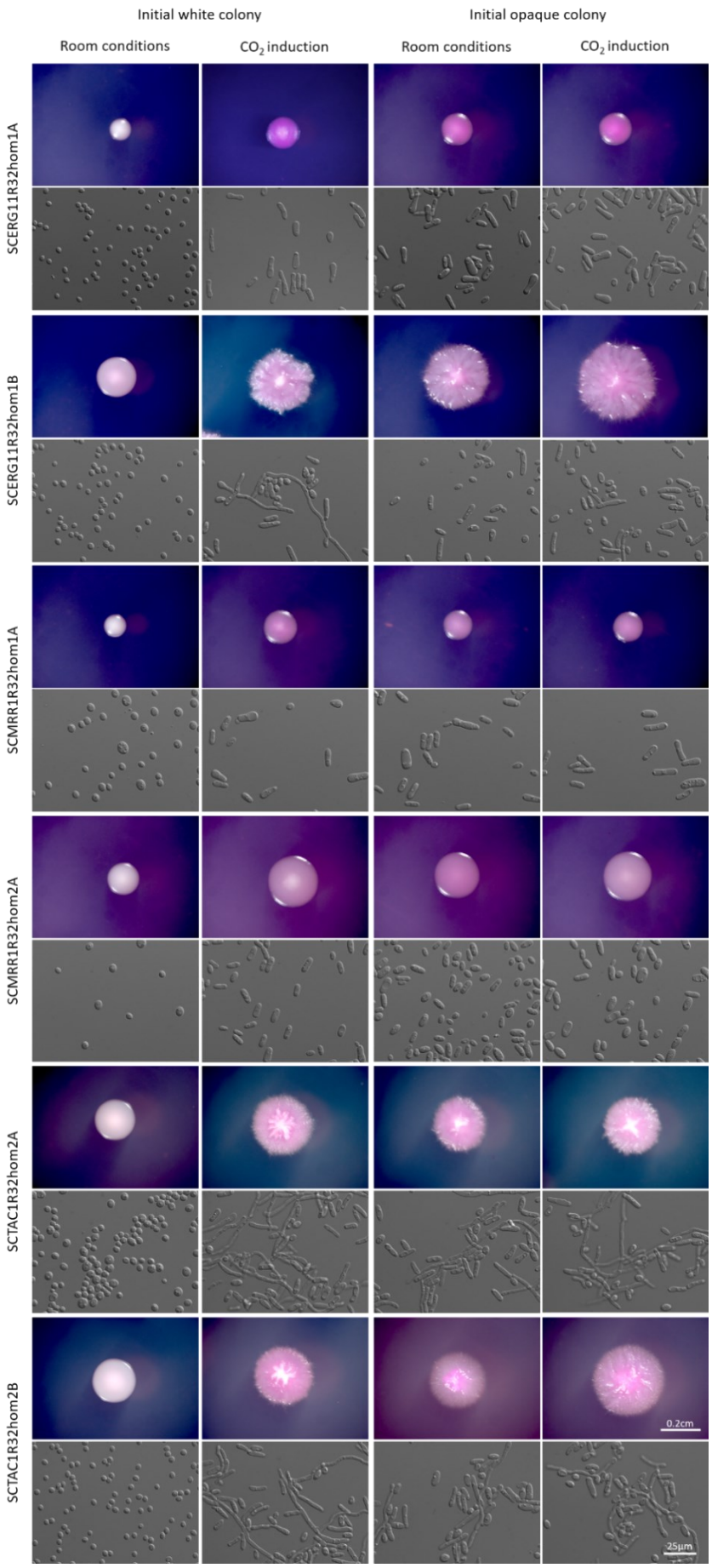

Figure 15 (continued on the next page)

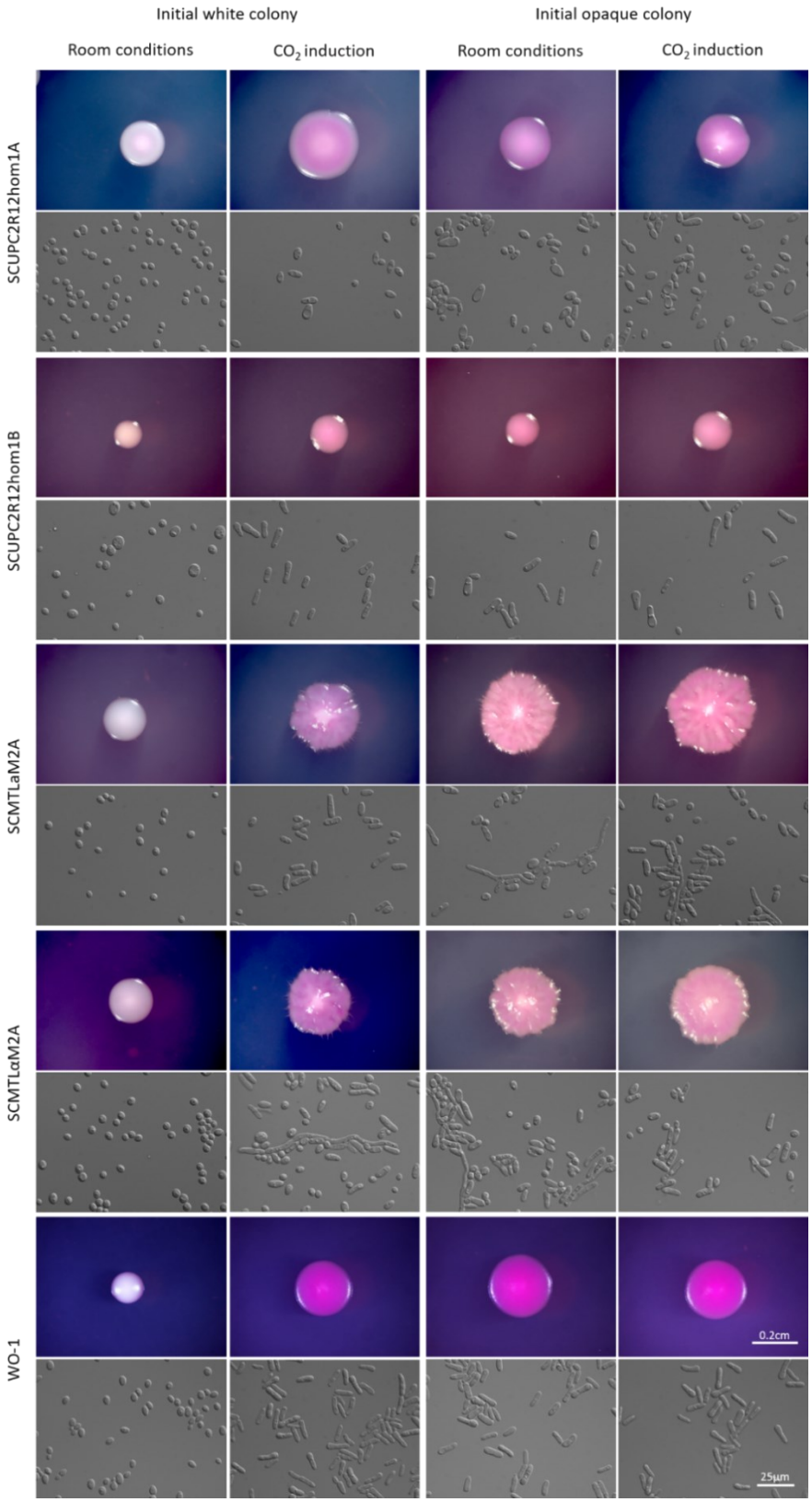

Figure 15: Colony and cell morphology of white and opaque phase cells of selected fluconazole-induced *MTL* homozygous strains. White and opaque cells were spread on Lee's agar plates with phloxine B (stains opaque colonies pink) and incubated for several days under room conditions, or at high CO_2 concentrations, followed by an incubation under room conditions. Afterwards, pictures of white and opaque colonies, as well as white and opaque cells were taken. Pictures of the selected *ERG11*^{G464S} homozygous strains SCERG11R32hom1A and SCERG11R32hom1B, *MRR1*^{P683S} homozygous strains SCMRR1R32hom1A and SCMRR1R32hom2A, *TAC1*^{G980E} homozygous strains SCTAC1R32hom2A and SCTAC1R32hom2B and *UPC2*^{G648D} heterozygous strains SCUPC2R12hom1A and SCUPC2R12hom1B are shown.

Based on the collected data, the two switching-competent *TAC1*^{G980E} homozygous isolates SCTAC1R32hom2A (*MTL*α homozygous) and SCTAC1R32hom2B (*MTL***a** homozygous) with a stable and reproducible white and opaque phenotype were chosen for mating experiments. These strains are derivatives of one of the independently constructed parental strains SCTAC1R32A and -B, respectively. Furthermore, strains with genomic recombination affecting as few loci as possible, besides the *MTL* and the *TAC1* locus, were selected. SCTAC1R32hom2A and SCTAC1R32hom2B are heterozygous for *GLN3*. This indicates that the genomic recombination event(s) during which the strains became homozygous for the *TAC1* and *MTL* locus did affect fewer loci than in strains that became homozygous for *GLN3-2*.

2.2.1.2. Isolation and characterization of *MRR1** and *MTL* homozygous strains

Strains which are homozygous for the *MRR1*^{P683S} allele grow faster on fluconazole-containing agar plates than strains which are heterozygous for the *MRR1*^{P683S} allele and were therefore distinguishable by colony size [271]. Hence, during the Master thesis by Popp [271] the two independently constructed *MRR1*^{P683S} heterozygous strains (SCMRR1R32A and -B) were passaged in the presence of fluconazole and plated on agar plates containing fluconazole, as described for *TAC1* GOF heterozygous strains in chapter 2.2.1.1. Using this strategy, strains that became homozygous for *MRR1*^{P683S} but retained both *MTL* loci were isolated [271]. In these strains, genomic rearrangements affecting at least two chromosomes (3 and 5) would have been necessary in order for them to become homozygous for both loci (the *MRR1*^{P683S} and the *MTL* locus, Figure 10).

Therefore, a different screening method was applied instead. Rather than screening for colony size, screening was done for *MTL* homozygous cells. In contrast to *MTL* heterozygous cells, *MTL* homozygous cells are white-to-opaque switching-competent when incubated in an 18% CO_2 atmosphere on solid agar [211]. As previously described, opaque colonies can be stained with phloxine B. Hence, the *MRR1*^{P683S} and *MTL* locus heterozygous strains SCMRR1R32A and -B were passaged in rich medium (YPD) in the presence of 1.75µg/ml and 2.5µg/ml fluconazole. Since GOF homozygous strains have a higher fluconazole resistance level than GOF heterozygous strains [121], resistance mutation homozygous strains have a selective advantage in the presence of fluconazole and were therefore enriched in the population over time. Each day, appropriate dilutions of the passages were plated on Lee's agar plates with phloxine B. The plates were incubated in an 18% CO_2 atmosphere for two days to induce white-to-opaque switching, followed by an incubation at a normal atmosphere and room temperature (room conditions) for several days. Under these conditions, *MTL* heterozygous strains

were expected to remain in the white phenotype and *MTL* homozygous strains were expected to switch to the opaque phenotype. Therefore, the opaque colonies were chosen for further analysis.

Three *MRR1*^{P683S} and *MTL* homozygous derivatives of the parental strain SCMRR1R32A (two *MTL*α homozygous, one *MTL***a** homozygous) and three *MRR1*^{P683S} and *MTL* homozygous derivatives of the parental strain SCMRR1R32B (one *MTL*α homozygous, two *MTL***a** homozygous) were isolated using this method (Table 5, Figure 12). This suggests that the LOH for the hyperactive *MRR1* allele, accompanied by increased fluconazole resistance, caused an enrichment of *MTL* homozygous strains in the population.

To examine whether genomic rearrangements also affected the right arm of chromosome 5, the restriction site polymorphism marker *GLN*3 was analyzed as described in chapter 2.2.1.1 (Table 5, Figure 12). All strains had lost one *GLN3* allele, indicating a loss of a chromosome 5 homolog. Strains which had become homozygous for the *MTL*α, had also become homozygous for the linked *GLN3-1*. According to this, strains which had become homozygous for the *MTL***a** locus had also become homozygous for the linked *GLN3-2* allele. In addition, the *CAP1* locus was analyzed, which lies on the left arm of chromosome 3 (Figure 10). Four of the *MRR1*^{P683S} and *MTL* homozygous mutants remained heterozygous for *CAP1*, indicating that LOH took place during mitotic recombination (Table 5, Figure 12). Two of the three derivatives of SCMRR1R32B lost the *CAP1-1* allele, implying a loss of the whole chromosome 3B and a linkage of the *CAP1-2* allele to the mutated *MRR1* allele in the parental strain SCMRR1R32B (Table 5, Figure 12). Note that Popp *et al.* [274] analyzed the *CAP1* locus with an additional probe due to unspecific bands in the Southern blots shown in Figure 12.

Table 5: *MRR1*^{P683S} and *MTL* homozygous strains isolated after passaging in the presence of fluconazole and their parental strains. Strains selected for mating experiments are highlighted in bold font.

Strain name[(a)]	**Parent**	**MIC [µg/ml]**	***MRR1* resistance mutation**	***MTL***	***GLN3***	***CAP-1***	**Fluconazole passages**
SC5314	-	0.5	-/-	*MTL***a**/ *MTL*α	*GLN3-1*/ *GLN3-2*	*CAP1-1*/ *CAP1-2*	-
SCMRR1R32A and -B	SC5314	4	-/ *MRR1*^{P683S}	*MTL***a**/ *MTL*α	*GLN3-1*/ *GLN3-2*	*CAP1-1*/ *CAP1-2*	-
SCMRR1R32hom1A (M2)	SCMRR1R32A	16	*MRR1*^{P683S}/ *MRR1*^{P683S}	*MTL*α/ *MTL*α	*GLN3-1*/ *GLN3-1*	*CAP1-1*/ *CAP1-2*	4x2.5µg/ml
M4	SCMRR1R32A	16	*MRR1*^{P683S}/ *MRR1*^{P683S}	*MTL*α/ *MTL*α	*GLN3-1*/ *GLN3-1*	*CAP1-1*/ *CAP1-2*	5x2.5µg/ml
SCMRR1R32hom2A (M8)	SCMRR1R32A	16	*MRR1*^{P683S}/ *MRR1*^{P683S}	*MTL***a**/ *MTL***a**	*GLN3-2*/ *GLN3-2*	*CAP1-1*/ *CAP1-2*	6x2.5µg/ml
SCMRR1R32hom1B (M2.1)	SCMRR1R32B	16	*MRR1*^{P683S}/ *MRR1*^{P683S}	*MTL***a**/ *MTL***a**	*GLN3-2*/ *GLN3-2*	*CAP1-2*/ *CAP1-2*	4x1.75µg/ml
SCMRR1R32hom2B (M2.2)	SCMRR1R32B	16	*MRR1*^{P683S}/ *MRR1*^{P683S}	*MTL*α/ *MTL*α	*GLN3-1*/ *GLN3-1*	*CAP1-1*/ *CAP1-2*	4x2.5µg/ml
M2.3	SCMRR1R32B	16	*MRR1*^{P683S}/ *MRR1*^{P683S}	*MTL***a**/ *MTL***a**	*GLN3-2*/ *GLN3-2*	*CAP1-2*/ *CAP1-2*	5x1.75µg/ml

[(a)] Originally used strain names are indicated in parentheses. Please note that initially randomly picked strains of all experiments were consecutively numbered. Subsequently, selected *MTL* homozygous strains were systematically renamed.

All *MRR1*^{P683S} and *MTL* homozygous strains had a $MIC_{fluconazole}$ of 16µg/ml, equivalent to the MIC of the genetically engineered strains SCMRR1R34A and -B with a homozygous P683S substitution in *MRR1*. This resistance level is two MIC values higher than the resistance level of the parental strains SCMRR1R32A and -B (Table 5, Figure 13).

As described in chapter 2.2.1.1, white-to-opaque switching competence, stability of the strains in the opaque phenotype and the phenotype of white and opaque colonies and cells were examined. After streaking of strain M4 from the glycerol stocks, white and opaque colonies of different sizes grew on the agar plates. Since strains with reproducible and preferably unobtrusive phenotypes should be selected for mating experiments, this strain was excluded from further characterization experiments. During experiments determining the stability of the strains in the opaque phenotype, strain SCMRR1R32hom2B was found to grow colonies of different sizes (Figure 16). This was observed when an opaque colony was spread on Lee's agar plates with phloxine B and incubated for two days with high CO_2 concentrations, followed by an incubation under room conditions. Therefore, also SCMRR1R32hom2B was also excluded from further analysis.

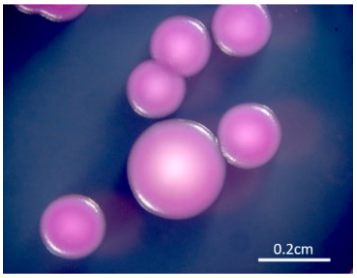

Figure 16: Opaque colonies of different sizes of the strain SCMRR1R32hom2B. An opaque colony of SCMRR1R32hom2B was plated for single colonies on Lee's agar plates with phloxine B. The plates were incubated for two days at 25°C and 18% CO_2, followed by an incubation for several days at room temperature and room atmosphere. In some cases, opaque colonies of different sizes grew on the plates.

Out of the two strains which had become homozygous for the *CAP1-2* allele, the strain SCMRR1R32hom1B was further analyzed. In addition, the strains SCMRR1R32hom1A and SCMRR1R32hom2A were characterized. These three strains were switching-competent, since after CO_2 induction, at least a mean of 99.9% of the colonies on the plates grew in the opaque and white-opaque mixed phenotype. Furthermore, mean spontaneous switching rates under room conditions did not exceed 0.6% of the colonies for each strain (Appendix A1). At least 99.4% of the colonies were in the opaque and white-opaque mixed phenotype after plating of opaque cells and incubation of the plates under room conditions (Appendix A2), suggesting that all strains are stable in the opaque phenotype. Switching rates of the strains SCMRR1R32hom1A and SCMRR1R32hom2A and pictures of white and opaque colonies of SCMRR1R32hom1A and SCMRR1R32hom2A are shown in Figure 14 and Figure 15, respectively. The colony size of SCMRR1R32hom1A is smaller than that of SCMRR1R32hom2A and the controls SCMTLaM2A, SCMTLαM2A and WO-1, under the tested conditions. Based on these findings, the *MTL*α homozygous strain SCMRR1R32hom1A and the *MTL***a** homozygous strain SCMRR1R32hom2A were selected for mating experiments. Both derivatives of the strain SCMRR1R32A

are heterozygous for the *CAP1* and *GLN3* locus, assuming that the genomic rearrangements causing the LOH for the hyperactive *MRR1* allele and the *MTL* locus affected smaller parts of the genome.

2.2.1.3. Isolation and characterization of *ERG11** and *MTL* homozygous strains

ERG11^{G464S} homozygous strains were not distinguishable from *ERG11*^{G464S} heterozygous strains by colony size on agar plates containing fluconazole [271], although the resistance level of these strains differed by one MIC value (SCERG11R32A and -B MIC 2µg/ml, SCERG11R34A and -B MIC 4µg/ml). Therefore, to isolate *ERG11*^{G464S} and *MTL* homozygous isolates, a screening for switching-competent cells was conducted, as described in 2.2.1.2. The *ERG11*^{G464S} and *MTL* locus heterozygous strains SCERG11R32A and -B were passaged in rich medium (YPD) with 2.5µg/ml fluconazole. Since *ERG11* and the *MTL* locus are both located on the left arm of chromosome 5 (Figure 10), it was not surprising that many mutants that became homozygous for both loci could be isolated.

Fourteen derivatives of the parental strain SCERG11R32A from different passages were analyzed by Southern hybridization (Table 6, Figure 12). All strains were homozygous for the *MTL*α, *ERG11*^{G464S} and *GLN3-1*. Probably, the LOH for these loci took place during a loss of the chromosome 5A, although several events cannot be excluded. It should be noted that all fourteen strains could be descendants of the same mutant, since they were isolated in the same experiment.

In addition, twenty derivatives of the parental strain SCERG11R32B of different passages were examined. All twenty mutants were homozygous for the *MTL* locus (9 *MTL*α, 11 *MTL***a**) and fifteen of these strains were homozygous for *ERG11*^{G464S} (4 *MTL*α, 11 *MTL***a**). It can be assumed that the LOH at the *MTL* locus in the five mutants which were still heterozygous for the *ERG11* locus was induced by fluconazole stress. All fifteen *ERG11*^{G464S} homozygous strains were still heterozygous for the *GLN3* locus, and hence, chromosome loss can be excluded. Four of these strains were *MTL*α homozygous, although the hyperactive *ERG11* allele is linked to the *MTL***a** locus in the parental strain SCERG11R32B (Figure 10). This suggests several recombination events leading to the LOH at the *ERG11* and the *MTL* locus.

Furthermore, the fluconazole resistance level of all twenty-nine *ERG11*^{G464S} and *MTL* homozygous strains was examined. The resistance level (8µg/ml) was two MIC values higher than the resistance level of the *ERG11*^{G464S} heterozygous parental strains SCERG11R32A and -B (Table 6) and one MIC value higher than the resistance level of the genetically engineered *ERG11*^{G464S} homozygous strains SCERG11R34A and -B (Figure 13). It is likely that in addition to the LOH for the *ERG11* resistance mutation, further mechanisms add to the fluconazole resistance level of the twenty-nine mutants.

Table 6: *ERG11*^{G464S} and *MTL* homozygous strains isolated after passaging in the presence of fluconazole and their parental strains. Strains selected for mating experiments are highlighted in bold font.

Strain name[a]	Parent	MIC [µg/ml][b]	*ERG11* resistance mutation	Mating type locus	*GLN3*[b]	Fluconazole passages
SC5314	-	0.5	-/-	*MTL***a**/ *MTL*α	*GLN3-1*/ *GLN3-2*	-
SCERG11R32A and -B	SC5314	2	-/*ERG11*^{G464S}	*MTL***a**/ *MTL*α	*GLN3-1*/ *GLN3-1*	-
SCERG11R32hom1A (E3A)	SCERG11R32A	8	*ERG11*^{G464S}/*ERG11*^{G464S}	*MTL*α/ *MTL*α	*GLN3-1*/ *GLN3-1*	2x2.5µg/ml
E4	SCERG11R32A	8	*ERG11*^{G464S}/*ERG11*^{G464S}	*MTL*α/ *MTL*α	*GLN3-1*/ *GLN3-1*	3x2.5µg/ml
E5	SCERG11R32A	8	*ERG11*^{G464S}/*ERG11*^{G464S}	*MTL*α/ *MTL*α	*GLN3-1*/ *GLN3-1*	3x2.5µg/ml
E6	SCERG11R32A	8	*ERG11*^{G464S}/*ERG11*^{G464S}	*MTL*α/ *MTL*α	*GLN3-1*/ *GLN3-1*	3x2.5µg/ml
E8	SCERG11R32A	8	*ERG11*^{G464S}/*ERG11*^{G464S}	*MTL*α/ *MTL*α	*GLN3-1*/ *GLN3-1*	3x2.5µg/ml
E10	SCERG11R32A	8	*ERG11*^{G464S}/*ERG11*^{G464S}	*MTL*α/ *MTL*α	*GLN3-1*/ *GLN3-1*	4x2.5µg/ml
E20	SCERG11R32A	8	*ERG11*^{G464S}/*ERG11*^{G464S}	*MTL*α/ *MTL*α	*GLN3-1*/ *GLN3-1*	5x2.5µg/ml
E25	SCERG11R32A	8	*ERG11*^{G464S}/*ERG11*^{G464S}	*MTL*α/ *MTL*α	*GLN3-1*/ *GLN3-1*	5x2.5µg/ml
E31	SCERG11R32A	8	*ERG11*^{G464S}/*ERG11*^{G464S}	*MTL*α/ *MTL*α	*GLN3-1*/ *GLN3-1*	6x2.5µg/ml
E36	SCERG11R32A	8	*ERG11*^{G464S}/*ERG11*^{G464S}	*MTL*α/ *MTL*α	*GLN3-1*/ *GLN3-1*	6x2.5µg/ml
E47	SCERG11R32A	8	*ERG11*^{G464S}/*ERG11*^{G464S}	*MTL*α/ *MTL*α	*GLN3-1*/ *GLN3-1*	7x2.5µg/ml
E51	SCERG11R32A	8	*ERG11*^{G464S}/*ERG11*^{G464S}	*MTL*α/ *MTL*α	*GLN3-1*/ *GLN3-1*	7x2.5µg/ml
E56	SCERG11R32A	8	*ERG11*^{G464S}/*ERG11*^{G464S}	*MTL*α/ *MTL*α	*GLN3-1*/ *GLN3-1*	8x2.5µg/ml
E61	SCERG11R32A	8	*ERG11*^{G464S}/*ERG11*^{G464S}	*MTL*α/ *MTL*α	*GLN3-1*/ *GLN3-1*	8x2.5µg/ml
SCERG11R32hom1B (E2.1)	SCERG11R32B	8	*ERG11*^{G464S}/*ERG11*^{G464S}	*MTL***a**/ *MTL***a**	*GLN3-1*/ *GLN3-2*	5x2.5µg/ml
E2.2	SCERG11R32B	n.t.	-/*ERG11*^{G464S}	*MTL*α/ *MTL*α	n.t.	6x2.5µg/ml
E2.3	SCERG11R32B	8	*ERG11*^{G464S}/*ERG11*^{G464S}	*MTL***a**/ *MTL***a**	*GLN3-1*/ *GLN3-2*	6x2.5µg/ml
E2.4	SCERG11R32B	8	*ERG11*^{G464S}/*ERG11*^{G464S}	*MTL***a**/ *MTL***a**	*GLN3-1*/ *GLN3-2*	6x2.5µg/ml
E2.5	SCERG11R32B	8	*ERG11*^{G464S}/*ERG11*^{G464S}	*MTL***a**/ *MTL***a**	*GLN3-1*/ *GLN3-2*	6x2.5µg/ml
E2.6	SCERG11R32B	8	*ERG11*^{G464S}/*ERG11*^{G464S}	*MTL***a**/ *MTL***a**	*GLN3-1*/ *GLN3-2*	6x2.5µg/ml
E2.7	SCERG11R32B	8	*ERG11*^{G464S}/*ERG11*^{G464S}	*MTL***a**/ *MTL***a**	*GLN3-1*/ *GLN3-2*	6x2.5µg/ml
E2.8	SCERG11R32B	n.t.	-/*ERG11*^{G464S}	*MTL*α/ *MTL*α	n.t.	6x2.5µg/ml
E2.19	SCERG11R32B	8	*ERG11*^{G464S}/*ERG11*^{G464S}	*MTL***a**/ *MTL***a**	*GLN3-1*/ *GLN3-2*	6x2.5µg/ml
E2.20	SCERG11R32B	n.t.	-/*ERG11*^{G464S}	*MTL*α/ *MTL*α	n.t.	7x2.5µg/ml
SCERG11R32hom2B (E2.21)	SCERG11R32B	8	*ERG11*^{G464S}/*ERG11*^{G464S}	*MTL*α/ *MTL*α	*GLN3-1*/ *GLN3-2*	7x2.5µg/ml
E2.22	SCERG11R32B	8	*ERG11*^{G464S}/*ERG11*^{G464S}	*MTL*α/ *MTL*α	*GLN3-1*/ *GLN3-2*	7x2.5µg/ml
E2.25	SCERG11R32B	8	*ERG11*^{G464S}/*ERG11*^{G464S}	*MTL***a**/ *MTL***a**	*GLN3-1*/ *GLN3-2*	7x2.5µg/ml

Strain name[a]	Parent	MIC [µg/ml][b]	*ERG11* resistance mutation	Mating type locus	*GLN3*[b]	Fluconazole passages
E2.26	SCERG11R32B	8	*ERG11*^{G464S}/*ERG11*^{G464S}	*MTL*α/ *MTL*α	*GLN3-1*/ *GLN3-2*	7x2.5µg/ml
E2.27	SCERG11R32B	8	*ERG11*^{G464S}/*ERG11*^{G464S}	*MTL*α/ *MTL*α	*GLN3-1*/ *GLN3-2*	7x2.5µg/ml
E2.35	SCERG11R32B	8	*ERG11*^{G464S}/*ERG11*^{G464S}	*MTL***a**/ *MTL***a**	*GLN3-1*/ *GLN3-2*	8x2.5µg/ml
E2.36	SCERG11R32B	n.t.	-/*ERG11*^{G464S}	*MTL*α/ *MTL*α	n.t.	8x2.5µg/ml
E2.37	SCERG11R32B	8	*ERG11*^{G464S}/*ERG11*^{G464S}	*MTL***a**/ *MTL***a**	*GLN3-1*/ *GLN3-2*	8x2.5µg/ml
E2.42	SCERG11R32B	8	*ERG11*^{G464S}/*ERG11*^{G464S}	*MTL***a**/ *MTL***a**	*GLN3-1*/ *GLN3-2*	8x2.5µg/ml
E2.43	SCERG11R32B	n.t.	-/*ERG11*^{G464S}	*MTL*α/ *MTL*α	n.t.	8x2.5µg/ml

[a] Originally used strain names are indicated in parentheses. Please note that initially randomly picked strains of all experiments were consecutively numbered. Subsequently, selected *MTL* homozygous strains were systematically renamed.
[b] n.t.: not tested

Next, white-to-opaque switching competence, stability of the strains in the opaque phenotype and the phenotype of white and opaque colonies and cells were examined, as previously described (chapter 2.2.1.1). The *MTL*α homozygous strain SCERG11R32hom1A and the *MTL***a** homozygous strain SCERG11R32hom1B were selected for this purpose. These strains were isolated in an early fluconazole passage. Both strains were homozygous for the *MTL* locus which was linked to the hyperactive *ERG11* allele in the parental strains (Figure 10). Therefore, probably only minor genomic recombination led to the LOH for both loci. Spontaneous white-to-opaque switching rates under room conditions did not exceed 2.2% (mean) of the colonies (Appendix A1, Figure 14). After CO_2 induction, at least 98.6% (mean) of the colonies were in the opaque phenotype and white-opaque mixed phenotype. Furthermore, all strains grew stably in the opaque phenotype (Appendix A2, Figure 14). After plating of opaque cells on Lee's agar plates and incubation under room conditions, a mean of at least 88.4% of the colonies grew in the opaque and mixed phenotype. Pictures of white and opaque colonies of SCERG11R32hom1A and SCERG11R32hom1B grown in the two tested conditions are shown in Figure 15. Colony size of SCERG11R32hom1A is smaller than that of SCERG11R32hom1B and the controls SCMTLaM2A, SCMTLαM2A and WO-1. Based on these findings, both strains were selected for mating experiments.

2.2.1.4. Isolation and characterization of *UPC2** heterozygous and *MTL* homozygous strains

To isolate strains which had become homozygous for the *UPC2*^{G648D} allele and simultaneously for the *MTL* locus, the independently constructed parental strains SCUPC2R12A and -B were passaged in the presence of fluconazole. Genomic recombination events affecting at least two chromosomes are necessary for an LOH at both loci, since *UPC2* is located on chromosome 1 and the *MTL* locus on

chromosome 5 (Figure 10). For this reason, after passaging of the parental strains in rich medium (YPD) in the presence of fluconazole, Lee's agar plates with phloxine B were screened for white-to-opaque switching-competent cells, as described in 2.2.1.2. Fluconazole concentrations of 2.5µg/ml and 5µg/ml in the shaking culture were chosen.

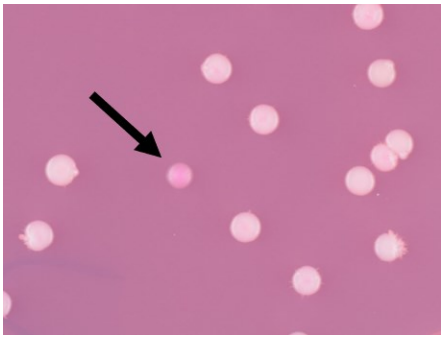

Figure 17: Picture of part of a Lee's plate with phloxine B of a screening experiment for fluconazole-induced *MTL* and *UPC2*^{G648D} homozygous strains. The pink color of the agar plate is caused by phloxine B, which selectively stains opaque colonies pink. The arrow highlights the opaque colony, which was later characterized as *UPC2*^{G648D} heterozygous and *MTL*α homozygous and termed SCUPC2R12hom1B.

Eight *MTL* homozygous derivatives were recovered from the parental strain SCUPC2R12A (Table 7). Southern hybridization showed that six strains were *MTL***a** homozygous and two strains *MTL*α homozygous. One *MTL*α locus homozygous derivative of the parental strain SCUPC2R12B was isolated (Figure 17). All nine isolated strains were still heterozygous for the hyperactive *UPC2* allele. A homozygous resistance mutation in *UPC2* causes only a minor gain of resistance [121], which was probably not enough to select for the LOH at this locus. The isolated strains presumably became homozygous by fluconazole stress-induced genomic recombination events. Furthermore, the restriction site polymorphism marker *GLN3* was examined by Southern hybridization. Eight of the nine isolated *MTL* homozygous strains were also homozygous for either *GLN3-1* or *GLN3-2*, indicating a loss of a whole chromosome. Nevertheless, it cannot be excluded that several events lead to this genetic configuration. The relevant genotype of the strains is listed in Table 7 and Southern blots of selected strains are shown in Figure 12.

In addition, the fluconazole resistance level of the strains was examined. The fluconazole-induced *MTL* homozygous and *UPC2*^{G648D} heterozygous strains had the same resistance level as their parental strains (MIC 2µg/ml), which are also heterozygous for the hyperactive *UPC2* allele. Only the strain U10 showed an increased MIC of 16µg/ml, which is even higher than the resistance level of the genetically engineered strains SCUPC2R14A and -B with homozygous *UPC2*^{G648D} alleles (MIC 4µg/ml). U10 presumably obtained a further resistance mutation during passaging in the presence of fluconazole and was therefore excluded from further analysis. MICs of the *MTL* homozygous isolates are listed in Table 7 and the MICs of selected strains and controls are shown in Figure 13.

Table 7: *UPC2*^{G648D} heterozygous and *MTL* homozygous strains isolated after passaging in the presence of fluconazole and their parental strains. Strains selected for mating experiments are highlighted in bold font.

Strain name[(a)]	Parent	MIC [µg/ml]	*UPC2* resistance mutation	Mating type locus	*GLN3*	Fluconazole passages
SC5314	-	0.5	-/-	*MTL***a**/*MTL*α	*GLN3-1/GLN3-2*	-
SCUPC2R12A and -B	SC5314	2	-/*UPC2*^{G648D}	*MTL***a**/*MTL*α	*GLN3-1/GLN3-2*	-
SCUPC2R12hom1A (U3)	SCUPC2R12A	2	-/*UPC2*^{G648D}	*MTL***a**/*MTL***a**	*GLN3-2/GLN3-2*	1x2.5µg/ml
U4	SCUPC2R12A	2	-/*UPC2*^{G648D}	*MTL***a**/*MTL***a**	*GLN3-2/GLN3-2*	1x5µg/ml
U5	SCUPC2R12A	2	-/*UPC2*^{G648D}	*MTL***a**/*MTL***a**	*GLN3-2/GLN3-2*	2x2.5µg/ml
U7	SCUPC2R12A	2	-/*UPC2*^{G648D}	*MTL*α/*MTL*α	*GLN3-1/GLN3-1*	3x2.5µg/ml
U9	SCUPC2R12A	2	-/*UPC2*^{G648D}	*MTL***a**/*MTL***a**	*GLN3-2/GLN3-2*	3x2.5µg/ml
U10	SCUPC2R12A	16	-/*UPC2*^{G648D}	*MTL*α/*MTL*α	*GLN3-1/GLN3-1*	5x2.5µg/ml
U11	SCUPC2R12A	2	-/*UPC2*^{G648D}	*MTL***a**/*MTL***a**	*GLN3-2/GLN3-2*	5x2.5µg/ml
U12	SCUPC2R12A	2	-/*UPC2*^{G648D}	*MTL***a**/*MTL***a**	*GLN3-1/GLN3-2*	5x5µg/ml
SCUPC2R12hom1B (U2.3)	SCUPC2R12B	2	-/*UPC2*^{G648D}	*MTL*α/*MTL*α	*GLN3-1/GLN3-1*	6x2.5µg/ml

[(a)] Originally used strain names are indicated in parentheses. Please note that initially randomly picked strains of all experiments were consecutively numbered. Subsequently, selected *MTL* homozygous strains were systematically renamed.

As described in chapter 2.2.1.1, white-to-opaque switching competence, stability of the strains in the opaque phenotype and the phenotype of white and opaque colonies and cells was examined. After exclusion of U10, the two *MTL*α homozygous isolates U7 and SCUPCR12hom1B (U2.3) remained as candidates for mating experiments. After streaking of strain U7 from glycerol stocks on Lee's agar plates with phloxine B, white and opaque colonies of different sizes grew (white and opaque phenotype see Figure 18). Therefore, this isolate was excluded from further experiments and only SCUPC2R12hom1B (derivative of SCUPC2R12B) was characterized. In addition, the *MTL***a** homozygous strains SCUPC2R12hom1A and U12 (derivatives of SCUPC2R12A) were chosen for characterization experiments. These strains were selected since SCUPC2R12hom1A was isolated after the first passage with 2.5µg/ml fluconazole and U12 remained heterozygous for *GLN3*, indicating a local genomic rearrangement causing the LOH for the *MTL* locus.

As expected, SCUPC2R12hom1B, SCUPC2R12hom1A and U12 were switching-competent. After plating of white cells on Lee's agar plates with phloxine B and an incubation at high CO_2 concentrations, a mean of at least 99.9% of the colonies were in the opaque and white-opaque mixed phenotype. Furthermore, mean spontaneous switching rates under room conditions did not exceed 1.8% of the colonies (Appendix A1, Figure 14). In addition, all strains remained stable in the opaque phenotype (Appendix A2, Figure 14). After plating of opaque cells on Lee's agar with phloxine B and incubation under room conditions, at least 83.6% (mean) of the strains remained in the opaque and white-opaque mixed phenotype. Pictures of white and opaque colonies and cells of SCUPC2R12hom1A and SCUPC2R12hom1B are shown in Figure 15. The colony size of SCUPC2R12hom1B is smaller than that of SCUPC2R12hom1A and the controls SCMTLaM2A, SCMTLαM2A and WO-1. Note that SCUPC2R12hom1A opaque colonies were slightly wrinkled when they grew from opaque cells plated on Lee's agar plates with phloxine B.

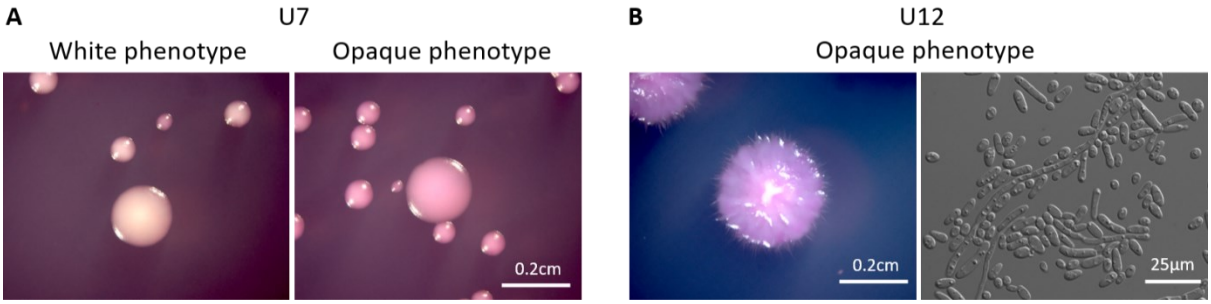

Figure 18: Colony phenotypes of white and opaque colonies of U7 and colony and cell morphology of U12 on Lee's agar plates with phloxine B. (A) Different white and opaque colony sizes of the *MTL* homozygous strain U7 were observed. (B) Opaque colonies of the *MTL* homozygous strain U12 were usually wrinkled and filamentation was found.

Although U12 remained heterozygous for the *GLN3* locus, in contrast to SCUPC2R12hom1A, this strain was not chosen for mating experiments since it had a strongly wrinkled opaque colony phenotype (Figure 18). Furthermore, SCUPC2R12hom1A grew more stably in the opaque phenotype. After plating of opaque cells on Lee's agar plates with phloxine B and incubation under room conditions, a mean of 93.3% of the colonies of SCUPC2R12hom1A and a mean of 83.6% of the colonies of U12 grew in the opaque and white-opaque mixed phenotype (Appendix A2). Since SCUPC2R12hom1B was the only derivative of strain SCUPC2R12B, it was chosen for mating experiments. In conclusion, the *MTL***a** homozygous strain SCUPC2R12hom1A and the *MTL*α homozygous strain SCUPC2R12hom1B were selected for mating experiments.

2.2.2. Mating of fluconazole-induced *MTL* homozygous strains with different resistance mutations

In order to examine whether the selected *MTL* homozygous strains can mate with eachother to generate recombinant mating progeny with different resistance mechanisms, mating experiments were performed. Selected fluconazole-induced *MTL* homozygous strains (Table 8) with a homozygous *ERG11*, *MRR1* or *TAC1* or heterozygous *UPC2* resistance mutation in the mating-competent opaque phenotype were mated with each other in all twelve possible combinations (Figure 19). An *MTL***a** homozygous strain with a resistance mutation (e.g. *MRR1**/*MRR1**) was mated with an *MTL*α homozygous strain with a different resistance mutation (e.g. *ERG11**/*ERG11**, *TAC1**/*TAC1** or *UPC2*/*UPC2**).

MTLa / MTLα	***ERG11**** SCERG11R32hom1B	***MRR1**** SCMRR1R32hom2A	***TAC1**** SCTACR32hom2B	***UPC2**** het. SCUPC2R12hom1A
ERG11* SCERG11R32hom1A		ME (3)	TE (6)	UE (3)
MRR1* SCMRR1R32hom1A	EM (17)		TM (2)	UM (18)
TAC1* SCTAC1R32hom2A	ET (2)	MT (7)		UT (2)
UPC2* het. SCUPC2R12hom1B	EU (5)	MU (10)	TU (4)	

Figure 19: Overview of the twelve mating crosses of the fluconazole-induced *MTL* homozygous strains with resistance mutations in *ERG11*, *MRR1*, *TAC1* or *UPC2*. Resistance mutations in *ERG11*, *MRR1*, *TAC1* or *UPC2* are indicated by asterisks. *MTL***a** homozygous strains SCERG11R32hom1B (*ERG11**/*ERG11**), SCMRR1R32hom2A (*MRR1**/*MRR1**), SCTAC1R32hom2B (*TAC1**/*TAC1**) and SCUPC2R12hom1A (*UPC2*/*UPC2** = *UPC2** het.) were mated with the *MTL*α homozygous strains SCERG11R32hom1A (*ERG11**/*ERG11**), SCMRR1R32hom1A (*MRR1**/*MRR1**), SCTAC1R32hom2A (*TAC1**/*TAC1**) and SCUPC2R12hom1B (*UPC2*/*UPC2** = *UPC2** het.) in all possible combinations. Resulting mating products ME, TE, UE, EM, TM, UM, ET, MT, UT, EU, MU and TU were termed systematically. The first letter indicates the resistance mutation of the *MTL***a** homozygous parental strain (E for *ERG11**, M for *MRR1**, T for *TAC1** and U for *UPC2**) and the second letter indicates the resistance mutation of the *MTL*α homozygous parental strain. Number of isolated mating products of each cross is indicated in parentheses. Note that the mating products of one cross can be related, since they were isolated in most cases in one experiment.

Table 8: Overview of selected fluconazole-induced *MTL* homozygous strains with resistance mutations in *ERG11*, *MRR1*, *TAC1* or *UPC2* used for mating assays. Adapted from [274].

Strain name	Parent	Resistance-associated locus	Mating type locus	Analyzed polymorphism marker	Fluconazole MIC [µg/ml]
SCERG11R32hom1A	SCERG11R32A	*ERG11*^{G464S}/*ERG11*^{G464S}	*MTL*α/*MTL*α	*GLN3-1*/*GLN3-1*	8
SCERG11R32hom1B	SCERG11R32B	*ERG11*^{G464S}/*ERG11*^{G464S}	*MTL***a**/*MTL***a**	*GLN3-1*/*GLN3-2*	8
SCMRR1R32hom1A	SCMRR1R32A	*MRR1*^{P683S}/*MRR1*^{P683S}	*MTL*α/*MTL*α	*GLN3-1*/*GLN3-1*; *CAP1-1*/*CAP1-2*	16
SCMRR1R32hom2A	SCMRR1R32A	*MRR1*^{P683S}/*MRR1*^{P683S}	*MTL***a**/*MTL***a**	*GLN3-2*/*GLN3-2*; *CAP1-1*/*CAP1-2*	16
SCTAC1R32hom2A	SCTAC1R32A	*TAC1*^{G980E}/ *TAC1*^{G980E}	*MTL*α/*MTL*α	*GLN3-1*/*GLN3-2*	8
SCTAC1R32hom2B	SCTAC1R32B	*TAC1*^{G980E}/ *TAC1*^{G980E}	*MTL***a**/*MTL***a**	*GLN3-1*/*GLN3-2*	8
SCUPC2R12hom1A	SCUPC2R12A	*UPC2*/*UPC2*^{G648D}	*MTL***a**/*MTL***a**	*GLN3-2*/*GLN3-2*	2
SCUPC2R12hom1B	SCUPC2R12B	*UPC2*/*UPC2*^{G648D}	*MTL*α/*MTL*α	*GLN3-1*/*GLN3-1*	2

2.2.2.1. Isolation of mating products with two different resistance mutations

First, a way to identify mating products among *MTL* homozygous parental strains needed to be established. The *MTL* homozygous parental strains have no dominant selection marker or auxotrophy. *TAC1* resistance mutation heterozygous strains are distinguishable from *TAC1* resistance mutation homozygous strains by colony size on agar containing fluconazole (Figure 11) [271]. Therefore, it was tested whether strains with two resistance mechanisms have an improved growth on agar plates

containing fluconazole in comparison to strains with only one resistance mechanism. Dilution spot assays were conducted on minimal medium SD agar and rich medium YPD agar with 5µg/ml fluconazole and as a control without fluconazole. Genetically engineered strains were examined into which one or two different GOF mutations in the relevant genes *ERG11*, *MRR1*, *TAC1* and/or *UPC2* had been introduced and which were already available in the laboratory's strain collection (Table 18).

Despite elevated MICs, strains with a combination of two resistance mechanisms were not distinguishable from either respective strain with only one resistance mechanism under the tested conditions. Even if one strain with a single resistance mutation grew considerably smaller colonies than the strain with the combination of two resistance mutations, the respective second strain with a single resistance mutation was not distinguishable from the strain with combined resistance mutations. For example, the *ERG11*^{G464S} homozygous strains SCERG11R34A and -B were distinguishable from the *ERG11*^{G464S} and *TAC1*^{G980E} homozygous strains SCETR34A and -B by colony size. Nevertheless, in comparison to the *TAC1*^{G980E} homozygous strains SCTAC1R34A and -B, the strains SCETR34A and -B did not show an improved growth on either type of agar containing fluconazole. Dilution spot assays on YPD agar are shown in Figure 20 and on SD agar in Figure 21.

Therefore, an alternate method was applied to identify mating products among the *MTL* locus homozygous parental strains. Instead of screening for colony size, screening was done for white-to-opaque switching-incompetent cells. Fluconazole-induced *MTL* homozygous strains in the mating-competent opaque phenotype were mixed together in all possible combinations in a 1:1 ratio (Figure 19). The suspension was spotted on a Spider agar plate so that cells were located close together. It has been described that in medium with alternative carbon sources, like Spider medium, the response of opaque cells to pheromones is enhanced [238]. Plates were incubated for two days at 18% CO_2 and 25°C to prevent a switching of the parental strains to the white phenotype. This was followed by an incubation for up to twelve days under room conditions in normal atmosphere. At various time points, fractions of the cell lawn were taken (for detailed information for single strains see Appendix A3).

During optimization of the experimental mating conditions, sonication of the suspensions with part of the cell lawn was applied for the mating crosses UT (parental strains SCUPC2R12hom1A and SCTAC1R32hom2A) and EM (parental strains SCERG11R32hom1B and SCMRR1R32hom1A) to disperse cell clumps. Strains EM26, EM27, EM28 and EM30 were isolated after one round of sonication. EM32, EM33, EM34 and UT1 were sonicated for two rounds (see chapter 4.2.4.2). Since sonication turned out to be unnecessary, this step was later eliminated.

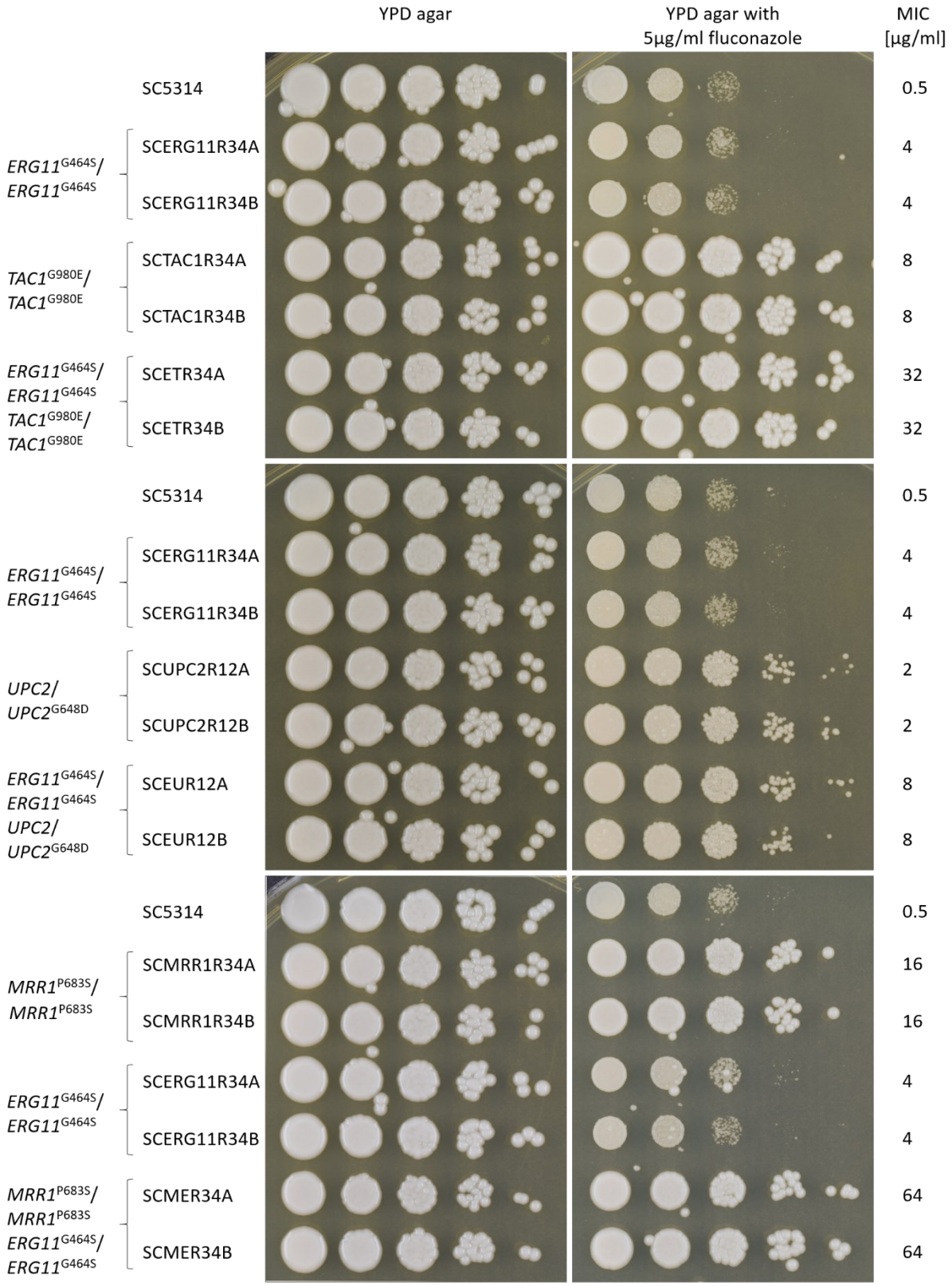

Figure 20 (continued on the next page)

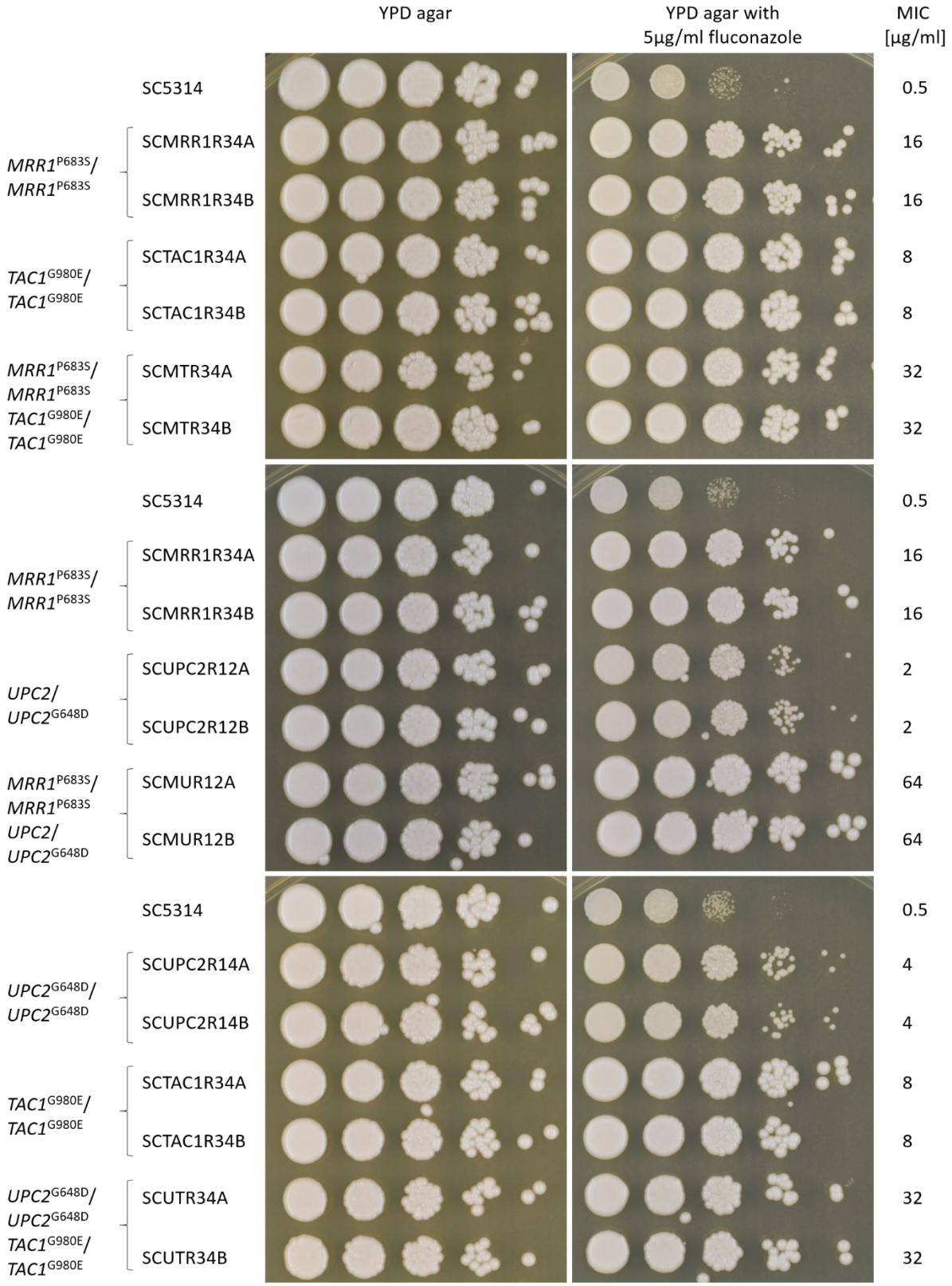

Figure 20: Comparison of growth of strains that have a single resistance mutation with strains that have a combination of two different resistance mutations on YPD agar containing fluconazole. The wild-type strain (SC5314), strains with a heterozygous or homozygous resistance mutation in *ERG11*, *MRR1*, *TAC1* or *UPC2* and strains with a combination of two different resistance mutations were plated on YPD agar with 5µg/ml fluconazole. As a growth control, strains were also plated on YPD agar without fluconazole. Furthermore, the MIC of the strains was determined.

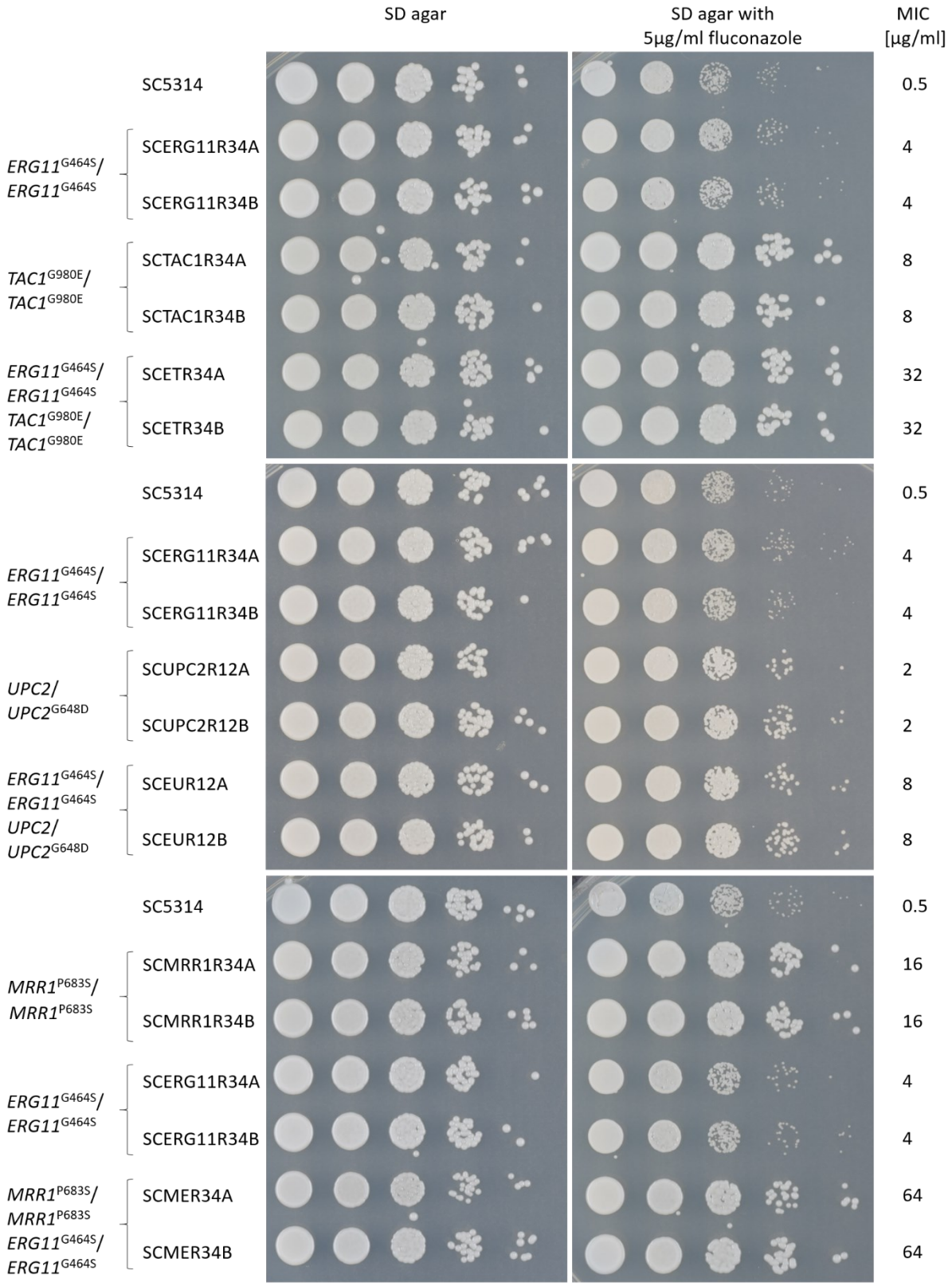

Figure 21 (continued on the next page)

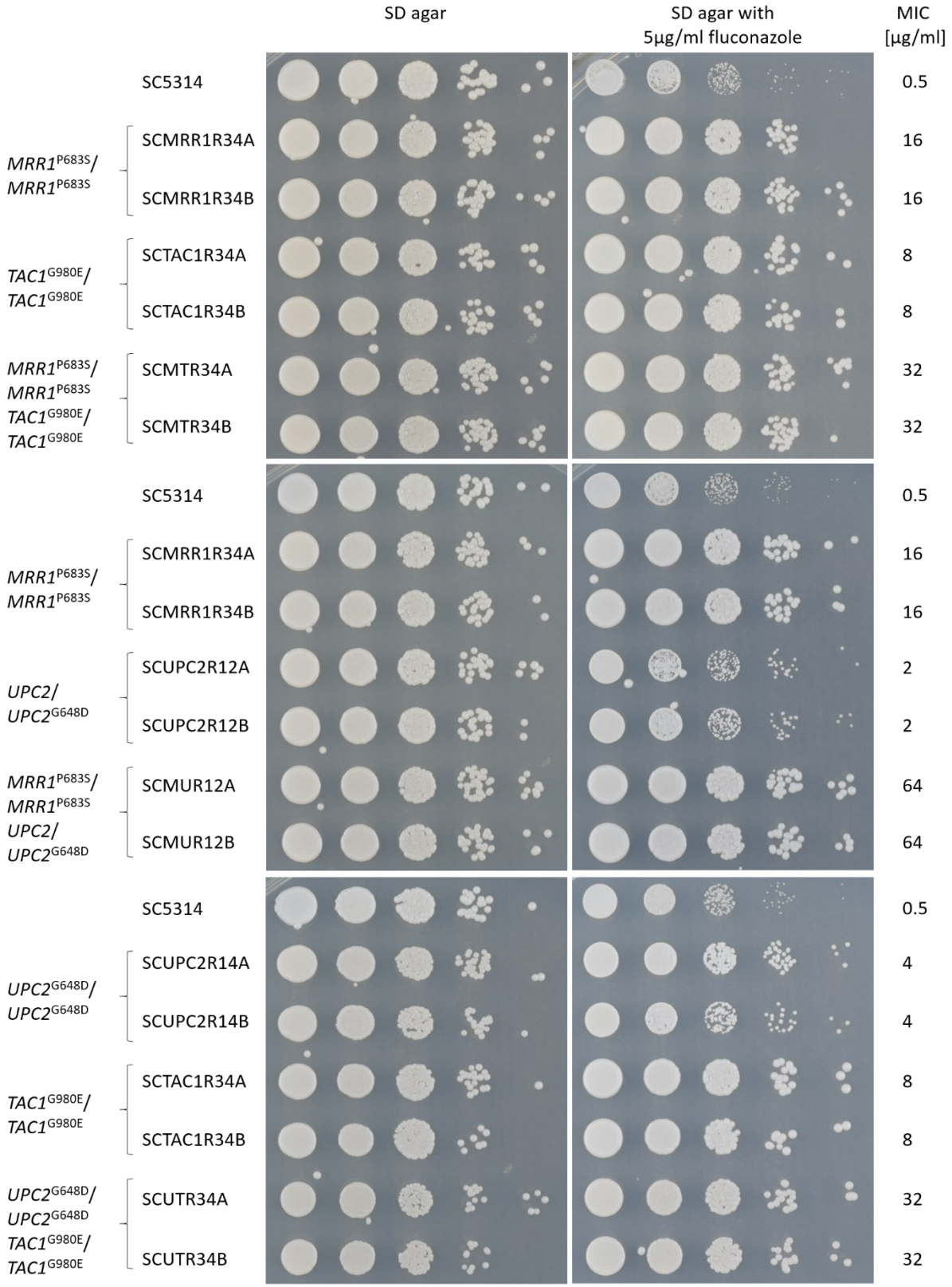

Figure 21: Comparison of growth of strains that have a single resistance mutation with strains that have a combination of two different resistance mutations on SD agar containing fluconazole. The wild-type strain (SC5314), strains with a heterozygous or homozygous resistance mutation in *ERG11*, *MRR1*, *TAC1* or *UPC2* and strains with a combination of two different resistance mutations were plated on SD agar with 5µg/ml fluconazole. As a growth control, strains were also plated on SD agar without fluconazole. Furthermore, the MIC of the strains is given for comparison.

An appropriate dilution of the cell lawn suspensions was spread for single colonies on Lee's agar with phloxine B, which selectively stains opaque colonies pink [218]. The plates were incubated for two days at 18% CO_2 and 25°C and afterwards for five days at room temperature and room atmosphere. Since the parental strains are *MTL* homozygous, they are able to switch to, or remain in the opaque phenotype after a switching stimulation with high CO_2 concentrations. In contrast, mating products are not able to switch to the opaque phenotype even with high CO_2 concentrations, as long as they are still *MTL* heterozygous. Consequently, white colonies were picked and further characterized. A picture of part of a Lee's agar plate with phloxine B with the mating cross EM is shown in Figure 22.

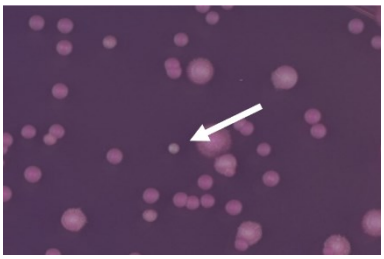

Figure 22: Picture of a part of a Lee's agar plate of a mating experiment of the *MTL*a homozygous strain SCERG11R32hom1B with the *MTL*α homozygous strain SCMRR1R32hom1A. The pink color of the agar plate is caused by phloxine B, which selectively stains opaque colonies pink. The white arrow highlights a white colony, a potential mating product, which was picked and further characterized.

First, the *MTL* locus of the potential mating products was examined by Southern hybridization. Mating products were expected to have both configurations of the *MTL* locus, as long as they had not already lost all *MTL***a** or *MTL*α alleles. Note that some white colonies turned out to be *MTL* homozygous parental strains (different frequency for different strains). At least two mating products of each cross were isolated (Appendix A3). The isolated mating products were termed systematically. The first letter indicates the resistance mutation of the *MTL***a** homozygous parental strain and the second letter the resistance mutation of the *MTL*α homozygous parental strain. For example, mating products EM were isolated from the cross of the *MTL***a** and *ERG11* GOF homozygous strain SCERG11R32hom1B with the *MTL*α and *MRR1* GOF homozygous strain SCMRR1R32hom1A. All mating products contained the genetic material of both parental strains, including the *MTL***a** and *MTL*α loci as well as hyperactive and wild-type alleles of resistance-associated genes *ERG11*, *MRR1*, *TAC1* and/or *UPC2*. Pictures of Southern blots of selected mating products are shown in Figure 23.

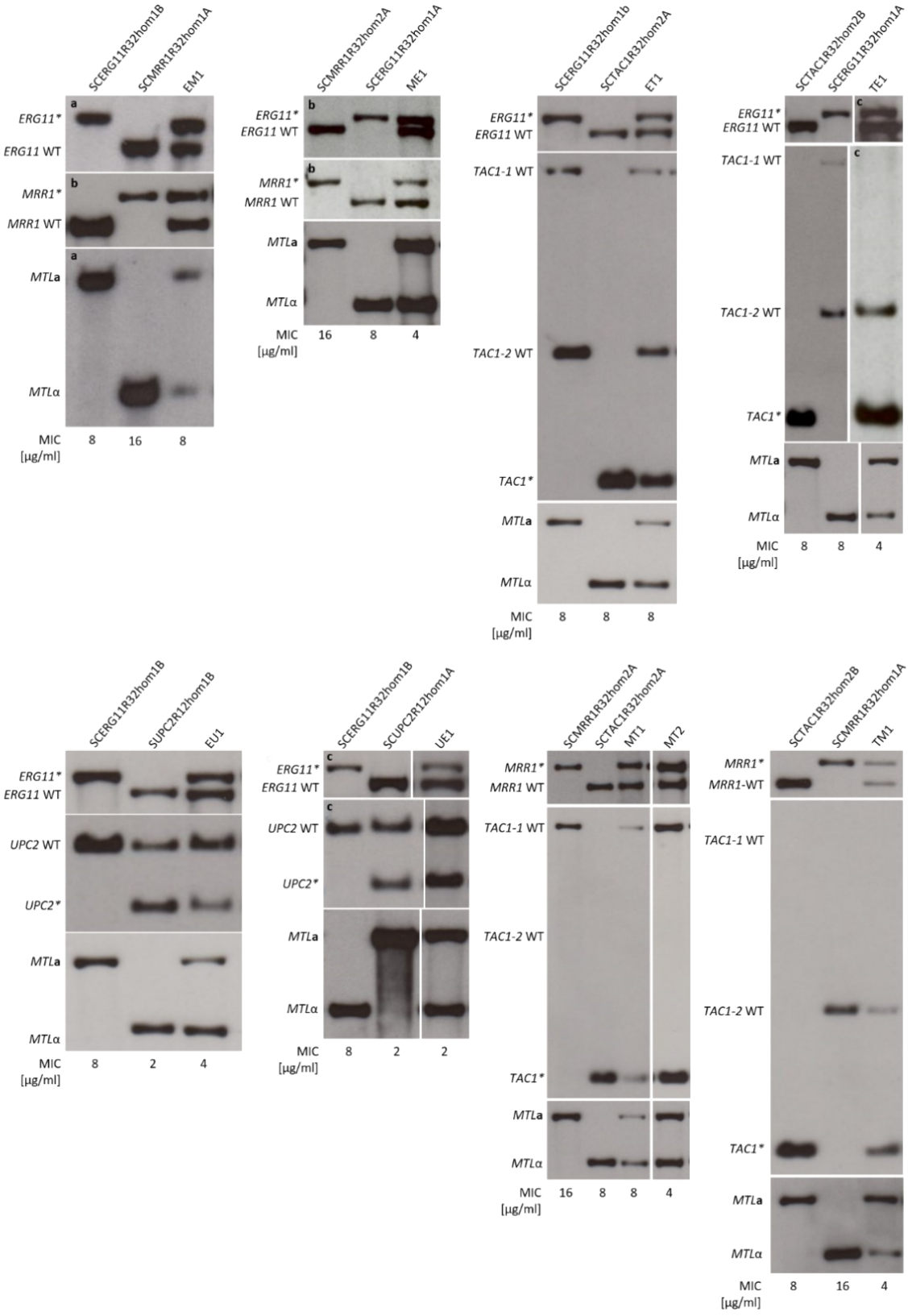

Figure 23 (continued on the next page)

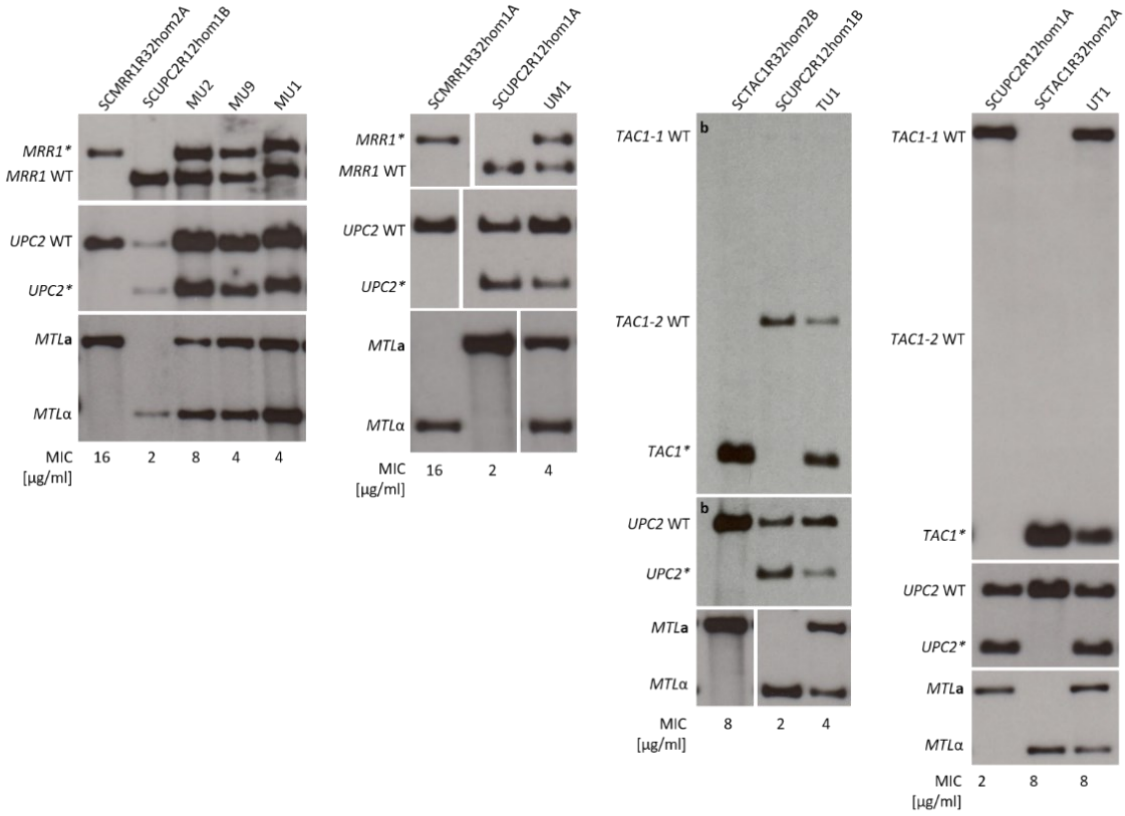

Figure 23: Genetic analysis of resistance-associated genes and the *MTL* locus of selected mating products and their respective parental strains. The *MTL* locus and resistance-associated genes *ERG11*, *MRR1*, *TAC1* and/or *UPC2* were analyzed by Southern hybridization. Restriction enzymes and probes used and a schematic showing the expected fragment sizes after hybridization are given in chapter 4.2.5.2 (Table 22, Figure 30, Figure 31). Note that the *MRR1* locus was analyzed with NsiI-digested chromosomal DNA and the *MTL* locus with EcoRI-digested chromosomal DNA and the 5'MTL probe. In some cases, different genomic DNA preparations were used for the blots. Signal intensities are caused by uneven DNA concentrations. MICs of the strains are indicated for comparison. Experiments were conducted with the help of Sabrina Schneider (a), Ines Krüger and Sonja Schwanfelder (b) and Nico Alexander Liebig (c). Parts published by Popp *et al.* [274].

2.2.2.2. Resistance level of the isolated mating products

An interesting question was what level of resistance the mating products would have, since they contained genetic material from both parental strains including two different resistance mechanisms. Surprisingly, mating products did not have a higher resistance level than their parental strains (Figure 24, Table 9, Appendix A3). In most cases, the MIC of the mating product was even lower than the MIC of one parent. For the crosses ME, TE, TM and for the strain MT2, the MIC was even lower than the MIC of both parental strains. The fluconazole-induced *MTL* homozygous strains with resistance mutations in *ERG11*, *MRR1* and *TAC1* no longer have any wild-type alleles (Figure 25). In contrast, the resulting mating products do have the genetic material of both parents and therefore also contain wild-type alleles. Hyperactive and wild-type alleles are present in a 1:1 ratio, except for *UPC2* (three wild-type alleles, one *UPC2** allele) as long as the mating products did not undergo genomic recombination already. It is possible that heterozygosity for the hyperactive alleles reduces the

resistance level in tetraploid mating products as it is the case for diploid strains. And it is conceivable that this would be the case when the strains carry two different resistance mutations.

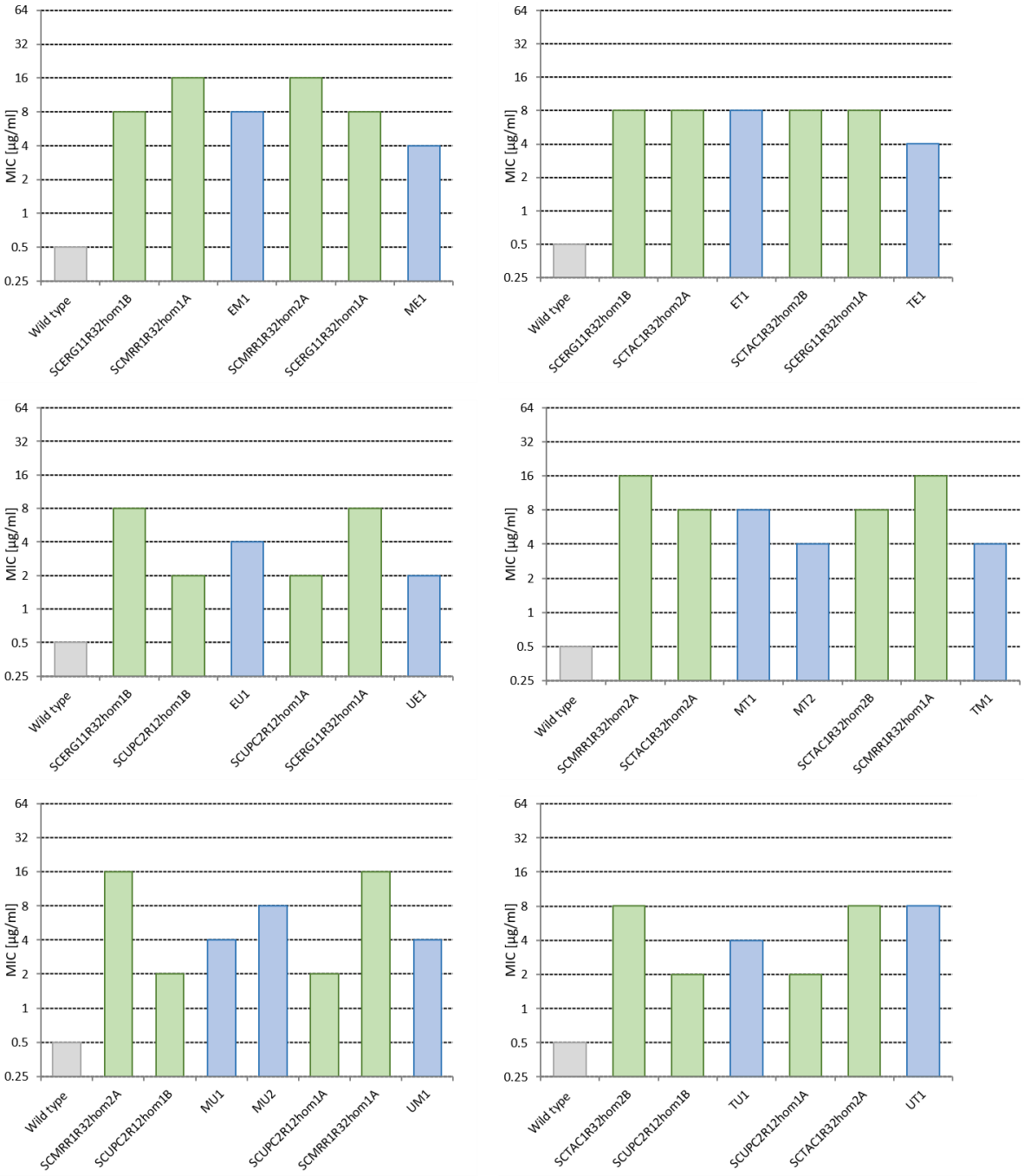

Figure 24: Fluconazole resistance level of selected mating products. Resistance mutations in the genes *ERG11*, *MRR1*, *TAC1* and *UPC2* are indicated by asterisks. MICs of the wild-type strain SC5314 (light gray bar), the fluconazole-induced *MTL*-homozygous parental strains (green bars) and the selected mating products (blue bars) are shown. Note that the growth of MU2 was already reduced at a fluconazole concentration of 8µg/ml.

All isolated mating products of one cross had the same resistance level, except for MT and MU. Out of seven mating products of the cross MT, six mating products had a MIC of 8µg/ml and one mating product a MIC of 4µg/ml. In addition, nine mating products of the cross MU had a MIC of 4µg/ml and one isolate a MIC of 8µg/ml.

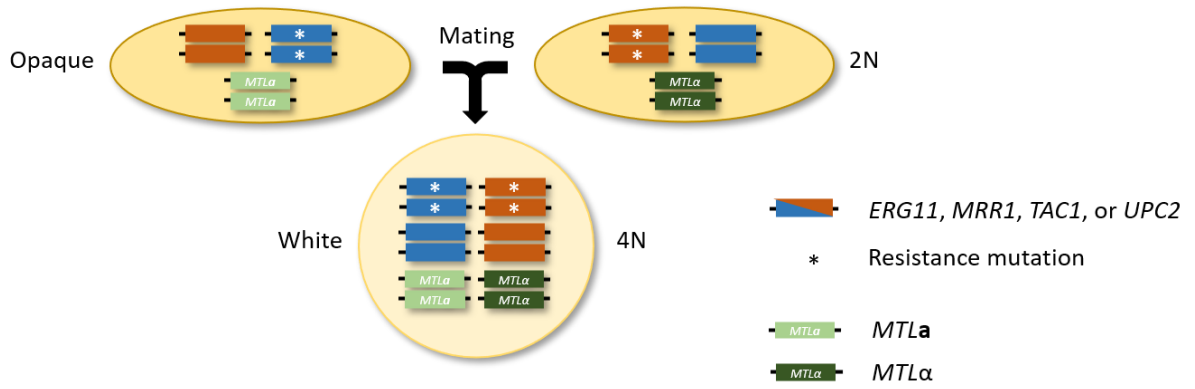

Figure 25: Schematic overview of the expected allelic composition of mating products and the fluconazole-induced *MTL* homozygous parental strains with a resistance mutation in *ERG11*, *MRR1* or *TAC1*. The two *MTL* configurations are indicated by a light green (*MTL***a**) and dark green (*MTL*α) bar. Alleles of the resistance-associated genes *ERG11*, *MRR1* and *TAC1* are indicated by blue or red bars and a resistance mutation by an asterisk. Mating products contain the genetic material of both parents and therefore contain the *MTL***a** locus, the *MTL*α locus and wild-type alleles of the resistance-associated genes in addition to the mutated alleles of the respective resistance-associated genes. Note that the number of alleles shown can differ for individual strains (chapter 2.2.2.3 and 2.2.3.2.).

As already mentioned, mating products can be related since they were often isolated in a single experiment. For consecutive experiments one mating product of every mating combination was selected. Since strains with two different MICs were isolated for the crosses MT and MU, two mating products were selected (Table 9).

Table 9: Overview of selected mating products with resistance mutations in *ERG11*, *MRR1*, *TAC1* and/or *UPC2*. Adapted from [274].

Strain name[a]	MIC [µg/ml]	*MTL***a homozygous parental strain**	*MTL*α **homozygous parental strain**	Time of co-incubation of both parental strains
EM1	8	SCERG11R32hom1B	SCMRR1R32hom1A	6 days
ME1 (ME3)	4	SCMRR1R32hom2A	SCERG11R32hom1A	6 days
ET1	8	SCER11R32hom1B	SCTAC1R32hom2A	3 days
TE1 (TE27)	4	SCTAC1R32hom2B	SCERG11R32hom1A	6 days
EU1	4	SCERG11R32hom1B	SCUPC2R12hom1B	6 days
UE1 (UE64)	2	SCUPC2R12hom1A	SCERG11R32hom1A	9 days
MT1 (MT3)	8	SCMRR1R32hom2A	SCTAC1R32hom2A	6 days
MT2 (MT6)	4			6 days
TM1 (TM8)	4	SCTAC1R32hom2B	SCMRR1R32hom1A	14 days
MU1 (MU13)	4	SCMRR1R32hom2A	SCUPC2R12hom1B	6 days
MU2 (MU8)	8[b]			3 days
UM1 (UM21)	4	SCUPC2R12hom1A	SCMRR1R32hom1A	3 days
TU1	4	SCTAC1R32hom2B	SCUPC2R12hom1B	6 days
UT1 (UT86)	8	SCUPC2R12hom1A	SCTAC1R32hom2A	3 days

[a] Originally used strain names are indicated in parentheses. Please note that initially randomly picked strains of all experiments were consecutively numbered. Subsequently, selected mating products strains were systematically renamed.
[b] Growth was already reduced at this fluconazole concentration.

2.2.2.3. Ploidy of the isolated mating products

To examine whether the isolated mating products were still tetraploid, or if they had already lost genetic material, ploidy level was analyzed by flow cytometry measurements (Figure 26). In addition, the ploidy levels were determined for the fluconazole-induced *MTL* homozygous parental strains and for the independently constructed *MTL* and resistance mutation heterozygous derivatives of the wild-type SC5314. The diploid wild-type strain SC5314 was analyzed as a reference strain. Peak profiles of all tested strains (red profile) are given in comparison to the 2C and 4C peaks (blue profile) of SC5314 in Figure 26. Each strain was analyzed at least three times independently.

All constructed derivatives of SC5314 with a heterozygous *ERG11*^{G464S} (SCERG11R32A and -B), *MRR1*^{P683S} (SCMRR1R32A and -B), *TAC1*^{G980E} (SCTAC1R32A and B), or *UPC2*^{G648D} (SCUPC2R12A and B) allele were diploid, as expected (Figure 26A). Their fluconazole-induced *MTL* homozygous derivatives SCERG11R32hom1B (*ERG11*^{G464S}/*ERG11*^{G464S}), SCTAC1R32hom2A and SCTAC1R32hom2B (*TAC1*^{G980E}/*TAC1*^{G980E}) were diploid as well (Figure 26B). The strains SCMRR1R32hom2A (*MRR1*^{P683S}/*MRR1*^{P683S}) and SCUPC2R12hom1A (*UPC2*/*UPC2*^{G648D}) were near-diploid. Peak profiles of SCMRR1R32hom2A (*MRR1*^{P683S}/*MRR1*^{P683S}) and SCUPC2R12hom1A (*UPC2*/*UPC2*^{G648D}) indicated a ploidy slightly higher than 2N. The strains SCERG11R32hom1A (*ERG11*^{G464S}/*ERG11*^{G464S}), SCMRR1R32hom1A (*MRR1*^{P683S}/*MRR1*^{P683S}) and SCUPC2R12hom1B (*UPC2*/*UPC2*^{G648D}) showed peak profiles with differing subpopulations.

Most of the analyzed mating products were tetraploid (Figure 26C). ME1 had already lost DNA content and was diploid, UT1 was hypertetraploid and MT2 peak profiles indicated population heterogeneity. TU1 showed population heterogeneity in two flow cytometry measurements (Appendix A5) and a tetraploid peak profile in one measurement (Figure 26C). This observation indicates that mating products are instable. Presumably, genomic changes had already taken place during the cell divisions prior to isolation and characterization of the strain.

Comparing the results of the flow cytometry experiments (Figure 26) and the Southern hybridization (Figure 23), loss of alleles and chromosomes was observed. Southern blots revealed that UE1 and TE1 had a weaker signal of the hyperactive *ERG11* allele in comparison to the wild-type *ERG11* allele. This was accompanied by a weaker signal of the *MTL*α allele (linked with the *ERG11** allele) in comparison to the signal of the *MTL***a** allele. For the strain UE1 this can be observed more clearly in Figure 28. In addition, TE1 had no *TAC1-1* wild-type alleles unlike its parent SCERG11R32hom1A, although TE1 (and UE1) appeared tetraploid in the flow cytometry analysis. Contrary to this observation, the signal of the mutated *ERG11* allele in comparison to the wild-type *ERG11* allele was stronger in Southern blots of strain EM1. Furthermore, the signal for the *MTL***a** locus (linked with *ERG11**) was stronger than that of

the *MTLα* locus. These three strains presumably lost one copy of Chr5B, although this was not recognizable in the FACS data.

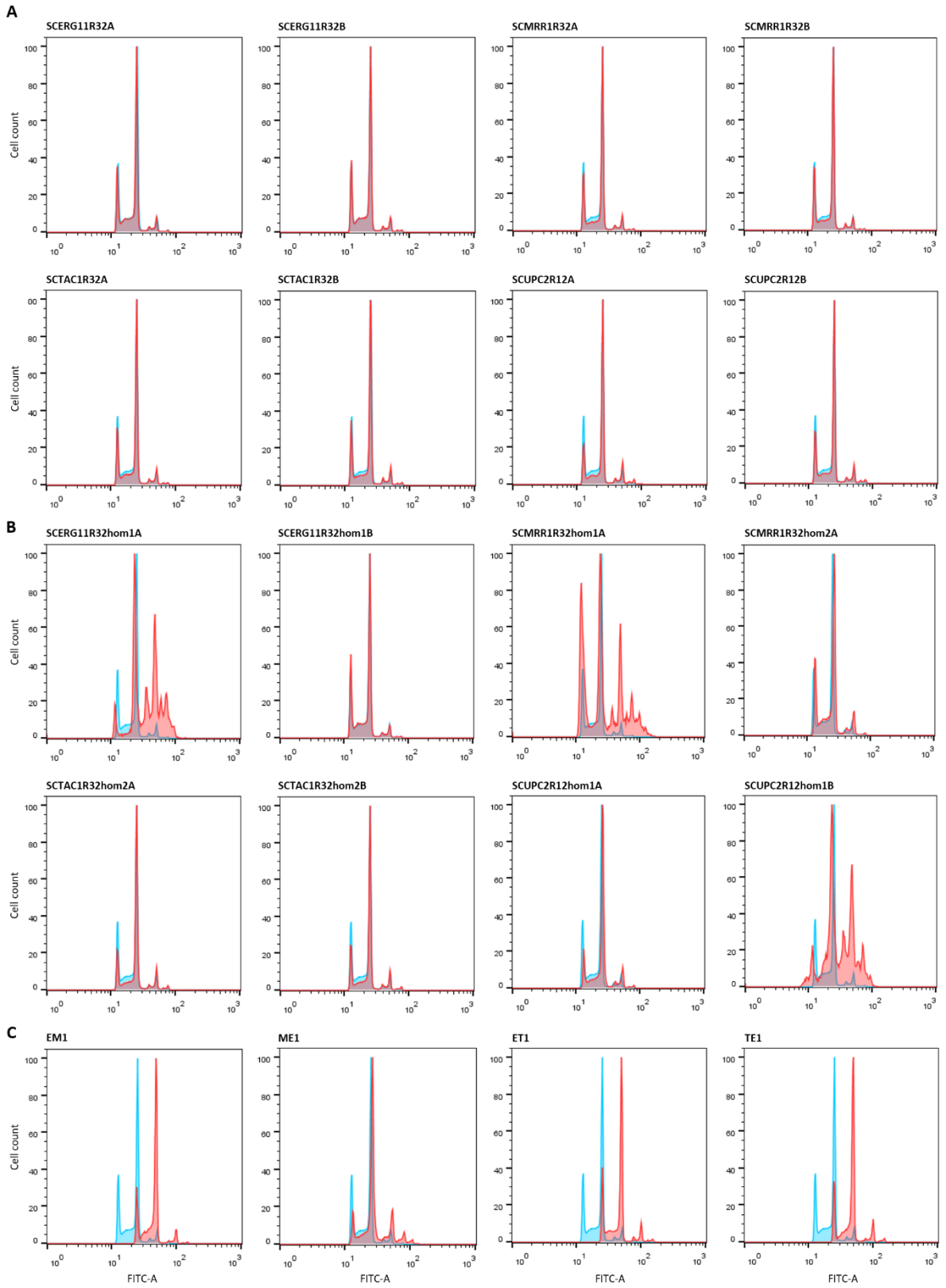

Figure 26 (continued on the next page)

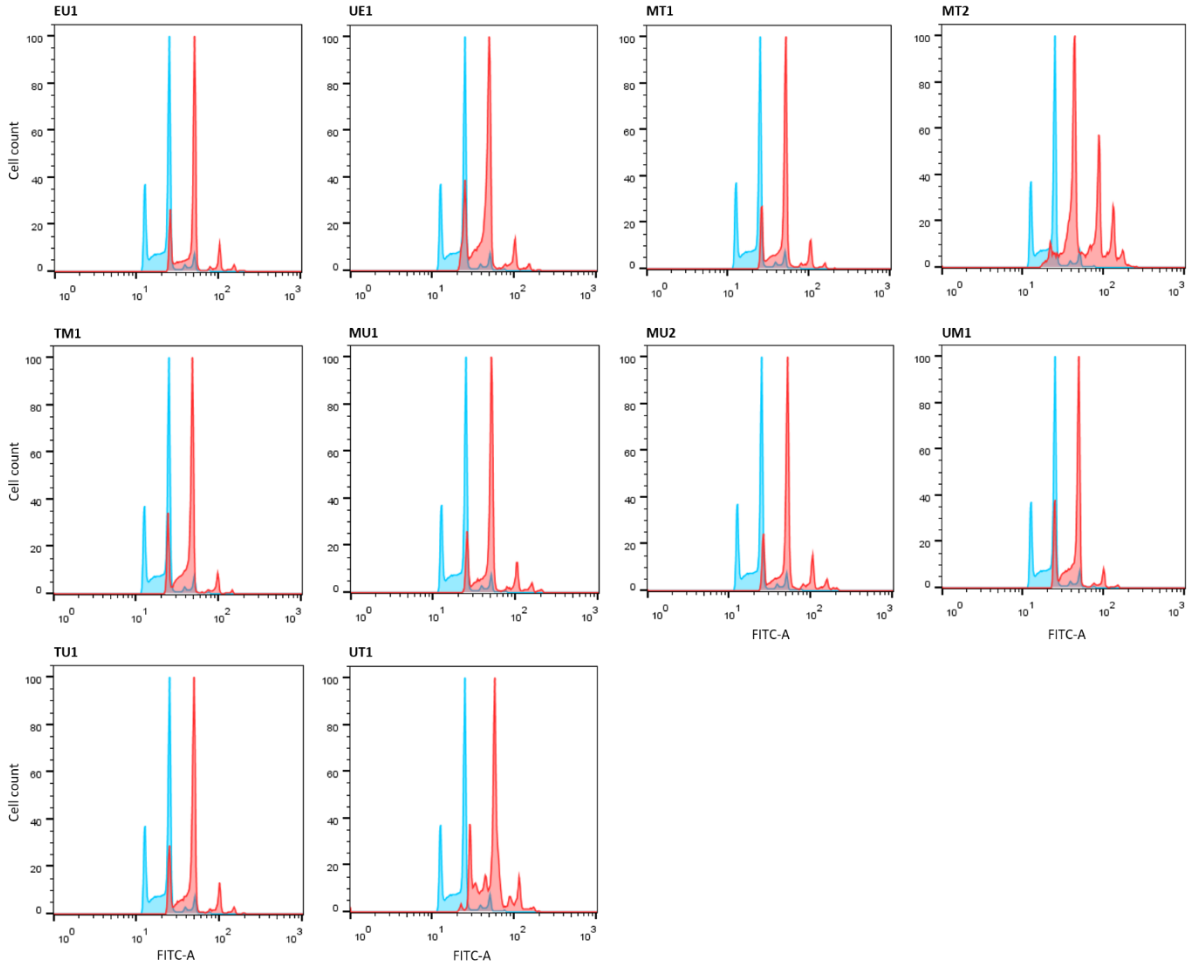

Figure 26: Ploidy of selected mating products and their parental strains. Flow cytometry profiles of the reference strain SC5314 is shown in blue. Profiles of the resistance mutation and *MTL* locus heterozygous strains (A), selected fluconazole-induced *MTL* homozygous strains (B) and selected mating products (C) are illustrated in red. Shown are profiles of one flow cytometry measurement. Comparison of different measurements is shown in Appendix A5. Adapted from [274].

In the Southern blots of MT2, the signal of the hyperactive *MRR1* allele was stronger than that of the wild-type *MRR1* allele. FACS analysis showed a heterogenous population structure. In contrast, Southern blots of ME1 indicated a loss of a copy of the hyperactive *MRR1* allele. It is possible that this strain lost a copy of chromosome 3 since flow cytometry measurements identified it as a diploid strain. Although a 3:1 ratio of wild-type and hyperactive *UPC2* alleles was expected for strain UT1 (two wild-type *UPC2* alleles from the parent SCTAC1R32hom2A, one wild-type and one hyperactive *UPC2* allele from the parent SCUPC2R12hom1A), signal intensities of *UPC2* and *UPC2** were similar in the Southern blots. This could be explained by a loss of two copies of chromosome 1, although UT1 had a hypertetraploid genome content. Therefore, genomic recombination events that amplified the chromosome with the hyperactive *UPC2* allele, or that lead to a replacement of one wild-type *UPC2* allele with the hyperactive *UPC2* allele, could also have taken place.

2.2.3. Reassortment of the genome of mating products in the presence of fluconazole

The instable tetraploid mating products can lose (parts of) chromosomes randomly and return through an aneuploid state to the diploid or near-diploid state [25, 181, 183, 186]. One aim of this study was to examine whether the mating products isolated during this study can reassort their chromosomes in an advantageous way in the presence of the selection pressure of fluconazole, thereby generating highly adapted progeny.

2.2.3.1. Isolation of highly fluconazole-resistant mating product progeny

Selected mating products (Table 9) were serially passaged in the presence of increasing fluconazole concentrations in rich medium (YPD). As a starting fluconazole concentration, half of the MIC of the respective mating product was chosen. Fluconazole concentrations were doubled stepwise every second passage until the maximum concentration of 256µg/ml was reached. During the first six passages and at least every second passage of the later passages, an appropriate dilution of the culture was plated on YPD agar. Three single colonies per passage were picked randomly and the fluconazole resistance level of the strains was examined (all analyzed strains are listed in Appendix A4). The one or two most resistant isolate(s) of the first six passages with an intermediate resistance level and the one or two isolate(s) with the overall highest resistance level of all passages were selected for further analysis. In the case that the most resistant derivative(s) was isolated in one of the later passages (≥ passage 8), the preceding passage was analyzed as well (if not already done) to ensure that the most resistant progeny was isolated at the earliest possible timepoint. Thus, two to four colonies of each passaging experiment were selected for further analysis of the genomic alterations, which accompany the development of fluconazole resistance. These strains are listed in Table 10.

For each passaged mating product, progeny with an increased fluconazole resistance level were isolated. Note that the derivative of mating product MU2, MU2P6A1 (passage 6) was very instable. After streaking of the strain from the glycerol stock, colonies of different sizes grew that had different fluconazole resistance levels (8, 16 and 32µg/ml). Therefore, an additional strain with the MIC of 16µg/ml from a later passage was selected for further analysis. No derivative of MU2 with a further increased MIC was isolated.

The most resistant derivative(s) of each mating product reached at least the resistance level of genetically engineered strains with homozygous resistance mutations in the respective same two resistance-associated genes. In some cases, the derivatives reached a resistance level of one MIC value higher (derivatives of EM1, MT2, TM1 and TU1) or two MIC values higher (derivatives of TE1 and EU1).

Only derivatives of the mating product MU2 acquired a decrease in resistance level by one MIC value in comparison to the MIC value of the genetically engineered strain SCMUR14A with homozygous resistance mutations in *MRR1* and *UPC2*. Presumably, more resistant isolates could have been isolated if further colonies would have been screened. MICs of the selected strains are shown in Figure 27.

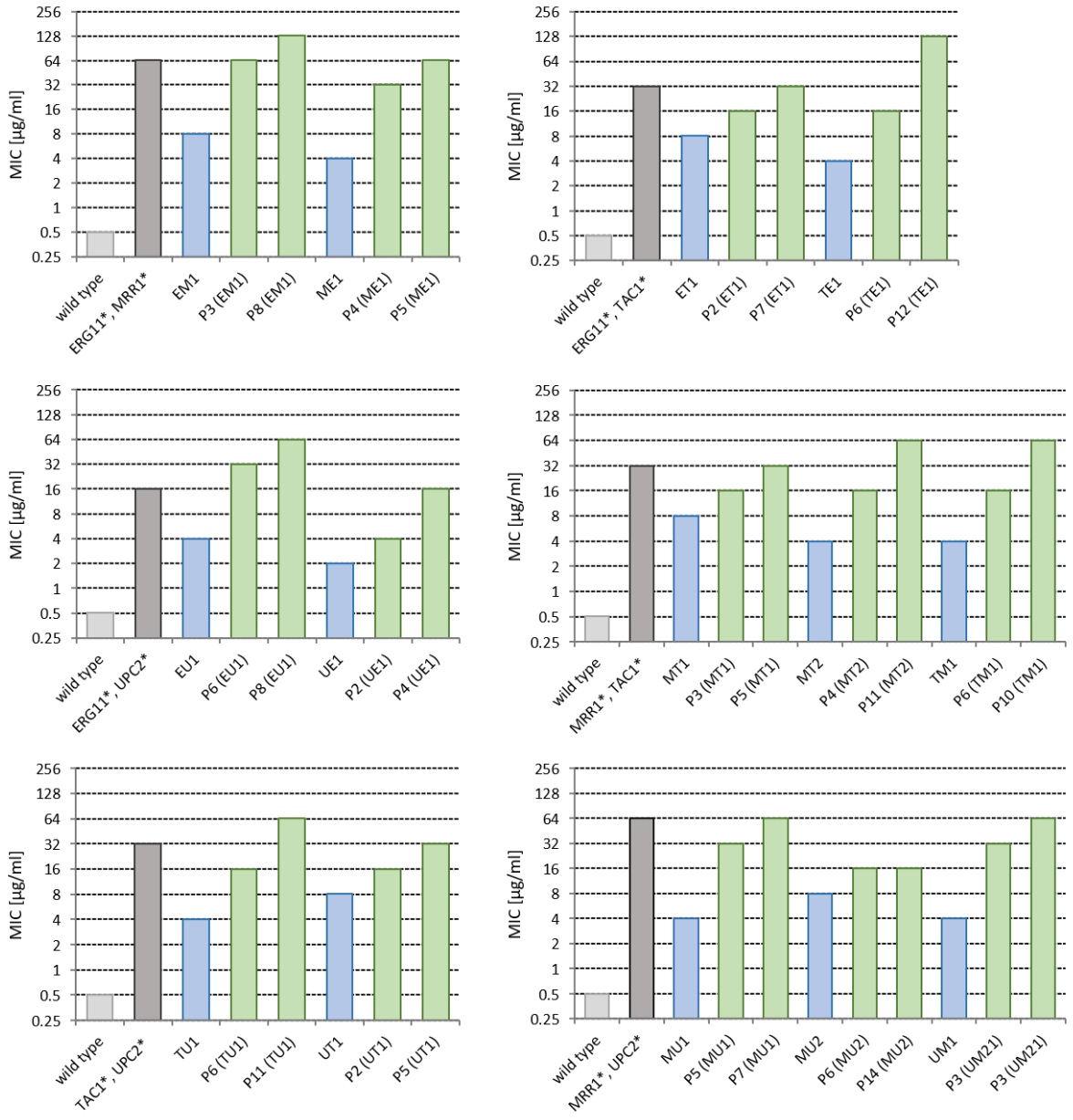

Figure 27: Fluconazole resistance level of selected mating product progeny. Resistance mutations in the genes *ERG11*, *MRR1*, *TAC1* and *UPC2* are indicated by asterisks. MICs of the wild-type strain SC5314 (light gray bar) and constructed diploid strains with a combination of two homozygous resistance mutations (dark gray bar) are given for comparison. Furthermore, MICs of parental mating products (blue bars) and the selected mating product progeny (green bars) are shown. Note that the growth of MU2 was already reduced at a fluconazole concentration of 8µg/ml. The derivative MU2P6A1 (passage 6) was very instable. After streaking of the strain from the glycerol stock, cells gave rise to colonies of different sizes and with different fluconazole resistance levels (8, 16 and 32µg/ml). Therefore, an additional strain with the same MIC of 16µg/ml from a later passage was selected for further analysis. Names of examined genetically engineered strains are listed as follows: SCMER34A and -B (*ERG11**, *MRR1**), SCETR34A and -B (*ERG11**, *TAC1**), SCEUR14A and -B (*ERG11**, *UPC2**), SCMTR34A and -B (*MRR1**, *TAC1**), SCMUR14A and -B (*MRR1**, *UPC2**) and SCUTR34A and -B (*TAC1**, *UPC2**).

Table 10: Overview of mating product derivates with intermediate and highest fluconazole resistance level. In addition, the passage in which the derivatives were isolated is given. Adapted from [274].

Strain name	MIC [µg/ml]	Genomic changes in comparison to the parental mating product[a]	Passage (fluconazole concentration in the passage)
Parental mating product EM1 (MIC 8µg/ml)			
EM1P3A-1	64	Loss of wild-type *ERG11*, wild-type *MRR1* and *MTL*α	3 (8µg/ml)
EM1P8A-1	128	Loss of wild-type *ERG11*, wild-type *MRR1* and *MTL*α	8 (32µg/ml)
EM1P8A-3	128	Loss of wild-type *ERG11*, wild-type *MRR1* and *MTL*α	
Parental mating product ME1 (MIC 4µg/ml)			
ME1P4A-2	32	Loss of wild-type *MRR1*	4 (4µg/ml)
ME1P4A-3	32	Loss of wild-type *MRR1*	
ME1P5A-2	64	Loss of wild-type *MRR1*	5 (8µg/ml)
Parental mating product ET1 (MIC 8µg/ml)			
ET1P2A-2	16		2 (4µg/ml)
ET1P7A-3	32	Loss of wild-type *TAC1,* decrease in *ERG11** and *MTL***a**	7 (32µg/ml)
Parental mating product TE1 (MIC 4µg/ml)			
TE1P6A-1	16	Decrease in *ERG11**, wild-type *TAC1* and *MTL*α	6 (8µg/ml)
TE1P6A-2	16	Loss of *ERG11**, wild-type *TAC1* and *MTLα*	
TE1P12A-1	128	Loss of wild-type *TAC1*, increase in *ERG11** and *MTL*α	12 (64µg/ml)
Parental mating product EU1 (MIC 4µg/ml)			
EU1P6A-3	32	Decrease in wild-type *ERG11* and *MTL*α	6 (8µg/ml)
EU1P8A-3	64	Loss of wild-type *ERG11* and *MTL*α, increase in *UPC2**	8 (16µg/ml)
Parental mating product UE1 (MIC 2µg/ml)			
UE1P2A-1	4	Increase in *UPC2**	2 (1µg/ml)
UE1P4A-3	16	Increase in *UPC2**, *ERG11** and *MTL*α	4 (2µg/ml)
Parental mating product MT1 (MIC 8µg/ml)			
MT1P3A-3	16	Decrease in wild-type *MRR1*	3 (8µg/ml)
MT1P5A-2	32	Loss of wild-type *MRR1*	5 (16µg/ml)
MT1P5A-3	32	Loss of wild-type *MRR1*, wild-type *TAC1* and *MTL***a**	
Parental mating product MT2 (MIC 4µg/ml)			
MT2P4A-3	16	Decrease in wild-type *TAC1* and *MTL*a	4 (4µg/ml)
MT2P11A-1	64	Loss of wild-type *MRR1*, decrease in wild-type *TAC1* and *MTL***a**	11 (64µg/ml)
Parental mating product TM1 (MIC 4µg/ml)			
TM1P6A-2	16	Loss of wild-type *TAC1* and *MTL*α	6 (8µg/ml)
TM1P6A-3	16	Loss of wild-type *TAC1* and *MTL*α	
TM1P10A-1	64	Loss of wild-type *MRR1*, wild-type *TAC1* and *MTL*α	10 (32µg/ml)
Parental mating product MU1 (MIC 4µg/ml)			
MU1P5A-1	32	Decrease in wild-type *MRR1*	5 (8µg/ml)
MU1P7A-1	64	Loss of wild-type *MRR1*	7 (16µg/ml)
Parental mating product MU2 (MIC 8µg/ml[b])			
MU2P6A-1	16[c]		6 (16µg/ml)
MU2P14A-1	16	Increase in *MRR1**	14 (256µg/ml)
Parental mating product UM1 (MIC 4µg/ml)			
UM1P3A-3	32	Loss of wild-type *MRR1*, increase in *UPC2**	3 (4µg/ml)
UM1P3A-1	64	Loss of wild-type *MRR1*	

Strain name	MIC [µg/ml]	Genomic changes in comparison to the parental mating product[a]	Passage (fluconazole concentration in the passage)
Parental mating product TU1 (MIC 4µg/ml)			
TU1P6A-3	16		6 (8µg/ml)
TU1P11A-1	64	Loss of wild-type *TAC1* and *MTL*α, increase in *UPC2**	11 (64µg/ml)
TU1P11A-3	64	Loss of wild-type *TAC1* and *MTL*α, increase in *UPC2**	
Parental mating product UT1 (MIC 8µg/ml)			
UT1P2A-2	16	Decrease in wild-type *TAC1* and *MTL***a**, increase in *UPC2**	2 (4µg/ml)
UT1P2A-3	16	Decrease in wild-type *TAC1* and *MTL***a**, increase in *UPC2**	
UT1P5A-1	32	Loss of wild-type *TAC1* and *MTL***a**	5 (16µg/ml)
UT1P5A-2	32	Decrease in wild-type *TAC1* and *MTL***a**, increase in *UPC2**	

[a] In relation to the other allele(s) (see Southern blots in Figure 28).
[b] Growth was already reduced at this fluconazole concentration.
[c] MU2P6A1 was very instable. After streaking of the strain from the glycerol stock, colonies of different sizes and with different fluconazole resistance levels (8, 16 and 32µg/ml) grew.

2.2.3.2. Genetic reassortment and drug resistance of mating product progeny

Interestingly, at least one analyzed derivative of most mating products had lost all or a part of the wild-type alleles of one or both of the resistance-associated genes *ERG11*, *MRR1*, *TAC1* or *UPC2* in comparison to the respective parental mating product (Table 10). The loss of wild-type alleles was analyzed by Southern hybridization in the present work (Figure 28) and confirmed by sequencing by Popp *et al.* [274].

Derivatives of mating product EM1 retained only hyperactive *ERG11* and *MRR1* alleles and the *MTL***a** locus, which was linked with the hyperactive *ERG11* allele in EM1. Derivatives of ME1 had lost all wild-type *MRR1* alleles. The most resistant progeny of ET1 (ET1P7A-3) had lost the wild-type *TAC1-1* allele and contained a decreased amount of the hyperactive *ERG11* and the linked *MTL***a**. TE1 progeny with the highest resistance level (128µg/ml) had lost all wild-type *TAC1* alleles but kept mutated *ERG11* alleles and the *MTL*α. The Southern blot signal of the hyperactive *ERG11* alleles and the *MTL*α locus were furthermore increased in comparison to the parental mating product. Interestingly, the wild-type *TAC1*, the hyperactive *ERG11* allele and the *MTL*α locus were located on the same chromosome in the parental mating product TE1, suggesting that a mitotic recombination event took place in this strain, by which the wild-type *TAC1* and the hyperactive *ERG11* alleles were separated from each other. In general, the high fluconazole resistance level cannot be explained only by the loss of wild-type alleles. Other mechanisms are likely responsible as well. The analyzed progeny of EU1 had lost wild-type *ERG11* alleles and alleles of the *MTL*α locus. Furthermore, the most resistant derivative EU1P8A-3 had an increased ratio of hyperactive *UPC2* alleles. Progeny of UE1 had a reduced number of wild-type *UPC2* alleles and the most resistant derivative UE1P4A-3 had, in addition, a decreased amount of wild-

type *ERG11* and linked *MTL***a** alleles. The most resistant derivatives of MT1 had lost all wild-type *MRR1* alleles. MT1P5A-3 in addition lost all wild-type *TAC1* alleles and the linked *MTL***a** locus. Similarly, the most resistant derivative of MT2 had lost all wild-type *MRR1* alleles and a decreased amount of wild-type *TAC1* and the linked *MTL***a** locus. TM1 progeny had lost the wild-type *TAC1* and the linked *MTL*α alleles. In addition, the most resistant derivative TM1P10A-1 retained only mutated *MRR1* alleles.

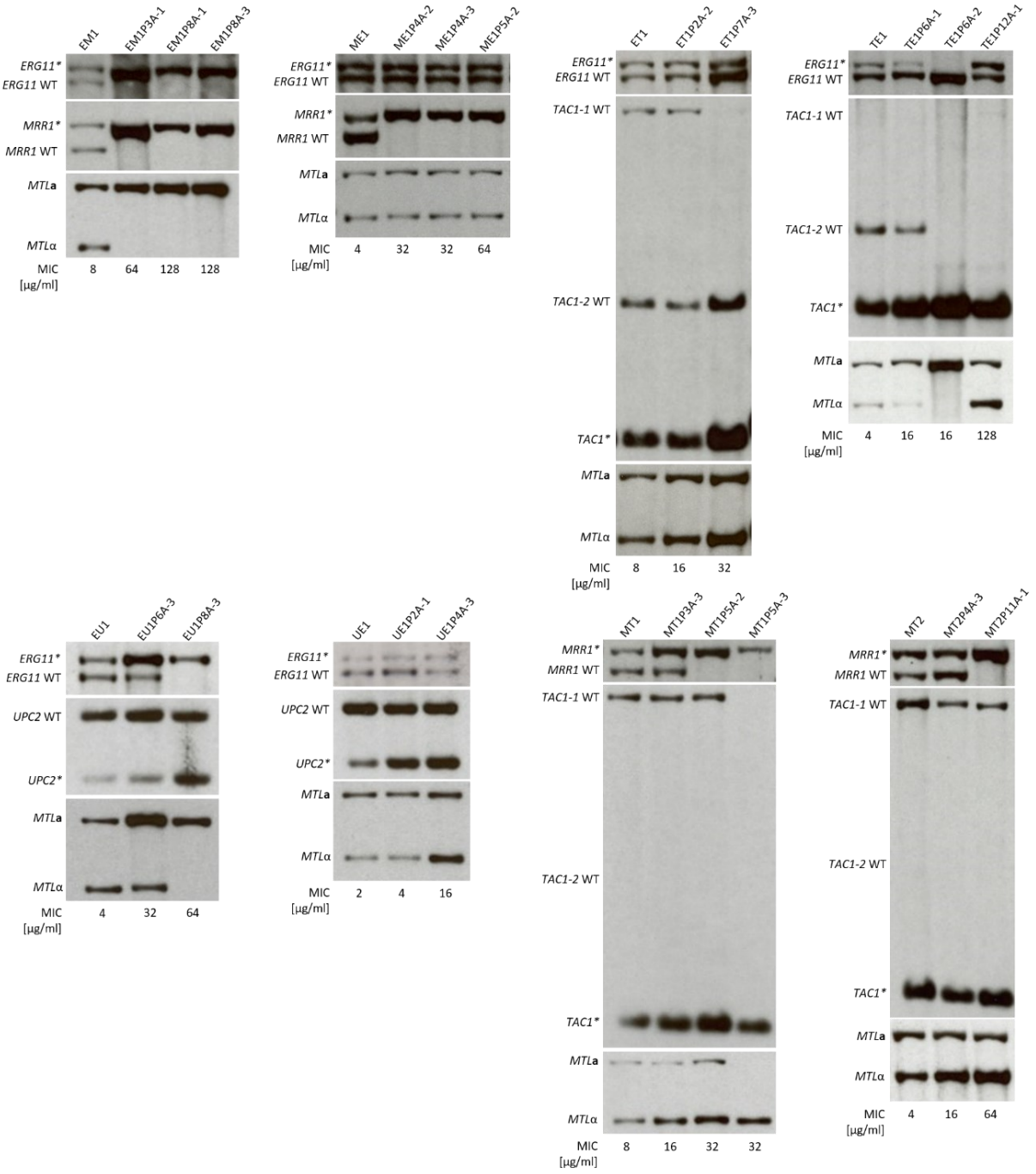

Figure 28 (continued on the next page)

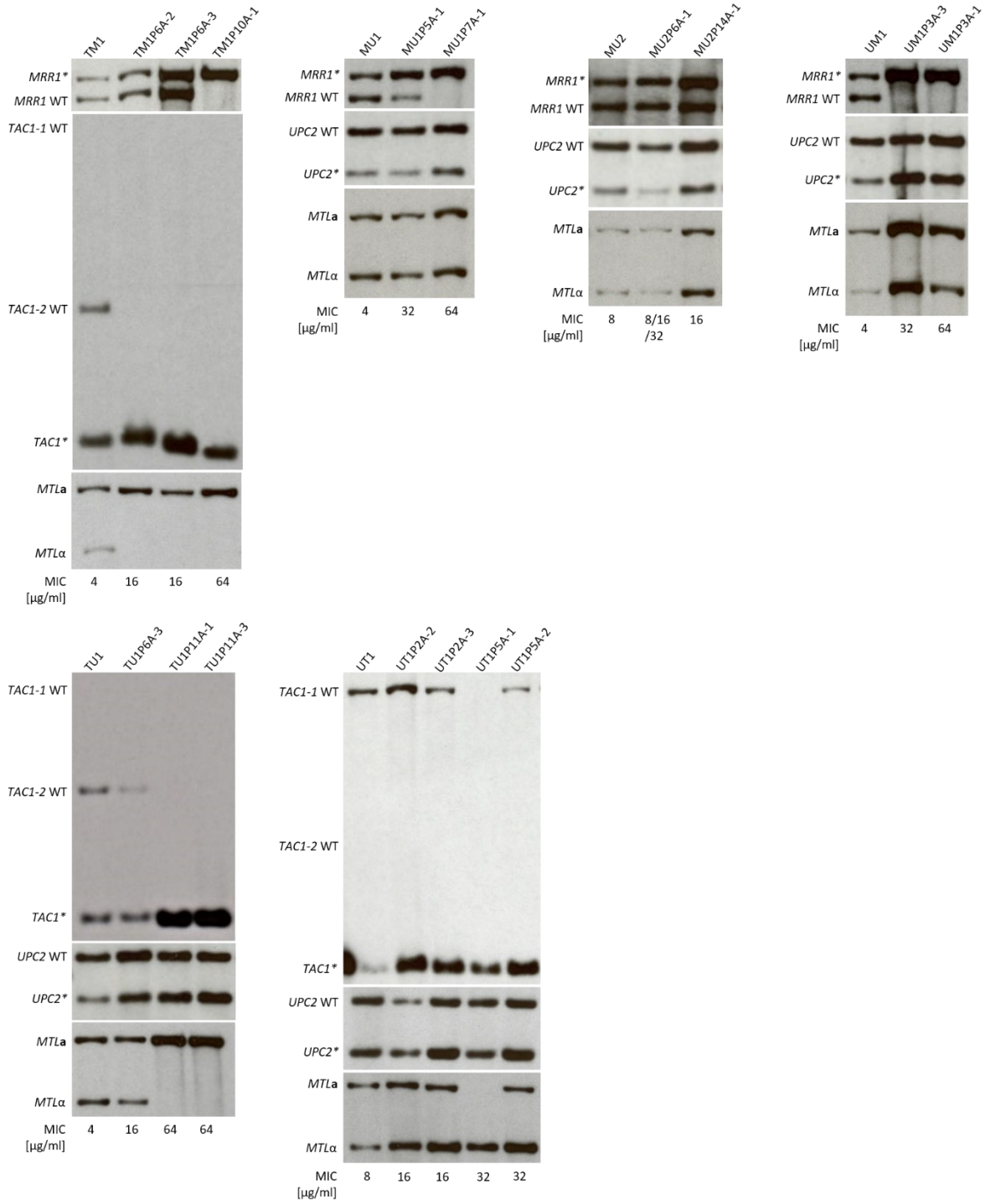

Figure 28: Genetic analysis of fluconazole resistance-associated genes and the *MTL* locus of mating product progeny and their parental strains. The *MTL* locus and resistance-associated genes *ERG11*, *MRR1*, *TAC1* and/or *UPC2* were analyzed by Southern hybridization. Restriction enzymes and probes used and a schematic showing the expected fragment sizes after hybridization are given in chapter 4.2.5.2 (Table 22, Figure 30, Figure 31). Note that the *MRR1* locus was analyzed with NsiI-digested chromosomal DNA and the *MTL* locus with EcoRI-digested chromosomal DNA and the 5'MTL probe. In some cases, different genomic DNA preparations were used for the blots. Signal intensities are caused by uneven DNA concentrations. MICs of the strains are indicated for comparison. Adapted from [274].

MU1 progeny sequentially lost wild-type *MRR1* alleles. The stable derivative of MU2 MU2P14A-1 also contained a lower amount of wild-type *MRR1* alleles. The derivatives of UM1 had lost all *MRR1* wild-type alleles. In addition, UM1P3A-3 with an intermediate resistance level had an increased ratio of

hyperactive *UPC2* alleles. The two most resistant derivatives of TU1 had lost all wild-type *TAC1* alleles together with the linked *MTL*α locus. Furthermore, the proportion of hyperactive *UPC2* alleles was increased. Most derivatives of UT1 had decreased levels of wild-type *TAC1* alleles and the linked *MTL***a** locus, as well as increased levels of hyperactive *UPC2*. The derivative UTAP5A-1 had even lost all wild-type *TAC1* and *MTL***a** alleles but did not show a changed ratio of *UPC2* alleles in comparison to the parental mating product in the Southern blots.

Ploidy of the mating product progeny was analyzed by flow cytometry measurements (Figure 29). In comparison to the parental mating products, ploidy of mating product derivatives changed. Some derivatives became diploid or near-diploid and subpopulations with different ploidies were observed. Instability of aneuploid strains became obvious by analyzing different subcultures of the same strain.

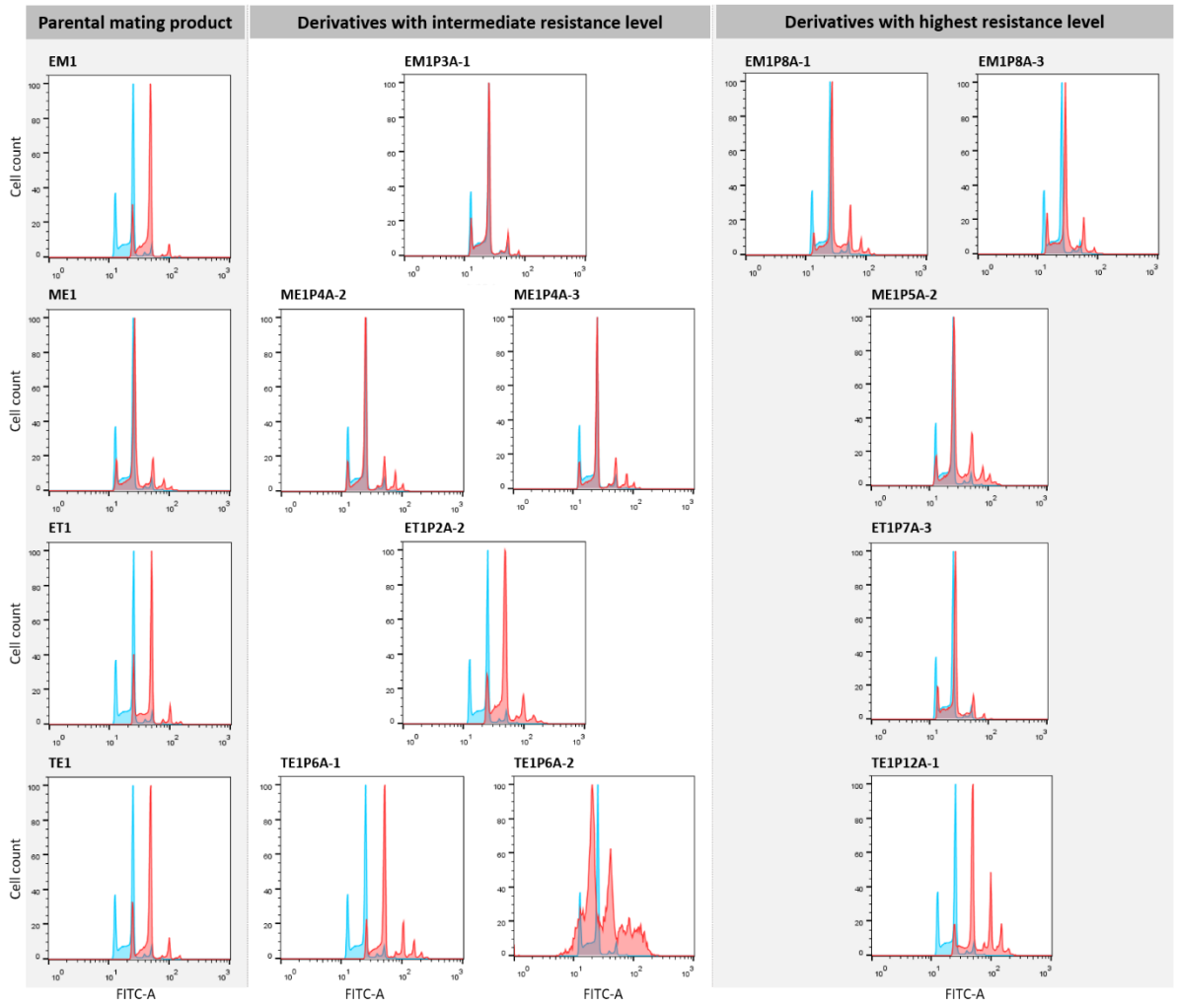

Figure 29 (continued on the next page)

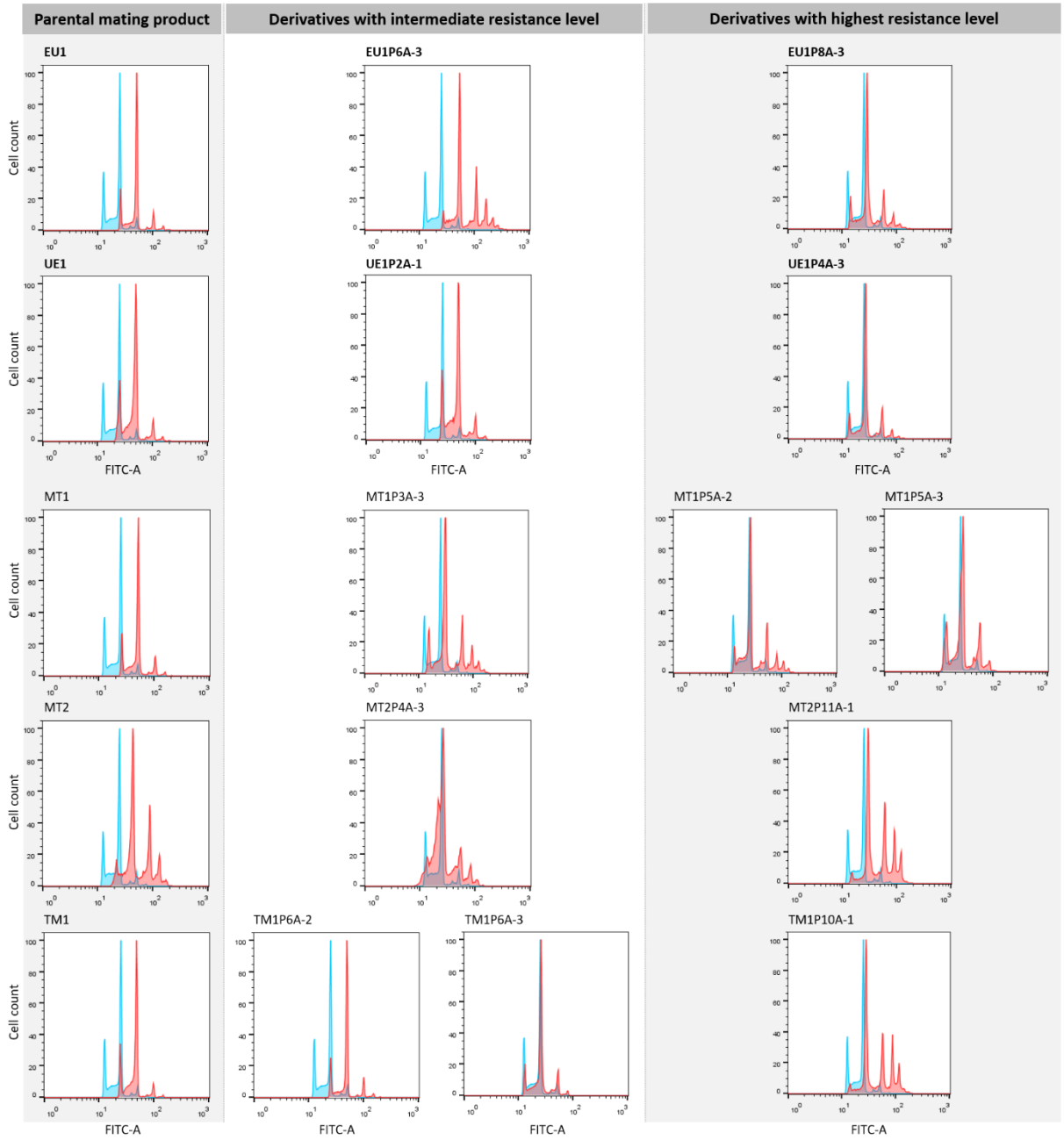

Figure 29 (continued on the next page)

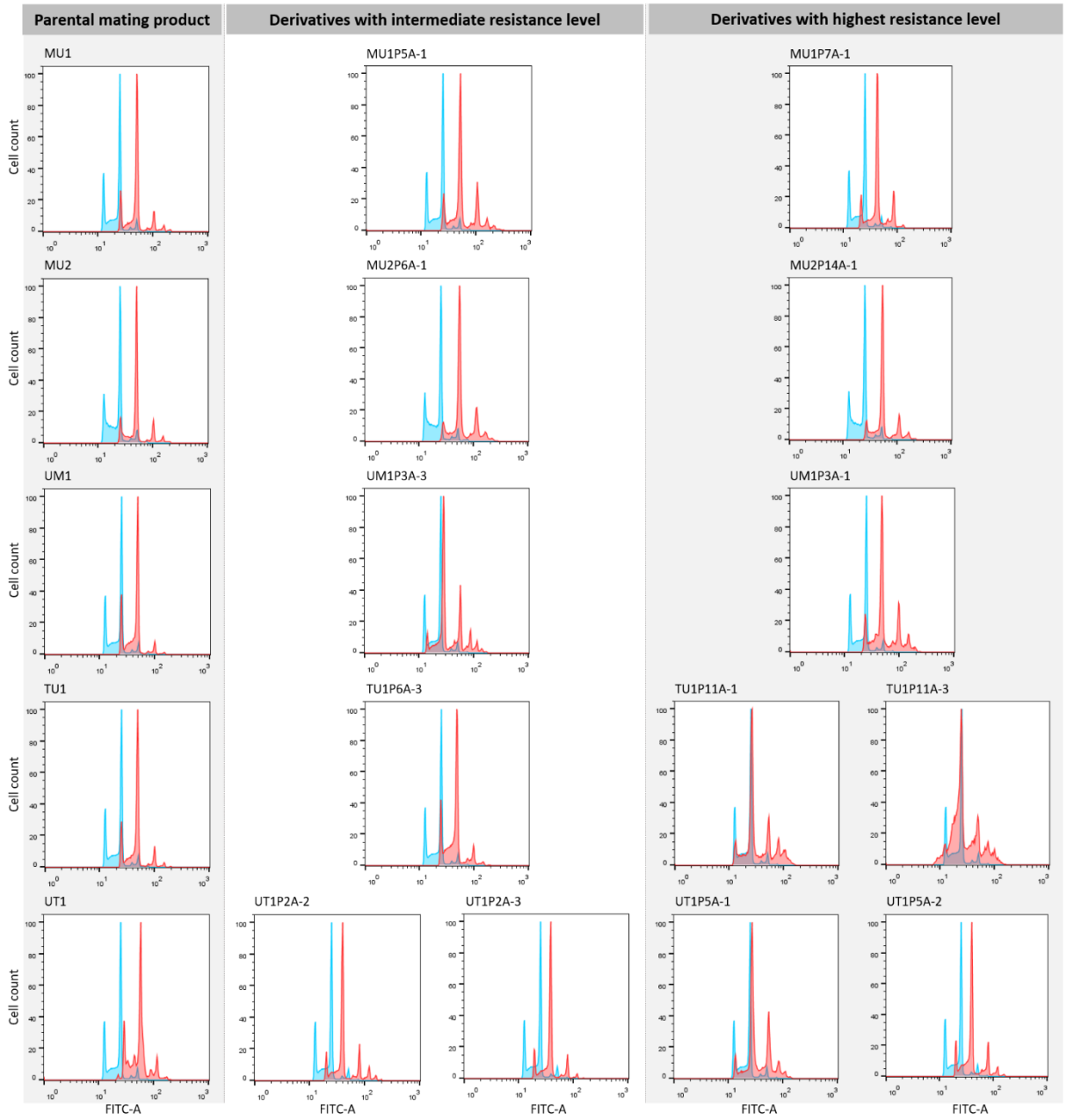

Figure 29: Ploidy of mating product progeny and their parental strains. Flow cytometry profile of the reference strain SC5314 is shown in blue and of the mating products and their progeny with intermediate and high resistance level in red. Shown are profiles of one flow cytometry measurement. Comparison of different measurements are given in Appendix A5. Adapted from [274].

Note that ET1 was passaged a second time as described in chapter 2.2.3.1 to test whether the isolation of highly fluconazole-resistant mating product progeny is reproducible for single strains. Isolated derivatives of this experiment are listed in Appendix A4. As in the first experiment, mating product progeny with an increased resistance level of 32µg/ml were also isolated in the second experiment (comparison in Appendix A6). One of both isolated strains (ET1P6B-1) had less *ERG11**, wild-type *TAC1-1* and *MTL***a** alleles like ET1P7A-3 (MIC 32µg/ml) isolated during the first experiment. Note that ET1P7A-3 lost all wild-type *TAC1-1* alleles. The FACS pattern was near-diploid for both strains. ET1P6B-3, an isolate from the second experiment, had also lost all wild-type *TAC1-1* alleles. A comparison of the Southern blots is shown in Appendix A7 and a comparison of the FACS profiles in

Appendix A8. Furthermore, a derivative with a resistance level of 64µg/ml was isolated during the second passaging experiment. This strain contained more mutated *ERG11** than wild-type *ERG11.* A further screening of more colonies of the later passages in the first experiment would have likely also resulted in the isolation of a strain with a MIC of 64µg/ml.

In conclusion, it may be stated that tetraploid mating products with a combination of different resistance mechanisms can rapidly adapt to environmental pressure conferred by fluconazole by reassorting the chromosomes in an advantageous way. In the present study, strains mostly became highly drug-resistant by the loss of wild-type alleles and retention of hyperactive alleles.

3. Discussion

3.1. Fitness costs of drug resistance are not easily compensated by *Candida albicans*

A key factor in the evolution and genomic stability of drug resistance in *C. albicans* is in how resistance mutations affect the fitness of this organism. Fitness is defined as the likelihood of a strain to grow as efficiently as other strains [276] and therefore, not being outcompeted by other strains in a population. Hyperactive zinc cluster transcription factors in *C. albicans* (*MRR1*, *TAC1* and *UPC2*) cause an increased fluconazole resistance and thereby confer a selective advantage in the presence of the drug [121]. Nevertheless, resistance mutations can come with a fitness cost [121]. In general, an appropriately regulated gene expression is necessary for cells to adapt to the environment. Several studies describe antifungal drug resistance as accompanied by complex changes in gene expression spanning the whole transcriptome, even when only one resistance mutation was present. These changes also persisted in the absence of the drug [277-280]. This disequilibrium in gene expression could lead to a waste of energy since unnecessary gene products are being produced [124]. The permanently altered gene expression could therefore cause an inadequate behavior in conditions other than drug challenge and reduce the capacity to adapt to host niches [124]. In line with this, many but not all changes in resistant cells are connected to drug resistance. Exactly which specific changes in resistant cells are linked to fitness costs in certain conditions is not known [124]. Presumably, the fitness defect has different causes [124], since, for example, different genes are controlled by the ZnTFs Mrr1, Tac1 and Upc2 [97, 98, 114].

Sasse *et al.* [121] analyzed the effect of resistance mutations in these ZnTFs *MRR1*, *TAC1* and *UPC2* on the resistance level and on the fitness of the strains in the absence and presence of fluconazole. For this purpose, isogenic strains with the resistance mutations P683S in *MRR1*, G980E in *TAC1* and G648D in *UPC2* were examined in the background of the wild-type SC5314. Indeed, each gain-of-function mutation (GOF), on one hand, caused a higher resistance level against fluconazole. On the other hand, the GOFs triggered a mild fitness defect under non-selective conditions particularly in rich medium. Nevertheless, the fitness defect of single hyperactive transcription factors depended on the environmental conditions. In minimal medium and in a mouse model of gastrointestinal colonization, no fitness defect was measured for strains with only a single GOF. In cells with a combination of two or three GOF mutations, the fitness defect was more evident. Furthermore, in a mouse model of gastrointestinal infection, strains with a combination of all three GOFs had a strongly reduced fitness, whereas in fluconazole-treated mice the triple mutant outcompeted the susceptible strain. Contrary to this observation, fluconazole-resistant clinical isolates did not show a fitness defect in other studies, either *in vitro* or *in vivo* in the absence of the drug [125, 141]. These strains could have compensated

for the costs of drug resistance by further evolution. Indeed, drug resistant strains isolated at earlier timepoints showed a lower fitness, while isolates from later timepoints exhibited an increased fitness [125], suggesting compensatory variations leveling out the costs of drug resistance. This is consistent with studies in antibiotic-resistant bacteria in which compensatory mutations are well-described [281, 282]. In the present study the fitness of clinical isolates with one or a combination of different resistance mutations in *MRR1*, *TAC1* and *UPC2* was analyzed to reveal whether they overcame the fitness defect caused by the hyperactive transcription factors through compensatory mutations. Note that a major part of the data described in chapter 2.1 and 3.1 was published and discussed by Popp *et al.* [266].

First, ten clinical isolate pairs with GOFs in *MRR1*, *TAC1* and/or *UPC2* were analyzed. The fitness of each fluconazole-resistant clinical strain with resistance mutation(s) was examined in competition with the matched fluconazole-susceptible partner. The fluconazole-resistant and the respective fluconazole-susceptible strains were sampled from the same patient who was clinically treated with fluconazole. Most fluconazole-resistant isolates showed a lower competitive fitness than their fluconazole-susceptible partner *in vitro* in rich medium (Figure 3). This suggests that the costs of drug resistance of a deregulated gene expression are not easily overcome. Interestingly, the three strains 1587, 6692 and F5 did not show a fitness defect when grown in competition with their respective partner. The common denominator of these strains is a GOF in *MRR1*, and these strains overcame the fitness defect presumably mainly caused by this hyperactive zinc cluster transcription factor. Note that F5 encodes an additional GOF in *UPC2*, where glycine is substituted by serine at the position 648. Sasse *et al.* [121] examined genetically engineered strains with a *UPC2* GOF at the same position in which glycine was exchanged by aspartic acid in the SC5314 genetic background. These strains exhibited a slight fitness defect when grown in competition with the wild-type strain SC5314 *in vitro* in rich medium. It is worth mentioning that all analyzed isolates originated from the human oral cavity and the fitness effect in YPD medium may not be reflected by the fitness in their original habitat.

Hyperactive *MRR1* regulates gene expression differently in various *C. albicans* strain backgrounds. Previous studies have found that the substitutions P683S and G997V cause an upregulation of a core set of genes in the genetic background of SC5314, F5 and G5. Nevertheless, gene expression patterns differed between the strains. Not all genes, that were upregulated in SC5314 containing hyperactive *MRR1* alleles were found to be upregulated in the clinical isolates F5 and G5. However, F5 and G5 did show an upregulation of additional genes in a Mrr1-dependent and -independent manner [98, 107]. Therefore, hyperactive *MRR1* alleles in distinct strain backgrounds could also affect the fitness of the strains in different ways. For this reason, all *MRR1* GOFs of the ten fluconazole-resistant clinical isolates were introduced into the SC5314 background.These strains were mixed with the wild-type strain

SC5314 in competition experiments. Indeed, each *MRR1* resistance mutation in the genetic background of the wild-type strain caused a significant fitness defect under non-selective conditions (Figure 4). Nevertheless, the strains 1587, 6692 and F5 did not show a fitness defect in competition with their respective fluconazole-susceptible partner under non-selective conditions *in vitro* and therefore, overcame the fitness defect caused by hyperactive *MRR1* alleles.

Two scenarios of how these strains compensated for the costs of drug resistance were conceivable. One possibility is that the strains developed a genetic background in which the resistance mutations do not cause a fitness defect during adaptation to the environment prior to the acquisition of the *MRR1* GOFs. Another possibility is that the strains acquired the resistance mutations, followed by the compensatory mutations. Therefore, *MRR1* resistance mutations of the strains 6692 and F5 were introduced into the genetic background of the fluconazole-susceptible partner 5833 and F2, respectively, and competition experiments were performed (chapter 2.1.6). Surprisingly, in the background of the matched fluconazole-susceptible partner, the *MRR1* GOF mutations did not cause a significant fitness defect *in vitro* (Figure 6). In conclusion, these strains had acquired a genetic background in which the acquisition of a *MRR1* resistance mutation did not cause a fitness defect.

It should be discussed that *TAC1* and *MRR1* resistance mutations in the genetic background of the wild-type SC5314 did not cause a fitness defect *in vitro* in a previous study by Lohberger *et al.* [106]. This observation stands in contrast to the results of the study of Sasse *et al.* [121] and of the present work in which each *MRR1* resistance mutation in the genetic background of SC5314 caused a significant fitness defect (Figure 4). Several reasons could be responsible for this difference. Lohberger *et al.* [106] used a different medium for *in vitro* competition experiments. Their yeast extract-peptone-dextrose medium contained half of the standard amount of peptone (1% rather than 2%) and yeast extract (0.5% rather than 1%). This medium resembles the minimal medium used by Sasse *et al*. [121], in which the fitness defect caused by GOFs was not obvious. Furthermore, Lohberger *et al*. [106] co-incubated the strains for around seven generations with a starting concentration of 3.7×10^6 cells in the culture. In contrast, Sasse *et al.* [121] incubated the co-cultures for 14-15 generations with a starting optical density of 0.002, and in the present study two co-cultures were grown for 14 generations each. Therefore, another reason for the observed differences might be in the growth of the strains for a greater number of generations, which enhanced growth differences and made fitness defects more clearly detectable.

Furthermore, a study by Ford *et al.* [125] observed a similar fitness of TW1 and TW17 *in vitro*, while in the present study TW17 showed a statistically significant fitness defect in competition with its fluconazole-susceptible partner TW1 *in vitro* (Figure 3). One possible reason for these differing findings is that Ford *et al*. [125] co-cultured the strains TW1 and TW17 with an unrelated, genetically marked

strain. In addition, Ford *et al*. [125] performed competition experiments in RPMI medium. *C. albicans* strains grow more slowly in RPMI medium than in rich medium (YPD), which was used in the present study. In addition, Ford *et al*. [125] co-incubated the strains for only five to ten generations. A longer time of co-incubation along with optimal growth conditions in the present study might be the reason that the fitness defect of TW17 was more clearly revealed.

The present study also examined the fitness of selected clinical isolate pairs *in vivo* in mouse models of gastrointestinal colonization (GI) and disseminated infection (IV). For these experiments, two strain pairs were selected, of which the fluconazole-resistant strains were outcompeted by their respective susceptible partner *in vitro* (B3/B4 and TW1/TW17). In addition, two strain pairs were chosen, of which the fluconazole-resistant strains were able to compete with the respective susceptible partner *in vitro* (5833/6692 and F2/F5). It was found in the mouse model of gastrointestinal colonization that B4, F5 and 6692 were outcompeted by their susceptible partners (Figure 7). Furthermore, TW17 showed a slight but significant fitness defect. In contrast, in the mouse model of disseminated infection only 6692 was slightly outcompeted by its susceptible partner, while the other strains did not show a significant fitness defect during infection of the kidneys (Figure 8). Although B4 showed a tendency of a fitness defect in competition with B3, it was not statistically significant. It can be concluded that in the present work the *in vitro* fitness did not reflect the *in vivo* fitness.

It should be mentioned that the *in vivo* fitness in mice may also not reflect the fitness of the strains in the human host. All clinical isolate pairs examined during the present study were isolated from HIV-infected patients with oropharyngeal candidiasis. The human environment profoundly differs from the conditions encountered by *C. albicans* in mice. For example, even though an oral candidiasis mouse model is well established, it differs from the environment of human oral infection. Histatin 5 is an antimicrobial peptide that is very active against *C. albicans* and present in the saliva of humans and other primates, but is not present in mice [283]. Furthermore, the successful colonization of *C. albicans* in the oral cavity and other niches is stronly dependent not only on the immune status, but also on the bacterial microflora of the host. The microflora varies between mice and humans, as well as among individuals. Therefore, the fitness effect further depends on the specific individual.

Note in this regard that the proportions of the strains isolated from individual mice infected with the same inoculum in an *in vivo* experiment varied highly in the present study. This phenomenon has been previously described in other studies as well [173, 174, 284, 285]. The less fit strain can sometimes outcompete the fitter strain in different mice infected with the same inoculum. One possible reason for this phenomenon is infection bottlenecks. In studies of population dynamics and evolution, this concept is used to describe events that drastically limit population size and frequently cause genetic drift [286]. Such host bottlenecks can represent defenses of infection and intrinsic characteristics of

the host environment such as nutritional limitations and innate and adaptive immune defenses [287]. It is also conceivable that the constitutive overexpression of target genes of hyperactive zinc cluster transcription factors causes a selective advantage in certain conditions in a particular mouse, comparable with the advantage under selective conditions like fluconazole exposure.

Interestingly, in the present study no fluconazole-resistant *C. albicans* strain was more fit than the respective susceptible partner in the tested *in vitro* and *in vivo* conditions. In contrast, in *Candida glabrata*, resistance mutations in Pdr1 confer azole resistance and increased virulence [288-291]. Furthermore, resistant *C. glabrata* strains probably get transmitted from patient to patient [292]. Although the tested drug-resistant *C. albicans* strains did not show a fitness defect in some conditions, there was not a single case in which they were more fit than the respective drug-susceptible partner. Therefore, in a population without the selective pressure of fluconazole, drug-resistant isolates would presumably be outcompeted by fluconazole-susceptible *C. albicans* strains.

3.2. Mating in clonal *C. albicans* populations is an adaptation mechanism to environmental stresses

Even though hyperactive *MRR1*, *TAC1* and *UPC2* alleles can cause a fitness defect under non-selective conditions depending on the growth conditions and the colonization/infection model (chapter 2.1 and 3.1), they confer a selective advantage in the presence of the drug fluconazole [121, 266]. This selective advantage is rooted in increased drug resistance caused by different mechanisms. Such mechanisms include the constitutive overexpression of the efflux pumps *MDR1* and *CDR1*/*CDR2*, which is provoked by the hyperactive zinc cluster transcription factors Mrr1 and Tac1, respectively [104-107, 109-112, 114, 266]. Another well-characterized resistance mechanism is the overexpression of the drug target *ERG11*, which is caused by hyperactive Upc2 [93-96, 266]. In addition, the drug target *ERG11* itself can be altered by resistance mutations whereby the efficiency of drug binding to this sterol 14α-demethylase is reduced [62, 73, 264, 265]. Diverse resistance mutations in *ERG11*, *MRR1*, *TAC1* and *UPC2* affect the resistance level of *C. albicans* differently and the combination of several of these resistance mechanisms in one strain increases drug resistance [121, 266]. Patients often harbor highly drug resistant strains with a combination of different resistance mutations [62, 73, 75, 104, 119, 121, 264, 266]. One example is isolate TW17, which was collected from an HIV-infected patient with recurrent oropharyngeal candidiasis who was treated with an azole drug [75]. This strain harbors resistance mutations in *MRR1*, *TAC1* and *UPC2* as described in Table 1. In this regard the question that arises is how such isolates acquire several different resistance mechanisms. One possibility is successively arising mutations [124]. It is also plausible that cells acquire different resistance mutations

independently, mate with each other and thereby exchange these mutations. From these mating products comprising the genetic material of both parental cells, genetically diverse offspring could be generated, some of which are highly drug-resistant and therefore better adapted to the stressful environment. This hypothesis was analyzed in the present work.

Mating between unrelated strains is expected to be beneficial, generating genetically diverse offspring that are better adapted to relevant conditions in the host niches [274]. Nevertheless, mating between genetically different strains is probably rare since patients are generally infected with their individual *C. albicans* strain [33-35]. Population genetic studies found that the population structure of *C. albicans* is clonal and that it reproduces mainly by mitosis [293-295]. In addition, a large proportion of isolated *C. albicans* strains is *MTL* heterozygous and thus not mating-competent [24]. For mating to be possible, strains need to be *MTL* homozygous and undergo a phenotypic transition to the opaque phenotype [24-26].

Although mating and the parasexual life cycle have been studied *in vitro* for a long time, the degree to which this phenomenon happens in nature has been critically discussed [296-299]. Through analysis of haploid mitochondrial genomes by MLST, early proof for mating in nature was found. Some of these genomes encoded allelic variants that were also identified in other lineages of *C. albicans* [298, 299]. Evidence for recombination between diverse *C. albicans* lineages in nature was also found by analysis of 182 isolates. This study found two genetic clusters with genetic signatures from two or more other clusters [153]. Wang *et al.* [166] found that in 21 sequenced *C. albicans* isolates of different clades, infection niches and countries, a subset of the strains had mosaic genomes as a result of mating between different clades. It should be noted that these events could be ancient as well.

The very fact that *C. albicans* has the ability to mate implies that this could be a relevant mechanism for adapting to a changing and stressful environment through the generation of diversity, upon which selection can act [23, 300, 301]. This adaptation is more rapid than is possible by asexual propagation [196, 302]. Therefore, genetic variation and new phenotypes could be generated by mating of genetically similar cells [181, 186]. Different *C. albicans* cells can develop different strategies to cope with the stress induced by drug exposure. Therefore, in a clonal population, cells could acquire different resistance mutations. In general, the mutation rate of *C. albicans* in standard laboratory medium is estimated at 1.2×10^{-10} per base pair per generation [156]. In other model yeasts, similar mutational frequencies are described [303, 304]. *In vivo* generation times are difficult to determine, making it more challenging to estimate mutational frequencies of *C. albicans*. Nevertheless, *in vivo* base substitution rates exceeded *in vitro* values in given time intervals. This observation is in line with the hypothesis that pressures in the host facilitate and/or preserve mutations [152, 156].

Furthermore it has been shown that strains that are homozygous for a resistance mutation have a selective advantage under drug exposure in comparison to strains that are heterozygous for the same resistance mutation due to an increased drug resistance [121]. Cells with individually acquired heterozygous resistance mutations could become homozygous for these resistance mutations and, at the same time, for the *MTL* locus under selective pressure. Indeed, genomic recombination can affect not only the resistance-associated locus, but also the *MTL* locus, causing a homozygosity at both loci [267, 269]. In turn, strains that are homozygous for the *MTL* locus are able to switch to the opaque phenotype which is the mating-competent form of the yeast [24, 25]. These cells could mate with each other and generate recombinant mating progeny with a combination of different resistance mechanisms.

In certain environmental conditions, the instable tetraploid mating products lose chromosomes randomly [23, 183]. Aneuploid derivatives of tetraploid mating products show broad fitness and virulence differences [186]. Out of a variety of strains generated in this way, the most adapted will dominate the population in a stressful environment. Therefore, an open question of the present work addresses how mating progeny with combined resistance mechanisms evolve under the selective pressure caused by fluconazole. Do highly adapted and therefore highly drug resistant strains arise by mating in the presence of fluconazole?

In general, fluconazole resistance is an ideal example for studying the role that parasexual recombination plays in adaptative evolution, since resistance can be acquired by diverse mechanisms and the combination of these mechanisms increases drug resistance. The acquisition of adaptative mutations of single cells in a clonal population and the exchange of these mutations by mating could be a way of adaptation to environmental stresses of *C. albicans* in general. An overview of the investigated hypothesis is outlined in Figure 9. Note that the majority of the data described in chapter 2.2 and 3.2 was published and discussed by Popp *et al.* [274].

3.2.1. Drug-induced *MTL* homozygous cells can mate with each other to generate mating products with combined genetic backgrounds

An important precondition for switching to the mating-competent opaque phenotype of *C. albicans* cells is a homozygous *MTL* locus (*MTL***a** or *MTL*α) [24, 25]. Nevertheless, most isolated *C. albicans* strains are heterozygous for the *MTL* locus [24, 269, 305]. LOH can take place spontaneously by mitotic recombination or by transient aneuploidies and the frequency of such events is increased under stress conditions like fluconazole exposure [130, 148]. In general, fluconazole-induced LOH in the absence of

GOFs is possible. Nevertheless, in a population under the selective pressure of fluconazole, cells with a homozygous resistance mutation would be enriched, due to an increased drug resistance [121].

In the present study, isogenic strains heterozygous for the *MTL* and a resistance mutation (*ERG11**, *MRR1**, *TAC1** or *UPC2**) were passaged in the presence of fluconazole to induce a LOH for both loci. The effect of these resistance mutations on the resistance level and on the fitness of the strains is described in detail in the study by Sasse *et al.* [121] (see chapter 3.1). The authors examined isogenic strains with a G646S mutation in *ERG11*, which affects the affinity of fluconazole to its target Erg11 [84]. It has been described that this amino acid substitution reduces the enzyme activity [84] and it was identified in a number of fluconazole-resistant clinical strains [62, 73, 119, 265, 306-311]. In addition, strains with a P683S resistance mutation in *MRR1*, which had been found in a number of fluconazole-resistant clinical isolates [104, 107], were analyzed. As an amino acid substitution in *TAC1*, G980E was chosen, which was already described in fluconazole-resistant clinical strains [109, 111], and the G648D substitution was selected for *UPC2*. All four resistance mutations did confer different levels of drug resistance, which was even potentiated when the strains were homozygous for the hyperactive allele [121].

Instead of using strains with different auxotrophies and then selecting prototrophic mating products or using a dominant selection marker, as it is often done, different screening methods were applied in the present study. First, a screening for faster growth of resistance mutation homozygous strains in comparison to resistance mutation heterozygous strains on solid agar containing fluconazole was tested. The aim was to isolate *MTL* and resistance mutation homozygous strains. Indeed, seven *MTL* and *TAC1** homozygous strains were isolated in this way (Table 4) [271]. In contrast, strains with a heterozygous resistance mutation in *ERG11* were not distinguishable by colony size from strains with a homozygous resistance mutation in *ERG11* [271]. In addition, although strains with a heterozygous resistance mutation in *MRR1* were distinguishable from strains with a homozygous resistance mutation by colony size, only resistance mutation homozygous strains which retained both *MTL* alleles were isolated in this way [271]. *MRR1* is located on chromosome 3 and the *MTL* locus on chromosome 5. Hence, genomic rearrangements affecting at least two chromosomes are necessary to obtain LOH at both loci (Figure 10). Nevertheless, only a few colonies were picked and examined for a LOH at the *MRR1* and *MTL* locus. It is possible that strains could have been isolated with a LOH for both loci, had more colonies been examined. Nevertheless, due to the low probability of isolating strains homozygous for both the *MRR1* and the *MTL* through screening for faster growth on agar plates containing fluconazole, a screening for white-to-opaque switching-competent cells was performed. Twenty-nine *ERG11** and *MTL* homozygous strains (Table 6) and six *MRR1** and *MTL* locus homozygous strains (Table 5) were isolated in this way. *UPC2** heterozygous strains were not distinguishable from

*UPC2** homozygous strains by colony size on agar containing fluconazole [271]. In addition, *UPC2* is located on a different chromosome (chromosome 1) than the *MTL* locus. Therefore, the screening for white-to-opaque switching-competent cells was applied for *UPC2** heterozygous strains as well. Nine *MTL* homozygous strains with a resistance mutation in *UPC2* were isolated (Table 7). These strains remained heterozygous for the mutated allele. Strains with a homozygous *UPC2*^{G648D} allele have only a slightly increased resistance level when compared to strains with a heterozygous mutated allele [121]. Presumably, this gain of resistance was not enough to select for a LOH at this locus under the tested conditions. Since at least 2 strains with opposing *MTL* configurations (*MTL***a** and *MTL*α) and a homozygous or heterozygous resistance mutation in *ERG11*, *MRR1*, *TAC1* and *UPC2* were isolated, no further efforts were made to improve the experimental conditions.

Interestingly, while screening for *MTL* homozygous strains with hyperactive *MRR1* alleles, all isolated *MTL* homozygous strains were homozygous for the hyperactive *MRR1* allele as well, although *MRR1* is located on a different chromosome. This sustains that in a *MTL* homozygous subpopulation under fluconazole exposure, the more resistant strains (e.g. *MRR1** homozygous) will outcompete strains with a lower resistance level (e.g. *MRR1** heterozygous) due to a selective advantage in this stressful condition, as it has been stated by Sasse *et al.* [121].

Furthermore, the resistance level of all isolated strains was examined (Table 4, Table 5, Table 6, Table 7). Strains which had become homozygous for the *MTL* locus and for *ERG11**, *MRR1** or *TAC1** had a one to two MIC values increased resistance level in comparison to their *MTL* and resistance mutation heterozygous parental strains. The *ERG11**, *MRR1** or *TAC1** homozygous strains reached the resistance level of constructed strains with homozygous resistance mutations in *ERG11*, *MRR1* or *TAC1*, respectively. Isolated strains with a homozygous *ERG11** allele reached even a one MIC value higher resistance level in comparison to strains in which the *ERG11* resistance mutation had been introduced by genetic engineering in both alleles. It is likely that further resistance mechanisms in addition to the homozygous *ERG11** are responsible for this difference. Unsurprisingly, *MTL* homozygous isolates, which remained heterozygous for the *UPC2* resistance mutation, exhibited the same resistance level as the parental strains. Only one isolate had an increased resistance level of 16µg/ml, probably caused by further mutations. It is worth mentioning that other studies did not find that *MTL* homozygous strains have a generally increased resistance level in comparison to *MTL* heterozygous strains [305, 312]. Nevertheless, resistance could be impaired by *PAP1* (encoding a poly(A) polymerase 1) which is contained in the *MTL* locus. *PAP1*α (encoded by the *MTL*α locus) induces hyperadenylation and enhanced stability of *CDR1* mRNA (efflux pump) when *PAP1***a** (encoded by the *MTL***a** locus) is not present [116]. However, in the present study no difference was observed in drug resistance between *MTL*α and *MTL***a** homozygous strains.

Out of all isolated strains, one *MTL***a** and one *MTL*α homozygous strain with homozygous *ERG11**, *MRR1**, *TAC1** or heterozygous *UPC2** were selected for mating experiments based on the following criteria (overview of the eight strains in Figure 13). Preferably, strains were chosen in which genomic recombination during LOH affected as few loci as possible (in addition to other criteria described below). Therefore, the polymorphism marker *GLN3* on the right arm of chromosome 5 of all relevant strains (*MTL*, *ERG11* and *TAC1* are located on the left arm of chromosome 5) and *CAP1* on the left arm of chromosome 3 of strains with LOH for the *MRR1* allele (*MRR1* is located on the right arm of chromosome 3) were analyzed (Figure 12). Strains with a LOH for *GLN3* or *CAP1* probably underwent a loss of a whole chromosome, although it cannot be excluded that several events caused the LOH at these loci. All three fluconazole-induced *TAC1** and *MTL* homozygous derivatives of SCTAC1R32A and one *TAC1** and *MTL* homozygous derivative of SCTAC1R32B were heterozygous for the *GLN3* locus, indicating a more local genomic recombination event. In contrast, three derivatives of SCTAC1R32B were homozygous for one *GLN3* allele, suggesting the loss of a whole chromosome. Two *TAC1** and *MTL* homozygous isolates that remained heterozygous for *GLN3* were selected for mating experiments. All isolates which were *MRR1** and *MTL* homozygous were homozygous for one *GLN3* allele, probably by loss of a homolog of chromosome 5. Four of the strains retained both *CAP1* alleles, indicating that LOH for *MRR1** was more likely to occur by a local event. Two of the three derivatives of SCMRR1R32B lost one *CAP1* allele, implying a loss of a whole chromosome 3. The two selected *MRR1** and *MTL* homozygous strains probably lost one homolog of chromosome 5 (homozygosity of *GLN3*) and became homozygous for *MRR1** by a more local event on chromosome 3 (heterozygosity of *CAP1*). All isolated *ERG11** and *MTL* homozygous derivatives of the parental strain SCERG11R32B were still heterozygous for the *GLN3* locus. However, all double-homozygous descendants from parental strain SCERG11R32A were homozygous for one *GLN3* allele. Of each parental strain one double-homozygous descendant was selected. Therefore, one *GLN3* homozygous and one heterozygous strain were used for mating experiments. All fluconazole-induced *MTL* homozygous and *UPC2** heterozygous strains underwent genomic rearrangements affecting larger parts of the genome, since these isolates were homozygous for *GLN3.* Only isolate U12 remained *GLN3* heterozygous. This strain was excluded from further analysis since it had a strongly wrinkled opaque colony phenotype. Therefore, both selected *MTL* homozygous and *UPC2** heterozygous strains were homozygous at the *GLN3* locus.

The mating-competent opaque form of the selected strains was needed for mating experiments. For a long time, it was believed that the epigenetic switch to the opaque phenotype happens only stochastically [26, 204, 206]. However, many different inputs are presumably responsible for the final switching frequency of a cell, since many genes have been described to be involved in switching [313], and it has been shown that depending on the environment, the frequency of white-to-opaque

switching can vary over several hundred-fold [314]. Interestingly, various conditions that reflect certain niches in the human host cause white-to-opaque switching [209, 211, 212, 214]. Therefore, an additional criterium for the selection of the strains was the white-to-opaque switching frequency and the stability of the cells in the opaque phenotype under different conditions (room conditions, conditions with high CO_2 concentrations). Indeed, all analyzed strains were switching-competent with a stable opaque phenotype. Furthermore, the isolates were supposed to grow white and opaque colonies with reproducible phenotypes. Hence, white and opaque cells were grown under room conditions for several days at least three times independently. In addition, cells of the same strains were also grown at least three times independently at high CO_2 concentrations for two days (induction of switching), followed by an incubation under room conditions for several days (Figure 15). Strains growing in different colony sizes under these conditions, as was the case for some *MRR1** and *MTL* homozygous isolates and *UPC2** heterozygous and *MTL* homozygous strains, were excluded from further characterization and mating experiments.

Some strains generally grew smaller white and opaque colonies on Lee's agar with phloxine B in comparison to the control strains SCMTLaM2A, SCMTLαM2A and WO-1 (Figure 15). Out of the selected strains this was observed for SCERG11R32hom1A, SCMRR1R32hom1A and SCUPC2R12hom1B (Figure 15). Ploidy analysis found that these strains had subpopulations with differing ploidy levels. Although *C. albicans* is quite tolerant of aneuploidy, it can come with a cost [267], which could be a possible explanation for the observed growth defect.

Furthermore, filamentation was found in opaque colonies of the *MTL* and *TAC1** homozygous isolates (Figure 15). These filaments could be white or opaque. Presumably loci relevant for filamentation were also affected by the genomic recombination events causing the LOH at the *TAC1* and *MTL* locus. Nevertheless, slight filamentation was also observed in opaque colonies of the *MTL* hemizygous control strains SCMTLaM2A and SCMTLαM2A under the tested conditions. Hence, the agar composition could be another reason for the observed filamentation. Lee's agar contains amino acids that have been described to induce filamentation in *C. albicans* [275].

An overview of the eight strains which were selected for mating experiments with the described criteria is given in Table 8. Mating experiments with these isolates were performed in all possible combinations (Figure 19). One challenge of the present work was the identification of mating products. Constructed strains with a combination of two homozygous or one homozygous and one heterozygous *ERG11**, *MRR1**, *TAC1** or *UPC2** allele(s) had a higher resistance level than strains with only one corresponding homozygous or heterozygous allele. Nevertheless, in an initial experiment these strains with a combination of different resistance mutations did not show an improved growth on agar containing fluconazole (Figure 20, Figure 21, Figure 21). For this reason, mating products were not

identified by colony size. As long as they did not undergo a genomic recombination event by which they lost alleles of one *MTL* type, mating products have alleles of both configurations of the *MTL* locus (see overview in Figure 9). Therefore, these cells are not capable of white-to-opaque switching in contrast to their *MTL* homozygous parental strains, which makes it possible to screen for switching-incompetent cells. With this method, mating products of all twelve crosses were isolated, even without applying selective pressure (overview in Figure 19).

The isolated mating products were quite unstable. This was obvious when ploidy analysis was performed with subcultures of the frozen mating products (Figure 26). Strains exhibited peak profiles indicating DNA content higher and lower than tetraploid. In addition, population heterogeneity and, for strain TU1, even wide-ranging peak profiles in different measurements, were observed (Appendix A5). Southern hybridization revealed that some mating products no longer contained all expected mutated and/or wild-type alleles. In general, as soon as tetraploid mating products begin to lose chromosomes, they will then start to lose further chromosomes, resulting in progeny with different aneuploidies and probably a more stable euploid status [181]. Nevertheless, other studies describe mating products as more stable. One reason for this alternative finding could be that in the present study no selection pressure was applied to identify mating products. Therefore, mating products were able to begin losing chromosomes straightaway following isolation. Another conceivable reason for the observed instability of the mating products could be stress caused by the addition of phloxine B, a derivative of fluorescein, to the agar plates.

Although mating products contained resistance mutations in two different resistance-associated genes, they did not exhibit a higher resistance level in comparison to their respective parental strains. Instead, fluconazole resistance was equal or even lower (Figure 24). In addition to the hyperactive *ERG11*, *MRR1*, *TAC1* and/or *UPC2* alleles, the mating products also contained corresponding wild-type alleles (schematic overview in Figure 25), which presumably affected the resistance level, comparable to resistance mutation heterozygous diploid strains. Popp *et al*. [274] examined this hypothesis. First, the resistance level of genetically engineered diploid strains with two heterozygous resistance mutations in all possible combinations (*ERG11**, *MRR1**, *TAC1** and *UPC2**) was tested. These strains had a lower fluconazole resistance level than constructed strains that were double homozygous for the two respective resistance mutations. Some strains had an even lower resistance in comparison to corresponding strains with only one homozygous resistance mutation. Second, mating experiments with fluconazole-induced *MTL* homozygous strains with resistance mutations in *MRR1* or *TAC1* were performed with strains with the same resistance mutation or wild-type alleles and the opposite mating type locus. Afterwards, the MIC of the resulting mating products was examined. Tetraploid mating products with four hyperactive alleles (*MRR1* or *TAC1*) had a higher resistance level than mating

products with two wild-type and two hyperactive alleles. The lowest resistance level was exhibited in the strain that contained only wild-type alleles.

Note that in the present study all isolated mating products had the same resistance level. Only isolates of the crosses MU and MT had a slightly different resistance level. The mating products could be related since most strains of the same cross were isolated in the same experiment. For each cross one mating product was selected for further experiments. From the crosses MU and MT, two strains were selected that differed in their fluconazole resistance level.

3.2.2. Mating product progeny can become highly fluconazole-resistant by reassorting the genome

Derivatives of tetraploid mating products reach the diploid or near-diploid state via an aneuploid state [25, 181, 183, 186]. During this random process of chromosome loss, genetic diversity arises since LOH of various parts of the genome, aneuploidy and recombination of homolog chromosomes takes place in a higher frequency than in diploid cells [181]. In the present study, the selected mating products (listed in Table 9) rapidly generated highly drug resistant derivatives during propagation in the presence of increasing concentrations of fluconazole. These strains reassorted their existing alleles in an advantageous way mainly by losing wild-type alleles. Nearly all mating products had derivates which were homozygous for one or both resistance-associated alleles. Some strains reached such high levels of drug resistance that other mechanisms of resistance in addition to a combination of hyperactive *ERG11*, *MRR1*, *TAC1* and/or *UPC2* alleles, likely also played a role in the development of fluconazole resistance. Hence, aneuploidy cannot be excluded as a contribution to drug resistance, since an involvement of aneuploidy in fluconazole resistance in strains without resistance mutations was shown by Hirakawa *et al.* [186]. In conclusion, in a population in which cells acquired resistance mechanisms in an independent fashion, *MTL* homozygous strains can be enriched during LOH for these advantageous mutations. These cells can mate with each other and, through the subsequent reassortment of chromosomes, better adapted and therefore highly fluconazole-resistant offspring can be generated rapidly.

As described above, during the loss of genetic material of tetraploids, intrachromosomal recombination takes place [184]. In the present study this was obvious in derivatives of the mating product TE1, in which the wild-type *TAC1*, the hyperactive *ERG11* allele and the *MTL*α locus were disconnected from each other.

In addition, mating product progeny that had become homozygous for the mating type locus was isolated. It is conceivable that these strains switch to the mating-competent opaque phenotype to mate with other strains with beneficial traits and generate progeny that is even better adapted to its environment. For example, it has been shown that strains with a combination of three or four different resistance mutations in *ERG11*, *MRR1*, *TAC1* and/or *UPC2* can achieve even higher fluconazole resistance levels than strains with two resistance mutations [121].

Furthermore, the ploidy level of the mating product progeny ranged from diploid to near-diploid to aneuploid. It has been described that fluconazole induces aneuploidies [130], which might interfere with the acquisition of a stable ploidy level during fluconazole exposure. In general, a high proportion of fluconazole-resistant clinical *C. albicans* strains is aneuploid [267]. These strains could be derived by fluconazole-induced aneuploidy of diploid cells. Nevertheless, it is also conceivable that such strains arose from mating in the host, promoting adaptation to disadvantageous conditions.

This study shows that *C. albicans* can utilize parasexual recombination in a clonal population to generate offspring that is better adapted to its stressful environment by combining drug resistance mechanisms. Furthermore, parasexual recombination may also play a role in adaptative evolution when LOH for other advantageous mutations is beneficial and *MTL* homozygous cells simultaneously accumulate. The hidden mating ability of *C. albicans* might thus play an important role in the evolution of better-adapted genetic variants, since parasexual recombination is enhanced by stress-induced genomic alterations that lead to the generation of mating competence in cells with adaptive mutations.

4. Material and Methods

4.1. Material

4.1.1. Growth media and agar

Table 11: Basic composition and optional supplements of media and agar

Growth media and agar	Basic composition	Additive substances
Amino acid stock solution	11.7g L-Leucine 9.0g L-Lysine 4.5g L-Alanine 4.5g L-Phenylalanine 4.5g Proline 4.5g L-Threonine 0.9g L-Methionine 0.63g L-Ornithine 0.63g L-Arginine Fill to 900ml with water	
Lee's	4.5g NaCl 4.5g $(NH_4)_2SO_4$ 2.25g K_2HPO_4 28ml 40% Glucose 100µl 1mM $ZnSO_4$ 810µl 1M $MgSO_4$ 1ml 1mg/ml Biotin 90ml 10x Amino Acid-stock solution Fill to 900ml with water pH 6.8	90µl 50mg/ml Phloxine B stock 18g Agar
LB (Lysogeny broth)	1% Peptone 0.5% Yeast Extract 0.5% NaCl	1.5% Agar 100µg/ml Ampicillin 50µg/ml Chloramphenicol
SD (Synthetic Defined)	0.67% Yeast nitrogen base with ammonium sulfate 2% Glucose pH 5.8	1,5% Agar 5µg/ml Fluconazole
SD with CSM (Complete Supplement Mixture)	1.34% Yeast nitrogen base with ammonium sulfate 4% Glucose 0.158% Complete supplement medium	
Spider	1% Nutrient broth 0.4% K_2HPO_4 2% Mannitol pH 7.2	1.35% Agar
YPD (Yeast peptone dextrose)	2% Peptone 1% Yeast extract 2% Glucose	1.5% Agar 50µg/ml Chloramphenicol 15µg/ml, 100µg/ml, or 200µg/ml Nourseothricin
YPM (Yeast peptone maltose)	1% Yeast extract 2% Peptone 2% Maltose	

4.1.2. General solutions

Table 12: General solutions with their basic composition used in this study.

Solution	Basic composition
5x DNA loading dye	25mM Tris-Cl pH 7.0, 25% Glycerol, 150mM EDTA, 0.05% Bromophenol blue, pH 8.0
10x PBS (Phosphate Buffered Saline)	2.7g KH_2PO_4, 14.2g Na_2HPO4, 2g KCl, 80g NaCl, added up to 1l with water, pH 7.4
10x TE	100mM Tris-HCl pH 7.5, 10mM EDTA pH 8.0
20x SSC	3M NaCl, 0.3M NaCitrat
50x TAE	2M Tris-Base, 1M Acetic acid, 0.05M EDTA, pH 8.0
50:50 TE	50mM Tris-Cl pH 8.0, 50mM EDTA pH 8.0
Breaking buffer	100mM NaCl, 10mM Tris-Cl pH 7.5, 1mM EDTA pH 8.0, 1% SDS, 2% Triton-X-100
PCI	Phenol/Chloroform/Isomylalcohol 25:24:1
Proteinase K solution	2.5mg/ml Proteinase K in 50:50 TE
RNase A solution	1mg/ml RNase A in 50:50 TE
Southern Blot Solution A	0.25M HCl
Southern Blot Solution B	1.5M NaCl, 0.5M NaOH
Southern Blot Solution C	1.5M NaCl, 0.5M Tris-Cl pH 7.5
SYBR Green solution	SYBR™ Green I diluted 1:100 in 50:50 TE
Urea wash buffer	6M Urea, 0.4% SDS, 0.5x SSC

4.1.3. Enzymes and chemicals

Table 13: Enzymes, chemicals and the company they were purchased from.

Enzymes and chemicals	Company
1kb Plus DNA ladder	ThermoFisher Scientific (Invitrogen™)
2-propanol	Roth
Acetic acid	Roth
Agarose	Roth / VWR life science (Peqlab)
Ammonium Sulfate	Roth
Ampicillin	Roth
Biotin	Applichem
Bromophenol blue	Applichem
Chloramphenicol	Roth
Chloroform/Isomylalcohol 21:1	AppliChem
CutSmart™ buffer	New England Biolabs
Complete supplement mixture (CSM)	MP Biomedicals
Dipotassium phosphate (K_2HPO_4)	Roth
DNase I and DNase buffer	New England Biolabs
D-Sorbitol	Roth
DTT (Dithiothreitol)	Roth
ECL™ (Enhanced chemiluminescence) DIRECT Nucleic acid labeling and detection system Kit	GE Healthcare
EDTA disodium salt dihydrate (titercomplex III)	Roth
Ethanol	Roth
Ethidium bromide	Applichem, Roth
Fluconazole	Sigma Aldrich
Formaldehyde	Roth
Glass beads (0.25-0.5mm diameter)	Roth
Glucose	Roth
Glycerol	Roth
Hydrochloric acid (HCl)	Roth
Isoamyl alcohol	Roth
L-Alanine	Roth
L-Arginine	Applichem

Enzymes and chemicals	Company
Lithium acetate	Roth
L-Leucine	Roth
L-Lysine	Applichem
L-Methionine	Applichem
L-Ornithine	Applichem
L-Phenylalanine	Roth
L-Threonine	Roth
Magnesium sulfate	Roth
Mannitol	Roth
Monopotassium phosphate (KH_2PO_4)	Roth
Nourseothricin	Werner BioAgents GmbH
Nucleotides (dNTPs)	New England Biolabs
Nutrient broth	Roth
Peptone	Roth
Phloxine B	Sigma Aldrich
Phusion high-fidelity DNA polymerase	New England Biolabs
Phenol	Roth
Potassium chloride (KCl)	Roth
Proline	Roth
Proteinase K	Roth
Restriction enzymes (ApaI, BglII, ClaI, EcoRI, EcoRV, SacI, SacII, SpeI, NsiI, XhoI)	New England Biolabs
RNase A	Sigma Aldrich
Roti® Phenol	Roth
SDS ultra pure	Roth
Sodium chloride (NaCl)	Roth
Sodium hydroxide (NaOH)	Roth
Sodium phosphate dibasic (Na_2HPO_4)	Roth
Sorbitol	Roth
SYBR™ Green I	Invitrogen
Taq DNA Polymerase	New England Biolabs
Tris PUFFERAN®	Roth
Triton-X-100	Roth
Tween 20	Applichem
Urea	Roth
Yeast extract	Beckton Dickinson
Zinc sulfate	Sigma Aldrich

4.1.4. Devices

Table 14: Devices, including the model and supplier.

Devices	Model	Company
Burner	Fuego Basic RF, Schuett Phoenix	WLD-Tec, Schuett Biotec
Centrifugal evaporator	Speed Vac SC110	Savant
Centrifuges	Megafuge 1.0R, Pico21, Biofuge Pico, Fresco 17, Fresco 21	Heraeus Instruments
Circular shaker	KS125 basic, Duomax 1030 Certomat® U, SM30	IKA Labortechnik, Heidolph, B.Braun Biotech International, Edmund Bühler GmbH
Colony counter pen	eCount	Heathrow Scientific
Developing machine	Cawomat 2000 IR	CAWO Photochemische Fabrik GmbH

Devices	Model	Company
Digital camera	AF-S MicroNIKKOR 40mm 1:2:8 G	Nicon
Electroporator	EasyjecT Prima	Eqibio
FACS machine	MACSQuantAnalyzer	Miltenyi Biotec
Gel chambers	Sub- cell®t GT, Sub- cell®t GT Mini	Bio-Rad
Gel documentation	Gel doc 2000	Intas science imaging
Hybridisation oven	Biometra OV2	Biometra
Incubators	Kelvitron®t B6200, Model 400	Heraeus Instruments, Memmert
MACSQuant Flow Cytometer	MACSQuant®Analyzer 10	Miltenyi Biotec
Microscopes	Eclipse 50, DMI 6000B, DM LS	Nikon, Leica, Leica
Microwave		Privileg
Milli-pore	TKA	ThermoFisher Scientific
Nanodrop spectrophotometer	Nanodrop® ND-1000 Spectrophotometer	peqLab Biotechnologie GmbH
Thermocycler	Peqstar, Cyclone 25, 96 Universal Gradient, Mastercycler gradient	VWR life science (Peqlab), VWR life science (Peqlab), VWR life science (Peqlab), Eppendorf
pH meter	inoLab pH Level 1	WTW
Photometer	Biophotometer	Eppendorf
Pipettes	Pipetman	Gilson, VWR, Eppendorf Research,
Power supply for gel chamber	Power Pac 300, Power Pac Basic	Bio-Rad, Bio-Rad
Replica plater for 96-well plate	8 x 6 Array	Sigma-Aldrich
Scanner	HP Scanjet 8300	HP Inc
Shaking incubator	TH15, Certomat® BS-1, Innova 4230	Edmund Bühler Johanna Otto GmbH, B. Braun Biotech International, New Brunswick Scientific
Southern Blot apparatus	VacuGene XL VP100C	GE Healthcare, VWR
Sterile benches	HERAsafe Heraeus	HERAsafe Heraeus
Stirrer	Heat Stir OB162, M21	Stuart, GLW
Ultrasonic homogenizer	Sonopuls HD 70	Bandelin
UV crosslinker	UV Stratalinker 1800	Stratagene
UV device	UVIS	Desaga
Vacuum pump	Vacu Gene pump	Pharmacia Biotech
Vacuum centrifuge	SpeedVac SC110	Savant
Vortexer	WiseStir MS-20A	Wisd Laboratory Instruments
Water bath	GFL1083	GFL

4.1.5. Oligonucleotides

Oligonucleotides were purchased from Eurofins MWG Operon as salt-free lyophilized powder. Water was added for rehydration.

Table 15: Oligonucleotides used in this study.

Name	5‘-end to 3‘-end oriented sequence
Act18	GAA TAC AAA ACC AGA TTT CCA G
Adh1.term1	AAG GTG CTG AAC CAA ACT GTG GTG A
Adh1.term2	GAC AAT CTT GAT TGG GCA TTT GAT C

Name	5‘-end to 3‘-end oriented sequence
CAP1-1	TCA GAT ATT GCC TCA CCA GC
CAP1-2	GCA GTA TTT ATC ACT ACT CCC
ERG4	GAA TCG AAA GAA AGG ATC CGT TTT ATT AA
ERG9	CAT TAA GAA AAG ATA GAG CTC C
GLN1	ATA ACG GGC CCT ACC TAG AGG AAT AAG TTC
GLN5	ATA TTG GAT CCT AGA GTT TGC AAA CAC GTA C
MTL3F	ATA TCC GCG GTT TGT TTA ACA CCA ATA ATT CCA TAA CC
MTL3R	ATA TGA GCT CCT TCT AAT TCC CCT CAA CTT TTA GGA GC
MTL5F	ATA TGG GCC CAA TCA AGA TTT ATT ACA TGT TGG TGA A
MTL5R	ATA TCT CGA GAT TTA ACT GGA GGA CAG AAG AAC ACA G
Prom.ADH1.fwd	TGA TAG AGA CCC AAT GCA AAG CC
Prom.ADH1.rev	GGC ACG AGA CGG AAA CTC TTT AGG
TAC1-9	TTT TGG ATC CTT AAA TCC CCA AAT TAT TGT CAA AG
TAC1-11	AAT TGA GCT CAG TTC AAG CAA GTA CTG GC
UPC2-1	ATA TCT CGA GAA TGA TGA TGA CAG TGA AAC AAG AAT C
UPC2-2	ATA TAG ATC TAT TTC ATA TTC ATA AAC CCA TTA TC
UPC2-4B	GCA TTC AAT ACT TGC CTT TAG TGC
UPC2-9	ATA TGG CGC CCC AAC TAA TCC ACT TAG TGC TTT G
ZCF36-1	TCT AAG TCG ACA AAA ATG TCA ATT GCC ACC ACC C
ZCF36-2	GCC AAT TCA CCA GAT CTA ATT TAA TTG C
ZCF36-3	GAA TAA TTC GGA GCT CAA TTT GCG TTT AGC C
ZCF36-6	ATA TTG GGC CCG CTA CCA TAA GCC TCG CTC G
ZCF36-7	CCA AAT GCA TTG ATT CTG GTG AAT TGG CAG C
ZCF36-8	AAT CGG ATC CAT TGG TAA AAA GTT GAT CAA ATG G
ZCF36-47	ATA TGG CGC CGG CAT CAA ACC GAA TTG GGA
ZCF36-52	ATA TGG CGC CGA AAT GTC ACC GCC ACG AAG TG
ZCF36-61	ATA TGG CGC CTG GAT AAA GTA AAC TGA AAA ACC TA
ZCF36-66	ATA TGG CGC CTA TTC TAT GGG TCT AAA TAG AGA AC
ZCF36seq2	CAG TTT ACT TTA TCC ATT TAT GCC
ZCF36seq4	GTT GGA ATT GCA GCT GTA TCC
ZCF36seq5	CCC TTG GTA ATC TTC CAC GC
ZCF36seq7	GAA GTC ACT ATT ACG TTG AGT G

4.1.6. Plasmids

Cloning was performed with the *Escherichia coli* strain DH5α (F-, endA1, hsdR17 [rk-, mk-], supE44, thi-1, recA1, gyrA96, relA1, Δ[argF-lac]U169, λ-, ϕ80dlacZΔM15) [315]. All plasmids used in this study are modifications of the vector pBluescript KS II(+) (Stratagene, Heidelberg, Germany).

Table 16: Plasmids used in this study

Name	Description	Reference
pADH1R1A	Contains *RFP* under the control of the *ADH1* promotor and the *caSAT1* marker	[121]
pMRR1R3	Contains the hyperactive *MRR1*^{P683S} allele and the *SAT1* flipper cassette with the *caFLP* recombinase under the control of the *MAL2* promotor	[98]
pMRR1R8	Contains the hyperactive *MRR1*^{T360I} allele and the *SAT1* flipper cassette with the *caFLP* recombinase under the control of the *MAL2* promotor	[316]
pMRR1R9	Contains the hyperactive *MRR1*^{K335N} allele and the *SAT1* flipper cassette with the *caFLP* recombinase under the control of the *MAL2* promotor	[316]

Abbreviations: ***caFLP***: *FLP* gene, adapted to the specific codon usage of *C. albicans*, encoding the site specific recombinase Flp; ***caSAT1***: Nourseothricin resistance marker (dominant), adapted to the specific codon usage of *C. albicans*; ***RFP***: Red fluorescent protein gene

4.1.7. *Candida albicans* strains

Each *Candida albicans* mutant was constructed twice in an independent manner consistent with laboratory quality standards. The resulting strains were labeled with the suffixes -A and -B.

Table 17: Clinical isolates used in this study.

Name[a]	Relevant genotype and description[b]	Reference	Additional references of sequence analysis of relevant genes
SC5314	*Candida albicans* wild-type strain; *MTL***a**/*MTL*α	[317]	
WO-1	*Candida albicans* wild-type strain; *MTL*α/*MTL*α	[26]	
Matched clinical isolate pairs			
1442	FLU^S clinical isolate from patient 9	[64]	
2271	FLU^R clinical isolate from patient 9; $MRR1^{Q350L}$/$MRR1^{Q350L}$	[64]	[104]
1490	FLU^S clinical isolate from patient 40	[64]	
1587	FLU^R clinical isolate from patient 40; $MRR1^{N803D}$/$MRR1^{N803D}$	[64]	[104]
5833	FLU^S clinical isolate from patient II	[318]	
6692	FLU^R clinical isolate from patient II; $MRR1^{K335N}$/$MRR1^{T360I}$	[318]	[104]
B3	FLU^S clinical isolate from patient B	[319]	
B4	FLU^R clinical isolate from patient B; $MRR1^{G878E}$/$MRR1^{G878E}$	[319]	[104]
DSY294 (C43)	FLU^S clinical isolate	[72]	
DSY296 (C56)	FLU^R clinical isolate; $TAC1^{N977D}$/$TAC1^{N977D}$	[72]	[110]
DSY2285 (26)	FLU^S clinical isolate	[320]	
DSY2286 (91)	FLU^R clinical isolate; $MRR1^{T896I}$/$MRR1^{T896I}$	[320]	[104]
F2	FLU^S clinical isolate from patient F	[62]	
F5	FLU^R clinical isolate from patient F; $MRR1^{P683S}$/$MRR1^{P683S}$; $UPC2^{G648S}$/$UPC2^{G648S}$	[62]	[107], This study
G2	FLU^S clinical isolate from patient G	[62]	
G5	FLU^R clinical isolate from patient G; $MRR1^{G997V}$/$MRR1^{G997V}$	[62]	[107]
Gu4	FLU^S clinical isolate from patient Gu	[319]	
Gu5	FLU^R clinical isolate from patient Gu; $TAC1^{G980E}$/$TAC1^{G980E}$	[319]	[266, 271]
TW1 (#1, DSY3534)	FLU^S clinical isolate	[321]	
TW17 (#17, DSY3448)	FLU^R clinical isolate; $MRR1^{G947S}$/$MRR1^{G947S}$; $TAC1^{A736V}$/$TAC1^{\Delta 962\text{-}969}$; *UPC2*/$UPC2^{A643V}$	[321]	[96, 106, 109], This study

[a] Strain names used in previous studies are indicated in parentheses.
[b] FLU^S: Fluconazole-susceptible; FLU^R: Fluconazole-resistant

Table 18: Genetically manipulated strains used in this study.

RFP-labeled strains	Parent	Relevant genotype	References
SCADH1R1A	SC5314	*ADH1/adh1::*P_{ADH1}*-RFP-caSAT1*	[121]
F2ADH1R1A and -B	F2	*ADH1/adh1::*P_{ADH1}*-RFP-caSAT1*	[266]
F5ADH1R1A and -B	F5	*ADH1/adh1::*P_{ADH1}*-RFP-caSAT1*	[266]
G2ADH1R1A and -B	G2	*ADH1/adh1::*P_{ADH1}*-RFP-caSAT1*	[266, 271]
G5ADH1R1A and -B	G5	*ADH1/adh1::*P_{ADH1}*-RFP-caSAT1*	[266, 271]
B3ADH1R1A and -B	B3	*ADH1/adh1::*P_{ADH1}*-RFP-caSAT1*	[266, 271]
B4ADH1R1A and -B	B4	*ADH1/adh1::*P_{ADH1}*-RFP-caSAT1*	[266, 271]
Gu4ADH1R1A and -B	Gu4	*ADH1/adh1::*P_{ADH1}*-RFP-caSAT1*	[266, 271]
Gu5ADH1R1A and -B	Gu5	*ADH1/adh1::*P_{ADH1}*-RFP-caSAT1*	[266, 271]
1442ADH1R1A and -B	1442	*ADH1/adh1::*P_{ADH1}*-RFP-caSAT1*	[266, 271]
2271ADH1R1A and -B	2271	*ADH1/adh1::*P_{ADH1}*-RFP-caSAT1*	[266, 271]
1490ADH1R1A and -B	1490	*ADH1/adh1::*P_{ADH1}*-RFP-caSAT1*	[266, 271]
1587ADH1R1A and -B	1587	*ADH1/adh1::*P_{ADH1}*-RFP-caSAT1*	[266, 271]
5833ADH1R1A and -B	5833	*ADH1/adh1::*P_{ADH1}*-RFP-caSAT1*	[266, 271]
6692ADH1R1A and -B	6692	*ADH1/adh1::*P_{ADH1}*-RFP-caSAT1*	[266, 271]
DSY294ADH1R1A and -B	DSY294	*ADH1/adh1::*P_{ADH1}*-RFP-caSAT1*	[266, 271]

***RFP*-labeled strains**	**Parent**	**Relevant genotype**	**References**
DSY296ADH1R1A and -B	DSY296	*ADH1/adh1::*P_{ADH1}*-RFP-caSAT1*	[266, 271]
DSY2285ADH1R1A and -B	DSY2285	*ADH1/adh1::*P_{ADH1}*-RFP-caSAT1*	[266, 271]
DSY2286ADH1R1A and -B	DSY2286	*ADH1/adh1::*P_{ADH1}*-RFP-caSAT1*	[266, 271]
TW1ADH1R1A and -B	TW1	*ADH1/adh1::*P_{ADH1}*-RFP-caSAT1*	[266]
TW17ADH1R1A and -B	TW17	*ADH1/adh1::*P_{ADH1}*-RFP-caSAT1*	[266]
Genetically engineered strains with *ERG11* resistance mutations			
SCERG11R32A	SC5314	*ERG11-1/ERG11*^{G464S}*-FRT*	[121]
SCERG11R32B	SC5314	*ERG11*^{G464S}*-FRT /ERG11-2*	[121]
SCERG11R34A	SCERG11R32A	*ERG11*^{G464S}*-FRT /ERG11*^{G464S}*-FRT*	[121]
SCERG11R34B	SCERG11R32B	*ERG11*^{G464S}*-FRT /ERG11*^{G464S}*-FRT*	[121]
Genetically engineered strains with *MRR1* resistance mutations			
SCMRR1R24A and -B	SC5314	*MRR1-FRT/MRR1-FRT*	[121]
SCMRR1R32A and -B	SC5314	*MRR1/MRR1*^{P683S}*-FRT*	[98]
SCMRR1R34A	SCMRR1R32A	*MRR1*^{P683S}*-FRT/MRR1* ^{P683S}*-FRT*	[98]
SCMRR1R34B	SCMRR1R32B	*MRR1*^{P683S}*-FRT/MRR1* ^{P683S}*-FRT*	[98]
SCMRR1R44A and -B	SC5314	*MRR1*^{G997V}*-FRT/MRR1* ^{G997V}*-FRT*	[316]
SCMRR1R54A and -B	SC5314	*MRR1*^{G878E}*-FRT/MRR1*^{G878E}*-FRT*	[316]
SCMRR1R64A and -B	SC5314	*MRR1*^{Q350L}*-FRT/MRR1*^{Q350L}*-FRT*	[316]
SCMRR1R74A and -B	SC5314	*MRR1*^{N803D}*-FRT/MRR1*^{N803D}*-FRT*	[316]
SCMRR1R84A and -B	SC5314	*MRR1*^{T360I}*-FRT/MRR1*^{T360I}*-FRT*	[316]
SCMRR1R94A and -B	SC5314	*MRR1*^{K335N}*-FRT/MRR1*^{K335N}*-FRT*	[316]
SCMRR1R982A and -B	SC5314	*MRR1*^{K335N}*-FRT/MRR1*^{T360I}*-FRT*	[316]
SCMRR1R104A and -B	SC5314	*MRR1*^{T896I}*-FRT/MRR1*^{T896I}*-FRT*	[316]
F2MRR1R31A and -B	F2	*MRR1/MRR1*^{P683S}*-SAT1-FLIP*	[266]
F2MRR1R32A	F2MRR1R31A	*MRR1/MRR1*^{P683S}*-FRT*	[266]
F2MRR1R32B	F2MRR1R31B	*MRR1/MRR1*^{P683S}*-FRT*	[266]
F2MRR1R33A	F2MRR1R32A	*MRR1*^{P683S}*-SAT1-FLIP /MRR1*^{P683S}*-FRT*	[266]
F2MRR1R33B	F2MRR1R32B	*MRR1*^{P683S}*-SAT1-FLIP/ MRR1*^{P683S}*-FRT*	[266]
F2MRR1R34A	F2MRR1R33A	*MRR1*^{P683S}*-FRT/MRR1*^{P683S}*-FRT*	[266]
F2MRR1R34B	F2MRR1R33B	*MRR1*^{P683S}*-FRT/MRR1*^{P683S}*-FRT*	[266]
5833MRR1R81A and -B	5833	*MRR1*^{T360I}*-SAT1-FLIP/MRR1*	[266]
5833MRR1R82A	5833MRR1R81A	*MRR1*^{T360I}*-FRT/MRR1*	[266]
5833MRR1R82B	5833MRR1R81B	*MRR1*^{T360I}*-FRT/MRR1*	[266]
5833MRR1R981A	5833MRR1R82A	*MRR1*^{T360I}*-FRT/MRR1*^{K335N}*-SAT1-FLIP*	[266]
5833MRR1R981B	5833MRR1R82B	*MRR1*^{T360I}*-FRT/MRR1*^{K335N}*-SAT1-FLIP*	[266]
5833MRR1R982A	5833MRR1R981A	*MRR1*^{T360I}*-FRT/MRR1*^{K335N}*-FRT*	[266]
5833MRR1R982B	5833MRR1R981B	*MRR1*^{T360I}*-FRT/MRR1*^{K335N}*-FRT*	[266]
Genetically engineered strains with *TAC1* resistance mutations			
SCTAC1R32A	SC5314	*TAC1-1/TAC1*^{G980E}*-FRT*	[322]
SCTAC1R32B	SC5314	*TAC1*^{G980E}*-FRT/TAC1-2*	[322]
SCTAC1R34A	SCTAC1R32A	*TAC1*^{G980E}*-FRT/TAC1*^{G980E}*-FRT*	[322]
SCTAC1R34B	SCTAC1R32B	*TAC1*^{G980E}*-FRT/TAC1*^{G980E}*-FRT*	[322]
Genetically engineered strains with *UPC2* resistance mutations			
SCUPC2R12A and -B	SC5314	*UPC2*^{G648D}*-FRT/UPC2-2*	[94]
SCUPC2R14A	SCUPC2R12A	*UPC2*^{G648D}*-FRT/UPC2*^{G648D}*-FRT*	[94]
SCUPC2R14B	SCUPC2R12B	*UPC2*^{G648D}*-FRT/UPC2*^{G648D}*-FRT*	[94]
Genetically engineered strains with a combination of different resistance mutations			
SCETR34A	SCERG11R34A	*ERG11*^{G464S}*-FRT/ERG11*^{G464S}*-FRT*; *TAC1*^{G980E}*-FRT/TAC1*^{G980E}*-FRT*	[121]
SCETR34B	SCERG11R34B	*ERG11*^{G464S}*-FRT/ERG11*^{G464S}*-FRT*; *TAC1*^{G980E}*-FRT/TAC1*^{G980E}*-FRT*	[121]
SCEUR12A	SCERG11R34A	*ERG11*^{G464S}*-FRT/ERG11*^{G464S}*-FRT*; *UPC2/UPC2*^{G648D}*-FRT*	[121]

***RFP*-labeled strains**	**Parent**	**Relevant genotype**	**References**
SCEUR12B	SCERG11R34A	*ERG11*^{G464S}*-FRT*/*ERG11*^{G464S}*-FRT*; *UPC2*/*UPC2*^{G648D}*-FRT*	[121]
SCEUR14A	SCEUR12A	*ERG11*^{G464S}*-FRT*/*ERG11*^{G464S}*-FRT*; *UPC2*^{G648D}*-FRT*/*UPC2*^{G648D}*-FRT*	[121]
SCEUR14B	SCEUR12B	*ERG11*^{G464S}*-FRT*/*ERG11*^{G464S}*-FRT*; *UPC2*^{G648D}*-FRT*/*UPC2*^{G648D}*-FRT*	[121]
SCMER34A	SCMRR1R34A	*ERG11*^{G464S}*-FRT*/*ERG11*^{G464S}*-FRT*; *MRR1*^{P683S}*-FRT*/*MRR1* ^{P683S}*-FRT*	[121]
SCMER34B	SCMRR1R34B	*ERG11*^{G464S}*-FRT*/*ERG11*^{G464S}*-FRT*; *MRR1*^{P683S}*-FRT*/*MRR1* ^{P683S}*-FRT*	[121]
SCMTR34A	SCMRR1R34A	*MRR1*^{P683S}*-FRT*/*MRR1* ^{P683S}*-FRT*; *TAC1*^{G980E}*-FRT*/*TAC1*^{G980E}*-FRT*	[121]
SCMTR34B	SCMRR1R34B	*MRR1*^{P683S}*-FRT*/*MRR1* ^{P683S}*-FRT*; *TAC1*^{G980E}*-FRT*/*TAC1*^{G980E}*-FRT*	[121]
SCMUR12A	SCMRR1R34A	*MRR1*^{P683S}*-FRT*/*MRR1* ^{P683S}*-FRT*; *UPC2*/*UPC2*^{G648D}*-FRT*	[121]
SCMUR12B	SCMRR1R34B	*MRR1*^{P683S}*-FRT*/*MRR1* ^{P683S}*-FRT*; *UPC2*/*UPC2*^{G648D}*-FRT*	[121]
SCMUR14A	SCMUR12A	*MRR1*^{P683S}*-FRT*/*MRR1* ^{P683S}*-FRT*; *UPC2*^{G648D}*-FRT*/*UPC2*^{G648D}*-FRT*	[121]
SCMUR14B	SCMUR12B	*MRR1*^{P683S}*-FRT*/*MRR1* ^{P683S}*-FRT*; *UPC2*^{G648D}*-FRT*/*UPC2*^{G648D}*-FRT*	[121]
SCUTR34A	SCUPC2R14A	*TAC1*^{G980E}*-FRT*/*TAC1*^{G980E}*-FRT*; *UPC2*^{G648D}*-FRT*/*UPC2*^{G648D}*-FRT*	[121]
SCUTR34B	SCUPC2R14B	*TAC1*^{G980E}*-FRT*/*TAC1*^{G980E}*-FRT*; *UPC2*^{G648D}*-FRT*/*UPC2*^{G648D}*-FRT*	[121]
Genetically engineered strains with hemizygous *MTL*			
SCMTLαM2A	SC5314	*MTL***a**/*mtl*α∆	[323]
SCMTLaM2A	SC5314	*mtl***a**∆/*MTL*α	[323]

Table 19: *MTL* homozygous strains derived after passaging in the presence of fluconazole.

Name[(a)]	**Parent**	**Relevant genotype**[(b)]	**References**
Strains with an *ERG11* resistance mutation			
SCERG11R32hom1A (E3A)	SCERG11R32A	*ERG11*^{G464S}/*ERG11*^{G464S}; *GLN3-1*/*GLN3-1*; *MTL*α/α	[274], this study
E4	SCERG11R32A	*ERG11*^{G464S}/*ERG11*^{G464S}; *GLN3-1*/*GLN3-1*; *MTL*α/α	[274], this study
E5	SCERG11R32A	*ERG11*^{G464S}/*ERG11*^{G464S}; *GLN3-1*/*GLN3-1*; *MTL*α/α	[274], this study
E6	SCERG11R32A	*ERG11*^{G464S}/*ERG11*^{G464S}; *GLN3-1*/*GLN3-1*; *MTL*α/α	[274], this study
E8	SCERG11R32A	*ERG11*^{G464S}/*ERG11*^{G464S}; *GLN3-1*/*GLN3-1*; *MTL*α/α	[274], this study
E10	SCERG11R32A	*ERG11*^{G464S}/*ERG11*^{G464S}; *GLN3-1*/*GLN3-1*; *MTL*α/α	[274], this study
E20	SCERG11R32A	*ERG11*^{G464S}/*ERG11*^{G464S}; *GLN3-1*/*GLN3-1*; *MTL*α/α	[274], this study
E25	SCERG11R32A	*ERG11*^{G464S}/*ERG11*^{G464S}; *GLN3-1*/*GLN3-1*; *MTL*α/α	[274], this study
E31	SCERG11R32A	*ERG11*^{G464S}/*ERG11*^{G464S}; *GLN3-1*/*GLN3-1*; *MTL*α/α	[274], this study
E36	SCERG11R32A	*ERG11*^{G464S}/*ERG11*^{G464S}; *GLN3-1*/*GLN3-1*; *MTL*α/α	[274], this study
E47	SCERG11R32A	*ERG11*^{G464S}/*ERG11*^{G464S}; *GLN3-1*/*GLN3-1*; *MTL*α/α	[274], this study
E51	SCERG11R32A	*ERG11*^{G464S}/*ERG11*^{G464S}; *GLN3-1*/*GLN3-1*; *MTL*α/α	[274], this study
E56	SCERG11R32A	*ERG11*^{G464S}/*ERG11*^{G464S}; *GLN3-1*/*GLN3-1*; *MTL*α/α	[274], this study
E61	SCERG11R32A	*ERG11*^{G464S}/*ERG11*^{G464S}; *GLN3-1*/*GLN3-1*; *MTL*α/α	[274], this study
SCERG11R32hom1B (E2.1)	SCERG11R32B	*ERG11*^{G464S}/*ERG11*^{G464S}; *GLN3-1*/*GLN3-2*; *MTL***a**/**a**	[274], this study
E2.2	SCERG11R32B	*ERG11*/*ERG11*^{G464S}; *MTL*α/α	[274], this study
E2.3	SCERG11R32B	*ERG11*^{G464S}/*ERG11*^{G464S}; *GLN3-1*/*GLN3-2*; *MTL***a**/**a**	[274], this study
E2.4	SCERG11R32B	*ERG11*^{G464S}/*ERG11*^{G464S}; *GLN3-1*/*GLN3-2*; *MTL***a**/**a**	[274], this study
E2.5	SCERG11R32B	*ERG11*^{G464S}/*ERG11*^{G464S}; *GLN3-1*/*GLN3-2*; *MTL***a**/**a**	[274], this study
E2.6	SCERG11R32B	*ERG11*^{G464S}/*ERG11*^{G464S}; *GLN3-1*/*GLN3-2*; *MTL***a**/**a**	[274], this study
E2.7	SCERG11R32B	*ERG11*^{G464S}/*ERG11*^{G464S}; *GLN3-1*/*GLN3-2*; *MTL***a**/**a**	[274], this study
E2.8	SCERG11R32B	*ERG11*^{G464S}*-*/*ERG11; MTL*α/α	[274], this study
E2.19	SCERG11R32B	*ERG11*^{G464S}/*ERG11*^{G464S}; *GLN3-1*/*GLN3-2*; *MTL***a**/**a**	[274], this study
E2.20	SCERG11R32B	*ERG11*/*ERG11*^{G464S}; *MTL*α/α	[274], this study
SCERG11R32hom2B (E2.21)	SCERG11R32B	*ERG11*^{G464S}/*ERG11*^{G464S}; *GLN3-1*/*GLN3-2*; *MTL*α/α	[274], this study
E2.22	SCERG11R32B	*ERG11*^{G464S}/*ERG11*^{G464S}; *GLN3-1*/*GLN3-2*; *MTL*α/α	[274], this study

Name[a]	Parent	Relevant genotype[b]	References
E2.25	SCERG11R32B	*ERG11*^{G464S}/*ERG11*^{G464S}; *GLN3-1/GLN3-2*; *MTL***a**/**a**	[274], this study
E2.26	SCERG11R32B	*ERG11*^{G464S}/*ERG11*^{G464S}; *GLN3-1/GLN3-2*; *MTL*α/α	[274], this study
E2.27	SCERG11R32B	*ERG11*^{G464S}/*ERG11*^{G464S}; *GLN3-1/GLN3-2*; *MTL*α/α	[274], this study
E2.35	SCERG11R32B	*ERG11*^{G464S}/*ERG11*^{G464S}; *GLN3-1/GLN3-2*; *MTL***a**/**a**	[274], this study
E2.36	SCERG11R32B	*ERG11/ERG11*^{G464S}*; MTL*α/α	[274], this study
E2.37	SCERG11R32B	*ERG11*^{G464S}/*ERG11*^{G464S}; *GLN3-1/GLN3-2*; *MTL***a**/**a**	[274], this study
E2.42	SCERG11R32B	*ERG11*^{G464S}/*ERG11*^{G464S}; *GLN3-1/GLN3-2*; *MTL***a**/**a**	[274], this study
E2.43	SCERG11R32B	*ERG11/ERG11*^{G464S}*; MTL*α/α	[274], this study
Strains with a *MRR1* resistance mutation			
SCMRR1R32hom1A (M2)	SCMRR1R32A	*CAP1-1/CAP1-2*; *GLN3-1/GLN3-1*; *MRR1*^{P683S}/*MRR1* ^{P683S}; *MTL*α/α	[274], this study
M4	SCMRR1R32A	*CAP1-1/CAP1-2*; *GLN3-1/GLN3-1*; *MRR1*^{P683S}/*MRR1* ^{P683S}; *MTL*α/α	[274], this study
SCMRR1R32hom2A (M8)	SCMRR1R32A	*CAP1-1/CAP1-2*; *GLN3-2/GLN3-2*; *MRR1*^{P683S}/*MRR1* ^{P683S}; *MTL***a**/**a**	[274], this study
SCMRR1R32hom1B (M2.1)	SCMRR1R32B	*CAP1-2/CAP1-2; GLN3-2/GLN3-2*; *MRR1*^{P683S}/*MRR1* ^{P683S}; *MTL***a**/**a**	[274], this study
SCMRR1R32hom2B (M2.2)	SCMRR1R32B	*CAP1-1/CAP1-2*; *GLN3-1/GLN3-1*; *MRR1*^{P683S}/*MRR1* ^{P683S}; *MTL*α/α	[274], this study
M2.3	SCMRR1R32B	*CAP1-2/CAP1-2*; *GLN3-2/GLN3-2*; *MRR1*^{P683S}/*MRR1* ^{P683S}; *MTL***a**/**a**	[274], this study
Strains with a *TAC1* resistance mutation			
SCTAC1R32hom1A (A1)	SCTAC1R32A	*GLN3-1/GLN3-2*; *MTL*α/α; *TAC1*^{G980E}/*TAC1*^{G980E}	[274], this study
SCTAC1R32hom2A (A2)	SCTAC1R32A	*GLN3-1/GLN3-2*; *MTL*α/α; *TAC1*^{G980E}/*TAC1*^{G980E}	[274], this study
SCTAC1R32hom3A (A5)	SCTAC1R32A	*GLN3-1/GLN3-2*; *MTL*α/α; *TAC1*^{G980E}/*TAC1*^{G980E}	[274], this study
SCTAC1R32hom1B (B2)	SCTAC1R32B	*GLN3-2/GLN3-2*; *MTL***a**/**a**; *TAC1*^{G980E}/*TAC1*^{G980E}	[274], this study
SCTAC1R32hom2B (B3)	SCTAC1R32B	*GLN3-1/GLN3-2*; *MTL***a**/**a**; *TAC1*^{G980E}/*TAC1*^{G980E}	[274], this study
SCTAC1R32hom3B (B4)	SCTAC1R32B	*GLN3-2/GLN3-2*; *MTL***a**/**a**; *TAC1*^{G980E}/*TAC1*^{G980E}	[274], this study
SCTAC1R32hom4B (B6)	SCTAC1R32B	*GLN3-2/GLN3-2*; *MTL***a**/**a**; *TAC1*^{G980E}/*TAC1*^{G980E}	[274], this study
Strains with an *UPC2* resistance mutation			
SCUPC2R12hom1A (U3)	SCUPC2R12A	*GLN3-2/GLN3-2*; *MTL***a**/**a**; *UPC2*^{G648D}/*UPC2-2*	[274], this study
U4	SCUPC2R12A	*GLN3-2/GLN3-2*; *MTL***a**/**a**; *UPC2*^{G648D}/*UPC2-2*	[274], this study
U5	SCUPC2R12A	*GLN3-2/GLN3-2; MTL***a**/**a**; *UPC2*^{G648D}/*UPC2-2*	[274], this study
U7	SCUPC2R12A	*GLN3-1/GLN3-1*; *MTL*α/α; *UPC2*^{G648D}/*UPC2-2*	[274], this study
U9	SCUPC2R12A	*GLN3-2/GLN3-2; MTL***a**/**a**; *UPC2*^{G648D}/*UPC2-2*	[274], this study
U10	SCUPC2R12A	*GLN3-1/GLN3-1*; *MTL*α/α; *UPC2*^{G648D}/*UPC2-2*	[274], this study
U11	SCUPC2R12A	*GLN3-2/GLN3-2*; *MTL***a**/**a**; *UPC2*^{G648D}/*UPC2-2*	[274], this study
U12	SCUPC2R12A	*GLN3-1/GLN3-2*; *MTL***a**/**a**; *UPC2*^{G648D}/*UPC2-2*	[274], this study
SCUPC2R12hom1B (U2.3)	SCUPC2R12B	*GLN3-1/GLN3-1*; *MTL*α/α; *UPC2*^{G648D}/*UPC2-2*	[274], this study

[a] Originally used strain names are indicated in parentheses. Please note that initially randomly picked strains of all experiments were consecutively numbered. Subsequently, selected *MTL* homozygous strains were systematically renamed.
[b] *FRT* sites are not listed. Exact number of mentioned alleles was not examined and may differ from 2.

Table 20: Mating products isolated during this study.

Name[a]	*MTL***a**/**a** parent	*MTL*α/α parent	Relevant genotype[b]	References
EM1	SCERG11R32hom1B	SCMRR1R32hom1A	*ERG11/ERG11*^{G464S}; *MRR1/MRR1* ^{P683S}; *MTL***a**/α	[274], this study
EM16	SCERG11R32hom1B	SCMRR1R32hom1A	*ERG11/ERG11*^{G464S}; *MRR1/MRR1* ^{P683S}; *MTL***a**/α	[274], this study
EM17	SCERG11R32hom1B	SCMRR1R32hom1A	*ERG11/ERG11*^{G464S}; *MRR1/MRR1* ^{P683S}; *MTL***a**/α	[274], this study
EM19	SCERG11R32hom1B	SCMRR1R32hom1A	*ERG11/ERG11*^{G464S}; *MRR1/MRR1* ^{P683S}; *MTL***a**/α	[274], this study
EM20	SCERG11R32hom1B	SCMRR1R32hom1A	*ERG11/ERG11*^{G464S}; *MRR1/MRR1* ^{P683S}; *MTL***a**/α	[274], this study
EM21	SCERG11R32hom1B	SCMRR1R32hom1A	*ERG11/ERG11*^{G464S}; *MRR1/MRR1* ^{P683S}; *MTL***a**/α	[274], this study

Name[a]	*MTL***a**/a parent	*MTL*α/α parent	Relevant genotype[b]	References
EM22	SCERG11R32hom1B	SCMRR1R32hom1A	*ERG11*/*ERG11*^{G464S}; *MRR1*/*MRR1*^{P683S}; *MTL***a**/α	[274], this study
EM23	SCERG11R32hom1B	SCMRR1R32hom1A	*ERG11*/*ERG11*^{G464S}; *MRR1*/*MRR1*^{P683S}; *MTL***a**/α	[274], this study
EM24	SCERG11R32hom1B	SCMRR1R32hom1A	*ERG11*/*ERG11*^{G464S}; *MRR1*/*MRR1*^{P683S}; *MTL***a**/α	[274], this study
EM25	SCERG11R32hom1B	SCMRR1R32hom1A	*ERG11*/*ERG11*^{G464S}; *MRR1*/*MRR1*^{P683S}; *MTL***a**/α	[274], this study
EM26	SCERG11R32hom1B	SCMRR1R32hom1A	*ERG11*/*ERG11*^{G464S}; *MRR1*/*MRR1*^{P683S}; *MTL***a**/α	[274], this study
EM27	SCERG11R32hom1B	SCMRR1R32hom1A	*ERG11*/*ERG11*^{G464S}; *MRR1*/*MRR1*^{P683S}; *MTL***a**/α	[274], this study
EM28	SCERG11R32hom1B	SCMRR1R32hom1A	*ERG11*/*ERG11*^{G464S}; *MRR1*/*MRR1*^{P683S}; *MTL***a**/α	[274], this study
EM30	SCERG11R32hom1B	SCMRR1R32hom1A	*ERG11*/*ERG11*^{G464S}; *MRR1*/*MRR1*^{P683S}; *MTL***a**/α	[274], this study
EM32	SCERG11R32hom1B	SCMRR1R32hom1A	*ERG11*/*ERG11*^{G464S}; *MRR1*/*MRR1*^{P683S}; *MTL***a**/α	[274], this study
EM33	SCERG11R32hom1B	SCMRR1R32hom1A	*ERG11*/*ERG11*^{G464S}; *MRR1*/*MRR1*^{P683S}; *MTL***a**/α	[274], this study
EM34	SCERG11R32hom1B	SCMRR1R32hom1A	*ERG11*/*ERG11*^{G464S}; *MRR1*/*MRR1*^{P683S}; *MTL***a**/α	[274], this study
ME1 (ME3)[c]	SCMRR1R32hom2A	SCERG11R32hom1A	*ERG11*/*ERG11*^{G464S}; *MRR1*/*MRR1*^{P683S}; *MTL***a**/α	[274], this study
ME35[c]	SCMRR1R32hom2A	SCERG11R32hom1A	*ERG11*/*ERG11*^{G464S}; *MRR1*/*MRR1*^{P683S}; *MTL***a**/α	[274], this study
ME36[c]	SCMRR1R32hom2A	SCERG11R32hom1A	*ERG11*/*ERG11*^{G464S}; *MRR1*/*MRR1*^{P683S}; *MTL***a**/α	[274], this study
ET1[c]	SCERG11R32hom1B	SCTAC1R32hom2A	*ERG11*/*ERG11*^{G464S}; *TAC1-1*/*TAC1-2*/*TAC1*^{G980E}; *MTL***a**/α	[274], this study
ET2[c]	SCERG11R32hom1B	SCTAC1R32hom2A	*ERG11*/*ERG11*^{G464S}; *TAC1-1*/*TAC1-2*/*TAC1*^{G980E}; *MTL***a**/α	[274], this study
TE1 (TE27)	SCTAC1R32hom2B	SCERG11R32hom1A	*ERG11*/*ERG11*^{G464S}; *TAC1-2*/*TAC1*^{G980E}; *MTL***a**/α	[274], this study
TE3[c]	SCTAC1R32hom2B	SCERG11R32hom1A	*ERG11*/*ERG11*^{G464S}; *TAC1-2*/*TAC1*^{G980E}; *MTL***a**/α	[274], this study
TE25	SCTAC1R32hom2B	SCERG11R32hom1A	*ERG11*/*ERG11*^{G464S}; *TAC1-2*/*TAC1*^{G980E}; *MTL***a**/α	[274], this study
TE33	SCTAC1R32hom2B	SCERG11R32hom1A	*ERG11*/*ERG11*^{G464S}; *TAC1-2*/*TAC1*^{G980E}; *MTL***a**/α	[274], this study
TE35	SCTAC1R32hom2B	SCERG11R32hom1A	*ERG11*/*ERG11*^{G464S}; *TAC1-2*/*TAC1*^{G980E}; *MTL***a**/α	[274], this study
TE42	SCTAC1R32hom2B	SCERG11R32hom1A	*ERG11*/*ERG11*^{G464S}; *TAC1-2*/*TAC1*^{G980E}; *MTL***a**/α	[274], this study
EU1[c]	SCERG11R32hom1B	SCUPC2R12hom1B	*ERG11*/*ERG11*^{G464S}; *UPC2*/*UPC2*^{G648D}; *MTL***a**/α	[274], this study
EU2[c]	SCERG11R32hom1B	SCUPC2R12hom1B	*ERG11*/*ERG11*^{G464S}; *UPC2*/*UPC2*^{G648D}; *MTL***a**/α	[274], this study
EU3[c]	SCERG11R32hom1B	SCUPC2R12hom1B	*ERG11*/*ERG11*^{G464S}; *UPC2*/*UPC2*^{G648D}; *MTL***a**/α	[274], this study
EU4[c]	SCERG11R32hom1B	SCUPC2R12hom1B	*ERG11*/*ERG11*^{G464S}; *UPC2*/*UPC2*^{G648D}; *MTL***a**/α	[274], this study
EU5[c]	SCERG11R32hom1B	SCUPC2R12hom1B	*ERG11*/*ERG11*^{G464S}; *UPC2*/*UPC2*^{G648D}; *MTL***a**/α	[274], this study
UE1 (UE64)	SCUPC2R12hom1A	SCERG11R32hom1A	*ERG11*/*ERG11*^{G464S}; *UPC2*/*UPC2*^{G648D}; *MTL***a**/α	[274], this study
UE59	SCUPC2R12hom1A	SCERG11R32hom1A	*ERG11*/*ERG11*^{G464S}; *UPC2*/*UPC2*^{G648D}; *MTL***a**/α	[274], this study
UE65	SCUPC2R12hom1A	SCERG11R32hom1A	*ERG11*/ *ERG11*^{G464S}; *UPC2*/*UPC2*^{G648D}; *MTL***a**/α	[274], this study

Name[a]	*MTL*a/a parent	*MTL*α/α parent	Relevant genotype[b]	References
MT1 (MT3)[c]	SCMRR1R32hom2A	SCTAC1R32hom2A	*MRR1*/*MRR1* ^{P683S}; *TAC1-1*/*TAC1* ^{G980E}; *MTL*a/α	[274], this study
MT2 (MT6)[c]	SCMRR1R32hom2A	SCTAC1R32hom2A	*MRR1*/*MRR1* ^{P683S}; *TAC1-1*/*TAC1* ^{G980E}; *MTL*a/α	[274], this study
MT5[c]	SCMRR1R32hom2A	SCTAC1R32hom2A	*MRR1*/*MRR1* ^{P683S}; *TAC1-1*/*TAC1* ^{G980E}; *MTL*a/α	[274], this study
MT8[c]	SCMRR1R32hom2A	SCTAC1R32hom2A	*MRR1*/*MRR1* ^{P683S}; *TAC1-1*/*TAC1* ^{G980E}; *MTL*a/α	[274], this study
MT12[c]	SCMRR1R32hom2A	SCTAC1R32hom2A	*MRR1*/*MRR1* ^{P683S}; *TAC1-1*/*TAC1* ^{G980E}; *MTL*a/α	[274], this study
MT13[c]	SCMRR1R32hom2A	SCTAC1R32hom2A	*MRR1*/*MRR1* ^{P683S}; *TAC1-1*/*TAC1* ^{G980E}; *MTL*a/α	[274], this study
MT16[c]	SCMRR1R32hom2A	SCTAC1R32hom2A	*MRR1*/*MRR1* ^{P683S}; *TAC1-1*/*TAC1* ^{G980E}; *MTL*a/α	[274], this study
TM1 (TM8)	SCTAC1R32hom2B	SCMRR1R32hom1A	*MRR1*/*MRR1* ^{P683S}; *TAC1-2*/*TAC1* ^{G980E}; *MTL*a/α	[274], this study
TM2	SCTAC1R32hom2B	SCMRR1R32hom1A	*MRR1*/*MRR1* ^{P683S}; *TAC1-1*/*TAC1* ^{G980E}; *MTL*a/α	[274], this study
MU1 (MU13)	SCMRR1R32hom2A	SCUPC2R12hom1B	*MRR1*/*MRR1* ^{P683S}; *UPC2*/*UPC2* ^{G648D}; *MTL*a/α	[274], this study
MU2 (MU8)	SCMRR1R32hom2A	SCUPC2R12hom1B	*MRR1*/*MRR1* ^{P683S}; *UPC2*/*UPC2* ^{G648D}; *MTL*a/α	[274], this study
MU9	SCMRR1R32hom2A	SCUPC2R12hom1B	*MRR1*/*MRR1* ^{P683S}; *UPC2*/*UPC2* ^{G648D}; *MTL*a/α	[274], this study
MU16	SCMRR1R32hom2A	SCUPC2R12hom1B	*MRR1*/*MRR1* ^{P683S}; *UPC2*/*UPC2* ^{G648D}; *MTL*a/α	[274], this study
MU18	SCMRR1R32hom2A	SCUPC2R12hom1B	*MRR1*/*MRR1* ^{P683S}; *UPC2*/*UPC2* ^{G648D}; *MTL*a/α	[274], this study
MU20	SCMRR1R32hom2A	SCUPC2R12hom1B	*MRR1*/*MRR1* ^{P683S}; *UPC2*/*UPC2* ^{G648D}; *MTL*a/α	[274], this study
MU21	SCMRR1R32hom2A	SCUPC2R12hom1B	*MRR1*/*MRR1* ^{P683S}; *UPC2*/*UPC2* ^{G648D}; *MTL*a/α	[274], this study
MU22	SCMRR1R32hom2A	SCUPC2R12hom1B	*MRR1*/*MRR1* ^{P683S}; *UPC2*/*UPC2* ^{G648D}; *MTL*a/α	[274], this study
MU23	SCMRR1R32hom2A	SCUPC2R12hom1B	*MRR1*/*MRR1* ^{P683S}; *UPC2*/*UPC2* ^{G648D}; *MTL*a/α	[274], this study
MU29	SCMRR1R32hom2A	SCUPC2R12hom1B	*MRR1*/*MRR1* ^{P683S}; *UPC2*/*UPC2* ^{G648D}; *MTL*a/α	[274], this study
UM1 (UM21)	SCUPC2R12hom1A	SCMRR1R32hom1A	*MRR1*/*MRR1* ^{P683S}; *UPC2*/*UPC2* ^{G648D}; *MTL*a/α	[274], this study
UM3[c]	SCUPC2R12hom1A	SCMRR1R32hom1A	*MRR1*/*MRR1* ^{P683S}; *UPC2*/*UPC2* ^{G648D}; *MTL*a/α	[274], this study
UM22	SCUPC2R12hom1A	SCMRR1R32hom1A	*MRR1*/*MRR1* ^{P683S}; *UPC2*/*UPC2* ^{G648D}; *MTL*a/α	[274], this study
UM24	SCUPC2R12hom1A	SCMRR1R32hom1A	*MRR1*/*MRR1* ^{P683S}; *UPC2*/*UPC2* ^{G648D}; *MTL*a/α	[274], this study
UM25	SCUPC2R12hom1A	SCMRR1R32hom1A	*MRR1*/*MRR1* ^{P683S}; *UPC2*/*UPC2* ^{G648D}; *MTL*a/α	[274], this study
UM26	SCUPC2R12hom1A	SCMRR1R32hom1A	*MRR1*/*MRR1* ^{P683S}; *UPC2*/*UPC2* ^{G648D}; *MTL*a/α	[274], this study
UM28	SCUPC2R12hom1A	SCMRR1R32hom1A	*MRR1*/*MRR1* ^{P683S}; *UPC2*/*UPC2* ^{G648D}; *MTL*a/α	[274], this study
UM29	SCUPC2R12hom1A	SCMRR1R32hom1A	*MRR1*/*MRR1* ^{P683S}; *UPC2*/*UPC2* ^{G648D}; *MTL*a/α	[274], this study
UM30	SCUPC2R12hom1A	SCMRR1R32hom1A	*MRR1*/*MRR1* ^{P683S}; *UPC2*/*UPC2* ^{G648D}; *MTL*a/α	[274], this study
UM31	SCUPC2R12hom1A	SCMRR1R32hom1A	*MRR1*/*MRR1* ^{P683S}; *UPC2*/*UPC2* ^{G648D}; *MTL*a/α	[274], this study
UM32	SCUPC2R12hom1A	SCMRR1R32hom1A	*MRR1*/*MRR1* ^{P683S}; *UPC2*/*UPC2* ^{G648D}; *MTL*a/α	[274], this study

Name[a]	*MTL***a**/a parent	*MTL*α/α parent	Relevant genotype[b]	References
UM34	SCUPC2R12hom1A	SCMRR1R32hom1A	*MRR1*/*MRR1* ^{P683S}; *UPC2*/*UPC2* ^{G648D}; *MTL***a**/α	[274], this study
UM35	SCUPC2R12hom1A	SCMRR1R32hom1A	*MRR1*/*MRR1* ^{P683S}; *UPC2*/*UPC2* ^{G648D}; *MTL***a**/α	[274], this study
UM36	SCUPC2R12hom1A	SCMRR1R32hom1A	*MRR1*/*MRR1* ^{P683S}; *UPC2*/*UPC2* ^{G648D}; *MTL***a**/α	[274], this study
UM37	SCUPC2R12hom1A	SCMRR1R32hom1A	*MRR1*/*MRR1* ^{P683S}; *UPC2*/*UPC2* ^{G648D}; *MTL***a**/α	[274], this study
UM38	SCUPC2R12hom1A	SCMRR1R32hom1A	*MRR1*/*MRR1* ^{P683S}; *UPC2*/*UPC2* ^{G648D}; *MTL***a**/α	[274], this study
UM39	SCUPC2R12hom1A	SCMRR1R32hom1A	*MRR1*/*MRR1* ^{P683S}; *UPC2*/*UPC2* ^{G648D}; *MTL***a**/α	[274], this study
UM40	SCUPC2R12hom1A	SCMRR1R32hom1A	*MRR1*/*MRR1* ^{P683S}; *UPC2*/*UPC2* ^{G648D}; *MTL***a**/α	[274], this study
TU1[c]	SCTAC1R32hom2B	SCUPC2R12hom1B	*TAC1-2*/*TAC1* ^{G980E}; *UPC2*/*UPC2* ^{G648D}; *MTL***a**/α	[274], this study
TU2[c]	SCTAC1R32hom2B	SCUPC2R12hom1B	*TAC1-2*/*TAC1* ^{G980E}; *UPC2*/*UPC2* ^{G648D}; *MTL***a**/α	[274], this study
TU4[c]	SCTAC1R32hom2B	SCUPC2R12hom1B	*TAC1-2*/*TAC1* ^{G980E}; *UPC2*/*UPC2* ^{G648D}; *MTL***a**/α	[274], this study
TU6[c]	SCTAC1R32hom2B	SCUPC2R12hom1B	*TAC1-2*/*TAC1* ^{G980E}; *UPC2*/*UPC2* ^{G648D}; *MTL***a**/α	[274], this study
UT1 (UT86)	SCUPC2R12hom1A	SCTAC1R32hom2A	*TAC1-2*/*TAC1* ^{G980E}; *UPC2*/*UPC2* ^{G648D}; *MTL***a**/α	[274], this study
UT85	SCUPC2R12hom1A	SCTAC1R32hom2A	*TAC1-1*/*TAC1* ^{G980E}; *UPC2*/*UPC2* ^{G648D}; *MTL***a**/α	[274], this study

[a] Originally used strain names are indicated in parentheses. Please note that initially randomly picked strains of all experiments were consecutively numbered. Subsequently, selected mating products were systematically renamed.
[b] *FRT* sites are not listed. Exact number of mentioned alleles was not determined. Given alleles indicate at least one copy of the respective form.
[c] Isolated with the help of Nico Alexander Liebig.

Table 21: Mating product progeny isolated during this study.

Name[a]	Parent	Relevant genotype and description[b][c]	References
Parental mating product EM1			
1EM1P1-1	EM1	n.t.	[274], this study
1EM1P1-2	EM1	n.t.	[274], this study
1EM1P1-3	EM1	n.t.	[274], this study
1EM1P2-1	EM1	n.t.	[274], this study
1EM1P2-2	EM1	n.t.	[274], this study
1EM1P2-3	EM1	n.t.	[274], this study
EM1P3A-1 (1EM1P3-1)	EM1	*ERG11* ^{G464S}; *MRR1* ^{P683S}; *MTL***a**	[274], this study
1EM1P3-2	EM1	n.t.	[274], this study
1EM1P3-3	EM1	n.t.	[274], this study
1EM1P4-1	EM1	n.t.	[274], this study
1EM1P4-2	EM1	n.t.	[274], this study
1EM1P4-3	EM1	n.t.	[274], this study
1EM1P5-1	EM1	n.t.	[274], this study
1EM1P5-2	EM1	n.t.	[274], this study
1EM1P5-3	EM1	n.t.	[274], this study
1EM1P6-1	EM1	n.t.	[274], this study
1EM1P6-2	EM1	n.t.	[274], this study
1EM1P6-3	EM1	n.t.	[274], this study
1EM1P7-1	EM1	n.t.	[274], this study
1EM1P7-2	EM1	n.t.	[274], this study
1EM1P7-3	EM1	n.t.	[274], this study
EM1P8A-1 (1EM1P8-1)	EM1	*ERG11* ^{G464S}; *MRR1* ^{P683S}; *MTL***a**	[274], this study
1EM1P8-2	EM1	n.t.	[274], this study
EM1P8A-3 (1EM1P8-3)	EM1	*ERG11* ^{G464S}; *MRR1* ^{P683S}; *MTL***a**	[274], this study
1EM1P10-1	EM1	n.t.	[274], this study

Name[a]	Parent	Relevant genotype and description[b][c]	References
1EM1P10-2	EM1	n.t.	[274], this study
1EM1P10-3	EM1	n.t.	[274], this study
1EM1P12-1	EM1	n.t.	[274], this study
1EM1P12-2	EM1	n.t.	[274], this study
1EM1P12-3	EM1	n.t.	[274], this study
1EM1P14-1	EM1	n.t.	This study
1EM1P14-2	EM1	n.t.	This study
1EM1P14-3	EM1	n.t.	This study
Parental mating product ME1			
1ME3P1-1	ME1 (ME3)	n.t.	[274], this study
1ME3P1-2	ME1 (ME3)	n.t.	[274], this study
1ME3P1-3	ME1 (ME3)	n.t.	[274], this study
1ME3P2-1	ME1 (ME3)	n.t.	[274], this study
1ME3P2-2	ME1 (ME3)	n.t.	[274], this study
1ME3P2-3	ME1 (ME3)	n.t.	[274], this study
1ME3P3-1	ME1 (ME3)	n.t.	[274], this study
1ME3P3-2	ME1 (ME3)	n.t.	[274], this study
1ME3P3-3	ME1 (ME3)	n.t.	[274], this study
1ME3P4-1	ME1 (ME3)	n.t.	[274], this study
ME1P4A-2 (1ME3P4-2)	ME1 (ME3)	*ERG11*/*ERG11*^{G464S}; *MRR1* ^{P683S}; *MTL***a**/α	[274], this study
ME1P4A-3 (1ME3P4-3)	ME1 (ME3)	*ERG11*/*ERG11*^{G464S}; *MRR1* ^{P683S}; *MTL***a**/α	[274], this study
1ME3P5-1	ME1 (ME3)	n.t.	[274], this study
ME1P5A-2 (1ME3P5-2)	ME1 (ME3)	*ERG11*/*ERG11*^{G464S}; *MRR1* ^{P683S}; *MTL***a**/α	[274], this study
1ME3P5-3	ME1 (ME3)	n.t.	[274], this study
1ME3P6-1	ME1 (ME3)	n.t.	[274], this study
1ME3P6-2	ME1 (ME3)	n.t.	[274], this study
1ME3P6-3	ME1 (ME3)	n.t.	[274], this study
1ME3P8-1	ME1 (ME3)	n.t.	[274], this study
1ME3P8-2	ME1 (ME3)	n.t.	[274], this study
1ME3P8-3	ME1 (ME3)	n.t.	[274], this study
1ME3P9-1	ME1 (ME3)	n.t.	[274], this study
1ME3P9-2	ME1 (ME3)	n.t.	[274], this study
1ME3P9-3	ME1 (ME3)	n.t.	[274], this study
1ME3P10-1	ME1 (ME3)	n.t.	[274], this study
1ME3P10-2	ME1 (ME3)	n.t.	[274], this study
1ME3P10-3	ME1 (ME3)	n.t.	[274], this study
1ME3P11-1	ME1 (ME3)	n.t.	[274], this study
1ME3P11-2	ME1 (ME3)	n.t.	[274], this study
1ME3P11-3	ME1 (ME3)	n.t.	[274], this study
1ME3P12-1	ME1 (ME3)	n.t.	[274], this study
1ME3P12-2	ME1 (ME3)	n.t.	[274], this study
1ME3P12-3	ME1 (ME3)	n.t.	[274], this study
1ME3P14-1	ME1 (ME3)	n.t.	This study
1ME3P14-2	ME1 (ME3)	n.t.	This study
1ME3P14-3	ME1 (ME3)	n.t.	This study
1ME3P16-1	ME1 (ME3)	n.t.	This study
1ME3P16-2	ME1 (ME3)	n.t.	This study
1ME3P16-3	ME1 (ME3)	n.t.	This study
Parental mating product ET1			
1ET1P1-1	ET1	n.t.	[274], this study
1ET1P1-2	ET1	n.t.	[274], this study
1ET1P1-3	ET1	n.t.	[274], this study
1ET1P2-1	ET1	n.t.	[274], this study
ET1P2A-2 (1ET1P2-2)	ET1	*ERG11*/*ERG11*^{G464S}; *MTL***a**/α; *TAC1-1*/*TAC1-2*/*TAC1*^{G980E}	[274], this study
1ET1P2-3	ET1	n.t.	[274], this study
1ET1P3-1	ET1	n.t.	[274], this study
1ET1P3-2	ET1	n.t.	[274], this study

Name[(a)]	Parent	Relevant genotype and description[(b)(c)]	References
1ET1P3-3	ET1	n.t.	[274], this study
1ET1P4-1	ET1	n.t.	[274], this study
1ET1P4-2	ET1	n.t.	[274], this study
1ET1P4-3	ET1	n.t.	[274], this study
1ET1P5-1	ET1	n.t.	[274], this study
1ET1P5-2	ET1	n.t.	[274], this study
1ET1P5-3	ET1	n.t.	[274], this study
1ET1P6-1	ET1	n.t.	[274], this study
1ET1P6-2	ET1	n.t.	[274], this study
1ET1P6-3	ET1	n.t.	[274], this study
1ET1P7-1	ET1	n.t.	[274], this study
1ET1P7-2	ET1	n.t.	[274], this study
ET1P7A-3 (1ET1P7-3)	ET1	*ERG11*/*ERG11*^{G464S}; *TAC1-2*/*TAC1*^{G980E}; *MTL***a**/α	[274], this study
1ET1P8-1	ET1	n.t.	[274], this study
1ET1P8-2	ET1	n.t.	[274], this study
1ET1P8-3	ET1	n.t.	[274], this study
1ET1P10-1	ET1	n.t.	[274], this study
1ET1P10-2	ET1	n.t.	[274], this study
1ET1P10-3	ET1	n.t.	[274], this study
1ET1P12-1	ET1	n.t.	[274], this study
1ET1P12-2	ET1	n.t.	[274], this study
1ET1P12-3	ET1	n.t.	[274], this study
1ET1P14-1	ET1	n.t.	This study
1ET1P14-2	ET1	n.t.	This study
1ET1P14-3	ET1	n.t.	This study
2ET1P1-1	ET1	n.t.	This study
2ET1P1-2	ET1	n.t.	This study
2ET1P1-3	ET1	n.t.	This study
2ET1P2-1	ET1	n.t.	This study
2ET1P2-2	ET1	n.t.	This study
2ET1P2-3	ET1	n.t.	This study
2ET1P3-1	ET1	n.t.	This study
2ET1P3-2	ET1	n.t.	This study
2ET1P3-3	ET1	n.t.	This study
2ET1P4-1	ET1	n.t.	This study
2ET1P4-2	ET1	n.t.	This study
2ET1P4-3	ET1	n.t.	This study
2ET1P5-1	ET1	n.t.	This study
2ET1P5-2	ET1	n.t.	This study
2ET1P5-3	ET1	n.t.	This study
ET1P6B-1 (2ET1P6-1)	ET1	*ERG11*/*ERG11*^{G464S}; *MTL***a**/α; *TAC1-1*/*TAC1-2*/*TAC1*^{G980E}	This study
2ET1P6-2	ET1	n.t.	This study
ET1P6B-3 (2ET1P6-3)	ET1	*ERG11*/*ERG11*^{G464S}; *MTL***a**/α; *TAC1-2*/*TAC1*^{G980E}	This study
2ET1P7-1	ET1	n.t.	This study
2ET1P7-2	ET1	n.t.	This study
2ET1P7-3	ET1	n.t.	This study
2ET1P8-1	ET1	n.t.	This study
2ET1P8-2	ET1	n.t.	This study
ET1P8B-3 (2ET1P8-3)	ET1	*ERG11*/*ERG11*^{G464S}; *MTL***a**/α; *TAC1-1*/*TAC1-2*/*TAC1*^{G980E}	This study
2ET1P10-1	ET1	n.t.	This study
2ET1P10-2	ET1	n.t.	This study
2ET1P10-3	ET1	n.t.	This study
2ET1P12-1	ET1	n.t.	This study
2ET1P12-2	ET1	n.t.	This study
2ET1P12-3	ET1	n.t.	This study
2ET1P14-1	ET1	n.t.	This study

Name[a]	Parent	Relevant genotype and description[b][c]	References
2ET1P14-2	ET1	n.t.	This study
2ET1P14-3	ET1	n.t.	This study
Parental mating product TE1			
1TE27P1-1	TE1 (TE27)	n.t.	[274], this study
1TE27P1-2	TE1 (TE27)	n.t.	[274], this study
1TE27P1-3	TE1 (TE27)	n.t.	[274], this study
1TE27P2-1	TE1 (TE27)	n.t.	[274], this study
1TE27P2-2	TE1 (TE27)	n.t.	[274], this study
1TE27P2-3	TE1 (TE27)	n.t.	[274], this study
1TE27P3-1	TE1 (TE27)	n.t.	[274], this study
1TE27P3-2	TE1 (TE27)	n.t.	[274], this study
1TE27P3-3	TE1 (TE27)	n.t.	[274], this study
1TE27P4-1	TE1 (TE27)	n.t.	[274], this study
1TE27P4-2	TE1 (TE27)	n.t.	[274], this study
1TE27P4-3	TE1 (TE27)	n.t.	[274], this study
1TE27P5-1	TE1 (TE27)	n.t.	[274], this study
1TE27P5-2	TE1 (TE27)	n.t.	[274], this study
1TE27P5-3	TE1 (TE27)	n.t.	[274], this study
TE1P6A-1 (1TE27P6-1)	TE1 (TE27)	*ERG11*/*ERG11*^{G464S}; *MTL***a**/α; *TAC1-2*/*TAC1*^{G980E}	[274], this study
TE1P6A-2 (1TE27P6-2)	TE1 (TE27)	n.t.	[274], this study
1TE27P6-3	TE1 (TE27)	n.t.	[274], this study
1TE27P8-1	TE1 (TE27)	n.t.	[274], this study
1TE27P8-2	TE1 (TE27)	n.t.	[274], this study
1TE27P8-3	TE1 (TE27)	n.t.	[274], this study
1TE27P10-1	TE1 (TE27)	n.t.	[274], this study
1TE27P10-2	TE1 (TE27)	n.t.	[274], this study
1TE27P10-3	TE1 (TE27)	n.t.	[274], this study
1TE27P11-1	TE1 (TE27)	n.t.	[274], this study
1TE27P11-2	TE1 (TE27)	n.t.	[274], this study
1TE27P11-3	TE1 (TE27)	n.t.	[274], this study
TE1P12A-1 (1TE27P12-1)	TE1 (TE27)	*ERG11*/*ERG11*^{G464S}; *MTL***a**/α; *TAC1*^{G980E}	[274], this study
1TE27P12-2	TE1 (TE27)	n.t.	[274], this study
1TE27P12-3	TE1 (TE27)	n.t.	[274], this study
1TE27P14-1	TE1 (TE27)	n.t.	This study
1TE27P14-2	TE1 (TE27)	n.t.	This study
1TE27P14-3	TE1 (TE27)	n.t.	This study
1TE27P16-1	TE1 (TE27)	n.t.	This study
1TE27P16-2	TE1 (TE27)	n.t.	This study
1TE27P16-3	TE1 (TE27)	n.t.	This study
Parental mating product EU1			
1EU1P1-1	EU1	n.t.	[274], this study
1EU1P1-2	EU1	n.t.	[274], this study
1EU1P1-3	EU1	n.t.	[274], this study
1EU1P2-1	EU1	n.t.	[274], this study
1EU1P2-2	EU1	n.t.	[274], this study
1EU1P2-3	EU1	n.t.	[274], this study
1EU1P3-1	EU1	n.t.	[274], this study
1EU1P3-2	EU1	n.t.	[274], this study
1EU1P3-3	EU1	n.t.	[274], this study
1EU1P4-1	EU1	n.t.	[274], this study
1EU1P4-2	EU1	n.t.	[274], this study
1EU1P4-3	EU1	n.t.	[274], this study
1EU1P5-1	EU1	n.t.	[274], this study
1EU1P5-2	EU1	n.t.	[274], this study
1EU1P5-3	EU1	n.t.	[274], this study
1EU1P6-1	EU1	n.t.	[274], this study
1EU1P6-2	EU1	n.t.	[274], this study

Name[a]	Parent	Relevant genotype and description[b][c]	References
EU1P6A-3 (1EU1P6-3)	EU1	*ERG11*/*ERG11*^{G464S}; *MTL***a**/α; *UPC2*/*UPC2*^{G648D}	[274], this study
1EU1P7-1	EU1	n.t.	[274], this study
1EU1P7-2	EU1	n.t.	[274], this study
1EU1P7-3	EU1	n.t.	[274], this study
1EU1P8-1	EU1	n.t.	[274], this study
1EU1P8-2	EU1	n.t.	[274], this study
EU1P8A-3 (1EU1P8-3)	EU1	*ERG11*^{G464S}; *MTL***a**; *UPC2*/*UPC2*^{G648D}	[274], this study
1EU1P10-1	EU1	n.t.	[274], this study
1EU1P10-2	EU1	n.t.	[274], this study
1EU1P10-3	EU1	n.t.	[274], this study
1EU1P12-1	EU1	n.t.	[274], this study
1EU1P12-2	EU1	n.t.	[274], this study
1EU1P12-3	EU1	n.t.	[274], this study
1EU1P14-1	EU1	n.t.	This study
1EU1P14-2	EU1	n.t.	This study
1EU1P14-3	EU1	n.t.	This study
1EU1P16-1	EU1	n.t.	This study
1EU1P16-2	EU1	n.t.	This study
1EU1P16-3	EU1	n.t.	This study
Parental mating product UE1			
1UE64P1-1	UE1 (UE64)	n.t.	[274], this study
1UE64P1-2	UE1 (UE64)	n.t.	[274], this study
1UE64P1-3	UE1 (UE64)	n.t.	[274], this study
UE1P2A-1 (1UE64P2-1)	UE1 (UE64)	*ERG11*/*ERG11*^{G464S}; *MTL***a**/α; *UPC2*/*UPC2*^{G648D}	[274], this study
1UE64P2-2	UE1 (UE64)	n.t.	[274], this study
1UE64P2-3	UE1 (UE64)	n.t.	[274], this study
1UE64P3-1	UE1 (UE64)	n.t.	[274], this study
1UE64P3-2	UE1 (UE64)	n.t.	[274], this study
1UE64P3-3	UE1 (UE64)	n.t.	[274], this study
1UE64P4-1	UE1 (UE64)	n.t.	[274], this study
1UE64P4-2	UE1 (UE64)	n.t.	[274], this study
UE1P4A-3 (1UE64P4-3)	UE1 (UE64)	*ERG11*/*ERG11*^{G464S}; *MTL***a**/α; *UPC2*/*UPC2*^{G648D}	[274], this study
1UE64P5-1	UE1 (UE64)	n.t.	[274], this study
1UE64P5-2	UE1 (UE64)	n.t.	[274], this study
1UE64P5-3	UE1 (UE64)	n.t.	[274], this study
1UE64P6-1	UE1 (UE64)	n.t.	[274], this study
1UE64P6-2	UE1 (UE64)	n.t.	[274], this study
1UE64P6-3	UE1 (UE64)	n.t.	[274], this study
1UE64P8-1	UE1 (UE64)	n.t.	[274], this study
1UE64P8-2	UE1 (UE64)	n.t.	[274], this study
1UE64P8-3	UE1 (UE64)	n.t.	[274], this study
1UE64P10-1	UE1 (UE64)	n.t.	[274], this study
1UE64P10-2	UE1 (UE64)	n.t.	[274], this study
1UE64P10-3	UE1 (UE64)	n.t.	[274], this study
1UE64P12-1	UE1 (UE64)	n.t.	[274], this study
1UE64P12-2	UE1 (UE64)	n.t.	[274], this study
1UE64P12-3	UE1 (UE64)	n.t.	[274], this study
1UE64P14-1	UE1 (UE64)	n.t.	This study
1UE64P14-2	UE1 (UE64)	n.t.	This study
1UE64P14-3	UE1 (UE64)	n.t.	This study
1UE64P16-1	UE1 (UE64)	n.t.	This study
1UE64P16-2	UE1 (UE64)	n.t.	This study
1UE64P16-3	UE1 (UE64)	n.t.	This study
1UE64P18-1	UE1 (UE64)	n.t.	This study
1UE64P18-2	UE1 (UE64)	n.t.	This study
1UE64P18-3	UE1 (UE64)	n.t.	This study
Parental mating product MT1			
1MT3P1-1	MT1 (MT3)	n.t.	[274], this study

Name[a]	Parent	Relevant genotype and description[b][c]	References
1MT3P1-2	MT1 (MT3)	n.t.	[274], this study
1MT3P1-3	MT1 (MT3)	n.t.	[274], this study
1MT3P2-1	MT1 (MT3)	n.t.	[274], this study
1MT3P2-2	MT1 (MT3)	n.t.	[274], this study
1MT3P2-3	MT1 (MT3)	n.t.	[274], this study
1MT3P3-1	MT1 (MT3)	n.t.	[274], this study
1MT3P3-2	MT1 (MT3)	n.t.	[274], this study
MT1P3A-3 (1MT3P3-3)	MT1 (MT3)	*MRR1*/*MRR1* ^{P683S}; *MTL***a**/α; *TAC1-1*/*TAC1* ^{G980E}	[274], this study
1MT3P4-1	MT1 (MT3)	n.t.	[274], this study
1MT3P4-2	MT1 (MT3)	n.t.	[274], this study
1MT3P4-3	MT1 (MT3)	n.t.	[274], this study
1MT3P5-1	MT1 (MT3)	n.t.	[274], this study
MT1P5A-2 (1MT3P5-2)	MT1 (MT3)	*MRR1*/*MRR1* ^{P683S}; *MTL***a**/α; *TAC1-1*/*TAC1* ^{G980E}	[274], this study
MT1P5A-3 (1MT3P5-3)	MT1 (MT3)	*MRR1*/*MRR1* ^{P683S}; *MTL***a**/α; *TAC1* ^{G980E}	[274], this study
1MT3P6-1	MT1 (MT3)	n.t.	[274], this study
1MT3P6-2	MT1 (MT3)	n.t.	[274], this study
1MT3P6-3	MT1 (MT3)	n.t.	[274], this study
1MT3P8-1	MT1 (MT3)	n.t.	[274], this study
1MT3P8-2	MT1 (MT3)	n.t.	[274], this study
1MT3P8-3	MT1 (MT3)	n.t.	[274], this study
1MT3P10-1	MT1 (MT3)	n.t.	[274], this study
1MT3P10-2	MT1 (MT3)	n.t.	[274], this study
1MT3P10-3	MT1 (MT3)	n.t.	[274], this study
1MT3P12-1	MT1 (MT3)	n.t.	[274], this study
1MT3P12-2	MT1 (MT3)	n.t.	[274], this study
1MT3P12-3	MT1 (MT3)	n.t.	[274], this study
1MT3P14-1	MT1 (MT3)	n.t.	This study
1MT3P14-2	MT1 (MT3)	n.t.	This study
1MT3P14-3	MT1 (MT3)	n.t.	This study
Parental mating product MT2			
1MT6P1-1	MT2 (MT6)	n.t.	This study
1MT6P1-2	MT2 (MT6)	n.t.	This study
1MT6P1-3	MT2 (MT6)	n.t.	This study
1MT6P2-1	MT2 (MT6)	n.t.	This study
1MT6P2-2	MT2 (MT6)	n.t.	This study
1MT6P2-3	MT2 (MT6)	n.t.	This study
1MT6P3-1	MT2 (MT6)	n.t.	This study
1MT6P3-2	MT2 (MT6)	n.t.	This study
1MT6P3-3	MT2 (MT6)	n.t.	This study
1MT6P4-1	MT2 (MT6)	n.t.	This study
1MT6P4-2	MT2 (MT6)	n.t.	This study
MT2P4A-3 (1MT6P4-3)	MT2 (MT6)	*MRR1*/*MRR1* ^{P683S}; *MTL***a**/α; *TAC1-1*/*TAC1* ^{G980E}	This study
1MT6P5-1	MT2 (MT6)	n.t.	This study
1MT6P5-2	MT2 (MT6)	n.t.	This study
1MT6P5-3	MT2 (MT6)	n.t.	This study
1MT6P6-1	MT2 (MT6)	n.t.	This study
1MT6P6-2	MT2 (MT6)	n.t.	This study
1MT6P6-3	MT2 (MT6)	n.t.	This study
1MT6P8-1	MT2 (MT6)	n.t.	This study
1MT6P8-2	MT2 (MT6)	n.t.	This study
1MT6P8-3	MT2 (MT6)	n.t.	This study
1MT6P10-1	MT2 (MT6)	n.t.	This study
1MT6P10-2	MT2 (MT6)	n.t.	This study
1MT6P10-3	MT2 (MT6)	n.t.	This study
MT2P11A-1 (1MT6P11-1)	MT2 (MT6)	*MRR1* ^{P683S}; *MTL***a**/α; *TAC1-1*/*TAC1* ^{G980E}	This study
1MT6P11-2	MT2 (MT6)	n.t.	This study
1MT6P11-3	MT2 (MT6)	n.t.	This study
1MT6P12-1	MT2 (MT6)	n.t.	This study

Name[a]	Parent	Relevant genotype and description[b][c]	References
1MT6P12-2	MT2 (MT6)	n.t.	This study
1MT6P12-3	MT2 (MT6)	n.t.	This study
1MT6P14-1	MT2 (MT6)	n.t.	This study
1MT6P14-2	MT2 (MT6)	n.t.	This study
1MT6P14-3	MT2 (MT6)	n.t.	This study
1MT6P16-1	MT2 (MT6)	n.t.	This study
1MT6P16-2	MT2 (MT6)	n.t.	This study
1MT6P16-3	MT2 (MT6)	n.t.	This study
Parental mating product TM1			
2TM8P1-1	TM1 (TM8)	n.t.	[274], this study
2TM8P1-2	TM1 (TM8)	n.t.	[274], this study
2TM8P1-3	TM1 (TM8)	n.t.	[274], this study
2TM8P2-1	TM1 (TM8)	n.t.	[274], this study
2TM8P2-2	TM1 (TM8)	n.t.	[274], this study
2TM8P2-3	TM1 (TM8)	n.t.	[274], this study
2TM8P3-1	TM1 (TM8)	n.t.	[274], this study
2TM8P3-2	TM1 (TM8)	n.t.	[274], this study
2TM8P3-3	TM1 (TM8)	n.t.	[274], this study
2TM8P4-1	TM1 (TM8)	n.t.	[274], this study
2TM8P4-2	TM1 (TM8)	n.t.	[274], this study
2TM8P4-3	TM1 (TM8)	n.t.	[274], this study
2TM8P5-1	TM1 (TM8)	n.t.	[274], this study
2TM8P5-2	TM1 (TM8)	n.t.	[274], this study
2TM8P5-3	TM1 (TM8)	n.t.	[274], this study
2TM8P6-1	TM1 (TM8)	n.t.	[274], this study
TM1P6A-2 (2TM8P6-2)	TM1 (TM8)	*MRR1*/*MRR1* ^{P683S}; *MTL***a**; *TAC1*^{G980E}	[274], this study
TM1P6A-3 (2TM8P6-3)	TM1 (TM8)	*MRR1*/*MRR1* ^{P683S}; *MTL***a**; *TAC1*^{G980E}	[274], this study
2TM8P8-1	TM1 (TM8)	n.t.	[274], this study
2TM8P8-2	TM1 (TM8)	n.t.	[274], this study
2TM8P8-3	TM1 (TM8)	n.t.	[274], this study
2TM8P9-1	TM1 (TM8)	n.t.	[274], this study
2TM8P9-2	TM1 (TM8)	n.t.	[274], this study
2TM8P9-3	TM1 (TM8)	n.t.	[274], this study
TM1P10A-1 (2TM8P10-1)	TM1 (TM8)	*MRR1* ^{P683S}; *MTL***a**; *TAC1*^{G980E}	[274], this study
2TM8P10-2	TM1 (TM8)	n.t.	[274], this study
2TM8P10-3	TM1 (TM8)	n.t.	[274], this study
2TM8P12-1	TM1 (TM8)	n.t.	[274], this study
2TM8P12-2	TM1 (TM8)	n.t.	[274], this study
2TM8P12-3	TM1 (TM8)	n.t.	[274], this study
2TM8P14-1	TM1 (TM8)	n.t.	This study
2TM8P14-2	TM1 (TM8)	n.t.	This study
2TM8P14-3	TM1 (TM8)	n.t.	This study
2TM8P16-1	TM1 (TM8)	n.t.	This study
2TM8P16-2	TM1 (TM8)	n.t.	This study
2TM8P16-3	TM1 (TM8)	n.t.	This study
Parental mating product MU1			
1MU13P1-1	MU1 (MU13)	n.t.	[274], this study
1MU13P1-2	MU1 (MU13)	n.t.	[274], this study
1MU13P1-3	MU1 (MU13)	n.t.	[274], this study
1MU13P2-1	MU1 (MU13)	n.t.	[274], this study
1MU13P2-2	MU1 (MU13)	n.t.	[274], this study
1MU13P2-3	MU1 (MU13)	n.t.	[274], this study
1MU13P3-1	MU1 (MU13)	n.t.	[274], this study
1MU13P3-2	MU1 (MU13)	n.t.	[274], this study
1MU13P3-3	MU1 (MU13)	n.t.	[274], this study
1MU13P4-1	MU1 (MU13)	n.t.	[274], this study
1MU13P4-2	MU1 (MU13)	n.t.	[274], this study
1MU13P4-3	MU1 (MU13)	n.t.	[274], this study

Name[a]	Parent	Relevant genotype and description[b][c]	References
MU1P5A-1 (1MU13P5-1)	MU1 (MU13)	*MRR1*/*MRR1* ^{P683S}; *MTL***a**/α; *UPC2*/*UPC2* ^{G648D}	[274], this study
1MU13P5-2	MU1 (MU13)	n.t.	[274], this study
1MU13P5-3	MU1 (MU13)	n.t.	[274], this study
1MU13P6-1	MU1 (MU13)	n.t.	[274], this study
1MU13P6-2	MU1 (MU13)	n.t.	[274], this study
1MU13P6-3	MU1 (MU13)	n.t.	[274], this study
MU1P7A-1 (1MU13P7-1)	MU1 (MU13)	*MRR1* ^{P683S}; *MTL***a**/α; *UPC2*/*UPC2* ^{G648D}	[274], this study
1MU13P7-2	MU1 (MU13)	n.t.	[274], this study
1MU13P7-3	MU1 (MU13)	n.t.	[274], this study
1MU13P8-1	MU1 (MU13)	n.t.	[274], this study
1MU13P8-2	MU1 (MU13)	n.t.	[274], this study
1MU13P8-3	MU1 (MU13)	n.t.	[274], this study
1MU13P10-1	MU1 (MU13)	n.t.	[274], this study
1MU13P10-2	MU1 (MU13)	n.t.	[274], this study
1MU13P10-3	MU1 (MU13)	n.t.	[274], this study
1MU13P12-1	MU1 (MU13)	n.t.	[274], this study
1MU13P12-2	MU1 (MU13)	n.t.	[274], this study
1MU13P12-3	MU1 (MU13)	n.t.	[274], this study
1MU13P14-1	MU1 (MU13)	n.t.	This study
1MU13P14-2	MU1 (MU13)	n.t.	This study
1MU13P14-3	MU1 (MU13)	n.t.	This study
1MU13P16-1	MU1 (MU13)	n.t.	This study
1MU13P16-2	MU1 (MU13)	n.t.	This study
1MU13P16-3	MU1 (MU13)	n.t.	This study
Parental mating product MU2			
1MU8P1-1	MU2 (MU8)	n.t.	This study
1MU8P1-2	MU2 (MU8)	n.t.	This study
1MU8P1-3	MU2 (MU8)	n.t.	This study
1MU8P2-1	MU2 (MU8)	n.t.	This study
1MU8P2-2	MU2 (MU8)	n.t.	This study
1MU8P2-3	MU2 (MU8)	n.t.	This study
1MU8P3-1	MU2 (MU8)	n.t.	This study
1MU8P3-2	MU2 (MU8)	n.t.	This study
1MU8P3-3	MU2 (MU8)	n.t.	This study
1MU8P4-1	MU2 (MU8)	n.t.	This study
1MU8P4-2	MU2 (MU8)	n.t.	This study
1MU8P4-3	MU2 (MU8)	n.t.	This study
1MU8P5-1	MU2 (MU8)	n.t.	This study
1MU8P5-2	MU2 (MU8)	n.t.	This study
1MU8P5-3	MU2 (MU8)	n.t.	This study
MU2P6A-1 (1MU8P6-1)	MU2 (MU8)	*MRR1*/*MRR1* ^{P683S}; *MTL***a**/α; *UPC2*/*UPC2* ^{G648D}	This study
1MU8P6-2	MU2 (MU8)	n.t.	This study
1MU8P6-3	MU2 (MU8)	n.t.	This study
1MU8P8-1	MU2 (MU8)	n.t.	This study
1MU8P8-2	MU2 (MU8)	n.t.	This study
1MU8P8-3	MU2 (MU8)	n.t.	This study
1MU8P10-1	MU2 (MU8)	n.t.	This study
1MU8P10-2	MU2 (MU8)	n.t.	This study
1MU8P10-3	MU2 (MU8)	n.t.	This study
1MU8P12-1	MU2 (MU8)	n.t.	This study
1MU8P12-2	MU2 (MU8)	n.t.	This study
1MU8P12-3	MU2 (MU8)	n.t.	This study
MU2P14A-1 (1MU8P14-1)	MU2 (MU8)	*MRR1*/*MRR1* ^{P683S}; *MTL***a**/α; *UPC2*/*UPC2* ^{G648D}	This study
1MU8P14-2	MU2 (MU8)	n.t.	This study
1MU8P14-3	MU2 (MU8)	n.t.	This study
Parental mating product UM1			
1UM21P1-1	UM1 (UM21)	n.t.	[274], this study

Name[a]	Parent	Relevant genotype and description[b][c]	References
1UM21P1-2	UM1 (UM21)	n.t.	[274], this study
1UM21P1-3	UM1 (UM21)	n.t.	[274], this study
1UM21P2-1	UM1 (UM21)	n.t.	[274], this study
1UM21P2-2	UM1 (UM21)	n.t.	[274], this study
1UM21P2-3	UM1 (UM21)	n.t.	[274], this study
UM1P3A-1 (1UM21P3-1)	UM1 (UM21)	*MRR1* ^{P683S}; *MTL***a**/α; *UPC2*/*UPC2*^{G648D}	[274], this study
1UM21P3-2	UM1 (UM21)	n.t.	[274], this study
UM1P3A-3 (1UM21P3-3)	UM1 (UM21)	*MRR1* ^{P683S}; *MTL***a**/α; *UPC2*/*UPC2*^{G648D}	[274], this study
1UM21P4-1	UM1 (UM21)	n.t.	[274], this study
1UM21P4-2	UM1 (UM21)	n.t.	[274], this study
1UM21P4-3	UM1 (UM21)	n.t.	[274], this study
1UM21P5-1	UM1 (UM21)	n.t.	[274], this study
1UM21P5-2	UM1 (UM21)	n.t.	[274], this study
1UM21P5-3	UM1 (UM21)	n.t.	[274], this study
1UM21P6-1	UM1 (UM21)	n.t.	[274], this study
1UM21P6-2	UM1 (UM21)	n.t.	[274], this study
1UM21P6-3	UM1 (UM21)	n.t.	[274], this study
1UM21P8-1	UM1 (UM21)	n.t.	[274], this study
1UM21P8-2	UM1 (UM21)	n.t.	[274], this study
1UM21P8-3	UM1 (UM21)	n.t.	[274], this study
1UM21P10-1	UM1 (UM21)	n.t.	[274], this study
1UM21P10-2	UM1 (UM21)	n.t.	[274], this study
1UM21P10-3	UM1 (UM21)	n.t.	[274], this study
1UM21P12-1	UM1 (UM21)	n.t.	[274], this study
1UM21P12-2	UM1 (UM21)	n.t.	[274], this study
1UM21P12-3	UM1 (UM21)	n.t.	[274], this study
1UM21P14-1	UM1 (UM21)	n.t.	This study
1UM21P14-2	UM1 (UM21)	n.t.	This study
1UM21P14-3	UM1 (UM21)	n.t.	This study
1UM21P16-1	UM1 (UM21)	n.t.	This study
1UM21P16-2	UM1 (UM21)	n.t.	This study
1UM21P16-3	UM1 (UM21)	n.t.	This study
Parental mating product TU1			
1TU1P1-1	TU1	n.t.	[274], this study
1TU1P1-2	TU1	n.t.	[274], this study
1TU1P1-3	TU1	n.t.	[274], this study
1TU1P2-1	TU1	n.t.	[274], this study
1TU1P2-2	TU1	n.t.	[274], this study
1TU1P2-3	TU1	n.t.	[274], this study
1TU1P3-1	TU1	n.t.	[274], this study
1TU1P3-2	TU1	n.t.	[274], this study
1TU1P3-3	TU1	n.t.	[274], this study
1TU1P4-1	TU1	n.t.	[274], this study
1TU1P4-2	TU1	n.t.	[274], this study
1TU1P4-3	TU1	n.t.	[274], this study
1TU1P5-1	TU1	n.t.	[274], this study
1TU1P5-2	TU1	n.t.	[274], this study
1TU1P5-3	TU1	n.t.	[274], this study
1TU1P6-1	TU1	n.t.	[274], this study
1TU1P6-2	TU1	n.t.	[274], this study
TU1P6A-3 (1TU1P6-3)	TU1	*MTL***a**/α; *TAC1-2*/*TAC1*^{G980E}; *UPC2*/*UPC2*^{G648D}	[274], this study
1TU1P8-1	TU1	n.t.	[274], this study
1TU1P8-2	TU1	n.t.	[274], this study
1TU1P8-3	TU1	n.t.	[274], this study
1TU1P10-1	TU1	n.t.	[274], this study
1TU1P10-2	TU1	n.t.	[274], this study
1TU1P10-3	TU1	n.t.	[274], this study
TU1P11A-1 (1TU1P11-1)	TU1	*MTL***a**; *TAC1*^{G980E}; *UPC2*/*UPC2*^{G648D}	[274], this study

Name[a]	Parent	Relevant genotype and description[b][c]	References
1TU1P11-2	TU1	n.t.	[274], this study
TU1P11A-3 (1TU1P11-3)	TU1	*MTL***a**; *TAC1*^{G980E}; *UPC2*/*UPC2*^{G648D}	[274], this study
1TU1P12-1	TU1	n.t.	[274], this study
1TU1P12-2	TU1	n.t.	[274], this study
1TU1P12-3	TU1	n.t.	[274], this study
1TU1P14-1	TU1	n.t.	This study
1TU1P14-2	TU1	n.t.	This study
1TU1P14-3	TU1	n.t.	This study
1TU1P16-1	TU1	n.t.	This study
1TU1P16-2	TU1	n.t.	This study
1TU1P16-3	TU1	n.t.	This study
Parental mating product UT1			
1UT86P1-1	UT1 (UT86)	n.t.	[274], this study
1UT86P1-2	UT1 (UT86)	n.t.	[274], this study
1UT86P1-3	UT1 (UT86)	n.t.	[274], this study
1UT86P2-1	UT1 (UT86)	n.t.	[274], this study
UT1P2A-2 (1UT86P2-2)	UT1 (UT86)	*MTL***a**/α; *TAC1-1*/*TAC1*^{G980E}; *UPC2*/*UPC2*^{G648D}	[274], this study
UT1P2A-3 (1UT86P2-3)	UT1 (UT86)	*MTL***a**/α; *TAC1-1*/*TAC1*^{G980E}; *UPC2*/*UPC2*^{G648D}	[274], this study
1UT86P3-1	UT1 (UT86)	n.t.	[274], this study
1UT86P3-2	UT1 (UT86)	n.t.	[274], this study
1UT86P3-3	UT1 (UT86)	n.t.	[274], this study
1UT86P4-1	UT1 (UT86)	n.t.	[274], this study
1UT86P4-2	UT1 (UT86)	n.t.	[274], this study
1UT86P4-3	UT1 (UT86)	n.t.	[274], this study
UT1P5A-1 (1UT86P5-1)	UT1 (UT86)	*MTL*α; *TAC1*^{G980E}; *UPC2*/*UPC2*^{G648D}	[274], this study
UT1P5A-2 (1UT86P5-2)	UT1 (UT86)	*MTL***a**/α; *TAC1-1*/*TAC1*^{G980E}; *UPC2*/*UPC2*^{G648D}	[274], this study
1UT86P5-3	UT1 (UT86)	n.t.	[274], this study
1UT86P6-1	UT1 (UT86)	n.t.	[274], this study
1UT86P6-2	UT1 (UT86)	n.t.	[274], this study
1UT86P6-3	UT1 (UT86)	n.t.	[274], this study
1UT86P8-1	UT1 (UT86)	n.t.	[274], this study
1UT86P8-2	UT1 (UT86)	n.t.	[274], this study
1UT86P8-3	UT1 (UT86)	n.t.	[274], this study
1UT86P10-1	UT1 (UT86)	n.t.	[274], this study
1UT86P10-2	UT1 (UT86)	n.t.	[274], this study
1UT86P10-3	UT1 (UT86)	n.t.	[274], this study
1UT86P12-1	UT1 (UT86)	n.t.	[274], this study
1UT86P12-2	UT1 (UT86)	n.t.	[274], this study
1UT86P12-3	UT1 (UT86)	n.t.	[274], this study
1UT86P13-1	UT1 (UT86)	n.t.	This study
1UT86P13-2	UT1 (UT86)	n.t.	This study
1UT86P13-3	UT1 (UT86)	n.t.	This study
1UT86P14-1	UT1 (UT86)	n.t.	This study
1UT86P14-2	UT1 (UT86)	n.t.	This study
1UT86P14-3	UT1 (UT86)	n.t.	This study

[a] Originally used strain names are indicated in parentheses. Please note that initially randomly picked strains of all experiments were consecutively numbered. Subsequently, selected strains were systematically renamed.

[b] *FRT* sites are not listed. Exact number of mentioned alleles was not examined. Given alleles indicate at least one copy of the respective form.

[c] n.t.: not tested

4.2. Methods

4.2.1. Growth of *Escherichia coli* strains

Escherichia coli strains were grown overnight in LB medium in a shaking incubator at 200rpm or on solid LB agar at 37°C. Optionally, 100µg/ml Ampicillin or 50µg/ml Chloramphenicol was added to prevent a loss of the plasmid. For storage, 17.2% glycerol was added and stocks were frozen at -80°C.

4.2.2. Growth of *Candida albicans* strains

All *Candida albicans* strains were frozen as stocks with 17.2% glycerol and stored at -80°C. In general, strains were grown in YPD liquid medium in a shaking incubator at 220rpm or on YPD agar plates. Cells in the white phenotype were cultivated at 30°C and strains in the opaque phenotype at 25°C. For the identification of opaque and white colonies, strains were grown on Lee's agar, pH 6.8 [324] at room temperature (RT). Additionally, phloxine B was supplemented, which selectively stains opaque colonies pink [218]. YPD agar plates with 200µg/ml of the dominant marker nourseothricin were used for the selection of nourseothricin-resistant transformants (strains harboring the correctly integrated *caSAT1* selection marker). For the recycling of the *SAT1* flipper (*SAT1* flipper cassette with the maltose-induced *MAL2* promoter), strains were cultivated in YPM medium.

4.2.3. Construction of *Candida albicans* strains

4.2.3.1. Gel-electrophoresis

To visualize DNA fragments and estimate their size, agarose gel-electrophoresis was performed. This method allows the separation of charged molecules, like DNA, in an electric field. Generally, 1% agarose gels were prepared with 1x TAE. DNA samples, supplemented with loading dye (1x), were loaded on the gels. After separation of the DNA fragments, the gel was stained in an ethidium bromide bath (10mg/ml ethidium bromide, which incorporates with DNA). The stained DNA was visualized using UV-light and pictures were taken with a gel documentation system. Determination of DNA fragment sizes were done in comparison to a 1kb ladder with known molecular size.

4.2.3.2. Isolation of DNA fragments from *Escherichia coli*

Plasmid isolation from *E. coli* cultures was carried out with the NucleoSpin® Plasmid Kit from Macherey-Nagel according to the manufacturer's instructions. The isolated DNA was digested, followed by separation by gel-electrophoresis using a 1% agarose gel. Hereafter required DNA fragments (inserts) were excised from the agarose gel and purified with the NucleoSpin® Gel Kit from Macherey-Nagel according to the manufacturer's instructions.

4.2.3.3. Transformation of *Candida albicans*

Gel-purified inserts from the *SAT1*flipper cassette or the plasmid pADH1R1A were used to replace endogenous alleles in *C. albicans* strains by electroporation [325], following the protocol published by Köhler *et al*. [326]. Unless stated otherwise, all centrifugation steps were done at 4000rpm for 5min at 4°C.

A *C. albicans* culture was inoculated and grown overnight at 30°C in a shaking incubator to the stationary phase. A subculture was inoculated and grown overnight at 30°C to the mid log phase. After centrifugation, the pellet was resuspended in a 10ml solution of 100mM Lithium acetate and TE Buffer, pH 7.5. After incubation of the suspension in a shaking incubator for 1h at 30°C, 250µl 1M DDT was added. Thereafter, the suspension was incubated in a shaking incubator for 30min at 30°C. 40ml cold water was added, the suspension was pelleted and washed with 25ml cold water. The pellet was resuspended with 5ml cold 1M sorbitol, which stabilizes the cells osmotically. This was followed by a centrifugation step; the supernatant was discarded and the pellet was resuspended in the remaining fluid. 40µl of the cell suspension was mixed with 5µl of the DNA (insert) in a cold cuvette (electroporation cuvette with a 2mm electrode gap). The suspension was incubated for 5min on ice. Afterwards, electroporation was conducted at 1.8kV. 1ml YPD medium was added to the cells and the suspension was split into two Eppendorf tubes. After 4h incubation in a shaking incubator at 30°C, cells were pelleted for 2min at 8000rpm. The supernatant was discarded, cells were resuspended in the remaining fluid and plated on YPD agar plates containing 200µl nourseothricin. During the 4h incubation, successfully transformed cells synthesize streptothricin-N-acetyltransferase, which is contained in the *SAT1*flipper cassette and the plasmid pADH1R1A (Figure 2, Figure 5). Therefore, positive transformants can grow in the presence of the dominant selection marker nourseothricin on the agar plates. After 2 days of incubation at 30°C, colonies were picked and further analyzed.

4.2.3.4. Isolation of chromosomal *Candida albicans* DNA

To verify the correct integration of the inserts during transformation of *C. albicans* and a successful recycling of the *SAT1* flipper cassette, chromosomal DNA was isolated and afterwards, Southern hybridization was performed (chapter 4.2.3.5). Isolation of genomic DNA was performed as described previously [272] with slight modifications. If not mentioned otherwise, all centrifugation steps were done at 13000rpm for 3 to 5min.

Cells from an overnight culture were pelleted for 5min at 4000rpm and resuspended in 200µl breaking buffer. Afterwards, 200µl glass beads and 200µl phenol/chloroform/isoamyl alcohol (25:24:1) were added and the cells were lysed by vortexing for 10min. 200µl TE buffer was added, the suspension was shortly vortexed, followed by centrifugation. Optionally, 200µl chloroform/isoamyl alcohol was added, the suspension was vortexed for 2min and centrifuged. The DNA in the aqueous phase was precipitated with 100% isopropanol at -20°C, pelleted and washed with 70% ethanol. Thereafter, the DNA was dissolved in 50µl water and 2µl RNase A (2.86mg/ml).

For particular experiments, an exact amount of DNA was needed. DNA samples potentially contain trace amounts of RNA, therefore, samples where DNA was to be measured were treated as follows. DNA was precipitated with 100% isopropanol as described previously and dissolved in 400µl TE buffer. RNA was then degraded by the addition of 10µl RNase A (2.86mg/ml) and the mixture was incubated for 10min at 37°C. The sample was mixed with 100% ethanol in order to precipitate the DNA. Thereafter, the DNA was pelleted, dissolved in 50µl water and the DNA concentration was measured with the NanoDrop ND-1000 Spectrophotometer.

4.2.3.5. Southern hybridization

10-30µg of DNA was digested with appropriate restriction enzymes and separated on a 1% agarose gel. Afterwards, DNA was transferred onto a nylon membrane by vacuum blotting. Prior to the transfer, the Whatman™ Nytran® SPC nylon transfer membrane (0.45µm pore size) was incubated for 2min in water and 5min in 20x SSC. Thereafter, the Southern blot setup was assembled and the membrane was placed in the vacuum blotter. The gel with the digested DNA fragments was placed on the membrane and the vacuum was started. First, Solution A was incubated for 15min to depurinate DNA. This was followed by a 15min incubation step with Solution B during which denaturation took place and a 15min incubation with Solution C for neutralization. DNA transfer was conducted for at least 90min with 20x SSC. The Southern blot apparatus was disassembled and the membrane containing the DNA fragments was incubated for 20sec in 0.4N NaOH (denaturation), followed by a neutralization

step for 30sec in 0.2M Tris-Cl pH 7.5. The DNA was crosslinked to the membrane via UV-illumination (Stratalinker 1800 with the setting auto crosslink).

Southern hybridization with enhanced chemiluminescence-labeled probes (amplified by PCR, as described in chapter 4.2.3.6) was conducted with an Amersham ECL Direct Nucleic Acid Labeling and Detection System following the instructions of the manufacturer. The exposure of the Amersham Hyperfilm™ ECL-high-performance chemiluminescence film to the membrane depended on the signal intensity.

4.2.3.6. Polymerase chain reaction

For the amplification of DNA from plasmids or chromosomal DNA of *C. albicans*, polymerase chain reaction (PCR) was applied. Following the manufacturer's instructions, PCR mixtures and cycles were set. Different DNA-polymerases like Phusion or Taq were used. Taq DNA Polymerase was used in most cases for the probe synthesis, whereas the Phusion high fidelity DNA polymerase was preferably used for error-free sequences (necessary for sequencing reactions) and long sequences (e.g. some probes). Dependent on the size of the respective DNA-fragment, elongation time was adjusted. Annealing temperature was set according to the primers' melting points and was calculated with the online based tool OligoCalc (Oligonucleotide Properties Calculator) [327], or ncbi.nlm.nih.gov. Gel-electrophoresis was performed to verify the success of the PCR. Optionally, the PCR product was purified with the PCR Clean-up GeneClean® III-Kit (Macherey-Nagel).

4.2.3.7. Sequencing

To validate the introduction of *MRR1* resistance mutations (chapter 2.1.5), *MRR1* of the heterozygous and homozygous mutants was reamplified and the purified PCR products sequenced. The sequencing reactions were sent to Seqlab (Göttingen). Analysis of the sequences was performed with web-based sequence analysis tools like BLAST at candidagenome.org and ncbi.nlm.nih.gov. Furthermore, the sequence alignment tool BioEdit (Tom Hall, Ibis Therapeutics, Carlsbad) was used.

4.2.4. Microevolution assays

4.2.4.1. Isolation of strains that have become homozygous for the *MTL* by drug exposure

One aim of this work was to isolate strains with a fluconazole-induced homozygosity for the *MTL* locus and at the same time for the *ERG11*^{G464S}, *MRR1*^{P683S}, *TAC1*^{G980E} or *UPC2*^{G648D} allele. For this purpose, resistance mutation and at the same time *MTL* locus heterozygous strains were cultivated in rich medium (YPD) with 1.75, 2.5, or 5µg/ml fluconazole to allow for the enrichment of cells with increased resistance. Strains were transferred 1:100 daily in fresh YPD medium with fluconazole and in parallel an appropriate dilution was plated on agar plates. This step was repeated up to 8 times.

The above selected fluconazole concentrations were used based on the MIC values for the starting strains (Table 4-7). *TAC1*/*TAC1*^{G980E} strains were cultivated with a fluconazole concentration of 5µg/ml. Since the resistance mutations in *ERG11* and *UPC2* have a weaker effect on fluconazole resistance than the *TAC1* gain-of-function (GOF) mutation, a lower initial fluconazole concentration (2.5µg/ml) was used to cultivate *ERG11*/*ERG11*^{G464S} and *UPC2*/*UPC2*^{G648D} strains. With this fluconazole concentration no *MTL*-homozygous and at the same time *UPC2*^{G648D} homozygous clones were isolated. Therefore, *UPC2*/*UPC2*^{G648D} strains were additionally grown in the presence of 5µg/ml fluconazole. *MRR1*/*MRR1*^{P683S} strains were cultivated with 5µg/ml fluconazole. Since no *MTL*-homozygous clones were obtained, two further fluconazole concentrations, 2.5µg/ml and 1.75µg/ml, were used.

Genetically engineered *TAC1*^{G980E} homozygous strains grow better and produce considerably larger colonies than *TAC1*^{G980E} heterozygous strains on YPD agar plates containing 5µg/ml fluconazole (Figure 11). Therefore, subcultures of *TAC1*/*TAC1*^{G980E} strains were plated for single colonies on YPD agar plates containing 5µg/ml fluconazole and incubated for 2 days at 30°C. Large single colonies were picked and characterized.

Instead of screening for a changed colony size, passages of the strains with a heterozygous *ERG11*, *MRR1* or *UPC2* resistance mutation were screened for switching-competent cells. It has been shown that strains which are homozygous for the *MTL* locus can switch to the opaque phenotype [25]. Hence, appropriate dilutions of each passage were plated on Lee's agar plates, pH 6.8 [324] with 5µg/ml phloxine B, which selectively stains opaque colonies pink [218]. As white-to-opaque switching can be induced with high CO_2 concentrations [211], agar plates were incubated for 2 days at 18% CO_2 and 25°C and afterwards for 5 days at room temperature in normal atmosphere. Opaque colonies were characterized for homozygosity of the resistance mutation and the *MTL* locus by Southern hybridization.

4.2.4.2. Isolation of mating products with different resistance mechanisms

MTL homozygous strains with specific resistance mutations in the mating-competent opaque morphology were streaked from the glycerol stock on Lee's agar plates, pH 6.8 with 5µg/ml phloxine B and incubated for several days at room temperature. After inoculation of an opaque colony of each strain into YPD medium, the cultures were grown overnight at 25°C in a shaking incubator. The next day, $3x10^7$ cells of a *MTL***a** strain were mixed with $3x10^7$ cells of a *MTL*α strain. For cell counting, a hemocytometer Thoma (Thoma new, 0.0025mm^2, Hecht Assistent) was used. The suspension was spotted on Spider agar plates, pH 7.2 [243]. To prevent switching of the cells to the white phenotype and/or to induce white-to-opaque switching, the plates were incubated for 2 days at 18% CO_2 and 25°C, followed by an incubation for up to 12 days under room conditions. At various time points fractions of the cell lawn were taken, suspended in water and an appropriate dilution was plated on Lee's agar with phloxine B.

During optimization of the experimental mating conditions, part of the mating spot was taken, suspended in phosphate-buffered saline (PBS) and sonicated to disperse cell clumps. Sonication was performed for one, two or three rounds (one round = three times sonication for 10 seconds; 70% cycle) and the suspension was chilled between the single sonication steps on ice. This was done for UT (parental strains SCUPC2R12hom1A and SCTAC1R32hom2A) and EM (parental strains SCERG11R32hom1B and SCMRR1R32hom1A) crosses. Since sonication turned out to be unnecessary, this step was omitted later.

The agar plates were incubated for 2 days at 18% CO_2 and 25°C and afterwards for 5 days under room conditions. Since the parental strains are *MTL* homozygous, they are able to switch to, or remain in the opaque phenotype after a stimulation with high CO_2 concentrations. In contrast, mating products cannot maintain the opaque phenotype even in conditions with high CO_2 concentrations, as long as they are *MTL* heterozygous. Consequently, white colonies were picked and further characterized. Glycerol stocks of possible mating products were prepared from an overnight culture of an isolated colony.

4.2.4.3. Isolation of mating product progeny

A single colony of a mating product was picked from a YPD agar plate, inoculated in YPD medium with fluconazole and grown for 24h at 30°C in a shaking incubator. An aliquot of the passage was frozen with 17.2% glycerol and stored at -80°C. Part of the remaining culture was diluted 1:1000 in fresh YPD medium with fluconazole. The subculture was grown for 24h at 30°C in a shaking incubator. If

necessary, subcultures were inoculated from the respective glycerol stock. During the passaging, stepwise increasing concentrations of fluconazole were added. As starting fluconazole concentration, half the MIC of the chosen mating product was used. On every second passage the fluconazole concentration was doubled. This procedure was repeated until the passage with a fluconazole concentration of 256µg/ml was reached. An appropriate dilution of the subcultures, or if necessary, of the frozen stocks was spread on YPD agar plates. Three single colonies were randomly picked after 2 days of growth at 30°C. These colonies were used for $MIC_{fluconazole}$ assays and in parallel, to prepare frozen glycerol stocks. For further analysis, the most resistant isolates of the first 6 passages and the most resistant isolates of all passages were chosen.

4.2.5. Genotypic assays

4.2.5.1. Sequence analysis of clinical isolates

To identify resistance mutations in clinical isolates, sequence analysis was conducted, as described in chapter 4.2.3.7. *UPC2* from the strains F2ADH1R1A and F5ADH1R1A was amplified by PCR (see chapter 4.2.3.6) with the primer pair UPC2-1 and UPC2-2. Afterwards, the purified PCR products were sequenced with the primers UPC2-1, UPC2-4B and UPC2-9. Furthermore, *MRR1* from the isolates TW1, TW2, TW3, TW17ADH1R1A and -B were amplified with the PCR primers ZCF36-3 and ZCF36-6. The purified PCR products were sequenced with the primer ZCF36seq4.

4.2.5.2. Genetic analysis by Southern hybridization

The genetic identity of single loci was analyzed by Southern hybridization as described in chapter 4.2.3.5 and probes were amplified by PCR as described in chapter 4.2.3.6.

Wild-type and mutated alleles of *ERG11*, *MRR1*, *TAC1* and *UPC2,* as well as polymorphic wild-type alleles of *CAP1*, *GLN3* and *MTL* were analyzed (Figure 30, Figure 31). *CAP1*, *ERG11*, *GLN3*, *TAC1* and *UPC2* were digested with a single restriction enzyme. *MRR1* and the *MTL* locus were digested with two different restriction enzymes (Table 22). DNA fragment sizes were calculated with the help of candidagenome.org.

Table 22: Different loci analyzed by Southern hybridization during this study.

Locus	Detected fragment sizes	Restriction enzyme	Probe	Primers for probe amplification
CAP1	*CAP1-1*: 3808bp, *CAP1-2*: 1339bp[(a)]	EcoRI	CAP1	CAP1-1, CAP1-2
ERG11	*ERG11*: 6581bp, *ERG11*^{G464S}: 7045bp	EcoRV	ERG11-GOF	ERG4, ERG9
GLN3	*GLN3-1*: 4206bp, *GLN3-2*: 9661bp	ClaI	GLN3	GLN1, GLN5
MRR1	*MRR1*: 7732bp, *MRR1*^{P683S}: 5498bp	SpeI	MRR1-GOF	ZCF36-1, ZCF36-2
	MRR1: 4974bp, *MRR1*^{P683S}: 5508bp	NsiI		
MTL	*MTL***a**: 4331bp, *MTL*α: 3071bp	EcoRI	3'MTL	MTL3F, MTL3R
	*MTL***a**: 6465bp, *MTL*α: 4866bp		5'MTL	MTL5F, MTL5R
	*MTL***a**: 3950bp, *MTL*α: 16352bp	XhoI	5'MTL	MTL5F, MTL5R
TAC1	*TAC1-1*: 5692bp, *TAC1-2*: 2772bp, *TAC1*^{G980E}: 1721bp	SpeI	TAC1-GOF	Tac1-9, Tac1-11
UPC2	*UPC2*: 3235bp, *UPC2*^{G648D}: 2738bp	BglII	UPC2-GOF	UPC2-1, UPC2-2

[(a)] Please note that the *CAP1* probe binds an additional fragment with the size of 1868bp (*CAP1-2* allele). This fragment was not detected in the Southern blots during this study (see Figure 12) due to the chosen experimental conditions.

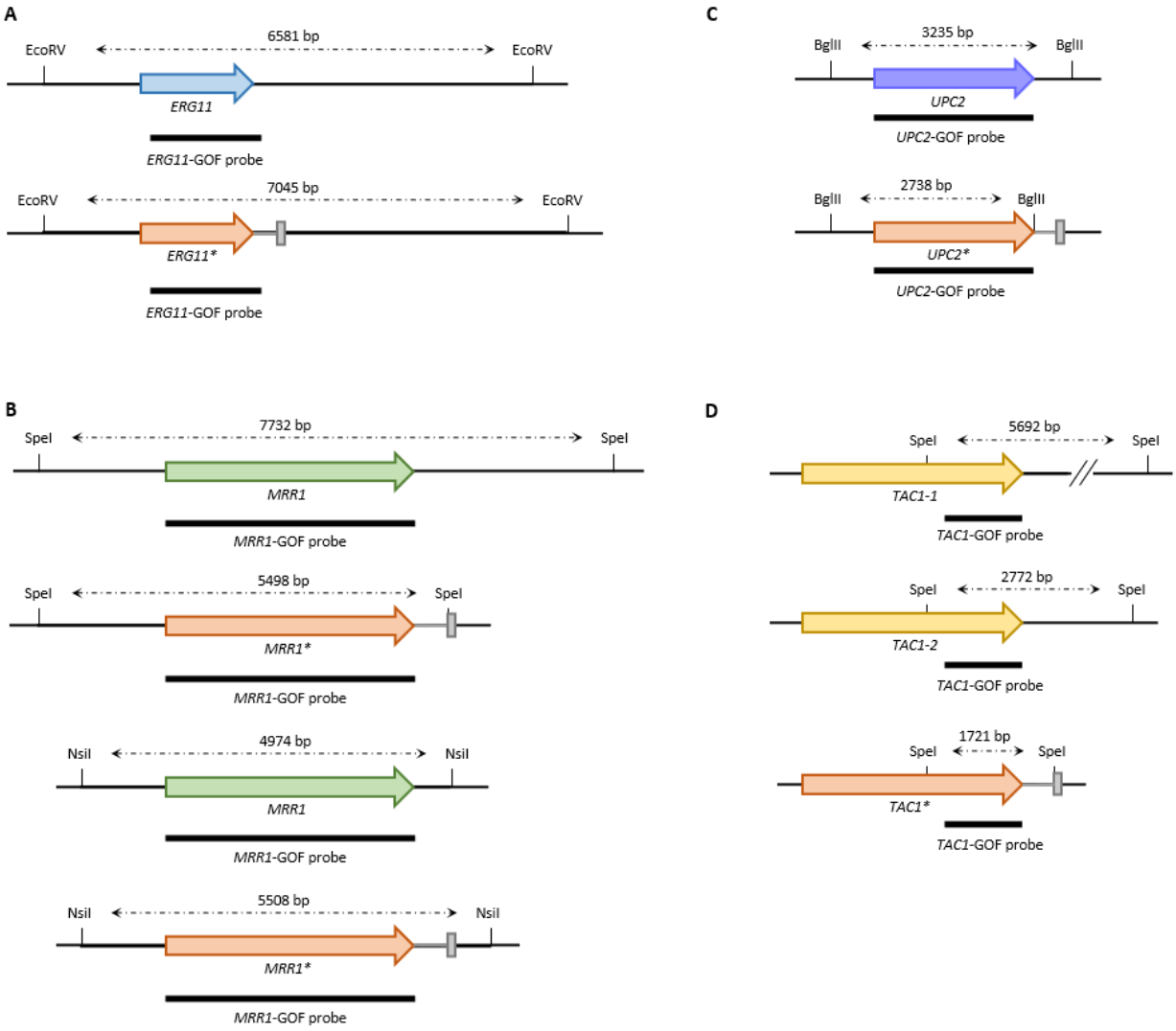

Figure 30: Schematic of the differentiation of wild-type and mutated alleles by Southern hybridization. Mutated alleles of (A) *ERG11*, (B) *MRR1*, (C) *UPC2* and (D) *TAC1* are indicated in red, used restriction sites are given and detected fragment sizes are shown. *MRR1* was analyzed with two different restriction enzymes and polymorphic *TAC1* wild-type alleles 1 and 2 were distinguished. Probes are indicated as black bars. Gray bars and boxes show the *ACT1* transcription termination sequence and *FRT* sites, which were introduced during transformation of the strains. Adapted from [274].

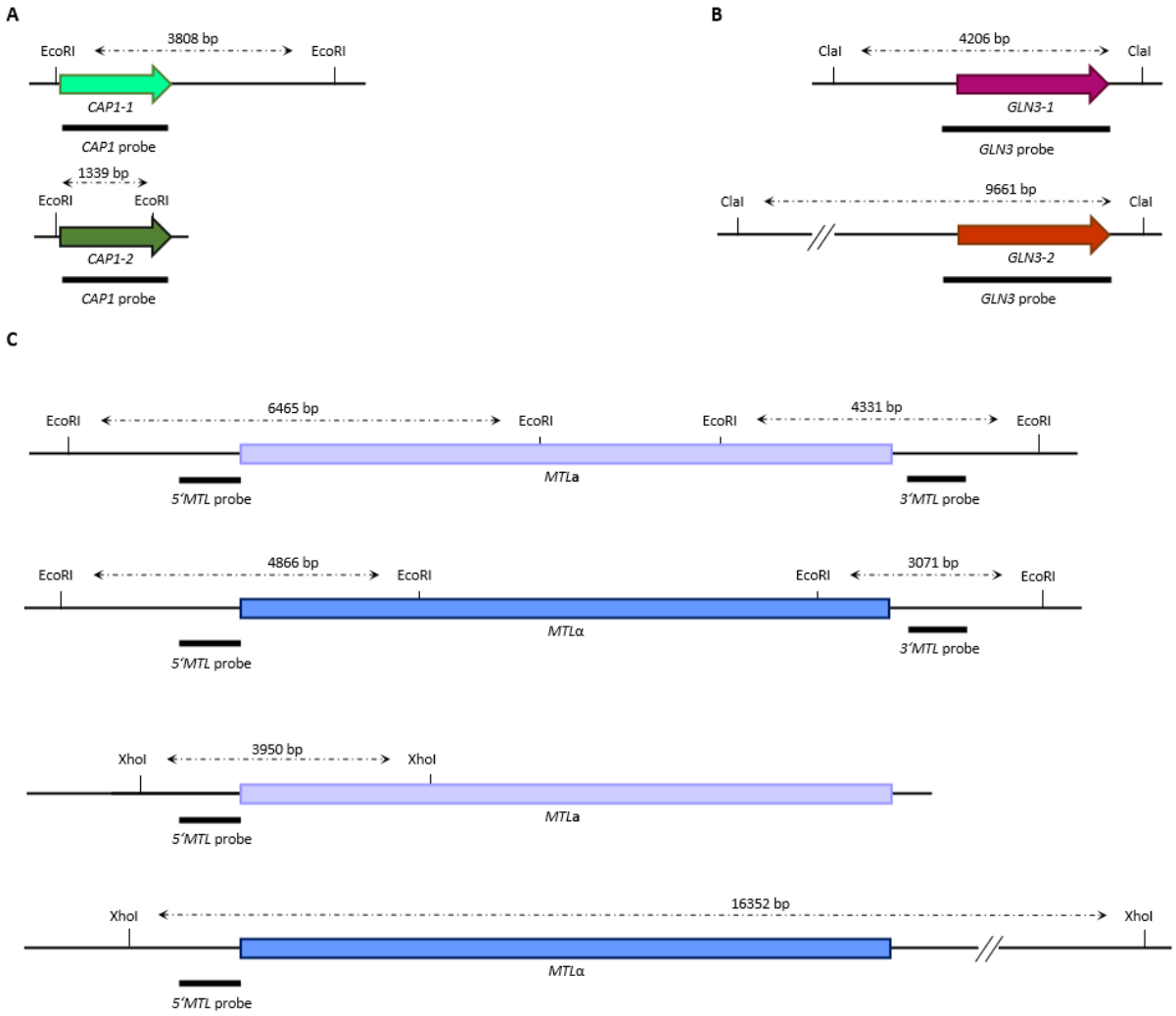

Figure 31: Schematic of the differentiation of polymorphic alleles by Southern hybridization. Alleles of (A) *CAP1*, (B) *GLN3* and (C) *MTL* are shown. Used restriction sites (*MTL* locus was analyzed with two different restriction enzymes) and detected fragment sizes are given. Probes are indicated as black bars. Please note that the *CAP1* probe binds an additional fragment with the size of 1868bp (*CAP1-2* allele). This fragment is not shown in this figure since it was not detected in the Southern blots during the present study due to the chosen experimental conditions. Adapted from [274].

4.2.5.3. Measurement of DNA content by flow cytometry

Ploidy of the chosen strains was determined by a previously described protocol [143] with some modifications. If not otherwise stated, all centrifugation steps were done at 1000g for 5min.

Strains were incubated in a shaking incubator in a 96-well microtiter plate at 30°C in YPD medium overnight. Afterwards, the cultures were subcultured in fresh YPD medium and grown in a shaking incubator for 4h at 30°C. Cells were pelleted and resuspended in 20µl of 50:50 TE. Cells were then fixed with 180µl of 90% ethanol overnight at -20°C. After two washing steps with 200µl 50:50 TE, cells were resuspended in 50µl RNase A solution and incubated for 3h at 37°C. The sample was treated with 50µl Proteinase K solution and incubated for 30min at 37°C in a shaking incubator. Cells were pelleted and resuspended in 50µl 50:50 TE and 50µl SYBR Green solution. Afterwards, they were incubated

overnight at room temperature and washed twice with 200µl 50:50 TE. Flow cytometry was conducted using a MACSQuantAnalyzer (Miltenyi Biotec, Bergisch Gladbach, Germany). After collection of data from at least 10,000 cells, data analysis was performed with FlowJo 10 (Becton, Dickinson and Company, USA).

4.2.6. Phenotypic assays

4.2.6.1. Fluconazole susceptibility assay

Determination of fluconazole susceptibilities was done by a broth microdilution method, also called MIC (minimal inhibitory concentration) assay, as already described [328] with slight changes. Strains were streaked on YPD agar plates and incubated for 2 days at 30°C. A single colony was suspended in 2ml 0.9% NaCl and 4µl of the suspension was mixed with 2ml 2xSD-CSM medium. Starting with a concentration of 512µg/ml of fluconazole, a 2-fold dilution series was prepared in water. After mixing 100µl of the cell suspension with 100µl of each fluconazole dilution in a 96-well microtiter plate, the plates were incubated for 48h at 37°C. The fluconazole concentration that abolished, or drastically reduced visible growth compared to a drug-free control of the wild-type strain SC5314 was defined as the MIC.

4.2.6.2. White-opaque switching frequency and phenotypic characterization of white and opaque colonies

To determine the white-opaque switching frequency of *C. albicans* strains, cells were streaked from frozen stocks on Lee's agar plates with phloxine B and grown for 7 days under room conditions. A single white and/or opaque colony was suspended in 200µl water and a dilution series was prepared. Appropriate dilutions were spread on two Lee's agar plates with phloxine B. One plate of each dilution was incubated for 7 days under room conditions and one plate for 2 days at 18% CO_2, 20% O_2 and 25°C, followed by an incubation under room conditions for 5 days. As already mentioned above, white-to-opaque switching can be induced with high CO_2 levels [211] and phloxine B stains opaque colonies pink [218]. White, opaque and mixed (white and opaque cells in a colony) colonies were counted. Pictures of the colonies and cells were taken with a stereo-microscope or brightfield microscope, respectively.

4.2.6.3. Dilution spot assay

In order to comparatively examine the ability of different strains to grow under fluconazole stresses, spot assays were used. Cultures of the strains were grown at 30°C in a shaking incubator in YPD or SD medium. After one night of growth, the cultures were diluted to an optical density (OD) at 600 nm of 2.0. A ten-fold dilution series was prepared (10^0 to 10^{-5}) in a 96-well microtiter plate and about 5µl of the cell suspension was transferred with a replicator onto YPD agar or SD agar plates with and without 5µg/ml fluconazole. Afterwards, plates were incubated for 2 days at 30°C and pictures were taken.

4.2.7. Competition assays

4.2.7.1. *In vitro* competitive fitness assay

Cultures of the strains were grown overnight in 10ml YPD medium at 30°C in a shaking incubator. An unlabeled and an *RFP*-labeled strain were mixed in a 1:1 ratio. Subcultures were inoculated in YPD medium with a starting OD_{600} of 0.002 and grown at 30°C for 24h in a shaking incubator. Next, the mixtures were diluted to an OD_{600} of 0.002 in fresh YPD medium, followed by 24h of growth in a shaking incubator at 30°C. After 24h and 48h of co-incubation appropriate dilutions of each co-culture were spread on YPD plates. After two days of growth at 30°C, colonies on the plates were counted. The different strains were distinguished by their colony color. Colonies of *RFP*-labeled strains appeared red and colonies of unlabeled strains white. The red color of the colonies was intensified by the storage of the plates at 4°C. Colonies of each color were counted and the ratio of white and red colonies calculated.

4.2.7.2. Mouse model of gastrointestinal colonization

Four days prior to infection with *C. albicans*, 6-8-week-old female BALB/c mice (Janvier Labs, Saint-Berthevin, France) were fed with 1mg/ml tetracycline, 2mg/ml streptomycin and 0.1mg/ml gentamicin in their drinking water. After an overnight growth of *C. albicans* strains in YPD medium at 30°C in a shaking incubator, the cultures were centrifuged for 2min at 4000rpm and resuspended in 5ml phosphate-buffered saline (PBS). The washing was repeated and the cell density was adjusted to 10^9cells/ml. For cell counting a hemocytometer Thoma (Thoma new, 0.0025mm^2, Hecht Assistent) was used. Competing strains were mixed in a 1:1 ratio and 50µl of the suspension (containing approximately $5x10^7$ cells) was fed to the mice. An appropriate dilution of the infection dosage was spread on YPD plates. 24h after infection and on the following 6 days, the feces of the mice were

collected, homogenized in PBS and a dilution series was prepared. Remaining homogenized feces were frozen with 8-10% glycerol at -80°C as a backup. Appropriate dilutions were plated on YPD plates containing 50µg/ml chloramphenicol, and if necessary, dilutions of the frozen stocks were plated as well. Proportions of the strains were determined by counting of the numbers of red and white colonies in the inoculum and in the populations recovered on each following day from the feces.

The colonization of different parts of the GI (gastrointestinal) tract is reflected by the CFUs (colony forming units) in fecal pellets [284]. To exclude contaminations and for the verification that the strains maintain their characteristic colony phenotype, two mice were infected with single *RFP*-labeled and unlabeled strains. For each pair of fluconazole-susceptible and fluconazole-resistant clinical isolates, four different mixtures were tested. The *RFP*-labeled fluconazole-susceptible strain (A and B isolate) was examined with the unlabeled fluconazole-resistant isolate twice. *Vice versa* the unlabeled fluconazole-susceptible strain was tested with the *RFP*-labeled fluconazole-resistant isolate two times (A and B isolate). Per mixture at least 3 mice were infected.

4.2.7.3. Mouse model of intravenous infection

After an overnight growth of the *Candida albicans* strains in YPD medium at 30°C in a shaking incubator, cultures were centrifuged for 2min at 4000rpm and resuspended in 5ml phosphate-buffered saline (PBS). The washing was repeated twice, and cell density was adjusted to $2x10^6$cells/ml. For cell counting a hemocytometer Thoma (Thoma new, 0.0025mm^2, Hecht Assistent) was used. For each pair of fluconazole-susceptible and fluconazole-resistant clinical isolates, four different mixtures were tested, as described in chapter 2.1.7. The competing strains were mixed in a 1:1 ratio. At least three 6-8 weeks old female BALB/c mice (Janvier Labs, Saint-Berthevin, France) were infected with one infection dosage mixture. As an additional control for each experiment, one mouse was infected with a single *RFP*-labeled strain. 100µl of the infection dosage was injected into the lateral tail vein. An appropriate dilution of the infection dosage was spread on YPD plates containing 50µg/ml chloramphenicol.

Mouse kidneys were collected 6 days after infection and stored at -20°C until they were processed. Afterwards, they were homogenized in sterile PBS and a dilution series was prepared. Appropriate dilutions were spread on YPD plates containing 50µg/ml chloramphenicol. The proportions of the strains were determined by counting white and red colonies. Remaining inoculum and homogenized organs were frozen with 8-10% glycerol at -80°C as a backup and if necessary, appropriate dilutions from these frozen stocks were plated.

4.2.7.4. Statistical analysis

For *in vitro* competition experiments the paired two-tailed t-test was applied due to the assumption that the collected data fit a standard normal distribution, as assays were performed in YPD medium under controlled conditions (30°C, room conditions). Relative proportions of the strains in the inoculum were compared to strains that were co-cultured for 1 or 2 days. Statistical analysis of the *in vivo* competition assays was conducted using the Wilcoxon signed-rank test. Proportions of strains in the inoculum and at the different days after infection (collected from infected mice) were compared. Every statistical analysis was performed with GraphPad Prism (version 6.07) software.

4.2.7.5. Ethics statement

Approval of the animal studies and protocols (permission number AZ 2531.01-07/12) was executed by the local government of Lower Franconia, Germany. According to the guidelines for animal care and experimentation of the German Animal Protection Law and the EU directive 2010/63/EU, every animal experiment was rigidly conducted.

5. Literature

[1] Perfect, J.R., 2017, *The antifungal pipeline: a reality check.* Nat Rev Drug Discov. 16: p. 603-616.

[2] Brown, G.D., D.W. Denning, N.A. Gow, S.M. Levitz, M.G. Netea, and T.C. White, 2012, *Hidden killers: human fungal infections.* Sci Transl Med. 4: p. 165rv13.

[3] Havlickova, B., V.A. Czaika, and M. Friedrich, 2008, *Epidemiological trends in skin mycoses worldwide.* Mycoses. 51 Suppl 4: p. 2-15.

[4] Sobel, J.D., 2007, *Vulvovaginal candidosis.* Lancet. 369: p. 1961-71.

[5] Saccente, M., 2009, *Clinical Mycology* ed. E. J. Anaissie, M. R. McGinnia, and M.A. Pfaller. Churchill Livingstone.

[6] Brown, G.D., D.W. Denning, and S.M. Levitz, 2012, *Tackling human fungal infections.* Science. 336: p. 647.

[7] Wisplinghoff, H., T. Bischoff, S.M. Tallent, H. Seifert, R.P. Wenzel, and M.B. Edmond, 2004, *Nosocomial bloodstream infections in US hospitals: analysis of 24,179 cases from a prospective nationwide surveillance study.* Clin Infect Dis. 39: p. 309-17.

[8] Pfaller, M.A. and D.J. Diekema, 2010, *Epidemiology of invasive mycoses in North America.* Crit Rev Microbiol. 36: p. 1-53.

[9] Pfaller, M.A. and D.J. Diekema, 2007, *Epidemiology of invasive candidiasis: a persistent public health problem.* Clin Microbiol Rev. 20: p. 133-63.

[10] Miceli, M.H., J.A. Diaz, and S.A. Lee, 2011, *Emerging opportunistic yeast infections.* Lancet Infect Dis. 11: p. 142-51.

[11] Bhattacharya, S., S. Sae-Tia, and B.C. Fries, 2020, *Candidiasis and Mechanisms of Antifungal Resistance.* Antibiotics (Basel). 9.

[12] Moran, G., C. Stokes, S. Thewes, B. Hube, D.C. Coleman, and D. Sullivan, 2004, *Comparative genomics using Candida albicans DNA microarrays reveals absence and divergence of virulence-associated genes in Candida dubliniensis.* Microbiology (Reading). 150: p. 3363-82.

[13] Thompson, G.R., 3rd, P.K. Patel, W.R. Kirkpatrick, S.D. Westbrook, D. Berg, J. Erlandsen, S.W. Redding, and T.F. Patterson, 2010, *Oropharyngeal candidiasis in the era of antiretroviral therapy.* Oral Surg Oral Med Oral Pathol Oral Radiol Endod. 109: p. 488-95.

[14] Zomorodian, K., N.N. Haghighi, N. Rajaee, K. Pakshir, B. Tarazooie, M. Vojdani, F. Sedaghat, and M. Vosoghi, 2011, *Assessment of Candida species colonization and denture-related stomatitis in complete denture wearers.* Med Mycol. 49: p. 208-11.

[15] Pfaller, M.A., M. Castanheira, S.A. Messer, G.J. Moet, and R.N. Jones, 2010, *Variation in Candida spp. distribution and antifungal resistance rates among bloodstream infection isolates by patient age: report from the SENTRY Antimicrobial Surveillance Program (2008-2009).* Diagn Microbiol Infect Dis. 68: p. 278-83.

[16] Berg, F.T., 1846, *Om Torsk hos Barn.* Stockholm: L. J. Hjerta.

[17] Berkhout, M., 1923, *De Schimmelgeschlachten Monilia, Oidium, Oospora en Toruta.* Dissertation, Utrecht.

[18] Kawaguchi, Y., H. Honda, J. Taniguchi-Morimura, and S. Iwasaki, 1989, *The codon CUG is read as serine in an asporogenic yeast Candida cylindracea.* Nature. 341: p. 164-6.

[19] Ohama, T., T. Suzuki, M. Mori, S. Osawa, T. Ueda, K. Watanabe, and T. Nakase, 1993, *Non-universal decoding of the leucine codon CUG in several Candida species.* Nucleic Acids Res. 21: p. 4039-45.

[20] Santos, M.A. and M.F. Tuite, 1995, *The CUG codon is decoded in vivo as serine and not leucine in Candida albicans.* Nucleic Acids Res. 23: p. 1481-6.

[21] Sugita, T. and T. Nakase, 1999, *Non-universal usage of the leucine CUG codon and the molecular phylogeny of the genus Candida.* Syst Appl Microbiol. 22: p. 79-86.

[22] Sugiyama, H., M. Ohkuma, Y. Masuda, S.M. Park, A. Ohta, and M. Takagi, 1995, *In vivo evidence for non-universal usage of the codon CUG in Candida maltosa.* Yeast. 11: p. 43-52.

[23] Bennett, R.J., 2015, *The parasexual lifestyle of Candida albicans.* Curr Opin Microbiol. 28: p. 10-7.
[24] Lockhart, S.R., C. Pujol, K.J. Daniels, M.G. Miller, A.D. Johnson, M.A. Pfaller, and D.R. Soll, 2002, *In Candida albicans, white-opaque switchers are homozygous for mating type.* Genetics. 162: p. 737-45.
[25] Miller, M.G. and A.D. Johnson, 2002, *White-opaque switching in Candida albicans is controlled by mating-type locus homeodomain proteins and allows efficient mating.* Cell. 110: p. 293-302.
[26] Slutsky, B., M. Staebell, J. Anderson, L. Risen, M. Pfaller, and D.R. Soll, 1987, *"White-opaque transition": a second high-frequency switching system in Candida albicans.* J Bacteriol. 169: p. 189-97.
[27] Lohse, M.B. and A.D. Johnson, 2009, *White-opaque switching in Candida albicans.* Curr Opin Microbiol. 12: p. 650-4.
[28] Staib, P. and J. Morschhauser, 2007, *Chlamydospore formation in Candida albicans and Candida dubliniensis--an enigmatic developmental programme.* Mycoses. 50: p. 1-12.
[29] Pande, K., C. Chen, and S.M. Noble, 2013, *Passage through the mammalian gut triggers a phenotypic switch that promotes Candida albicans commensalism.* Nat Genet. 45: p. 1088-91.
[30] Morschhauser, J., 2010, *Regulation of white-opaque switching in Candida albicans.* Med Microbiol Immunol. 199: p. 165-72.
[31] Barnett, J.A., 2008, *A history of research on yeasts 12: medical yeasts part 1, Candida albicans.* Yeast. 25: p. 385-417.
[32] Bensasson, D., J. Dicks, J.M. Ludwig, C.J. Bond, A. Elliston, I.N. Roberts, and S.A. James, 2019, *Diverse Lineages of Candida albicans Live on Old Oaks.* Genetics. 211: p. 277-288.
[33] Odds, F.C. and M.D. Jacobsen, 2008, *Multilocus sequence typing of pathogenic Candida species.* Eukaryot Cell. 7: p. 1075-84.
[34] Pfaller, M.A., 1995, *Epidemiology of fungal infections: the promise of molecular typing.* Clin Infect Dis. 20: p. 1535-9.
[35] Soll, D.R., 2000, *The ins and outs of DNA fingerprinting the infectious fungi.* Clin Microbiol Rev. 13: p. 332-70.
[36] Mayer, F.L., D. Wilson, and B. Hube, 2013, *Candida albicans pathogenicity mechanisms.* Virulence. 4: p. 119-28.
[37] Taylor, P., 2020, *Antifungal Drugs: Technologies and Global Markets.* BCC Publishing. PHM029G.
[38] Lupetti, A., R. Danesi, M. Campa, M. Del Tacca, and S. Kelly, 2002, *Molecular basis of resistance to azole antifungals.* Trends Mol Med. 8: p. 76-81.
[39] Petrikkos, G. and A. Skiada, 2007, *Recent advances in antifungal chemotherapy.* Int J Antimicrob Agents. 30: p. 108-17.
[40] Odds, F.C., A.J. Brown, and N.A. Gow, 2003, *Antifungal agents: mechanisms of action.* Trends Microbiol. 11: p. 272-9.
[41] Vanden Bossche, H., L. Koymans, and H. Moereels, 1995, *P450 inhibitors of use in medical treatment: focus on mechanisms of action.* Pharmacol Ther. 67: p. 79-100.
[42] Delattin, N., B.P. Cammue, and K. Thevissen, 2014, *Reactive oxygen species-inducing antifungal agents and their activity against fungal biofilms.* Future Med Chem. 6: p. 77-90.
[43] Efimova, S.S., L.V. Schagina, and O.S. Ostroumova, 2014, *Investigation of channel-forming activity of polyene macrolide antibiotics in planar lipid bilayers in the presence of dipole modifiers.* Acta Naturae. 6: p. 67-79.
[44] Bhattacharya, S., B.D. Esquivel, and T.C. White, 2018, *Overexpression or Deletion of Ergosterol Biosynthesis Genes Alters Doubling Time, Response to Stress Agents, and Drug Susceptibility in Saccharomyces cerevisiae.* mBio. 9.
[45] Perlin, D.S., 2011, *Current perspectives on echinocandin class drugs.* Future Microbiol. 6: p. 441-57.
[46] Shapiro, R.S., N. Robbins, and L.E. Cowen, 2011, *Regulatory circuitry governing fungal development, drug resistance, and disease.* Microbiol Mol Biol Rev. 75: p. 213-67.

[47] Douglas, C.M., 2001, *Fungal beta(1,3)-D-glucan synthesis.* Med Mycol. 39 Suppl 1: p. 55-66.
[48] Ripeau, J.S., F. Aumont, P. Belhumeur, L. Ostrosky-Zeichner, J.H. Rex, and L. de Repentigny, 2002, *Effect of the echinocandin caspofungin on expression of Candida albicans secretory aspartyl proteinases and phospholipase in vitro.* Antimicrob Agents Chemother. 46: p. 3096-100.
[49] Porollo, A., J. Meller, Y. Joshi, V. Jaiswal, A.G. Smulian, and M.T. Cushion, 2012, *Analysis of current antifungal agents and their targets within the Pneumocystis carinii genome.* Curr Drug Targets. 13: p. 1575-85.
[50] Munro, C.A., 2010, *Fungal echinocandin resistance.* F1000 Biol Rep. 2: p. 66.
[51] Pappas, P.G., C.A. Kauffman, D. Andes, D.K. Benjamin, Jr., T.F. Calandra, J.E. Edwards, Jr., S.G. Filler, J.F. Fisher, B.J. Kullberg, L. Ostrosky-Zeichner, A.C. Reboli, J.H. Rex, T.J. Walsh, J.D. Sobel, and A. Infectious Diseases Society of, 2009, *Clinical practice guidelines for the management of candidiasis: 2009 update by the Infectious Diseases Society of America.* Clin Infect Dis. 48: p. 503-35.
[52] Vermes, A., H.J. Guchelaar, and J. Dankert, 2000, *Flucytosine: a review of its pharmacology, clinical indications, pharmacokinetics, toxicity and drug interactions.* J Antimicrob Chemother. 46: p. 171-9.
[53] Denning, D.W. and W.W. Hope, 2010, *Therapy for fungal diseases: opportunities and priorities.* Trends Microbiol. 18: p. 195-204.
[54] Nishimoto, A.T., C. Sharma, and P.D. Rogers, 2020, *Molecular and genetic basis of azole antifungal resistance in the opportunistic pathogenic fungus Candida albicans.* J Antimicrob Chemother. 75: p. 257-270.
[55] Pfaller, M.A., D.J. Diekema, D.L. Gibbs, V.A. Newell, D. Ellis, V. Tullio, A. Rodloff, W. Fu, T.A. Ling, and G. Global Antifungal Surveillance, 2010, *Results from the ARTEMIS DISK Global Antifungal Surveillance Study, 1997 to 2007: a 10.5-year analysis of susceptibilities of Candida Species to fluconazole and voriconazole as determined by CLSI standardized disk diffusion.* J Clin Microbiol. 48: p. 1366-77.
[56] Lyon, G.M., S. Karatela, S. Sunay, Y. Adiri, and I. Candida Surveillance Study, 2010, *Antifungal susceptibility testing of Candida isolates from the Candida surveillance study.* J Clin Microbiol. 48: p. 1270-5.
[57] Pfaller, M.A., G.J. Moet, S.A. Messer, R.N. Jones, and M. Castanheira, 2011, *Candida bloodstream infections: comparison of species distributions and antifungal resistance patterns in community-onset and nosocomial isolates in the SENTRY Antimicrobial Surveillance Program, 2008-2009.* Antimicrob Agents Chemother. 55: p. 561-6.
[58] Pfaller, M.A., A. Espinel-Ingroff, E. Canton, M. Castanheira, M. Cuenca-Estrella, D.J. Diekema, A. Fothergill, J. Fuller, M. Ghannoum, R.N. Jones, S.R. Lockhart, E. Martin-Mazuelos, M.S. Melhem, L. Ostrosky-Zeichner, P. Pappas, T. Pelaez, J. Peman, J. Rex, and M.W. Szeszs, 2012, *Wild-type MIC distributions and epidemiological cutoff values for amphotericin B, flucytosine, and itraconazole and Candida spp. as determined by CLSI broth microdilution.* J Clin Microbiol. 50: p. 2040-6.
[59] Lockhart, S.R., N. Iqbal, A.A. Cleveland, M.M. Farley, L.H. Harrison, C.B. Bolden, W. Baughman, B. Stein, R. Hollick, B.J. Park, and T. Chiller, 2012, *Species identification and antifungal susceptibility testing of Candida bloodstream isolates from population-based surveillance studies in two U.S. cities from 2008 to 2011.* J Clin Microbiol. 50: p. 3435-42.
[60] Espinel-Ingroff, A., M.A. Pfaller, B. Bustamante, E. Canton, A. Fothergill, J. Fuller, G.M. Gonzalez, C. Lass-Florl, S.R. Lockhart, E. Martin-Mazuelos, J.F. Meis, M.S. Melhem, L. Ostrosky-Zeichner, T. Pelaez, M.W. Szeszs, G. St-Germain, L.X. Bonfietti, J. Guarro, and J. Turnidge, 2014, *Multilaboratory study of epidemiological cutoff values for detection of resistance in eight Candida species to fluconazole, posaconazole, and voriconazole.* Antimicrob Agents Chemother. 58: p. 2006-12.

[61] Fan-Havard, P., D. Capano, S.M. Smith, A. Mangia, and R.H. Eng, 1991, *Development of resistance in candida isolates from patients receiving prolonged antifungal therapy.* Antimicrob Agents Chemother. 35: p. 2302-5.

[62] Franz, R., S.L. Kelly, D.C. Lamb, D.E. Kelly, M. Ruhnke, and J. Morschhauser, 1998, *Multiple molecular mechanisms contribute to a stepwise development of fluconazole resistance in clinical Candida albicans strains.* Antimicrob Agents Chemother. 42: p. 3065-72.

[63] Hernaez, M.L., C. Gil, J. Pla, and C. Nombela, 1998, *Induced expression of the Candida albicans multidrug resistance gene CDR1 in response to fluconazole and other antifungals.* Yeast. 14: p. 517-26.

[64] Lopez-Ribot, J.L., R.K. McAtee, L.N. Lee, W.R. Kirkpatrick, T.C. White, D. Sanglard, and T.F. Patterson, 1998, *Distinct patterns of gene expression associated with development of fluconazole resistance in serial candida albicans isolates from human immunodeficiency virus-infected patients with oropharyngeal candidiasis.* Antimicrob Agents Chemother. 42: p. 2932-7.

[65] Lopez-Ribot, J.L., R.K. McAtee, S. Perea, W.R. Kirkpatrick, M.G. Rinaldi, and T.F. Patterson, 1999, *Multiple resistant phenotypes of Candida albicans coexist during episodes of oropharyngeal candidiasis in human immunodeficiency virus-infected patients.* Antimicrob Agents Chemother. 43: p. 1621-30.

[66] Marr, K.A., C.N. Lyons, T.R. Rustad, R.A. Bowden, and T.C. White, 1998, *Rapid, transient fluconazole resistance in Candida albicans is associated with increased mRNA levels of CDR.* Antimicrob Agents Chemother. 42: p. 2584-9.

[67] Marr, K.A., T.C. White, J.A. van Burik, and R.A. Bowden, 1997, *Development of fluconazole resistance in Candida albicans causing disseminated infection in a patient undergoing marrow transplantation.* Clin Infect Dis. 25: p. 908-10.

[68] Nolte, F.S., T. Parkinson, D.J. Falconer, S. Dix, J. Williams, C. Gilmore, R. Geller, and J.R. Wingard, 1997, *Isolation and characterization of fluconazole- and amphotericin B-resistant Candida albicans from blood of two patients with leukemia.* Antimicrob Agents Chemother. 41: p. 196-9.

[69] Pappas, P.G., J.H. Rex, J.D. Sobel, S.G. Filler, W.E. Dismukes, T.J. Walsh, J.E. Edwards, and A. Infectious Diseases Society of, 2004, *Guidelines for treatment of candidiasis.* Clin Infect Dis. 38: p. 161-89.

[70] Prasad, R., P. De Wergifosse, A. Goffeau, and E. Balzi, 1995, *Molecular cloning and characterization of a novel gene of Candida albicans, CDR1, conferring multiple resistance to drugs and antifungals.* Curr Genet. 27: p. 320-9.

[71] Sanglard, D., F. Ischer, M. Monod, and J. Bille, 1997, *Cloning of Candida albicans genes conferring resistance to azole antifungal agents: characterization of CDR2, a new multidrug ABC transporter gene.* Microbiology. 143 (Pt 2): p. 405-16.

[72] Sanglard, D., K. Kuchler, F. Ischer, J.L. Pagani, M. Monod, and J. Bille, 1995, *Mechanisms of resistance to azole antifungal agents in Candida albicans isolates from AIDS patients involve specific multidrug transporters.* Antimicrob Agents Chemother. 39: p. 2378-86.

[73] Sanglard, D., F. Ischer, L. Koymans, and J. Bille, 1998, *Amino acid substitutions in the cytochrome P-450 lanosterol 14alpha-demethylase (CYP51A1) from azole-resistant Candida albicans clinical isolates contribute to resistance to azole antifungal agents.* Antimicrob Agents Chemother. 42: p. 241-53.

[74] Sheehan, D.J., C.A. Hitchcock, and C.M. Sibley, 1999, *Current and emerging azole antifungal agents.* Clin Microbiol Rev. 12: p. 40-79.

[75] White, T.C., 1997, *Increased mRNA levels of ERG16, CDR, and MDR1 correlate with increases in azole resistance in Candida albicans isolates from a patient infected with human immunodeficiency virus.* Antimicrob Agents Chemother. 41: p. 1482-7.

[76] White, T.C., K.A. Marr, and R.A. Bowden, 1998, *Clinical, cellular, and molecular factors that contribute to antifungal drug resistance.* Clin Microbiol Rev. 11: p. 382-402.

[77] D'Costa, V.M., C.E. King, L. Kalan, M. Morar, W.W. Sung, C. Schwarz, D. Froese, G. Zazula, F. Calmels, R. Debruyne, G.B. Golding, H.N. Poinar, and G.D. Wright, 2011, *Antibiotic resistance is ancient.* Nature. 477: p. 457-61.

[78] Wright, G.D., 2007, *The antibiotic resistome: the nexus of chemical and genetic diversity.* Nat Rev Microbiol. 5: p. 175-86.

[79] Robbins, N., T. Caplan, and L.E. Cowen, 2017, *Molecular Evolution of Antifungal Drug Resistance.* Annu Rev Microbiol. 71: p. 753-775.

[80] Cowen, L.E. and W.J. Steinbach, 2008, *Stress, drugs, and evolution: the role of cellular signaling in fungal drug resistance.* Eukaryot Cell. 7: p. 747-64.

[81] Robbins, N., G.D. Wright, and L.E. Cowen, 2016, *Antifungal Drugs: The Current Armamentarium and Development of New Agents.* Microbiol Spectr. 4.

[82] Vincent, B.M., A.K. Lancaster, R. Scherz-Shouval, L. Whitesell, and S. Lindquist, 2013, *Fitness trade-offs restrict the evolution of resistance to amphotericin B.* PLoS Biol. 11: p. e1001692.

[83] Anderson, J.B., 2005, *Evolution of antifungal-drug resistance: mechanisms and pathogen fitness.* Nat Rev Microbiol. 3: p. 547-56.

[84] Kelly, S.L., D.C. Lamb, J. Loeffler, H. Einsele, and D.E. Kelly, 1999, *The G464S amino acid substitution in Candida albicans sterol 14alpha-demethylase causes fluconazole resistance in the clinic through reduced affinity.* Biochem Biophys Res Commun. 262: p. 174-9.

[85] Lamb, D.C., D.E. Kelly, T.C. White, and S.L. Kelly, 2000, *The R467K amino acid substitution in Candida albicans sterol 14alpha-demethylase causes drug resistance through reduced affinity.* Antimicrob Agents Chemother. 44: p. 63-7.

[86] Kelly, S.L., D.C. Lamb, and D.E. Kelly, 1999, *Y132H substitution in Candida albicans sterol 14alpha-demethylase confers fluconazole resistance by preventing binding to haem.* FEMS Microbiol Lett. 180: p. 171-5.

[87] Warrilow, A.G., A.T. Nishimoto, J.E. Parker, C.L. Price, S.A. Flowers, D.E. Kelly, P.D. Rogers, and S.L. Kelly, 2019, *The Evolution of Azole Resistance in Candida albicans Sterol 14alpha-Demethylase (CYP51) through Incremental Amino Acid Substitutions.* Antimicrob Agents Chemother. 63.

[88] Kelly, S.L., D.C. Lamb, D.E. Kelly, N.J. Manning, J. Loeffler, H. Hebart, U. Schumacher, and H. Einsele, 1997, *Resistance to fluconazole and cross-resistance to amphotericin B in Candida albicans from AIDS patients caused by defective sterol delta5,6-desaturation.* FEBS Lett. 400: p. 80-2.

[89] Sanglard, D., F. Ischer, T. Parkinson, D. Falconer, and J. Bille, 2003, *Candida albicans mutations in the ergosterol biosynthetic pathway and resistance to several antifungal agents.* Antimicrob Agents Chemother. 47: p. 2404-12.

[90] Miyazaki, T., Y. Miyazaki, K. Izumikawa, H. Kakeya, S. Miyakoshi, J.E. Bennett, and S. Kohno, 2006, *Fluconazole treatment is effective against a Candida albicans erg3/erg3 mutant in vivo despite in vitro resistance.* Antimicrob Agents Chemother. 50: p. 580-6.

[91] Silver, P.M., B.G. Oliver, and T.C. White, 2004, *Role of Candida albicans transcription factor Upc2p in drug resistance and sterol metabolism.* Eukaryot Cell. 3: p. 1391-7.

[92] MacPherson, S., B. Akache, S. Weber, X. De Deken, M. Raymond, and B. Turcotte, 2005, *Candida albicans zinc cluster protein Upc2p confers resistance to antifungal drugs and is an activator of ergosterol biosynthetic genes.* Antimicrob Agents Chemother. 49: p. 1745-52.

[93] Dunkel, N., T.T. Liu, K.S. Barker, R. Homayouni, J. Morschhauser, and P.D. Rogers, 2008, *A gain-of-function mutation in the transcription factor Upc2p causes upregulation of ergosterol biosynthesis genes and increased fluconazole resistance in a clinical Candida albicans isolate.* Eukaryot Cell. 7: p. 1180-90.

[94] Heilmann, C.J., S. Schneider, K.S. Barker, P.D. Rogers, and J. Morschhauser, 2010, *An A643T mutation in the transcription factor Upc2p causes constitutive ERG11 upregulation and increased fluconazole resistance in Candida albicans.* Antimicrob Agents Chemother. 54: p. 353-9.

[95] Flowers, S.A., K.S. Barker, E.L. Berkow, G. Toner, S.G. Chadwick, S.E. Gygax, J. Morschhauser, and P.D. Rogers, 2012, *Gain-of-function mutations in UPC2 are a frequent cause of ERG11 upregulation in azole-resistant clinical isolates of Candida albicans.* Eukaryot Cell. 11: p. 1289-99.

[96] Hoot, S.J., A.R. Smith, R.P. Brown, and T.C. White, 2011, *An A643V amino acid substitution in Upc2p contributes to azole resistance in well-characterized clinical isolates of Candida albicans.* Antimicrob Agents Chemother. 55: p. 940-2.

[97] Znaidi, S., S. Weber, O.Z. Al-Abdin, P. Bomme, S. Saidane, S. Drouin, S. Lemieux, X. De Deken, F. Robert, and M. Raymond, 2008, *Genomewide location analysis of Candida albicans Upc2p, a regulator of sterol metabolism and azole drug resistance.* Eukaryot Cell. 7: p. 836-47.

[98] Schubert, S., K.S. Barker, S. Znaidi, S. Schneider, F. Dierolf, N. Dunkel, M. Aid, G. Boucher, P.D. Rogers, M. Raymond, and J. Morschhauser, 2011, *Regulation of efflux pump expression and drug resistance by the transcription factors Mrr1, Upc2, and Cap1 in Candida albicans.* Antimicrob Agents Chemother. 55: p. 2212-23.

[99] Del Sorbo, G., H. Schoonbeek, and M.A. De Waard, 2000, *Fungal transporters involved in efflux of natural toxic compounds and fungicides.* Fungal Genet Biol. 30: p. 1-15.

[100] Sanglard, D., F. Ischer, M. Monod, and J. Bille, 1996, *Susceptibilities of Candida albicans multidrug transporter mutants to various antifungal agents and other metabolic inhibitors.* Antimicrob Agents Chemother. 40: p. 2300-5.

[101] Schillig, R. and J. Morschhauser, 2013, *Analysis of a fungus-specific transcription factor family, the Candida albicans zinc cluster proteins, by artificial activation.* Mol Microbiol. 89: p. 1003-17.

[102] Morschhauser, J., S. Michel, and P. Staib, 1999, *Sequential gene disruption in Candida albicans by FLP-mediated site-specific recombination.* Mol Microbiol. 32: p. 547-56.

[103] Branco, J., A.P. Silva, R.M. Silva, A. Silva-Dias, C. Pina-Vaz, G. Butler, A.G. Rodrigues, and I.M. Miranda, 2015, *Fluconazole and Voriconazole Resistance in Candida parapsilosis Is Conferred by Gain-of-Function Mutations in MRR1 Transcription Factor Gene.* Antimicrob Agents Chemother. 59: p. 6629-33.

[104] Dunkel, N., J. Blass, P.D. Rogers, and J. Morschhauser, 2008, *Mutations in the multi-drug resistance regulator MRR1, followed by loss of heterozygosity, are the main cause of MDR1 overexpression in fluconazole-resistant Candida albicans strains.* Mol Microbiol. 69: p. 827-40.

[105] Eddouzi, J., J.E. Parker, L.A. Vale-Silva, A. Coste, F. Ischer, S. Kelly, M. Manai, and D. Sanglard, 2013, *Molecular mechanisms of drug resistance in clinical Candida species isolated from Tunisian hospitals.* Antimicrob Agents Chemother. 57: p. 3182-93.

[106] Lohberger, A., A.T. Coste, and D. Sanglard, 2014, *Distinct roles of Candida albicans drug resistance transcription factors TAC1, MRR1, and UPC2 in virulence.* Eukaryot Cell. 13: p. 127-42.

[107] Morschhauser, J., K.S. Barker, T.T. Liu, B.W.J. Bla, R. Homayouni, and P.D. Rogers, 2007, *The transcription factor Mrr1p controls expression of the MDR1 efflux pump and mediates multidrug resistance in Candida albicans.* PLoS Pathog. 3: p. e164.

[108] Schubert, S., P.D. Rogers, and J. Morschhauser, 2008, *Gain-of-function mutations in the transcription factor MRR1 are responsible for overexpression of the MDR1 efflux pump in fluconazole-resistant Candida dubliniensis strains.* Antimicrob Agents Chemother. 52: p. 4274-80.

[109] Coste, A., A. Selmecki, A. Forche, D. Diogo, M.E. Bougnoux, C. d'Enfert, J. Berman, and D. Sanglard, 2007, *Genotypic evolution of azole resistance mechanisms in sequential Candida albicans isolates.* Eukaryot Cell. 6: p. 1889-904.

[110] Coste, A., V. Turner, F. Ischer, J. Morschhauser, A. Forche, A. Selmecki, J. Berman, J. Bille, and D. Sanglard, 2006, *A mutation in Tac1p, a transcription factor regulating CDR1 and CDR2, is coupled with loss of heterozygosity at chromosome 5 to mediate antifungal resistance in Candida albicans.* Genetics. 172: p. 2139-56.

[111] Coste, A.T., J. Crittin, C. Bauser, B. Rohde, and D. Sanglard, 2009, *Functional analysis of cis- and trans-acting elements of the Candida albicans CDR2 promoter with a novel promoter reporter system.* Eukaryot Cell. 8: p. 1250-67.

[112] Coste, A.T., M. Karababa, F. Ischer, J. Bille, and D. Sanglard, 2004, *TAC1, transcriptional activator of CDR genes, is a new transcription factor involved in the regulation of Candida albicans ABC transporters CDR1 and CDR2.* Eukaryot Cell. 3: p. 1639-52.

[113] Liu, T.T., S. Znaidi, K.S. Barker, L. Xu, R. Homayouni, S. Saidane, J. Morschhauser, A. Nantel, M. Raymond, and P.D. Rogers, 2007, *Genome-wide expression and location analyses of the Candida albicans Tac1p regulon.* Eukaryot Cell. 6: p. 2122-38.

[114] Znaidi, S., X. De Deken, S. Weber, T. Rigby, A. Nantel, and M. Raymond, 2007, *The zinc cluster transcription factor Tac1p regulates PDR16 expression in Candida albicans.* Mol Microbiol. 66: p. 440-52.

[115] Manoharlal, R., N.A. Gaur, S.L. Panwar, J. Morschhauser, and R. Prasad, 2008, *Transcriptional activation and increased mRNA stability contribute to overexpression of CDR1 in azole-resistant Candida albicans.* Antimicrob Agents Chemother. 52: p. 1481-92.

[116] Manoharlal, R., J. Gorantala, M. Sharma, D. Sanglard, and R. Prasad, 2010, *PAP1 [poly(A) polymerase 1] homozygosity and hyperadenylation are major determinants of increased mRNA stability of CDR1 in azole-resistant clinical isolates of Candida albicans.* Microbiology (Reading). 156: p. 313-26.

[117] Li, X., F. Yang, D. Li, M. Zhou, X. Wang, Q. Xu, Y. Zhang, L. Yan, and Y. Jiang, 2015, *Trisomy of chromosome R confers resistance to triazoles in Candida albicans.* Med Mycol. 53: p. 302-9.

[118] Nishimoto, A.T., Q. Zhang, B. Hazlett, J. Morschhauser, and P.D. Rogers, 2019, *Contribution of Clinically Derived Mutations in the Gene Encoding the Zinc Cluster Transcription Factor Mrr2 to Fluconazole Antifungal Resistance and CDR1 Expression in Candida albicans.* Antimicrob Agents Chemother. 63.

[119] Perea, S., J.L. Lopez-Ribot, W.R. Kirkpatrick, R.K. McAtee, R.A. Santillan, M. Martinez, D. Calabrese, D. Sanglard, and T.F. Patterson, 2001, *Prevalence of molecular mechanisms of resistance to azole antifungal agents in Candida albicans strains displaying high-level fluconazole resistance isolated from human immunodeficiency virus-infected patients.* Antimicrob Agents Chemother. 45: p. 2676-84.

[120] White, T.C., 1997, *The presence of an R467K amino acid substitution and loss of allelic variation correlate with an azole-resistant lanosterol 14alpha demethylase in Candida albicans.* Antimicrob Agents Chemother. 41: p. 1488-94.

[121] Sasse, C., N. Dunkel, T. Schafer, S. Schneider, F. Dierolf, K. Ohlsen, and J. Morschhauser, 2012, *The stepwise acquisition of fluconazole resistance mutations causes a gradual loss of fitness in Candida albicans.* Mol Microbiol. 86: p. 539-56.

[122] Asai, K., N. Tsuchimori, K. Okonogi, J.R. Perfect, O. Gotoh, and Y. Yoshida, 1999, *Formation of azole-resistant Candida albicans by mutation of sterol 14-demethylase P450.* Antimicrob Agents Chemother. 43: p. 1163-9.

[123] Forche, A., D. Abbey, T. Pisithkul, M.A. Weinzierl, T. Ringstrom, D. Bruck, K. Petersen, and J. Berman, 2011, *Stress alters rates and types of loss of heterozygosity in Candida albicans.* MBio. 2.

[124] Morschhauser, J., 2016, *The development of fluconazole resistance in Candida albicans - an example of microevolution of a fungal pathogen.* J Microbiol. 54: p. 192-201.

[125] Ford, C.B., J.M. Funt, D. Abbey, L. Issi, C. Guiducci, D.A. Martinez, T. Delorey, B.Y. Li, T.C. White, C. Cuomo, R.P. Rao, J. Berman, D.A. Thompson, and A. Regev, 2015, *The evolution of drug resistance in clinical isolates of Candida albicans.* Elife. 4: p. e00662.

[126] Selmecki, A., A. Forche, and J. Berman, 2006, *Aneuploidy and isochromosome formation in drug-resistant Candida albicans.* Science. 313: p. 367-70.

[127] Selmecki, A., M. Gerami-Nejad, C. Paulson, A. Forche, and J. Berman, 2008, *An isochromosome confers drug resistance in vivo by amplification of two genes, ERG11 and TAC1.* Mol Microbiol. 68: p. 624-41.

[128] Marr, K.A., C.N. Lyons, K. Ha, T.R. Rustad, and T.C. White, 2001, *Inducible azole resistance associated with a heterogeneous phenotype in Candida albicans.* Antimicrob Agents Chemother. 45: p. 52-9.

[129] Berman, J., 2016, *Ploidy plasticity: a rapid and reversible strategy for adaptation to stress.* FEMS Yeast Res. 16.

[130] Harrison, B.D., J. Hashemi, M. Bibi, R. Pulver, D. Bavli, Y. Nahmias, M. Wellington, G. Sapiro, and J. Berman, 2014, *A tetraploid intermediate precedes aneuploid formation in yeasts exposed to fluconazole.* PLoS Biol. 12: p. e1001815.

[131] Gao, J., H. Wang, Z. Li, A.H. Wong, Y.Z. Wang, Y. Guo, X. Lin, G. Zeng, H. Liu, Y. Wang, and J. Wang, 2018, *Candida albicans gains azole resistance by altering sphingolipid composition.* Nat Commun. 9: p. 4495.

[132] Andersson, D.I., 2003, *Persistence of antibiotic resistant bacteria.* Curr Opin Microbiol. 6: p. 452-6.

[133] Chau, A.S., M. Gurnani, R. Hawkinson, M. Laverdiere, A. Cacciapuoti, and P.M. McNicholas, 2005, *Inactivation of sterol Delta5,6-desaturase attenuates virulence in Candida albicans.* Antimicrob Agents Chemother. 49: p. 3646-51.

[134] Vale-Silva, L.A., A.T. Coste, F. Ischer, J.E. Parker, S.L. Kelly, E. Pinto, and D. Sanglard, 2012, *Azole resistance by loss of function of the sterol Delta(5),(6)-desaturase gene (ERG3) in Candida albicans does not necessarily decrease virulence.* Antimicrob Agents Chemother. 56: p. 1960-8.

[135] Selmecki, A.M., K. Dulmage, L.E. Cowen, J.B. Anderson, and J. Berman, 2009, *Acquisition of aneuploidy provides increased fitness during the evolution of antifungal drug resistance.* PLoS Genet. 5: p. e1000705.

[136] Calvet, H.M., M.R. Yeaman, and S.G. Filler, 1997, *Reversible fluconazole resistance in Candida albicans: a potential in vitro model.* Antimicrob Agents Chemother. 41: p. 535-9.

[137] Huang, M., M. McClellan, J. Berman, and K.C. Kao, 2011, *Evolutionary dynamics of Candida albicans during in vitro evolution.* Eukaryot Cell. 10: p. 1413-21.

[138] Angiolella, L., A.R. Stringaro, F. De Bernardis, B. Posteraro, M. Bonito, L. Toccacieli, A. Torosantucci, M. Colone, M. Sanguinetti, A. Cassone, and A.T. Palamara, 2008, *Increase of virulence and its phenotypic traits in drug-resistant strains of Candida albicans.* Antimicrob Agents Chemother. 52: p. 927-36.

[139] Hayama, K., H. Ishibashi, S.A. Ishijima, K. Niimi, S. Tansho, Y. Ono, B.C. Monk, A.R. Holmes, D.R. Harding, R.D. Cannon, and S. Abe, 2012, *A D-octapeptide drug efflux pump inhibitor acts synergistically with azoles in a murine oral candidiasis infection model.* FEMS Microbiol Lett. 328: p. 130-7.

[140] Schulz, B., K. Weber, A. Schmidt, M. Borg-von Zepelin, and M. Ruhnke, 2011, *Difference in virulence between fluconazole-susceptible and fluconazole-resistant Candida albicans in a mouse model.* Mycoses. 54: p. e522-30.

[141] Andes, D., A. Forrest, A. Lepak, J. Nett, K. Marchillo, and L. Lincoln, 2006, *Impact of antimicrobial dosing regimen on evolution of drug resistance in vivo: fluconazole and Candida albicans.* Antimicrob Agents Chemother. 50: p. 2374-83.

[142] Cowen, L.E., L.M. Kohn, and J.B. Anderson, 2001, *Divergence in fitness and evolution of drug resistance in experimental populations of Candida albicans.* J Bacteriol. 183: p. 2971-8.

[143] Hickman, M.A., G. Zeng, A. Forche, M.P. Hirakawa, D. Abbey, B.D. Harrison, Y.M. Wang, C.H. Su, R.J. Bennett, Y. Wang, and J. Berman, 2013, *The 'obligate diploid' Candida albicans forms mating-competent haploids.* Nature. 494: p. 55-9.

[144] Gerstein, A.C., H. Lim, J. Berman, and M.A. Hickman, 2017, *Ploidy tug-of-war: Evolutionary and genetic environments influence the rate of ploidy drive in a human fungal pathogen.* Evolution. 71: p. 1025-1038.

[145] Kravets, A., F. Yang, G. Bethlendy, Y. Cao, F. Sherman, and E. Rustchenko, 2014, *Adaptation of Candida albicans to growth on sorbose via monosomy of chromosome 5 accompanied by*

duplication of another chromosome carrying a gene responsible for sorbose utilization. FEMS Yeast Res. 14: p. 708-13.

[146] Rustchenko, E., 2007, *Chromosome instability in Candida albicans.* FEMS Yeast Res. 7: p. 2-11.

[147] Hirakawa, M.P., D.A. Martinez, S. Sakthikumar, M.Z. Anderson, A. Berlin, S. Gujja, Q. Zeng, E. Zisson, J.M. Wang, J.M. Greenberg, J. Berman, R.J. Bennett, and C.A. Cuomo, 2015, *Genetic and phenotypic intra-species variation in Candida albicans.* Genome Res. 25: p. 413-25.

[148] Forche, A., P.T. Magee, A. Selmecki, J. Berman, and G. May, 2009, *Evolution in Candida albicans populations during a single passage through a mouse host.* Genetics. 182: p. 799-811.

[149] Schulze, J. and U. Sonnenborn, 2009, *Yeasts in the gut: from commensals to infectious agents.* Dtsch Arztebl Int. 106: p. 837-42.

[150] Miramon, P. and M.C. Lorenz, 2017, *A feast for Candida: Metabolic plasticity confers an edge for virulence.* PLoS Pathog. 13: p. e1006144.

[151] Noble, S.M., B.A. Gianetti, and J.N. Witchley, 2017, *Candida albicans cell-type switching and functional plasticity in the mammalian host.* Nat Rev Microbiol. 15: p. 96-108.

[152] Forche, A., G. Cromie, A.C. Gerstein, N.V. Solis, T. Pisithkul, W. Srifa, E. Jeffery, D. Abbey, S.G. Filler, A.M. Dudley, and J. Berman, 2018, *Rapid Phenotypic and Genotypic Diversification After Exposure to the Oral Host Niche in Candida albicans.* Genetics. 209: p. 725-741.

[153] Ropars, J., C. Maufrais, D. Diogo, M. Marcet-Houben, A. Perin, N. Sertour, K. Mosca, E. Permal, G. Laval, C. Bouchier, L. Ma, K. Schwartz, K. Voelz, R.C. May, J. Poulain, C. Battail, P. Wincker, A.M. Borman, A. Chowdhary, S. Fan, S.H. Kim, P. Le Pape, O. Romeo, J.H. Shin, T. Gabaldon, G. Sherlock, M.E. Bougnoux, and C. d'Enfert, 2018, *Gene flow contributes to diversification of the major fungal pathogen Candida albicans.* Nat Commun. 9: p. 2253.

[154] Skrzypek, M.S., J. Binkley, G. Binkley, S.R. Miyasato, M. Simison, and G. Sherlock, 2017, *The Candida Genome Database (CGD): incorporation of Assembly 22, systematic identifiers and visualization of high throughput sequencing data.* Nucleic Acids Res. 45: p. D592-D596.

[155] Butler, G., M.D. Rasmussen, M.F. Lin, M.A. Santos, S. Sakthikumar, C.A. Munro, E. Rheinbay, M. Grabherr, A. Forche, J.L. Reedy, I. Agrafioti, M.B. Arnaud, S. Bates, A.J. Brown, S. Brunke, M.C. Costanzo, D.A. Fitzpatrick, P.W. de Groot, D. Harris, L.L. Hoyer, B. Hube, F.M. Klis, C. Kodira, N. Lennard, M.E. Logue, R. Martin, A.M. Neiman, E. Nikolaou, M.A. Quail, J. Quinn, M.C. Santos, F.F. Schmitzberger, G. Sherlock, P. Shah, K.A. Silverstein, M.S. Skrzypek, D. Soll, R. Staggs, I. Stansfield, M.P. Stumpf, P.E. Sudbery, T. Srikantha, Q. Zeng, J. Berman, M. Berriman, J. Heitman, N.A. Gow, M.C. Lorenz, B.W. Birren, M. Kellis, and C.A. Cuomo, 2009, *Evolution of pathogenicity and sexual reproduction in eight Candida genomes.* Nature. 459: p. 657-62.

[156] Ene, I.V., R.A. Farrer, M.P. Hirakawa, K. Agwamba, C.A. Cuomo, and R.J. Bennett, 2018, *Global analysis of mutations driving microevolution of a heterozygous diploid fungal pathogen.* Proc Natl Acad Sci U S A. 115: p. E8688-E8697.

[157] Muzzey, D., K. Schwartz, J.S. Weissman, and G. Sherlock, 2013, *Assembly of a phased diploid Candida albicans genome facilitates allele-specific measurements and provides a simple model for repeat and indel structure.* Genome Biol. 14: p. R97.

[158] Jones, T., N.A. Federspiel, H. Chibana, J. Dungan, S. Kalman, B.B. Magee, G. Newport, Y.R. Thorstenson, N. Agabian, P.T. Magee, R.W. Davis, and S. Scherer, 2004, *The diploid genome sequence of Candida albicans.* Proc Natl Acad Sci U S A. 101: p. 7329-34.

[159] Liang, S.H. and R.J. Bennett, 2019, *The Impact of Gene Dosage and Heterozygosity on The Diploid Pathobiont Candida albicans.* J Fungi (Basel). 6.

[160] Staib, P., M. Kretschmar, T. Nichterlein, H. Hof, and J. Morschhauser, 2002, *Host versus in vitro signals and intrastrain allelic differences in the expression of a Candida albicans virulence gene.* Mol Microbiol. 44: p. 1351-66.

[161] Muzzey, D., G. Sherlock, and J.S. Weissman, 2014, *Extensive and coordinated control of allele-specific expression by both transcription and translation in Candida albicans.* Genome Res. 24: p. 963-73.

[162] Zhao, X., S.H. Oh, R. Jajko, D.J. Diekema, M.A. Pfaller, C. Pujol, D.R. Soll, and L.L. Hoyer, 2007, *Analysis of ALS5 and ALS6 allelic variability in a geographically diverse collection of Candida albicans isolates.* Fungal Genet Biol. 44: p. 1298-309.

[163] Zhao, X., C. Pujol, D.R. Soll, and L.L. Hoyer, 2003, *Allelic variation in the contiguous loci encoding Candida albicans ALS5, ALS1 and ALS9.* Microbiology (Reading). 149: p. 2947-2960.

[164] Braun, B.R., M. van Het Hoog, C. d'Enfert, M. Martchenko, J. Dungan, A. Kuo, D.O. Inglis, M.A. Uhl, H. Hogues, M. Berriman, M. Lorenz, A. Levitin, U. Oberholzer, C. Bachewich, D. Harcus, A. Marcil, D. Dignard, T. Iouk, R. Zito, L. Frangeul, F. Tekaia, K. Rutherford, E. Wang, C.A. Munro, S. Bates, N.A. Gow, L.L. Hoyer, G. Kohler, J. Morschhauser, G. Newport, S. Znaidi, M. Raymond, B. Turcotte, G. Sherlock, M. Costanzo, J. Ihmels, J. Berman, D. Sanglard, N. Agabian, A.P. Mitchell, A.D. Johnson, M. Whiteway, and A. Nantel, 2005, *A human-curated annotation of the Candida albicans genome.* PLoS Genet. 1: p. 36-57.

[165] Wilkins, M., N. Zhang, and J. Schmid, 2018, *Biological Roles of Protein-Coding Tandem Repeats in the Yeast Candida Albicans.* J Fungi (Basel). 4.

[166] Wang, J.M., R.J. Bennett, and M.Z. Anderson, 2018, *The Genome of the Human Pathogen Candida albicans Is Shaped by Mutation and Cryptic Sexual Recombination.* MBio. 9.

[167] Feri, A., R. Loll-Krippleber, P.H. Commere, C. Maufrais, N. Sertour, K. Schwartz, G. Sherlock, M.E. Bougnoux, C. d'Enfert, and M. Legrand, 2016, *Analysis of Repair Mechanisms following an Induced Double-Strand Break Uncovers Recessive Deleterious Alleles in the Candida albicans Diploid Genome.* mBio. 7.

[168] Diogo, D., C. Bouchier, C. d'Enfert, and M.E. Bougnoux, 2009, *Loss of heterozygosity in commensal isolates of the asexual diploid yeast Candida albicans.* Fungal Genet Biol. 46: p. 159-68.

[169] Rosenberg, S.M., 2011, *Stress-induced loss of heterozygosity in Candida: a possible missing link in the ability to evolve.* mBio. 2.

[170] Forche, A., M. Steinbach, and J. Berman, 2009, *Efficient and rapid identification of Candida albicans allelic status using SNP-RFLP.* FEMS Yeast Res. 9: p. 1061-9.

[171] Tao, L., H. Du, G. Guan, Y. Dai, C.J. Nobile, W. Liang, C. Cao, Q. Zhang, J. Zhong, and G. Huang, 2014, *Discovery of a "white-gray-opaque" tristable phenotypic switching system in candida albicans: roles of non-genetic diversity in host adaptation.* PLoS Biol. 12: p. e1001830.

[172] Liang, S.H., M.Z. Anderson, M.P. Hirakawa, J.M. Wang, C. Frazer, L.M. Alaalm, G.J. Thomson, I.V. Ene, and R.J. Bennett, 2019, *Hemizygosity Enables a Mutational Transition Governing Fungal Virulence and Commensalism.* Cell Host Microbe. 25: p. 418-431 e6.

[173] Pierce, J.V. and C.A. Kumamoto, 2012, *Variation in Candida albicans EFG1 expression enables host-dependent changes in colonizing fungal populations.* MBio. 3: p. e00117-12.

[174] Pierce, J.V., D. Dignard, M. Whiteway, and C.A. Kumamoto, 2013, *Normal adaptation of Candida albicans to the murine gastrointestinal tract requires Efg1p-dependent regulation of metabolic and host defense genes.* Eukaryot Cell. 12: p. 37-49.

[175] Sitterle, E., C. Maufrais, N. Sertour, M. Palayret, C. d'Enfert, and M.E. Bougnoux, 2019, *Within-Host Genomic Diversity of Candida albicans in Healthy Carriers.* Sci Rep. 9: p. 2563.

[176] Bennett, R.J., A. Forche, and J. Berman, 2014, *Rapid mechanisms for generating genome diversity: whole ploidy shifts, aneuploidy, and loss of heterozygosity.* Cold Spring Harb Perspect Med. 4.

[177] Forche, A., G. May, and P.T. Magee, 2005, *Demonstration of loss of heterozygosity by single-nucleotide polymorphism microarray analysis and alterations in strain morphology in Candida albicans strains during infection.* Eukaryot Cell. 4: p. 156-65.

[178] Liu, J.Y., W.J. Li, C. Shi, Y. Wang, Y. Zhao, and M.J. Xiang, 2015, *Mutations in the Flo8 transcription factor contribute to virulence and phenotypic traits in Candida albicans strains.* Microbiol Res. 178: p. 1-8.

[179] Todd, R.T., T.D. Wikoff, A. Forche, and A. Selmecki, 2019, *Genome plasticity in Candida albicans is driven by long repeat sequences.* Elife. 8.

[180] Ene, I.V., R.J. Bennett, and M.Z. Anderson, 2019, *Mechanisms of genome evolution in Candida albicans.* Curr Opin Microbiol. 52: p. 47-54.
[181] Hickman, M.A., C. Paulson, A. Dudley, and J. Berman, 2015, *Parasexual Ploidy Reduction Drives Population Heterogeneity Through Random and Transient Aneuploidy in Candida albicans.* Genetics. 200: p. 781-94.
[182] Marton, T., A. Feri, P.H. Commere, C. Maufrais, C. d'Enfert, and M. Legrand, 2019, *Identification of Recessive Lethal Alleles in the Diploid Genome of a Candida albicans Laboratory Strain Unveils a Potential Role of Repetitive Sequences in Buffering Their Deleterious Impact.* mSphere. 4.
[183] Bennett, R.J. and A.D. Johnson, 2003, *Completion of a parasexual cycle in Candida albicans by induced chromosome loss in tetraploid strains.* EMBO J. 22: p. 2505-15.
[184] Forche, A., K. Alby, D. Schaefer, A.D. Johnson, J. Berman, and R.J. Bennett, 2008, *The parasexual cycle in Candida albicans provides an alternative pathway to meiosis for the formation of recombinant strains.* PLoS Biol. 6: p. e110.
[185] Ibrahim, A.S., B.B. Magee, D.C. Sheppard, M. Yang, S. Kauffman, J. Becker, J.E. Edwards, Jr., and P.T. Magee, 2005, *Effects of ploidy and mating type on virulence of Candida albicans.* Infect Immun. 73: p. 7366-74.
[186] Hirakawa, M.P., D.E. Chyou, D. Huang, A.R. Slan, and R.J. Bennett, 2017, *Parasex Generates Phenotypic Diversity de Novo and Impacts Drug Resistance and Virulence in Candida albicans.* Genetics. 207: p. 1195-1211.
[187] Lockhart, S.R., K.J. Daniels, R. Zhao, D. Wessels, and D.R. Soll, 2003, *Cell biology of mating in Candida albicans.* Eukaryot Cell. 2: p. 49-61.
[188] Hickman, M.A. *The Hickman Lab, Investigating how yeast species generate genetic variation, Fig. 1. Ploidy transitions in C. albicans*. [cited 2020 October 20th, 3:15 pm]; Available from: https://scholarblogs.emory.edu/hickmanlab/research/
[189] Hickman, M.A. *The Hickman Lab, Investigations into the rock and roll lifestyle (i.e. sex and drugs) of yeasts., The Candida albicans lifecycle*. [cited 2020 October 20th, 3:15 pm]; Available from: https://meleahhickman.wordpress.com/.
[190] Arbour, M., E. Epp, H. Hogues, A. Sellam, C. Lacroix, J. Rauceo, A. Mitchell, M. Whiteway, and A. Nantel, 2009, *Widespread occurrence of chromosomal aneuploidy following the routine production of Candida albicans mutants.* FEMS Yeast Res. 9: p. 1070-7.
[191] Forche, A., N.V. Solis, M. Swidergall, R. Thomas, A. Guyer, A. Beach, G.A. Cromie, G.T. Le, E. Lowell, N. Pavelka, J. Berman, A.M. Dudley, A. Selmecki, and S.G. Filler, 2019, *Selection of Candida albicans trisomy during oropharyngeal infection results in a commensal-like phenotype.* PLoS Genet. 15: p. e1008137.
[192] Tucker, C., S. Bhattacharya, H. Wakabayashi, S. Bellaousov, A. Kravets, S.L. Welle, J. Myers, J.J. Hayes, M. Bulger, and E. Rustchenko, 2018, *Transcriptional Regulation on Aneuploid Chromosomes in Divers Candida albicans Mutants.* Sci Rep. 8: p. 1630.
[193] Hose, J., C.M. Yong, M. Sardi, Z. Wang, M.A. Newton, and A.P. Gasch, 2015, *Dosage compensation can buffer copy-number variation in wild yeast.* Elife. 4.
[194] Tang, Y.C. and A. Amon, 2013, *Gene copy-number alterations: a cost-benefit analysis.* Cell. 152: p. 394-405.
[195] Goddard, M.R., H.C. Godfray, and A. Burt, 2005, *Sex increases the efficacy of natural selection in experimental yeast populations.* Nature. 434: p. 636-40.
[196] McDonald, M.J., D.P. Rice, and M.M. Desai, 2016, *Sex speeds adaptation by altering the dynamics of molecular evolution.* Nature. 531: p. 233-6.
[197] Zhang, L., L. Yan, J. Jiang, Y. Wang, Y. Jiang, T. Yan, and Y. Cao, 2014, *The structure and retrotransposition mechanism of LTR-retrotransposons in the asexual yeast Candida albicans.* Virulence. 5: p. 655-64.
[198] Magee, B.B. and P.T. Magee, 2000, *Induction of mating in Candida albicans by construction of MTLa and MTLalpha strains.* Science. 289: p. 310-3.

[199] Hull, C.M., R.M. Raisner, and A.D. Johnson, 2000, *Evidence for mating of the "asexual" yeast Candida albicans in a mammalian host.* Science. 289: p. 307-10.
[200] Anderson, M.Z., G.J. Thomson, M.P. Hirakawa, and R.J. Bennett, 2019, *A 'parameiosis' drives depolyploidization and homologous recombination in Candida albicans.* Nat Commun. 10: p. 4388.
[201] Hull, C.M. and A.D. Johnson, 1999, *Identification of a mating type-like locus in the asexual pathogenic yeast Candida albicans.* Science. 285: p. 1271-5.
[202] Huang, G., H. Wang, S. Chou, X. Nie, J. Chen, and H. Liu, 2006, *Bistable expression of WOR1, a master regulator of white-opaque switching in Candida albicans.* Proc Natl Acad Sci U S A. 103: p. 12813-8.
[203] Srikantha, T., A.R. Borneman, K.J. Daniels, C. Pujol, W. Wu, M.R. Seringhaus, M. Gerstein, S. Yi, M. Snyder, and D.R. Soll, 2006, *TOS9 regulates white-opaque switching in Candida albicans.* Eukaryot Cell. 5: p. 1674-87.
[204] Zordan, R.E., D.J. Galgoczy, and A.D. Johnson, 2006, *Epigenetic properties of white-opaque switching in Candida albicans are based on a self-sustaining transcriptional feedback loop.* Proc Natl Acad Sci U S A. 103: p. 12807-12.
[205] Perry, A.M., A.D. Hernday, and C.J. Nobile, 2020, *Unraveling How Candida albicans Forms Sexual Biofilms.* J Fungi (Basel). 6.
[206] Zordan, R.E., M.G. Miller, D.J. Galgoczy, B.B. Tuch, and A.D. Johnson, 2007, *Interlocking transcriptional feedback loops control white-opaque switching in Candida albicans.* PLoS Biol. 5: p. e256.
[207] Hernday, A.D., M.B. Lohse, P.M. Fordyce, C.J. Nobile, J.L. DeRisi, and A.D. Johnson, 2013, *Structure of the transcriptional network controlling white-opaque switching in Candida albicans.* Mol Microbiol. 90: p. 22-35.
[208] Soll, D.R., 2014, *The role of phenotypic switching in the basic biology and pathogenesis of Candida albicans.* J Oral Microbiol. 6.
[209] Huang, G., S. Yi, N. Sahni, K.J. Daniels, T. Srikantha, and D.R. Soll, 2010, *N-acetylglucosamine induces white to opaque switching, a mating prerequisite in Candida albicans.* PLoS Pathog. 6: p. e1000806.
[210] Xie, J., L. Tao, C.J. Nobile, Y. Tong, G. Guan, Y. Sun, C. Cao, A.D. Hernday, A.D. Johnson, L. Zhang, F.Y. Bai, and G. Huang, 2013, *White-opaque switching in natural MTLa/alpha isolates of Candida albicans: evolutionary implications for roles in host adaptation, pathogenesis, and sex.* PLoS Biol. 11: p. e1001525.
[211] Huang, G., T. Srikantha, N. Sahni, S. Yi, and D.R. Soll, 2009, *CO(2) regulates white-to-opaque switching in Candida albicans.* Curr Biol. 19: p. 330-4.
[212] Ramirez-Zavala, B., O. Reuss, Y.N. Park, K. Ohlsen, and J. Morschhauser, 2008, *Environmental induction of white-opaque switching in Candida albicans.* PLoS Pathog. 4: p. e1000089.
[213] Tong, Y., C. Cao, J. Xie, J. Ni, G. Guan, L. Tao, L. Zhang, and G. Huang, 2014, *N-acetylglucosamine-induced white-to-opaque switching in Candida albicans is independent of the Wor2 transcription factor.* Fungal Genet Biol. 62: p. 71-7.
[214] Alby, K. and R.J. Bennett, 2009, *Stress-induced phenotypic switching in Candida albicans.* Mol Biol Cell. 20: p. 3178-91.
[215] Rikkerink, E.H., B.B. Magee, and P.T. Magee, 1988, *Opaque-white phenotype transition: a programmed morphological transition in Candida albicans.* J Bacteriol. 170: p. 895-9.
[216] Srikantha, T. and D.R. Soll, 1993, *A white-specific gene in the white-opaque switching system of Candida albicans.* Gene. 131: p. 53-60.
[217] Lachke, S.A., S.R. Lockhart, K.J. Daniels, and D.R. Soll, 2003, *Skin facilitates Candida albicans mating.* Infect Immun. 71: p. 4970-6.
[218] Soll, D.R., B. Morrow, and T. Srikantha, 1993, *High-frequency phenotypic switching in Candida albicans.* Trends Genet. 9: p. 61-5.

[219] Tuch, B.B., Q.M. Mitrovich, O.R. Homann, A.D. Hernday, C.K. Monighetti, F.M. De La Vega, and A.D. Johnson, 2010, *The transcriptomes of two heritable cell types illuminate the circuit governing their differentiation.* PLoS Genet. 6: p. e1001070.

[220] Lan, C.Y., G. Newport, L.A. Murillo, T. Jones, S. Scherer, R.W. Davis, and N. Agabian, 2002, *Metabolic specialization associated with phenotypic switching in Candidaalbicans.* Proc Natl Acad Sci U S A. 99: p. 14907-12.

[221] Tsong, A.E., M.G. Miller, R.M. Raisner, and A.D. Johnson, 2003, *Evolution of a combinatorial transcriptional circuit: a case study in yeasts.* Cell. 115: p. 389-99.

[222] Si, H., A.D. Hernday, M.P. Hirakawa, A.D. Johnson, and R.J. Bennett, 2013, *Candida albicans white and opaque cells undergo distinct programs of filamentous growth.* PLoS Pathog. 9: p. e1003210.

[223] Dumitru, R., D.H. Navarathna, C.P. Semighini, C.G. Elowsky, R.V. Dumitru, D. Dignard, M. Whiteway, A.L. Atkin, and K.W. Nickerson, 2007, *In vivo and in vitro anaerobic mating in Candida albicans.* Eukaryot Cell. 6: p. 465-72.

[224] Huang, G., 2012, *Regulation of phenotypic transitions in the fungal pathogen Candida albicans.* Virulence. 3: p. 251-61.

[225] Ene, I.V., M.B. Lohse, A.V. Vladu, J. Morschhauser, A.D. Johnson, and R.J. Bennett, 2016, *Phenotypic Profiling Reveals that Candida albicans Opaque Cells Represent a Metabolically Specialized Cell State Compared to Default White Cells.* mBio. 7.

[226] Scaduto, C.M. and R.J. Bennett, 2015, *Candida albicans the chameleon: transitions and interactions between multiple phenotypic states confer phenotypic plasticity.* Curr Opin Microbiol. 26: p. 102-8.

[227] Geiger, J., D. Wessels, S.R. Lockhart, and D.R. Soll, 2004, *Release of a potent polymorphonuclear leukocyte chemoattractant is regulated by white-opaque switching in Candida albicans.* Infect Immun. 72: p. 667-77.

[228] Sasse, C., M. Hasenberg, M. Weyler, M. Gunzer, and J. Morschhauser, 2013, *White-opaque switching of Candida albicans allows immune evasion in an environment-dependent fashion.* Eukaryot Cell. 12: p. 50-8.

[229] Lohse, M.B. and A.D. Johnson, 2008, *Differential phagocytosis of white versus opaque Candida albicans by Drosophila and mouse phagocytes.* PLoS One. 3: p. e1473.

[230] Alby, K., D. Schaefer, and R.J. Bennett, 2009, *Homothallic and heterothallic mating in the opportunistic pathogen Candida albicans.* Nature. 460: p. 890-3.

[231] Dignard, D., A.L. El-Naggar, M.E. Logue, G. Butler, and M. Whiteway, 2007, *Identification and characterization of MFA1, the gene encoding Candida albicans a-factor pheromone.* Eukaryot Cell. 6: p. 487-94.

[232] Bennett, R.J., M.A. Uhl, M.G. Miller, and A.D. Johnson, 2003, *Identification and characterization of a Candida albicans mating pheromone.* Mol Cell Biol. 23: p. 8189-201.

[233] Panwar, S.L., M. Legrand, D. Dignard, M. Whiteway, and P.T. Magee, 2003, *MFalpha1, the gene encoding the alpha mating pheromone of Candida albicans.* Eukaryot Cell. 2: p. 1350-60.

[234] Julius, D., A. Brake, L. Blair, R. Kunisawa, and J. Thorner, 1984, *Isolation of the putative structural gene for the lysine-arginine-cleaving endopeptidase required for processing of yeast prepro-alpha-factor.* Cell. 37: p. 1075-89.

[235] Julius, D., L. Blair, A. Brake, G. Sprague, and J. Thorner, 1983, *Yeast alpha factor is processed from a larger precursor polypeptide: the essential role of a membrane-bound dipeptidyl aminopeptidase.* Cell. 32: p. 839-52.

[236] Newport, G. and N. Agabian, 1997, *KEX2 influences Candida albicans proteinase secretion and hyphal formation.* J Biol Chem. 272: p. 28954-61.

[237] Bautista-Munoz, C., C. Hernandez-Rodriguez, and L. Villa-Tanaca, 2005, *Analysis and expression of STE13ca gene encoding a putative X-prolyl dipeptidyl aminopeptidase from Candida albicans.* FEMS Immunol Med Microbiol. 45: p. 459-69.

[238] Bennett, R.J. and A.D. Johnson, 2006, *The role of nutrient regulation and the Gpa2 protein in the mating pheromone response of C. albicans.* Mol Microbiol. 62: p. 100-19.

[239] Lin, C.H., S. Kabrawala, E.P. Fox, C.J. Nobile, A.D. Johnson, and R.J. Bennett, 2013, *Genetic control of conventional and pheromone-stimulated biofilm formation in Candida albicans.* PLoS Pathog. 9: p. e1003305.

[240] Chen, P., S.K. Sapperstein, J.D. Choi, and S. Michaelis, 1997, *Biogenesis of the Saccharomyces cerevisiae mating pheromone a-factor.* J Cell Biol. 136: p. 251-69.

[241] Magee, B.B., M. Legrand, A.M. Alarco, M. Raymond, and P.T. Magee, 2002, *Many of the genes required for mating in Saccharomyces cerevisiae are also required for mating in Candida albicans.* Mol Microbiol. 46: p. 1345-51.

[242] Raymond, M., D. Dignard, A.M. Alarco, N. Mainville, B.B. Magee, and D.Y. Thomas, 1998, *A Ste6p/P-glycoprotein homologue from the asexual yeast Candida albicans transports the a-factor mating pheromone in Saccharomyces cerevisiae.* Mol Microbiol. 27: p. 587-98.

[243] Schaefer, D., P. Cote, M. Whiteway, and R.J. Bennett, 2007, *Barrier activity in Candida albicans mediates pheromone degradation and promotes mating.* Eukaryot Cell. 6: p. 907-18.

[244] Guan, G., L. Tao, H. Yue, W. Liang, J. Gong, J. Bing, Q. Zheng, A.O. Veri, S. Fan, N. Robbins, L.E. Cowen, and G. Huang, 2019, *Environment-induced same-sex mating in the yeast Candida albicans through the Hsf1-Hsp90 pathway.* PLoS Biol. 17: p. e2006966.

[245] Yi, S., N. Sahni, K.J. Daniels, C. Pujol, T. Srikantha, and D.R. Soll, 2008, *The same receptor, G protein, and mitogen-activated protein kinase pathway activate different downstream regulators in the alternative white and opaque pheromone responses of Candida albicans.* Mol Biol Cell. 19: p. 957-70.

[246] Chen, J., J. Chen, S. Lane, and H. Liu, 2002, *A conserved mitogen-activated protein kinase pathway is required for mating in Candida albicans.* Mol Microbiol. 46: p. 1335-44.

[247] Lockhart, S.R., R. Zhao, K.J. Daniels, and D.R. Soll, 2003, *Alpha-pheromone-induced "shmooing" and gene regulation require white-opaque switching during Candida albicans mating.* Eukaryot Cell. 2: p. 847-55.

[248] Daniels, K.J., T. Srikantha, S.R. Lockhart, C. Pujol, and D.R. Soll, 2006, *Opaque cells signal white cells to form biofilms in Candida albicans.* EMBO J. 25: p. 2240-52.

[249] Zhao, R., K.J. Daniels, S.R. Lockhart, K.M. Yeater, L.L. Hoyer, and D.R. Soll, 2005, *Unique aspects of gene expression during Candida albicans mating and possible G(1) dependency.* Eukaryot Cell. 4: p. 1175-90.

[250] Lehtonen, J., M.D. Jennions, and H. Kokko, 2012, *The many costs of sex.* Trends Ecol Evol. 27: p. 172-8.

[251] Roze, D. and S.P. Otto, 2012, *Differential selection between the sexes and selection for sex.* Evolution. 66: p. 558-74.

[252] Grimberg, B. and C. Zeyl, 2005, *The effects of sex and mutation rate on adaptation in test tubes and to mouse hosts by Saccharomyces cerevisiae.* Evolution. 59: p. 431-8.

[253] Nielsen, K. and J. Heitman, 2007, *Sex and virulence of human pathogenic fungi.* Adv Genet. 57: p. 143-73.

[254] Sun, S. and J. Heitman, 2011, *Is sex necessary?* BMC Biol. 9: p. 56.

[255] Heitman, J., 2015, *Evolution of sexual reproduction: a view from the Fungal Kingdom supports an evolutionary epoch with sex before sexes.* Fungal Biol Rev. 29: p. 108-117.

[256] Burt, A., 2000, *Perspective: sex, recombination, and the efficacy of selection--was Weismann right?* Evolution. 54: p. 337-51.

[257] Jokela, J., M.F. Dybdahl, and C.M. Lively, 2009, *The maintenance of sex, clonal dynamics, and host-parasite coevolution in a mixed population of sexual and asexual snails.* Am Nat. 174 Suppl 1: p. S43-53.

[258] Lively, C.M., 2010, *A review of Red Queen models for the persistence of obligate sexual reproduction.* J Hered. 101 Suppl 1: p. S13-20.

[259] Morran, L.T., O.G. Schmidt, I.A. Gelarden, R.C. Parrish, 2nd, and C.M. Lively, 2011, *Running with the Red Queen: host-parasite coevolution selects for biparental sex.* Science. 333: p. 216-8.

[260] Carroll, L., 1871, *Through the Looking-Glass*. London: Macmillan.

[261] Morschhauser, J., 2002, *The genetic basis of fluconazole resistance development in Candida albicans.* Biochim Biophys Acta. 1587: p. 240-8.
[262] Morschhauser, J., 2010, *Regulation of multidrug resistance in pathogenic fungi.* Fungal Genet Biol. 47: p. 94-106.
[263] Sanglard, D., A. Coste, and S. Ferrari, 2009, *Antifungal drug resistance mechanisms in fungal pathogens from the perspective of transcriptional gene regulation.* FEMS Yeast Res. 9: p. 1029-50.
[264] Flowers, S.A., B. Colon, S.G. Whaley, M.A. Schuler, and P.D. Rogers, 2015, *Contribution of clinically derived mutations in ERG11 to azole resistance in Candida albicans.* Antimicrob Agents Chemother. 59: p. 450-60.
[265] Morio, F., C. Loge, B. Besse, C. Hennequin, and P. Le Pape, 2010, *Screening for amino acid substitutions in the Candida albicans Erg11 protein of azole-susceptible and azole-resistant clinical isolates: new substitutions and a review of the literature.* Diagn Microbiol Infect Dis. 66: p. 373-84.
[266] Popp, C., I.A.I. Hampe, T. Hertlein, K. Ohlsen, P.D. Rogers, and J. Morschhauser, 2017, *Competitive Fitness of Fluconazole-Resistant Clinical Candida albicans Strains.* Antimicrob Agents Chemother. 61.
[267] Selmecki, A., A. Forche, and J. Berman, 2010, *Genomic plasticity of the human fungal pathogen Candida albicans.* Eukaryot Cell. 9: p. 991-1008.
[268] Wu, W., C. Pujol, S.R. Lockhart, and D.R. Soll, 2005, *Chromosome loss followed by duplication is the major mechanism of spontaneous mating-type locus homozygosis in Candida albicans.* Genetics. 169: p. 1311-27.
[269] Rustad, T.R., D.A. Stevens, M.A. Pfaller, and T.C. White, 2002, *Homozygosity at the Candida albicans MTL locus associated with azole resistance.* Microbiology. 148: p. 1061-72.
[270] Schubert, S., C. Popp, P.D. Rogers, and J. Morschhauser, 2011, *Functional dissection of a Candida albicans zinc cluster transcription factor, the multidrug resistance regulator Mrr1.* Eukaryot Cell. 10: p. 1110-21.
[271] Popp, C., *Evolution der Antimykotikaresistenz in Candida albicans*. 2014. Unpublished master's thesis, Institute for Molecular Infection Biology (IMIB), Julius-Maximilians-Universität Würzburg, Germany, Würzburg.
[272] Reuss, O., A. Vik, R. Kolter, and J. Morschhauser, 2004, *The SAT1 flipper, an optimized tool for gene disruption in Candida albicans.* Gene. 341: p. 119-27.
[273] Sasse, C. and J. Morschhauser, 2012, *Gene deletion in Candida albicans wild-type strains using the SAT1-flipping strategy.* Methods Mol Biol. 845: p. 3-17.
[274] Popp, C., B. Ramirez-Zavala, S. Schwanfelder, I. Kruger, and J. Morschhauser, 2019, *Evolution of Fluconazole-Resistant Candida albicans Strains by Drug-Induced Mating Competence and Parasexual Recombination.* MBio. 10.
[275] Garbe, E. and S. Vylkova, 2019, *Role of Amino Acid Metabolism in the Virulence of Human Pathogenic Fungi.* Current Clinical Microbiology Reports. 6: p. 108-119.
[276] Elena, S.F. and R.E. Lenski, 2003, *Evolution experiments with microorganisms: the dynamics and genetic bases of adaptation.* Nat Rev Genet. 4: p. 457-69.
[277] Cowen, L.E., A. Nantel, M.S. Whiteway, D.Y. Thomas, D.C. Tessier, L.M. Kohn, and J.B. Anderson, 2002, *Population genomics of drug resistance in Candida albicans.* Proc Natl Acad Sci U S A. 99: p. 9284-9.
[278] Barker, K.S., S. Crisp, N. Wiederhold, R.E. Lewis, B. Bareither, J. Eckstein, R. Barbuch, M. Bard, and P.D. Rogers, 2004, *Genome-wide expression profiling reveals genes associated with amphotericin B and fluconazole resistance in experimentally induced antifungal resistant isolates of Candida albicans.* J Antimicrob Chemother. 54: p. 376-85.
[279] DeRisi, J., B. van den Hazel, P. Marc, E. Balzi, P. Brown, C. Jacq, and A. Goffeau, 2000, *Genome microarray analysis of transcriptional activation in multidrug resistance yeast mutants.* FEBS Lett. 470: p. 156-60.

[280] Rogers, P.D. and K.S. Barker, 2003, *Genome-wide expression profile analysis reveals coordinately regulated genes associated with stepwise acquisition of azole resistance in Candida albicans clinical isolates.* Antimicrob Agents Chemother. 47: p. 1220-7.

[281] Andersson, D.I. and B.R. Levin, 1999, *The biological cost of antibiotic resistance.* Curr Opin Microbiol. 2: p. 489-93.

[282] Maisnier-Patin, S. and D.I. Andersson, 2004, *Adaptation to the deleterious effects of antimicrobial drug resistance mutations by compensatory evolution.* Res Microbiol. 155: p. 360-9.

[283] Puri, S. and M. Edgerton, 2014, *How does it kill?: understanding the candidacidal mechanism of salivary histatin 5.* Eukaryot Cell. 13: p. 958-64.

[284] White, S.J., A. Rosenbach, P. Lephart, D. Nguyen, A. Benjamin, S. Tzipori, M. Whiteway, J. Mecsas, and C.A. Kumamoto, 2007, *Self-regulation of Candida albicans population size during GI colonization.* PLoS Pathog. 3: p. e184.

[285] Perez, J.C., C.A. Kumamoto, and A.D. Johnson, 2013, *Candida albicans commensalism and pathogenicity are intertwined traits directed by a tightly knit transcriptional regulatory circuit.* PLoS Biol. 11: p. e1001510.

[286] Reece, J., 2014, *Campbell biology*. Boston: Pearson.

[287] Abel, S., P. Abel zur Wiesch, B.M. Davis, and M.K. Waldor, 2015, *Analysis of Bottlenecks in Experimental Models of Infection.* PLoS Pathog. 11: p. e1004823.

[288] Ferrari, S., F. Ischer, D. Calabrese, B. Posteraro, M. Sanguinetti, G. Fadda, B. Rohde, C. Bauser, O. Bader, and D. Sanglard, 2009, *Gain of function mutations in CgPDR1 of Candida glabrata not only mediate antifungal resistance but also enhance virulence.* PLoS Pathog. 5: p. e1000268.

[289] Ferrari, S., M. Sanguinetti, R. Torelli, B. Posteraro, and D. Sanglard, 2011, *Contribution of CgPDR1-regulated genes in enhanced virulence of azole-resistant Candida glabrata.* PLoS One. 6: p. e17589.

[290] Vale-Silva, L., F. Ischer, S. Leibundgut-Landmann, and D. Sanglard, 2013, *Gain-of-function mutations in PDR1, a regulator of antifungal drug resistance in Candida glabrata, control adherence to host cells.* Infect Immun. 81: p. 1709-20.

[291] Vale-Silva, L.A., B. Moeckli, R. Torelli, B. Posteraro, M. Sanguinetti, and D. Sanglard, 2016, *Upregulation of the Adhesin Gene EPA1 Mediated by PDR1 in Candida glabrata Leads to Enhanced Host Colonization.* mSphere. 1.

[292] Cleveland, A.A., L.H. Harrison, M.M. Farley, R. Hollick, B. Stein, T.M. Chiller, S.R. Lockhart, and B.J. Park, 2015, *Declining incidence of candidemia and the shifting epidemiology of Candida resistance in two US metropolitan areas, 2008-2013: results from population-based surveillance.* PLoS One. 10: p. e0120452.

[293] Graser, Y., M. Volovsek, J. Arrington, G. Schonian, W. Presber, T.G. Mitchell, and R. Vilgalys, 1996, *Molecular markers reveal that population structure of the human pathogen Candida albicans exhibits both clonality and recombination.* Proc Natl Acad Sci U S A. 93: p. 12473-7.

[294] Xu, J., T.G. Mitchell, and R. Vilgalys, 1999, *PCR-restriction fragment length polymorphism (RFLP) analyses reveal both extensive clonality and local genetic differences in Candida albicans.* Mol Ecol. 8: p. 59-73.

[295] Forche, A., G. Schonian, Y. Graser, R. Vilgalys, and T.G. Mitchell, 1999, *Genetic structure of typical and atypical populations of Candida albicans from Africa.* Fungal Genet Biol. 28: p. 107-25.

[296] Odds, F.C., M.E. Bougnoux, D.J. Shaw, J.M. Bain, A.D. Davidson, D. Diogo, M.D. Jacobsen, M. Lecomte, S.Y. Li, A. Tavanti, M.C. Maiden, N.A. Gow, and C. d'Enfert, 2007, *Molecular phylogenetics of Candida albicans.* Eukaryot Cell. 6: p. 1041-52.

[297] Tavanti, A., A.D. Davidson, M.J. Fordyce, N.A. Gow, M.C. Maiden, and F.C. Odds, 2005, *Population structure and properties of Candida albicans, as determined by multilocus sequence typing.* J Clin Microbiol. 43: p. 5601-13.

[298] Jacobsen, M.D., A.M. Rattray, N.A. Gow, F.C. Odds, and D.J. Shaw, 2008, *Mitochondrial haplotypes and recombination in Candida albicans.* Med Mycol. 46: p. 647-54.

[299] Anderson, J.B., C. Wickens, M. Khan, L.E. Cowen, N. Federspiel, T. Jones, and L.M. Kohn, 2001, *Infrequent genetic exchange and recombination in the mitochondrial genome of Candida albicans.* J Bacteriol. 183: p. 865-72.
[300] Berman, J. and L. Hadany, 2012, *Does stress induce (para)sex? Implications for Candida albicans evolution.* Trends Genet. 28: p. 197-203.
[301] Heitman, J., 2010, *Evolution of eukaryotic microbial pathogens via covert sexual reproduction.* Cell Host Microbe. 8: p. 86-99.
[302] Goddard, M.R., 2016, *Molecular evolution: Sex accelerates adaptation.* Nature. 531: p. 176-7.
[303] Zhu, Y.O., M.L. Siegal, D.W. Hall, and D.A. Petrov, 2014, *Precise estimates of mutation rate and spectrum in yeast.* Proc Natl Acad Sci U S A. 111: p. E2310-8.
[304] Farlow, A., H. Long, S. Arnoux, W. Sung, T.G. Doak, M. Nordborg, and M. Lynch, 2015, *The Spontaneous Mutation Rate in the Fission Yeast Schizosaccharomyces pombe.* Genetics. 201: p. 737-44.
[305] Legrand, M., P. Lephart, A. Forche, F.M. Mueller, T. Walsh, P.T. Magee, and B.B. Magee, 2004, *Homozygosity at the MTL locus in clinical strains of Candida albicans: karyotypic rearrangements and tetraploid formation.* Mol Microbiol. 52: p. 1451-62.
[306] Loffler, J., S.L. Kelly, H. Hebart, U. Schumacher, C. Lass-Florl, and H. Einsele, 1997, *Molecular analysis of cyp51 from fluconazole-resistant Candida albicans strains.* FEMS Microbiol Lett. 151: p. 263-8.
[307] Marichal, P., L. Koymans, S. Willemsens, D. Bellens, P. Verhasselt, W. Luyten, M. Borgers, F.C.S. Ramaekers, F.C. Odds, and H. Vanden Bossche, 1999, *Contribution of mutations in the cytochrome P450 14alpha-demethylase (Erg11p, Cyp51p) to azole resistance in Candida albicans.* Microbiology. 145 (Pt 10): p. 2701-2713.
[308] Martinez, M., J.L. Lopez-Ribot, W.R. Kirkpatrick, S.P. Bachmann, S. Perea, M.T. Ruesga, and T.F. Patterson, 2002, *Heterogeneous mechanisms of azole resistance in Candida albicans clinical isolates from an HIV-infected patient on continuous fluconazole therapy for oropharyngeal candidosis.* J Antimicrob Chemother. 49: p. 515-24.
[309] Chau, A.S., C.A. Mendrick, F.J. Sabatelli, D. Loebenberg, and P.M. McNicholas, 2004, *Application of real-time quantitative PCR to molecular analysis of Candida albicans strains exhibiting reduced susceptibility to azoles.* Antimicrob Agents Chemother. 48: p. 2124-31.
[310] Li, X., N. Brown, A.S. Chau, J.L. Lopez-Ribot, M.T. Ruesga, G. Quindos, C.A. Mendrick, R.S. Hare, D. Loebenberg, B. DiDomenico, and P.M. McNicholas, 2004, *Changes in susceptibility to posaconazole in clinical isolates of Candida albicans.* J Antimicrob Chemother. 53: p. 74-80.
[311] Siikala, E., R. Rautemaa, M. Richardson, H. Saxen, P. Bowyer, and D. Sanglard, 2010, *Persistent Candida albicans colonization and molecular mechanisms of azole resistance in autoimmune polyendocrinopathy-candidiasis-ectodermal dystrophy (APECED) patients.* J Antimicrob Chemother. 65: p. 2505-13.
[312] Pujol, C., S.A. Messer, M. Pfaller, and D.R. Soll, 2003, *Drug resistance is not directly affected by mating type locus zygosity in Candida albicans.* Antimicrob Agents Chemother. 47: p. 1207-12.
[313] Brenes, L.R., M.B. Lohse, N. Hartooni, and A.D. Johnson, 2020, *A Set of Diverse Genes Influence the Frequency of White-Opaque Switching in Candida albicans.* G3 (Bethesda).
[314] Dalal, C.K., I.A. Zuleta, M.B. Lohse, R.E. Zordan, H. El-Samad, and A.D. Johnson, 2019, *A population shift between two heritable cell types of the pathogen Candida albicans is based both on switching and selective proliferation.* Proc Natl Acad Sci U S A.
[315] 1986, *Bethesda Research Laboratories.*
[316] Hampe, I.A.I., J. Friedman, M. Edgerton, and J. Morschhauser, 2017, *An acquired mechanism of antifungal drug resistance simultaneously enables Candida albicans to escape from intrinsic host defenses.* PLoS Pathog. 13: p. e1006655.
[317] Gillum, A.M., E.Y. Tsay, and D.R. Kirsch, 1984, *Isolation of the Candida albicans gene for orotidine-5'-phosphate decarboxylase by complementation of S. cerevisiae ura3 and E. coli pyrF mutations.* Mol Gen Genet. 198: p. 179-82.

[318] Saidane, S., S. Weber, X. De Deken, G. St-Germain, and M. Raymond, 2006, *PDR16-mediated azole resistance in Candida albicans.* Mol Microbiol. 60: p. 1546-62.

[319] Franz, R., M. Ruhnke, and J. Morschhauser, 1999, *Molecular aspects of fluconazole resistance development in Candida albicans.* Mycoses. 42: p. 453-8.

[320] Calabrese, D., J. Bille, and D. Sanglard, 2000, *A novel multidrug efflux transporter gene of the major facilitator superfamily from Candida albicans (FLU1) conferring resistance to fluconazole.* Microbiology. 146 (Pt 11): p. 2743-54.

[321] White, T.C., M.A. Pfaller, M.G. Rinaldi, J. Smith, and S.W. Redding, 1997, *Stable azole drug resistance associated with a substrain of Candida albicans from an HIV-infected patient.* Oral Dis. 3 Suppl 1: p. S102-9.

[322] Sasse, C., R. Schillig, F. Dierolf, M. Weyler, S. Schneider, S. Mogavero, P.D. Rogers, and J. Morschhauser, 2011, *The transcription factor Ndt80 does not contribute to Mrr1-, Tac1-, and Upc2-mediated fluconazole resistance in Candida albicans.* PLoS One. 6: p. e25623.

[323] Ramirez-Zavala, B., M. Weyler, T. Gildor, C. Schmauch, D. Kornitzer, R. Arkowitz, and J. Morschhauser, 2013, *Activation of the Cph1-dependent MAP kinase signaling pathway induces white-opaque switching in Candida albicans.* PLoS Pathog. 9: p. e1003696.

[324] Bedell, G.W. and D.R. Soll, 1979, *Effects of low concentrations of zinc on the growth and dimorphism of Candida albicans: evidence for zinc-resistant and -sensitive pathways for mycelium formation.* Infect Immun. 26: p. 348-54.

[325] De Backer, M.D., D. Maes, S. Vandoninck, M. Logghe, R. Contreras, and W.H. Luyten, 1999, *Transformation of Candida albicans by electroporation.* Yeast. 15: p. 1609-18.

[326] Kohler, G.A., T.C. White, and N. Agabian, 1997, *Overexpression of a cloned IMP dehydrogenase gene of Candida albicans confers resistance to the specific inhibitor mycophenolic acid.* J Bacteriol. 179: p. 2331-8.

[327] Kibbe, W.A., 2007, *OligoCalc: an online oligonucleotide properties calculator.* Nucleic Acids Res. 35: p. W43-6.

[328] Ruhnke, M., A. Eigler, I. Tennagen, B. Geiseler, E. Engelmann, and M. Trautmann, 1994, *Emergence of fluconazole-resistant strains of Candida albicans in patients with recurrent oropharyngeal candidosis and human immunodeficiency virus infection.* J Clin Microbiol. 32: p. 2092-8.

6. Appendix

Appendix A1

White-to-opaque switching competence of fluconazole-induced *MTL* homozygous isolates and control strains. White phase cells were spread for single colonies on Lee's agar plates with phloxine B. One share of the plates was incubated under room conditions for several days as a control. The other share of the plates was incubated for 2 days at a high CO_2 concertation (18% CO_2) and 25°C to induce white-to-opaque switching. This step was followed by an incubation for several days under room conditions. The experiment was conducted at least three times independently for each strain. The exact number of experiments and mean values of counted opaque colonies, white-opaque mixed colonies and white colonies are given.

Strain[(a)]	**Incubation under room conditions**				**Incubation at 18% CO_2 and 25°C, followed by an incubation under room conditions**			
	Opaque colonies mean (%]	**Mixed colonies mean [%]**	**Opaque and mixed colonies total mean [%]**	**Number of experiments**	**Opaque colonies mean [%]**	**Mixed colonies mean [%]**	**Opaque and mixed colonies total mean [%]**	**Number of experiments**
SCMTLaM2A	0.0	0.0	0.0	5	98.6	1.2	99.3	4
SCMTLαM2A	0.0	0.3	0.3	5	98.5	1.3	99.9	5
WO-1	0.8	1.7	2.5	3	46.3	35.6	81.9	3
SCERG11R32hom1A (E3A)	0.1	2.1	2.2	5	69.5	29.1	98.6	3
SCERG11R32hom1B (E2.1)	0.0	0.0	0.0	5	100.0	0.0	100.0	4
SCMRR1R32hom1A (M2)	0.1	0.1	0.2	3	98.9	1.1	100.0	3
SCMRR1R32hom2A (M8)	0.0	0.0	0.0	4	96.6	3.4	100.0	3
SCMRR1R32hom1B (M2.1)	0.0	0.1	0.1	5	66.6	33.3	99.9	3
SCMRR1R32hom2B (M2.2)	0.2	0.4	0.6	4	93.7	6.3	100.0	4
SCTAC1R32hom1A (A1)	0.0	0.3	0.3	6	87.6	2.3	89.9	6
SCTAC1R32hom2A (A2)	0.0	0.8	0.8	4	98.4	1.3	99.7	4
SCTAC1R32hom3A (A5)	0.0	0.5	0.5	4	80.8	18.9	99.7	4
SCTAC1R32hom1B (B2)	0.0	0.1	0.1	3	99.9	0.1	100.0	3
SCTAC1R32hom2B (B3)	0.1	0.3	0.4	6	99.9	0.0	99.9	6
SCTAC1R32hom3B (B4)	0.0	1.2	1.2	4	99.7	0.1	99.8	4
SCTAC1R32hom4B (B6)	0.0	0.7	0.7	4	95.8	4.2	100.0	4
SCUPC2R12hom1A (U3)	0.0	0.7	0.7	3	99.9	0.0	99.9	4
U12	0.0	0.6	0.6	3	98.2	1.8	100.0	3
SCUPC2R12hom1B (U2.3)	0.0	1.8	1.8	5	99.7	0.3	100.0	5

[(a)] Originally used strain names are indicated in parentheses. Please note that initially randomly picked strains of all experiments were consecutively numbered. Subsequently, selected *MTL* homozygous strains were systematically renamed.

Appendix A2

Stability of opaque phase cells of fluconazole-induced *MTL* homozygous isolates and control strains in two different conditions. Opaque phase cells were spread for single colonies on Lee's agar plates with phloxine B. One share of the plates was incubated under room conditions for several days. The other share of the plates was incubated for 2 days at a high CO_2 concertation (18% CO_2) and 25°C (induction of white-opaque switching). This step was followed by an incubation for several days under room conditions. The experiment was conducted at least three times independently for each strain. The exact number of experiments and mean values of counted opaque colonies, white-opaque mixed colonies and white colonies are given.

Strain[(a)]	**Incubation under room conditions**				**Incubation at 18% CO_2 and 25°C, followed by an incubation under room conditions**			
	Opaque colonies mean [%]	**Mixed colonies mean [%]**	**Opaque and mixed colonies total mean [%]**	**Number of experiments**	**Opaque colonies mean [%]**	**Mixed colonies mean [%]**	**Opaque and mixed colonies total mean [%]**	**Number of experiments**
SCMTLaM2A	81.1	3.9	85.0	4	100.0	0.0	100.0	5
SCMTLαM2A	83.8	3.4	87.2	3	100.0	0.0	100.0	5
WO-1	100.0	0.0	100.0	3	100.0	0.0	100.0	3
SCERG11R32hom1A (E3A)	97.5	1.1	98.6	4	99.8	0.2	100.0	3
SCERG11R32hom1B (E2.1)	84.8	3.6	88.4	5	100.0	0.0	100.0	4
SCMRR1R32hom1A (M2)	99.6	0.0	99.6	4	99.7	0.0	99.7	3
SCMRR1R32hom2A (M8)	99.3	0.1	99.4	4	100.0	0.0	100.0	3
SCMRR1R32hom1B (M2.1)	98.8	0.0	98.8	4	100.0	0.0	100.0	3
SCMRR1R32hom2B (M2.2)	94.5	0.3	94.8	5	100.0	0.0	100.0	4
SCTAC1R32hom1A (A1)	90.3	3.2	93.5	4	100.0	0.0	100.0	4
SCTAC1R32hom2A (A2)	95.8	1.7	97.5	4	100.0	0.0	100.0	4
SCTAC1R32hom3A (A5)	94.0	1.8	95.8	4	99.9	0.1	100.0	4
SCTAC1R32hom1B (B2)	80.2	5.5	85.7	3	100.0	0.0	100.0	3
SCTAC1R32hom2B (B3)	82.0	2.7	84.7	3	100.0	0.0	100.0	3
SCTAC1R32hom3B (B4)	85.5	2.2	87.7	4	100.0	0.0	100.0	4
SCTAC1R32hom4B (B6)	93.9	1.9	95.8	4	99.8	0.2	100.0	4
SCUPC2R12hom1A (U3)	91.5	1.8	93.3	4	100.0	0.0	100.0	4
U12	82.1	1.5	83.6	3	98.3	0.6	98.9	3
SCUPC2R12hom1B (U2.3)	95.5	1.6	97.1	5	100.0	0.0	100.0	5

[(a)] Originally used strain names are indicated in parentheses. Please note that initially randomly picked strains of all experiments were consecutively numbered. Subsequently, selected *MTL* homozygous strains were systematically renamed.

Appendix A3

Mating products isolated during this study and their fluconazole resistance level (MIC). Selected mating products for passaging experiments are highlighted in italic font. Time of co-incubation of the *MTL* homozygous parental strains before the cell lawn was partly taken and plated for single colonies to identify mating products is indicated (detailed information in chapter 4.2.4.2). Parts published by Popp *et al.* [274].

Mating product[(a)]	**MIC [µg/ml]**	**Time of co-incubation of the *MTL* homozygous parental strains**
Cross of SCERG11R32hom1B (*MTL*a parent) and SCMRR1R32hom1A (*MTL*α parent)		
EM1	8	6 days
EM16	8	6 days
EM17	8	6 days
EM19	8	6 days
EM20	8	6 days
EM21	8	6 days
EM22	8	6 days
EM23	8	6 days
EM24	8	6 days
EM25	8	6 days
EM26	8	6 days
EM27	8	6 days
EM28	8	6 days
EM30	8	6 days
EM32	8	6 days
EM33	8	6 days
EM34	8	6 days
Cross of SCMRR1R32hom2A (*MTL*a parent) and SCERG11R32hom1A (*MTL*α parent)		
ME1 (ME3)	4	6 days
ME35	4	6 days
ME36	4	6 days
Cross of SCER11R32hom1B (*MTL*a parent) and SCTAC1R32hom2A (*MTL*α parent)		
ET1	8	3 days
ET2	8	6 days
Cross of SCTAC1R32hom2B (*MTL*a parent) and SCERG11R32hom1A (*MTL*α parent)		
TE1 (TE27)	4	6 days
TE3	4	6 days
TE25	4	6 days
TE33	4	6 days
TE35	4	9 days
TE42	4	9 days
Cross of SCERG11R32hom1B (*MTL*a parent) and SCUPC2R12hom1B (*MTL*α parent)		
EU1	4	6 days
EU2	4	14 days
EU3	4	14 days
EU4	4	14 days
EU5	4	14 days
Cross of SCUPC2R12hom1A (*MTL*a parent) and SCERG11R32hom1A (*MTL*α parent)		
UE1 (UE64)	2	9 days
UE59	2	6 days
UE65	2	9 days
Cross of SCMRR1R32hom2A (*MTL*a parent) and SCTAC1R32hom2A (*MTL*α parent)		
MT1 (MT3)	8	6 days
MT2 (MT6)	4	6 days
MT5	8	6 days
MT8	8	6 days
MT12	8	6 days
MT13	8	6 days
MT16	8	14 days

Mating product[a]	MIC [µg/ml]	Time of co-incubation of the *MTL* homozygous parental strains
Cross of SCTAC1R32hom2B (*MTL*a parent) and SCMRR1R32hom1A (*MTL*α parent)		
TM1 (TM8)	4	14 days
TM2	4	6 days
Cross of SCMRR1R32hom2A (*MTL*a parent) and SCUPC2R12hom1B (*MTL*α parent)		
MU1 (MU13)	4	6 days
MU2 (MU8)	8[b]	3 days
MU9	4	3 days
MU16	4	6 days
MU18	4	6 days
MU20	4	9 days
MU21	4	9 days
MU22	4	9 days
MU23	4	9 days
MU29	4	9 days
Cross of SCUPC2R12hom1A (*MTL*a parent) and SCMRR1R32hom1A (*MTL*α parent)		
UM1 (UM21)	4	3 days
UM3	4	14 days
UM22	4	3 days
UM24	4	6 days
UM25	4	6 days
UM26	4	6 days
UM28	4	6 days
UM29	4	6 days
UM30	4	6 days
UM31	4	9 days
UM32	4	9 days
UM34	4	9 days
UM35	4	9 days
UM36	4	9 days
UM37	4	9 days
UM38	4	9 days
UM39	4	9 days
UM40	4	9 days
Cross of SCTAC1R32hom2B (*MTL*a parent) and SCUPC2R12hom1B (*MTL*α parent)		
TU1	4	6 days
TU2	4	14 days
TU4	4	14 days
TU6	4	14 days
Cross of SCUPC2R12hom1A (*MTL*a parent) and SCTAC1R32hom2A (*MTL*α parent)		
UT1 (UT86)	8	3 days
UT85	8	3 days

[a] Originally used strain names are indicated in parentheses. Please note that initially randomly picked strains of all experiments were consecutively numbered. Subsequently, selected mating products were systematically renamed.
[b] Growth was already reduced at this fluconazole concentration.

Appendix A4

Mating product derivatives isolated during the present study and their fluconazole resistance level (MIC). Relevant genotypes and the passage in which the derivatives were isolated, including the fluconazole concentration in the passage are indicated. Note that ET1 was passaged twice independently. Parts published by Popp *et al.* [274].

MP Derivative[a]	MIC [µg/ml]	Relevant genotype[b]	Passage (fluconazole concentration in the culture)
Parental mating product EM1			
1EM1P1-1	8	n.t.	1 (4µg/ml)
1EM1P1-2	8	n.t.	
1EM1P1-3	8	n.t.	
1EM1P2-1	16	n.t.	2 (4µg/ml)
1EM1P2-2	16	n.t.	
1EM1P2-3	16	n.t.	
EM1P3A-1 (1EM1P3-1)	64	*ERG11*^{G464S}; *MRR1*^{P683S}; *MTL***a**	3 (8µg/ml)
1EM1P3-2	16	n.t.	
1EM1P3-3	16	n.t.	
1EM1P4-1	16	n.t.	4 (8µg/ml)
1EM1P4-2	64	n.t.	
1EM1P4-3	32	n.t.	
1EM1P5-1	8	n.t.	5 (16µg/ml)
1EM1P5-2	32	n.t.	
1EM1P5-3	32	n.t.	
1EM1P6-1	32	n.t.	6 (16µg/ml)
1EM1P6-2	32	n.t.	
1EM1P6-3	64	n.t.	
1EM1P7-1	16	n.t.	7 (32µg/ml)
1EM1P7-2	32	n.t.	
1EM1P7-3	64	n.t.	
EM1P8A-1 (1EM1P8-1)	128	*ERG11*^{G464S}; *MRR1*^{P683S}; *MTL***a**	8 (32µg/ml)
1EM1P8-2	8	n.t.	
EM1P8A-3 (1EM1P8-3)	128	*ERG11*^{G464S}; *MRR1*^{P683S}; *MTL***a**	
1EM1P10-1	32	n.t.	10 (64µg/ml)
1EM1P10-2	32	n.t.	
1EM1P10-3	32	n.t.	
1EM1P12-1	32	n.t.	12 (128µg/ml)
1EM1P12-2	16	n.t.	
1EM1P12-3	32	n.t.	
1EM1P14-1	32	n.t.	14 (256µg/ml)
1EM1P14-2	32	n.t.	
1EM1P14-3	32	n.t.	
Parental mating product ME1			
1ME3P1-1	8	n.t.	1 (2µg/ml)
1ME3P1-2	4	n.t.	
1ME3P1-3	8	n.t.	
1ME3P2-1	8	n.t.	2 (2µg/ml)
1ME3P2-2	4	n.t.	
1ME3P2-3	4	n.t.	
1ME3P3-1	16	n.t.	3 (4µg/ml)
1ME3P3-2	4	n.t.	
1ME3P3-3	16	n.t.	
1ME3P4-1	16	n.t.	4 (4µg/ml)
ME1P4A-2 (1ME3P4-2)	32	*ERG11*/*ERG11*^{G464S}; *MRR1*^{P683S}; *MTL***a**/α	
ME1P4A-3 (1ME3P4-3)	32	*ERG11*/*ERG11*^{G464S}; *MRR1*^{P683S}; *MTL***a**/α	
1ME3P5-1	32	n.t.	5 (8µg/ml)
ME1P5A-2 (1ME3P5-2)	64	*ERG11*/*ERG11*^{G464S}; *MRR1*^{P683S}; *MTL***a**/α	
1ME3P5-3	16	n.t.	

MP Derivative[a]	MIC [µg/ml]	Relevant genotype[b]	Passage (fluconazole concentration in the culture)
1ME3P6-1	64	n.t.	6 (8µg/ml)
1ME3P6-2	64	n.t.	
1ME3P6-3	64	n.t.	
1ME3P8-1	64	n.t.	8 (16µg/ml)
1ME3P8-2	64	n.t.	
1ME3P8-3	64	n.t.	
1ME3P9-1	64	n.t.	9 (32µg/ml)
1ME3P9-2	64	n.t.	
1ME3P9-3	64	n.t.	
1ME3P10-1	64	n.t.	10 (32µg/ml)
1ME3P10-2	64	n.t.	
1ME3P10-3	64	n.t.	
1ME3P11-1	64	n.t.	11 (64µg/ml)
1ME3P11-2	64	n.t.	
1ME3P11-3	64	n.t.	
1ME3P12-1	64	n.t.	12 (64µg/ml)
1ME3P12-2	32	n.t.	
1ME3P12-3	64	n.t.	
1ME3P14-1	32	n.t.	14 (128µg/ml)
1ME3P14-2	32	n.t.	
1ME3P14-3	32	n.t.	
1ME3P16-1	16	n.t.	16 (256µg/ml)
1ME3P16-2	32	n.t.	
1ME3P16-3	32	n.t.	
Parental mating product ET1			
1ET1P1-1	8	n.t.	1 (4µg/ml)
1ET1P1-2	8	n.t.	
1ET1P1-3	8	n.t.	
1ET1P2-1	8	n.t.	2 (4µg/ml)
ET1P2A-2 (1ET1P2-2)	16	*ERG11*/*ERG11*^{G464S}; *MTL***a**/α; *TAC1-1*/*TAC1-2*/*TAC1*^{G980E}	
1ET1P2-3	8	n.t.	
1ET1P3-1	16	n.t.	3 (8µg/ml)
1ET1P3-2	16	n.t.	
1ET1P3-3	8	n.t.	
1ET1P4-1	16	n.t.	4 (8µg/ml)
1ET1P4-2	16	n.t.	
1ET1P4-3	16	n.t.	
1ET1P5-1	16	n.t.	5 (16µg/ml)
1ET1P5-2	16	n.t.	
1ET1P5-3	16	n.t.	
1ET1P6-1	16	n.t.	6 (16µg/ml)
1ET1P6-2	16	n.t.	
1ET1P6-3	16	n.t.	
1ET1P7-1	16	n.t.	7 (32µg/ml)
1ET1P7-2	16	n.t.	
ET1P7A-3 (1ET1P7-3)	32	*ERG11*/*ERG11*^{G464S}; *TAC1-2*/*TAC1*^{G980E}; *MTL***a**/α	
1ET1P8-1	32	n.t.	8 (32µg/ml)
1ET1P8-2	16	n.t.	
1ET1P8-3	16	n.t.	
1ET1P10-1	16	n.t.	10 (64µg/ml)
1ET1P10-2	8	n.t.	
1ET1P10-3	16	n.t.	
1ET1P12-1	16	n.t.	12 (128µg/ml)
1ET1P12-2	16	n.t.	
1ET1P12-3	8	n.t.	

MP Derivative[a]	MIC [µg/ml]	Relevant genotype[b]	Passage (fluconazole concentration in the culture)
1ET1P14-1	16	n.t.	14 (256µg/ml)
1ET1P14-2	16	n.t.	
1ET1P14-3	16	n.t.	
Parental mating product ET1 In the following derivatives isolated during the second passaging experiment are listed.			
2ET1P1-1	8	n.t.	1 (4µg/ml)
2ET1P1-2	8	n.t.	
2ET1P1-3	8	n.t.	
2ET1P2-1	8	n.t.	2(4µg/ml)
2ET1P2-2	8	n.t.	
2ET1P2-3	16	n.t.	
2ET1P3-1	16	n.t.	3(8µg/ml)
2ET1P3-2	16	n.t.	
2ET1P3-3	16	n.t.	
2ET1P4-1	16	n.t.	4 (8µg/ml)
2ET1P4-2	16	n.t.	
2ET1P4-3	16	n.t.	
2ET1P5-1	16	n.t.	5 (16µg/ml)
2ET1P5-2	16	n.t.	
2ET1P5-3	16	n.t.	
ET1P6B-1 (2ET1P6-1)	32	*ERG11*/*ERG11*^{G464S}; *MTL***a**/α; *TAC1-1*/*TAC1-2*/*TAC1*^{G980E}	6 (16µg/ml)
2ET1P6-2	16	n.t.	
ET1P6B-3 (2ET1P6-3)	32	*ERG11*/*ERG11*^{G464S}; *MTL***a**/α; *TAC1-2*/*TAC1*^{G980E}	
2ET1P7-1	32	n.t.	7 (32µg/ml)
2ET1P7-2	16	n.t.	
2ET1P7-3	16	n.t.	
2ET1P8-1	16	n.t.	8 (32µg/ml)
2ET1P8-2	16	n.t.	
ET1P8B-3 (2ET1P8-3)	64	*ERG11*/*ERG11*^{G464S}; *MTL***a**/α; *TAC1-1*/*TAC1-2*/*TAC1*^{G980E}	
2ET1P10-1	16	n.t.	10 (64µg/ml)
2ET1P10-2	16	n.t.	
2ET1P10-3	16	n.t.	
2ET1P12-1	-	n.t.	12 (128µg/ml)
2ET1P12-2	-	n.t.	
2ET1P12-3	-	n.t.	
2ET1P14-1	-	n.t.	14 (256µg/ml)
2ET1P14-2	-	n.t.	
2ET1P14-3	-	n.t.	
Parental mating product TE1			
1TE27P1-1	4	n.t.	1 (2µg/ml)
1TE27P1-2	4	n.t.	
1TE27P1-3	4	n.t.	
1TE27P2-1	4	n.t.	2 (2µg/ml)
1TE27P2-2	4	n.t.	
1TE27P2-3	4	n.t.	
1TE27P3-1	8	n.t.	3 (4µg/ml)
1TE27P3-2	8	n.t.	
1TE27P3-3	8	n.t.	
1TE27P4-1	8	n.t.	4 (4µg/ml)
1TE27P4-2	8	n.t.	
1TE27P4-3	8	n.t.	
1TE27P5-1	8	n.t.	5 (8µg/ml)
1TE27P5-2	8	n.t.	
1TE27P5-3	8	n.t.	

MP Derivative[a]	MIC [µg/ml]	Relevant genotype[b]	Passage (fluconazole concentration in the culture)
TE1P6A-1 (1TE27P6-1)	16	*ERG11*/*ERG11*^{G464S}; *MTL***a**/α; *TAC1-2*/*TAC1*^{G980E}	6 (8µg/ml)
TE1P6A-2 (1TE27P6-2)	16	*ERG11*; *MTL***a**; *TAC1*^{G980E}	
1TE27P6-3	8	n.t.	
1TE27P8-1	32	n.t.	8 (16µg/ml)
1TE27P8-2	32	n.t.	
1TE27P8-3	32	n.t.	
1TE27P10-1	64	n.t.	10 (32µg/ml)
1TE27P10-2	64	n.t.	
1TE27P10-3	16	n.t.	
1TE27P11-1	8	n.t.	11 (64µg/ml)
1TE27P11-2	64	n.t.	
1TE27P11-3	64	n.t.	
TE1P12A-1 (1TE27P12-1)	128	*ERG11*/*ERG11*^{G464S}; *MTL***a**/α; *TAC1*^{G980E}	12 (64µg/ml)
1TE27P12-2	32	n.t.	
1TE27P12-3	8	n.t.	
1TE27P14-1	4	n.t.	14 (128µg/ml)
1TE27P14-2	8	n.t.	
1TE27P14-3	8	n.t.	
1TE27P16-1	16	n.t.	16 (256µg/ml)
1TE27P16-2	16	n.t.	
1TE27P16-3	8	n.t.	
Parental mating product EU1			
1EU1P1-1	4	n.t.	1 (2µg/ml)
1EU1P1-2	4	n.t.	
1EU1P1-3	4	n.t.	
1EU1P2-1	8	n.t.	2 (2µg/ml)
1EU1P2-2	4	n.t.	
1EU1P2-3	8	n.t.	
1EU1P3-1	8	n.t.	3 (4µg/ml)
1EU1P3-2	8	n.t.	
1EU1P3-3	8	n.t.	
1EU1P4-1	8	n.t.	4 (4µg/ml)
1EU1P4-2	16	n.t.	
1EU1P4-3	8	n.t.	
1EU1P5-1	16	n.t.	5 (8µg/ml)
1EU1P5-2	8	n.t.	
1EU1P5-3	16	n.t.	
1EU1P6-1	16	n.t.	6 (8µg/ml)
1EU1P6-2	16	n.t.	
EU1P6A-3 (1EU1P6-3)	32	*ERG11*/*ERG11*^{G464S}; *MTL***a**/α; *UPC2*/*UPC2*^{G648D}	
1EU1P7-1	16	n.t.	7 (16µg/ml)
1EU1P7-2	16	n.t.	
1EU1P7-3	16	n.t.	
1EU1P8-1	16	n.t.	8 (16µg/ml)
1EU1P8-2	16	n.t.	
EU1P8A-3 (1EU1P8-3)	64	*ERG11*^{G464S}; *MTL***a**; *UPC2*/*UPC2*^{G648D}	
1EU1P10-1	16	n.t.	10 (32µg/ml)
1EU1P10-2	16	n.t.	
1EU1P10-3	16	n.t.	
1EU1P12-1	16	n.t.	12 (64µg/ml)
1EU1P12-2	16	n.t.	
1EU1P12-3	32	n.t.	
1EU1P14-1	16	n.t.	14 (128µg/ml)
1EU1P14-2	32	n.t.	
1EU1P14-3	32	n.t.	

MP Derivative[a]	MIC [µg/ml]	Relevant genotype[b]	Passage (fluconazole concentration in the culture)
1EU1P16-1	32	n.t.	16 (256µg/ml)
1EU1P16-2	32	n.t.	
1EU1P16-3	32	n.t.	
Parental mating product UE1			
1UE64P1-1	2	n.t.	1 (1µg/ml)
1UE64P1-2	2	n.t.	
1UE64P1-3	2	n.t.	
UE1P2A-1 (1UE64P2-1)	4	*ERG11*/*ERG11*^{G464S}; *MTL***a**/α; *UPC2*/*UPC2*^{G648D}	2 (1µg/ml)
1UE64P2-2	2	n.t.	
1UE64P2-3	2	n.t.	
1UE64P3-1	4	n.t.	3 (2µg/ml)
1UE64P3-2	2	n.t.	
1UE64P3-3	4	n.t.	
1UE64P4-1	8	n.t.	4 (2µg/ml)
1UE64P4-2	4	n.t.	
UE1P4A-3 (1UE64P4-3)	16	*ERG11*/*ERG11*^{G464S}; *MTL***a**/α; *UPC2*/*UPC2*^{G648D}	
1UE64P5-1	8	n.t.	5 (4µg/ml)
1UE64P5-2	16	n.t.	
1UE64P5-3	2	n.t.	
1UE64P6-1	4	n.t.	6 (4µg/ml)
1UE64P6-2	8	n.t.	
1UE64P6-3	4	n.t.	
1UE64P8-1	8	n.t.	8 (8µg/ml)
1UE64P8-2	8	n.t.	
1UE64P8-3	4	n.t.	
1UE64P10-1	2	n.t.	10 (16µg/ml)
1UE64P10-2	2	n.t.	
1UE64P10-3	2	n.t.	
1UE64P12-1	2	n.t.	12 (32µg/ml)
1UE64P12-2	2	n.t.	
1UE64P12-3	2	n.t.	
1UE64P14-1	2	n.t.	14 (64µg/ml)
1UE64P14-2	2	n.t.	
1UE64P14-3	2	n.t.	
1UE64P16-1	2	n.t.	16 (128µg/ml)
1UE64P16-2	2	n.t.	
1UE64P16-3	2	n.t.	
1UE64P18-1	2	n.t.	18 (256µg/ml)
1UE64P18-2	2	n.t.	
1UE64P18-3	2	n.t.	
Parental mating product MT1			
1MT3P1-1	8	n.t.	1 (4µg/ml)
1MT3P1-2	8	n.t.	
1MT3P1-3	8	n.t.	
1MT3P2-1	8	n.t.	2 (4µg/ml)
1MT3P2-2	8	n.t.	
1MT3P2-3	8	n.t.	
1MT3P3-1	8	n.t.	3 (8µg/ml)
1MT3P3-2	8	n.t.	
MT1P3A-3 (1MT3P3-3)	16	*MRR1*/*MRR1* ^{P683S}; *MTL***a**/α; *TAC1-1*/*TAC1*^{G980E}	
1MT3P4-1	16	n.t.	4 (8µg/ml)
1MT3P4-2	8	n.t.	
1MT3P4-3	16	n.t.	
1MT3P5-1	16	n.t.	5 (16µg/ml)
MT1P5A-2 (1MT3P5-2)	32	*MRR1*/*MRR1* ^{P683S}; *MTL***a**/α; *TAC1-1*/*TAC1*^{G980E}	
MT1P5A-3 (1MT3P5-3)	32	*MRR1*/*MRR1* ^{P683S}; *MTL***a**/α; *TAC1*^{G980E}	

MP Derivative[a]	MIC [µg/ml]	Relevant genotype[b]	Passage (fluconazole concentration in the culture)
1MT3P6-1	16	n.t.	6 (16µg/ml)
1MT3P6-2	16	n.t.	
1MT3P6-3	32	n.t.	
1MT3P8-1	8	n.t.	8 (32µg/ml)
1MT3P8-2	8	n.t.	
1MT3P8-3	8	n.t.	
1MT3P10-1	8	n.t.	10 (64µg/ml)
1MT3P10-2	16	n.t.	
1MT3P10-3	16	n.t.	
1MT3P12-1	8	n.t.	12 (128µg/ml)
1MT3P12-2	8	n.t.	
1MT3P12-3	16	n.t.	
1MT3P14-1	8	n.t.	14 (256µg/ml)
1MT3P14-2	8	n.t.	
1MT3P14-3	8	n.t.	
Parental mating product MT2			
1MT6P1-1	8	n.t.	1 (2µg/ml)
1MT6P1-2	8	n.t.	
1MT6P1-3	8	n.t.	
1MT6P2-1	8	n.t.	2 (2µg/ml)
1MT6P2-2	8	n.t.	
1MT6P2-3	8	n.t.	
1MT6P3-1	8	n.t.	3 (4µg/ml)
1MT6P3-2	8	n.t.	
1MT6P3-3	8	n.t.	
1MT6P4-1	8	n.t.	4 (4µg/ml)
1MT6P4-2	8	n.t.	
MT2P4A-3 (1MT6P4-3)	16	*MRR1*/*MRR1*^{P683S}; *MTL***a**/α; *TAC1-1*/*TAC1*^{G980E}	
1MT6P5-1	16	n.t.	5 (8µg/ml)
1MT6P5-2	16	n.t.	
1MT6P5-3	16	n.t.	
1MT6P6-1	16	n.t.	6 (8µg/ml)
1MT6P6-2	16	n.t.	
1MT6P6-3	16	n.t.	
1MT6P8-1	32	n.t.	8 (16µg/ml)
1MT6P8-2	32	n.t.	
1MT6P8-3	32	n.t.	
1MT6P10-1	32	n.t.	10 (32µg/ml)
1MT6P10-2	32	n.t.	
1MT6P10-3	32	n.t.	
MT2P11A-1 (1MT6P11-1)	64	*MRR1*^{P683S}; *MTL***a**/α; *TAC1-1*/*TAC1*^{G980E}	11 (64µg/ml)
1MT6P11-2	16	n.t.	
1MT6P11-3	32	n.t.	
1MT6P12-1	16	n.t.	12 (64µg/ml)
1MT6P12-2	32	n.t.	
1MT6P12-3	64	n.t.	
1MT6P14-1	32	n.t.	14 (128µg/ml)
1MT6P14-2	32	n.t.	
1MT6P14-3	32	n.t.	
1MT6P16-1	16	n.t.	16 (256µg/ml)
1MT6P16-2	32	n.t.	
1MT6P16-3	8	n.t.	
Parental mating product TM1			
2TM8P1-1	4	n.t.	1 (2µg/ml)
2TM8P1-2	4	n.t.	
2TM8P1-3	4	n.t.	

MP Derivative[a]	MIC [µg/ml]	Relevant genotype[b]	Passage (fluconazole concentration in the culture)
2TM8P2-1	8	n.t.	2 (2µg/ml)
2TM8P2-2	4	n.t.	
2TM8P2-3	4	n.t.	
2TM8P3-1	8	n.t.	3 (4µg/ml)
2TM8P3-2	8	n.t.	
2TM8P3-3	8	n.t.	
2TM8P4-1	8	n.t.	4 (4µg/ml)
2TM8P4-2	8	n.t.	
2TM8P4-3	8	n.t.	
2TM8P5-1	8	n.t.	5 (8µg/ml)
2TM8P5-2	8	n.t.	
2TM8P5-3	8	n.t.	
2TM8P6-1	8	n.t.	6 (8µg/ml)
TM1P6A-2 (2TM8P6-2)	16	*MRR1*/*MRR1* ^{P683S}; *MTL***a**; *TAC1*^{G980E};	
TM1P6A-3 (2TM8P6-3)	16	*MRR1*/*MRR1* ^{P683S}; *MTL***a**; *TAC1*^{G980E}	
2TM8P8-1	32	n.t.	8 (16µg/ml)
2TM8P8-2	32	n.t.	
2TM8P8-3	32	n.t.	
2TM8P9-1	16	n.t.	9 (32µg/ml)
2TM8P9-2	16	n.t.	
2TM8P9-3	16	n.t.	
TM1P10A-1 (2TM8P10-1)	64	*MRR1* ^{P683S}; *MTL***a**; *TAC1*^{G980E}	10 (32µg/ml)
2TM8P10-2	32	n.t.	
2TM8P10-3	8	n.t.	
2TM8P12-1	8	n.t.	12 (64µg/ml)
2TM8P12-2	16	n.t.	
2TM8P12-3	8	n.t.	
2TM8P14-1	8	n.t.	14 (128µg/ml)
2TM8P14-2	16	n.t.	
2TM8P14-3	16	n.t.	
2TM8P16-1	8	n.t.	16 (256µg/ml)
2TM8P16-2	8	n.t.	
2TM8P16-3	8	n.t.	
Parental mating product MU1			
1MU13P1-1	8	n.t.	1 (2µg/ml)
1MU13P1-2	8	n.t.	
1MU13P1-3	8	n.t.	
1MU13P2-1	8	n.t.	2 (2µg/ml)
1MU13P2-2	8	n.t.	
1MU13P2-3	8	n.t.	
1MU13P3-1	16	n.t.	3 (4µg/ml)
1MU13P3-2	8	n.t.	
1MU13P3-3	8	n.t.	
1MU13P4-1	8	n.t.	4 (4µg/ml)
1MU13P4-2	8	n.t.	
1MU13P4-3	8	n.t.	
MU1P5A-1 (1MU13P5-1)	32	*MRR1*/*MRR1* ^{P683S}; *MTL***a**/α; *UPC2*/*UPC2*^{G648D}	5 (8µg/ml)
1MU13P5-2	8	n.t.	
1MU13P5-3	16	n.t.	
1MU13P6-1	32	n.t.	6 (8µg/ml)
1MU13P6-2	32	n.t.	
1MU13P6-3	8	n.t.	
MU1P7A-1 (1MU13P7-1)	64	*MRR1* ^{P683S}; *MTL***a**/α; *UPC2*/*UPC2*^{G648D}	7 (16µg/ml)
1MU13P7-2	8	n.t.	
1MU13P7-3	2	n.t.	

MP Derivative[a]	MIC [µg/ml]	Relevant genotype[b]	Passage (fluconazole concentration in the culture)
1MU13P8-1	64	n.t.	8 (16µg/ml)
1MU13P8-2	8	n.t.	
1MU13P8-3	8	n.t.	
1MU13P10-1	4	n.t.	10 (32µg/ml)
1MU13P10-2	4	n.t.	
1MU13P10-3	4	n.t.	
1MU13P12-1	4	n.t.	12 (64µg/ml)
1MU13P12-2	4	n.t.	
1MU13P12-3	4	n.t.	
1MU13P14-1	4	n.t.	14 (128µg/ml)
1MU13P14-2	4	n.t.	
1MU13P14-3	4	n.t.	
1MU13P16-1	2	n.t.	16 (256µg/ml)
1MU13P16-2	2	n.t.	
1MU13P16-3	2	n.t.	
Parental mating product MU2			
1MU8P1-1	8[c]	n.t.	1 (4µg/ml)
1MU8P1-2	8[c]	n.t.	
1MU8P1-3	8[c]	n.t.	
1MU8P2-1	8	n.t.	2 (4µg/ml)
1MU8P2-2	8[c]	n.t.	
1MU8P2-3	8[c]	n.t.	
1MU8P3-1	8	n.t.	3 (8µg/ml)
1MU8P3-2	8[c]	n.t.	
1MU8P3-3	8[c]	n.t.	
1MU8P4-1	8	n.t.	4 (8µg/ml)
1MU8P4-2	8[c]	n.t.	
1MU8P4-3	8	n.t.	
1MU8P5-1	8[c]	n.t.	5 (16µg/ml)
1MU8P5-2	8	n.t.	
1MU8P5-3	8	n.t.	
MU2P6A-1 (1MU8P6-1)	8/16/32[d]	*MRR1*/*MRR1* ^{P683S}; *MTL***a**/α; *UPC2*/*UPC2* ^{G648D}	6 (16µg/ml)
1MU8P6-2	8	n.t.	
1MU8P6-3	4	n.t.	
1MU8P8-1	1	n.t.	8 (32µg/ml)
1MU8P8-2	4	n.t.	
1MU8P8-3	4	n.t.	
1MU8P10-1	2	n.t.	10 (64µg/ml)
1MU8P10-2	8	n.t.	
1MU8P10-3	4	n.t.	
1MU8P12-1	8	n.t.	12 (128µg/ml)
1MU8P12-2	8	n.t.	
1MU8P12-3	4	n.t.	
MU2P14A-1 (1MU8P14-1)	16	*MRR1*/*MRR1* ^{P683S}; *MTL***a**/α; *UPC2*/*UPC2* ^{G648D}	14 (256µg/ml)
1MU8P14-2	4	n.t.	
1MU8P14-3	4	n.t.	
Parental mating product UM1			
1UM21P1-1	4	n.t.	1 (2µg/ml)
1UM21P1-2	4	n.t.	
1UM21P1-3	4	n.t.	
1UM21P2-1	4	n.t.	2 (2µg/ml)
1UM21P2-2	4	n.t.	
1UM21P2-3	4	n.t.	
UM1P3A-1 (1UM21P3-1)	64	*MRR1* ^{P683S}; *MTL***a**/α; *UPC2*/*UPC2* ^{G648D}	3 (4µg/ml)
1UM21P3-2	4	n.t.	
UM1P3A-3 (1UM21P3-3)	32	*MRR1* ^{P683S}; *MTL***a**/α; *UPC2*/*UPC2* ^{G648D}	

MP Derivative[a]	MIC [µg/ml]	Relevant genotype[b]	Passage (fluconazole concentration in the culture)
1UM21P4-1	32	n.t.	4 (4µg/ml)
1UM21P4-2	4[d]	n.t.	
1UM21P4-3	64	n.t.	
1UM21P5-1	32	n.t.	5 (8µg/ml)
1UM21P5-2	32	n.t.	
1UM21P5-3	32	n.t.	
1UM21P6-1	32	n.t.	6 (8µg/ml)
1UM21P6-2	32	n.t.	
1UM21P6-3	32	n.t.	
1UM21P8-1	32	n.t.	8 (16µg/ml)
1UM21P8-2	32	n.t.	
1UM21P8-3	64	n.t.	
1UM21P10-1	32	n.t.	10 (32µg/ml)
1UM21P10-2	32	n.t.	
1UM21P10-3	32	n.t.	
1UM21P12-1	32	n.t.	12 (64µg/ml)
1UM21P12-2	32	n.t.	
1UM21P12-3	32	n.t.	
1UM21P14-1	32	n.t.	14 (128µg/ml)
1UM21P14-2	32	n.t.	
1UM21P14-3	32	n.t.	
1UM21P16-1	32	n.t.	16 (256µg/ml)
1UM21P16-2	32	n.t.	
1UM21P16-3	32	n.t.	
Parental mating product TU1			
1TU1P1-1	4	n.t.	1 (2µg/ml)
1TU1P1-2	4	n.t.	
1TU1P1-3	4	n.t.	
1TU1P2-1	4	n.t.	2 (2µg/ml)
1TU1P2-2	4	n.t.	
1TU1P2-3	4	n.t.	
1TU1P3-1	4	n.t.	3 (4µg/ml)
1TU1P3-2	4	n.t.	
1TU1P3-3	4	n.t.	
1TU1P4-1	4	n.t.	4 (4µg/ml)
1TU1P4-2	4	n.t.	
1TU1P4-3	8	n.t.	
1TU1P5-1	8	n.t.	5 (8µg/ml)
1TU1P5-2	8	n.t.	
1TU1P5-3	8	n.t.	
1TU1P6-1	8	n.t.	6 (8µg/ml)
1TU1P6-2	8	n.t.	
TU1P6A-3 (1TU1P6-3)	16	*MTL***a**/α; *TAC1-2*/*TAC1*^{G980E}; *UPC2*/*UPC2*^{G648D}	
1TU1P8-1	32	n.t.	8 (16µg/ml)
1TU1P8-2	32	n.t.	
1TU1P8-3	32	n.t.	
1TU1P10-1	32	n.t.	10 (32µg/ml)
1TU1P10-2	32	n.t.	
1TU1P10-3	32	n.t.	
TU1P11A-1 (1TU1P11-1)	64	*MTL***a**; *TAC1*^{G980E}; *UPC2*/*UPC2*^{G648D}	11 (64µg/ml)
1TU1P11-2	8	n.t.	
TU1P11A-3 (1TU1P11-3)	64	*MTL***a**; *TAC1*^{G980E}; *UPC2*/*UPC2*^{G648D}	
1TU1P12-1	8	n.t.	12 (64µg/ml)
1TU1P12-2	64	n.t.	
1TU1P12-3	64	n.t.	

MP Derivative[a]	MIC [µg/ml]	Relevant genotype[b]	Passage (fluconazole concentration in the culture)
1TU1P14-1	8	n.t.	14 (128µg/ml)
1TU1P14-2	8	n.t.	
1TU1P14-3	8	n.t.	
1TU1P16-1	8	n.t.	16 (256µg/ml)
1TU1P16-2	8	n.t.	
1TU1P16-3	8	n.t.	
Parental mating product UT1			
1UT86P1-1	8	n.t.	1 (4µg/ml)
1UT86P1-2	8	n.t.	
1UT86P1-3	8	n.t.	
1UT86P2-1	16	n.t.	2 (4µg/ml)
UT1P2A-2 (1UT86P2-2)	16	*MTL***a**/α; *TAC1-1*/*TAC1*^{G980E}; *UPC2*/*UPC2*^{G648D}	
UT1P2A-3 (1UT86P2-3)	16	*MTL***a**/α; *TAC1-1*/*TAC1*^{G980E}; *UPC2*/*UPC2*^{G648D}	
1UT86P3-1	16	n.t.	3 (8µg/ml)
1UT86P3-2	16	n.t.	
1UT86P3-3	8	n.t.	
1UT86P4-1	16	n.t.	4 (8µg/ml)
1UT86P4-2	16	n.t.	
1UT86P4-3	16	n.t.	
UT1P5A-1 (1UT86P5-1)	32	*MTL*α; *TAC1*^{G980E}; *UPC2*/*UPC2*^{G648D}	5 (16µg/ml)
UT1P5A-2 (1UT86P5-2)	32	*MTL***a**/α; *TAC1-1*/*TAC1*^{G980E}; *UPC2*/*UPC2*^{G648D}	
1UT86P5-3	16	n.t.	
1UT86P6-1	16	n.t.	6 (16µg/ml)
1UT86P6-2	32	n.t.	
1UT86P6-3	16	n.t.	
1UT86P8-1	16	n.t.	8 (32µg/ml)
1UT86P8-2	16	n.t.	
1UT86P8-3	16	n.t.	
1UT86P10-1	32	n.t.	10 (64µg/ml)
1UT86P10-2	16	n.t.	
1UT86P10-3	16	n.t.	
1UT86P12-1	32	n.t.	12 (128µg/ml)
1UT86P12-2	32	n.t.	
1UT86P12-3	32	n.t.	
1UT86P13-1	16	n.t.	13 (256µg/ml)
1UT86P13-2	16	n.t.	
1UT86P13-3	16	n.t.	
1UT86P14-1	16	n.t.	14 (256µg/ml)
1UT86P14-2	16	n.t.	
1UT86P14-3	32	n.t.	

[a] Originally used strain names are indicated in parentheses. Please note that initially randomly picked strains of all experiments were consecutively numbered. Subsequently, selected strains were systematically renamed.

[b] n.t.: not tested

[c] Growth was already reduced at this fluconazole concentration.

[d] Strains 1UM21P4-2 and MU2P6A-1 were very instable. After streaking of the strains from the glycerol stock, colonies of different sizes and with different fluconazole resistance levels (1UM21P4-2: 4 and 16µg/ml; MU2P6A-1: 4, 16 and 32µg/ml) grew.

Appendix A5

Independent flow cytometry measurements of genetically engineered *MTL* heterozygous parental strain, selected fluconazole-induced *MTL* homozygous strains, selected mating products and selected mating product progeny. Flow cytometry profiles of the reference strain SC5314 are shown in blue and of the analyzed strains in red. Ploidy of every strain was measured three times, except for strain MT2P11A-1 (two times). Adapted from [274].

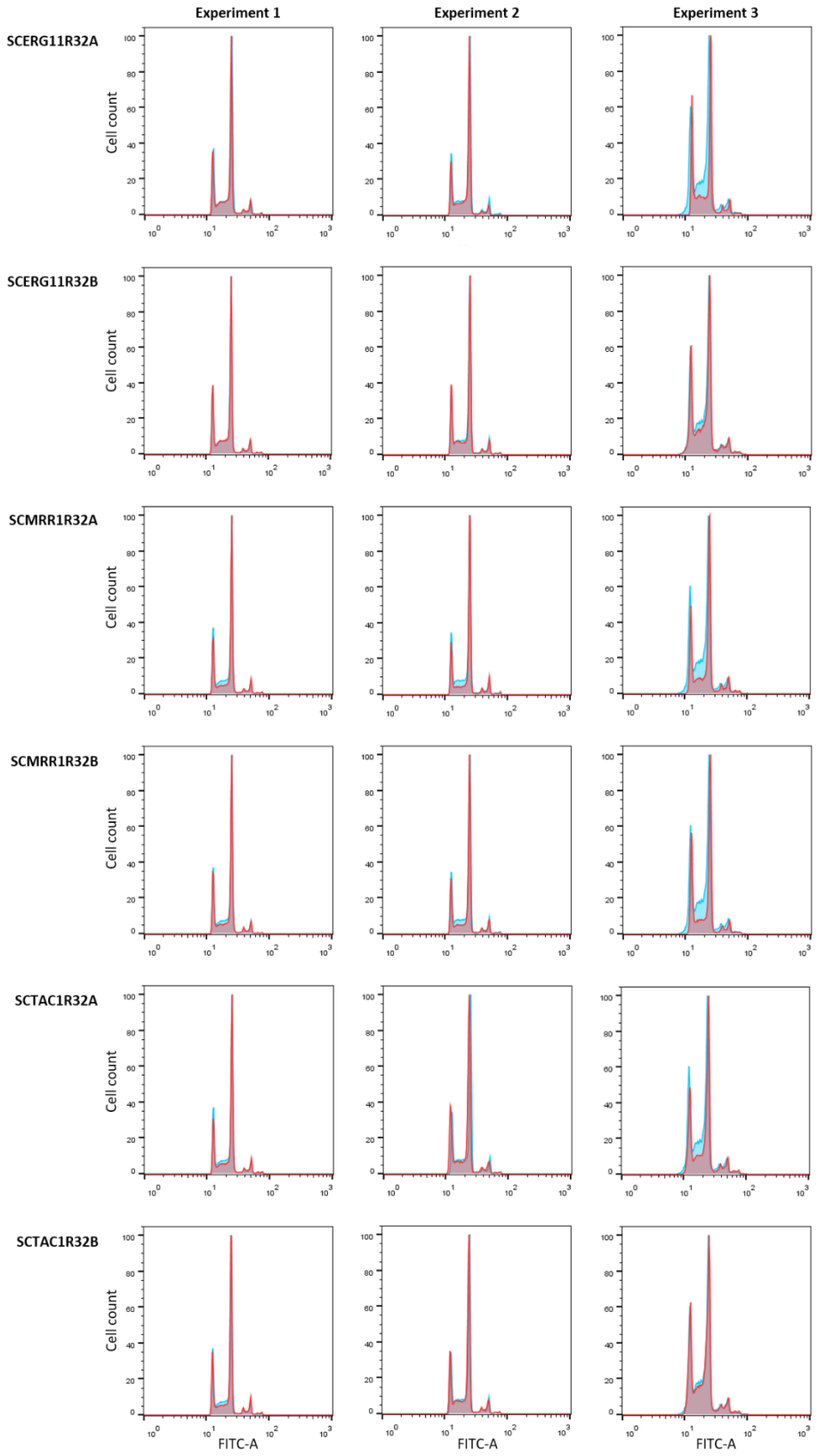

Appendix A5 (continued on the next page)

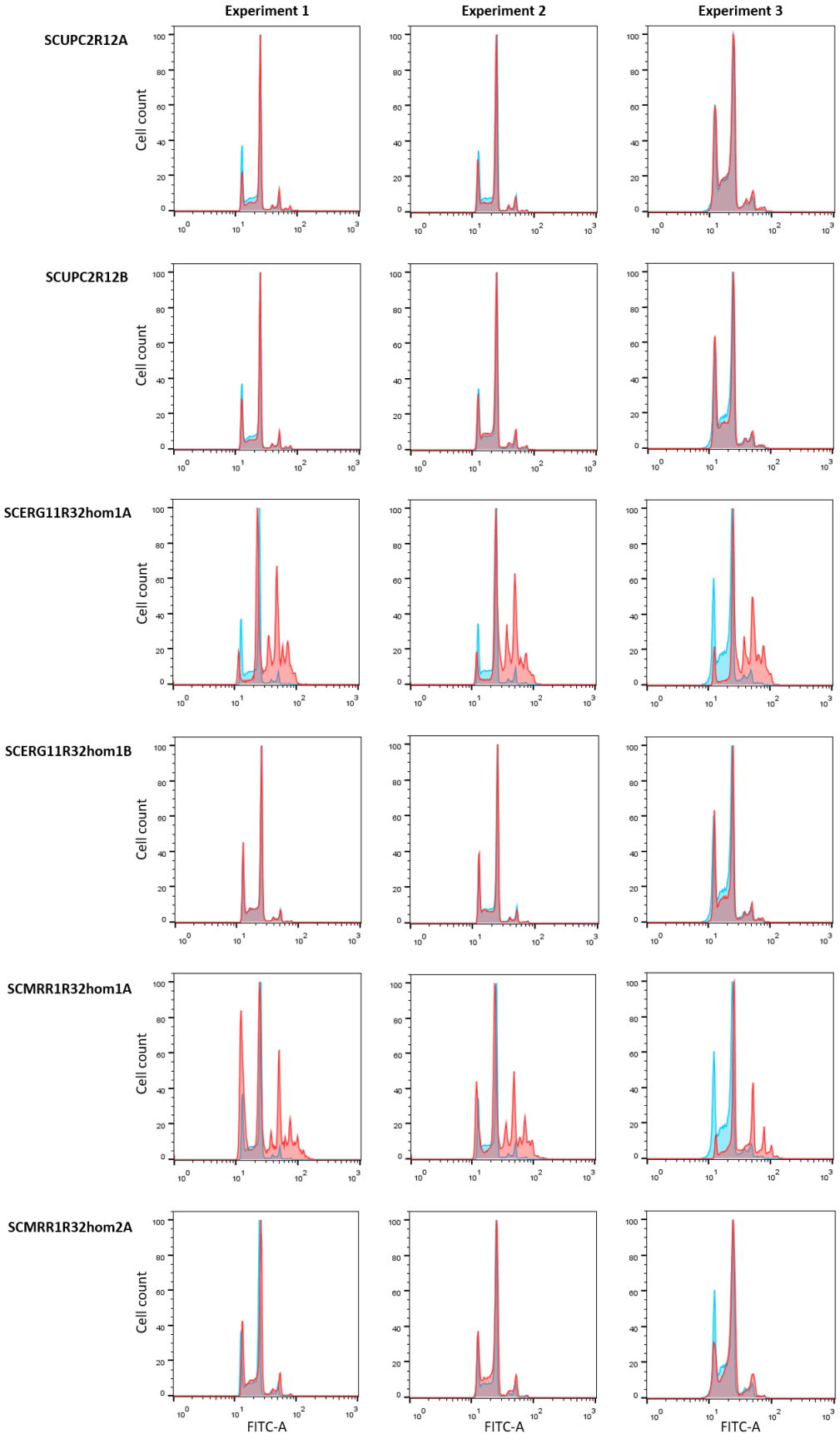

Appendix A5 (continued on the next page)

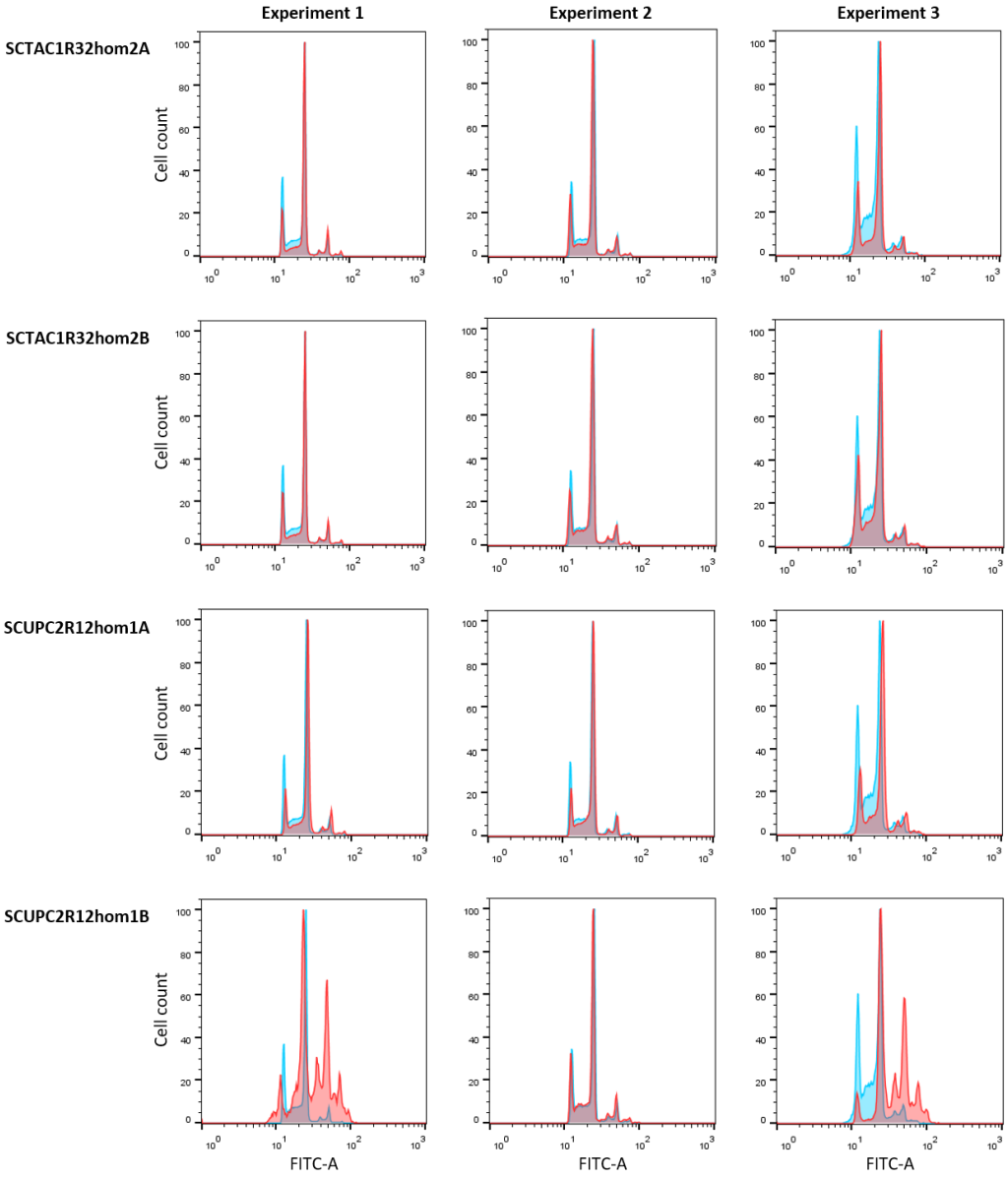

Appendix A5 (continued on the next page)

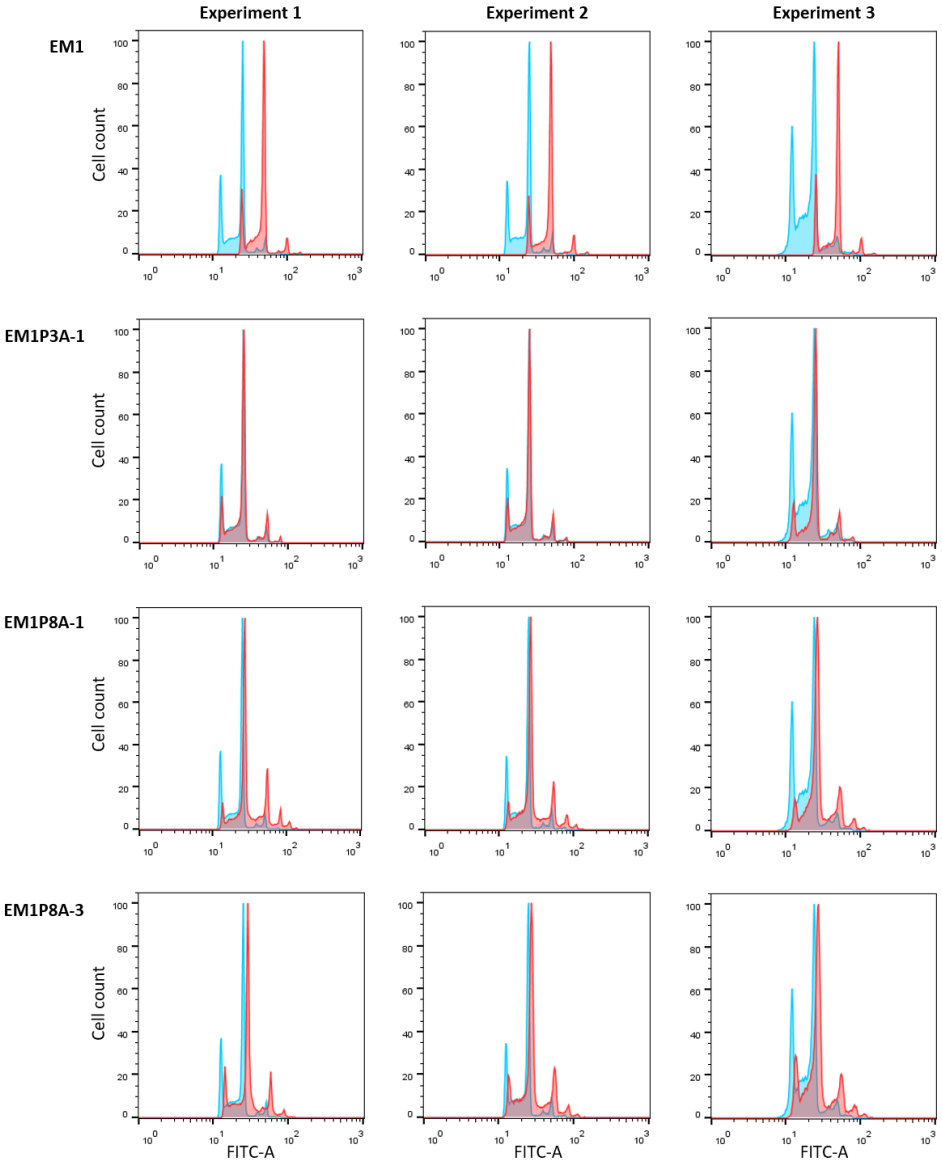

Appendix A5 (continued on the next page)

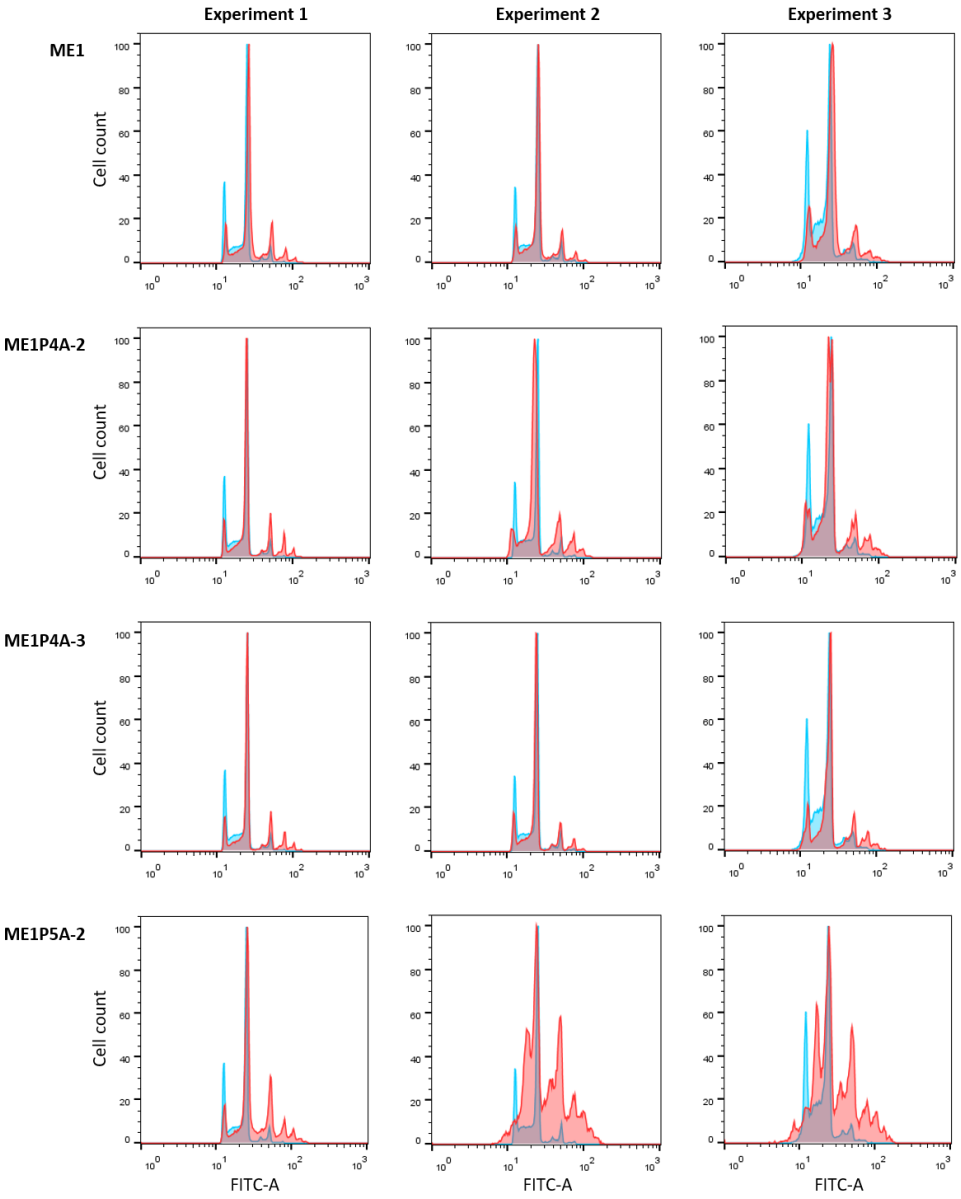

Appendix A5 (continued on the next page)

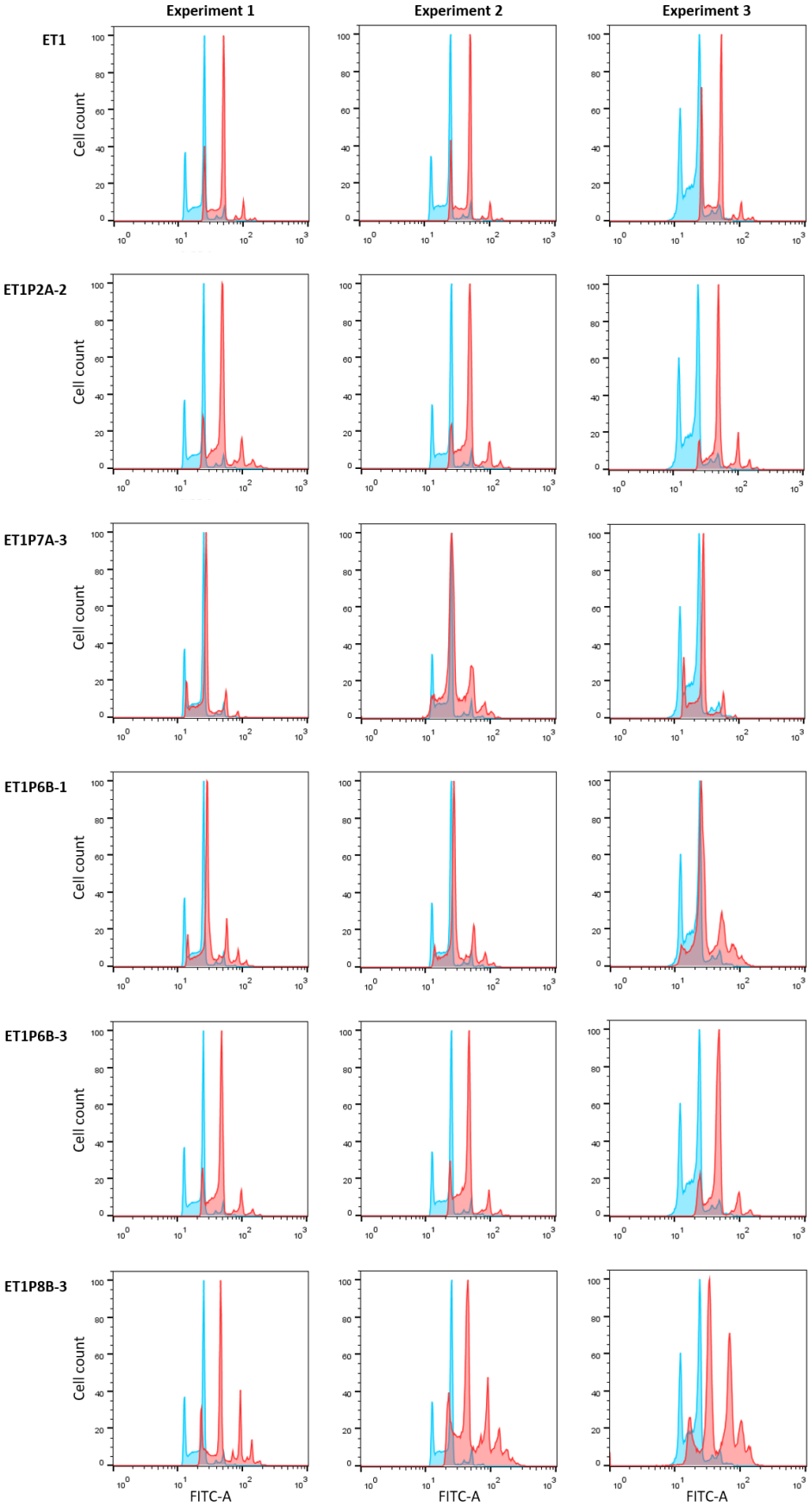

Appendix A5 (continued on the next page)

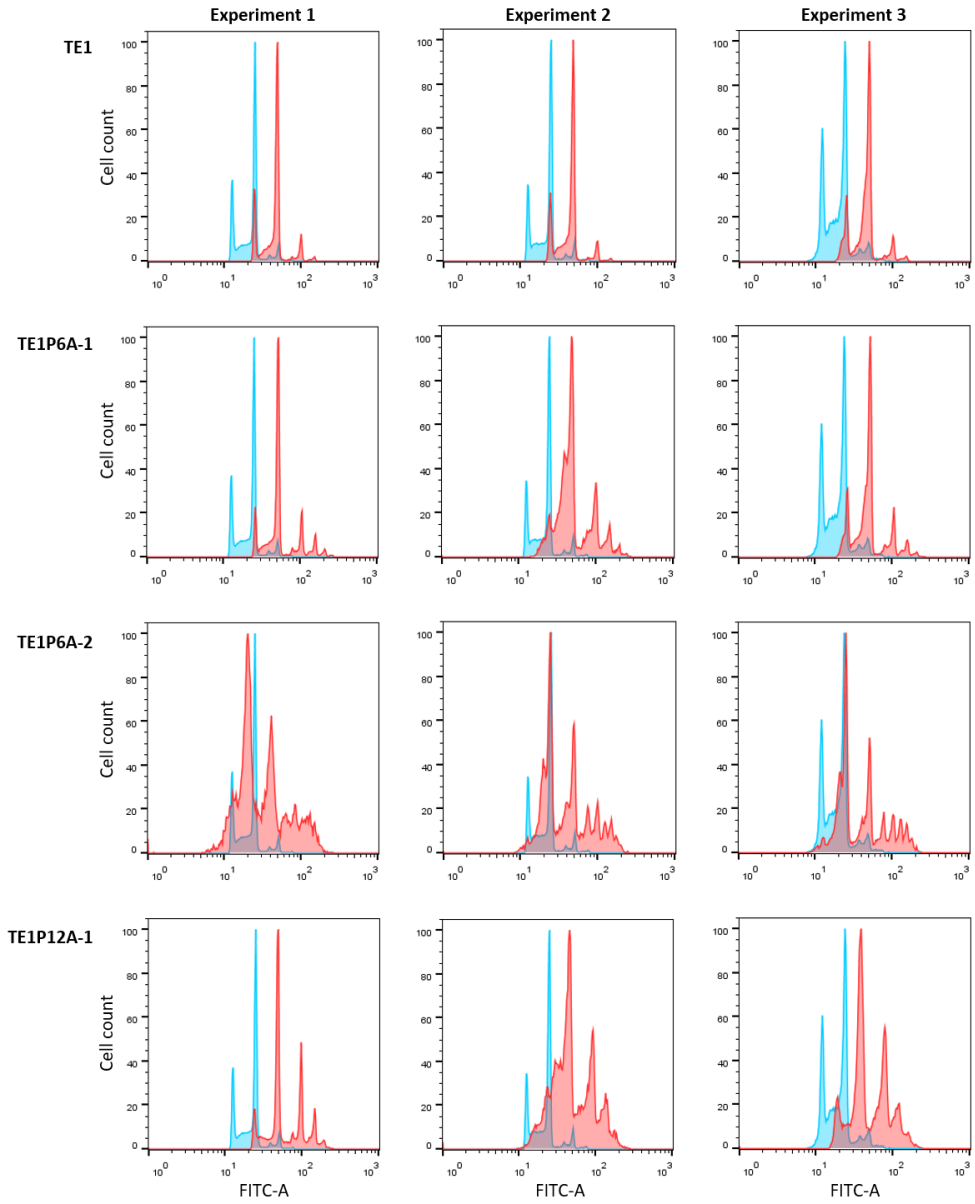

Appendix A5 (continued on the next page)

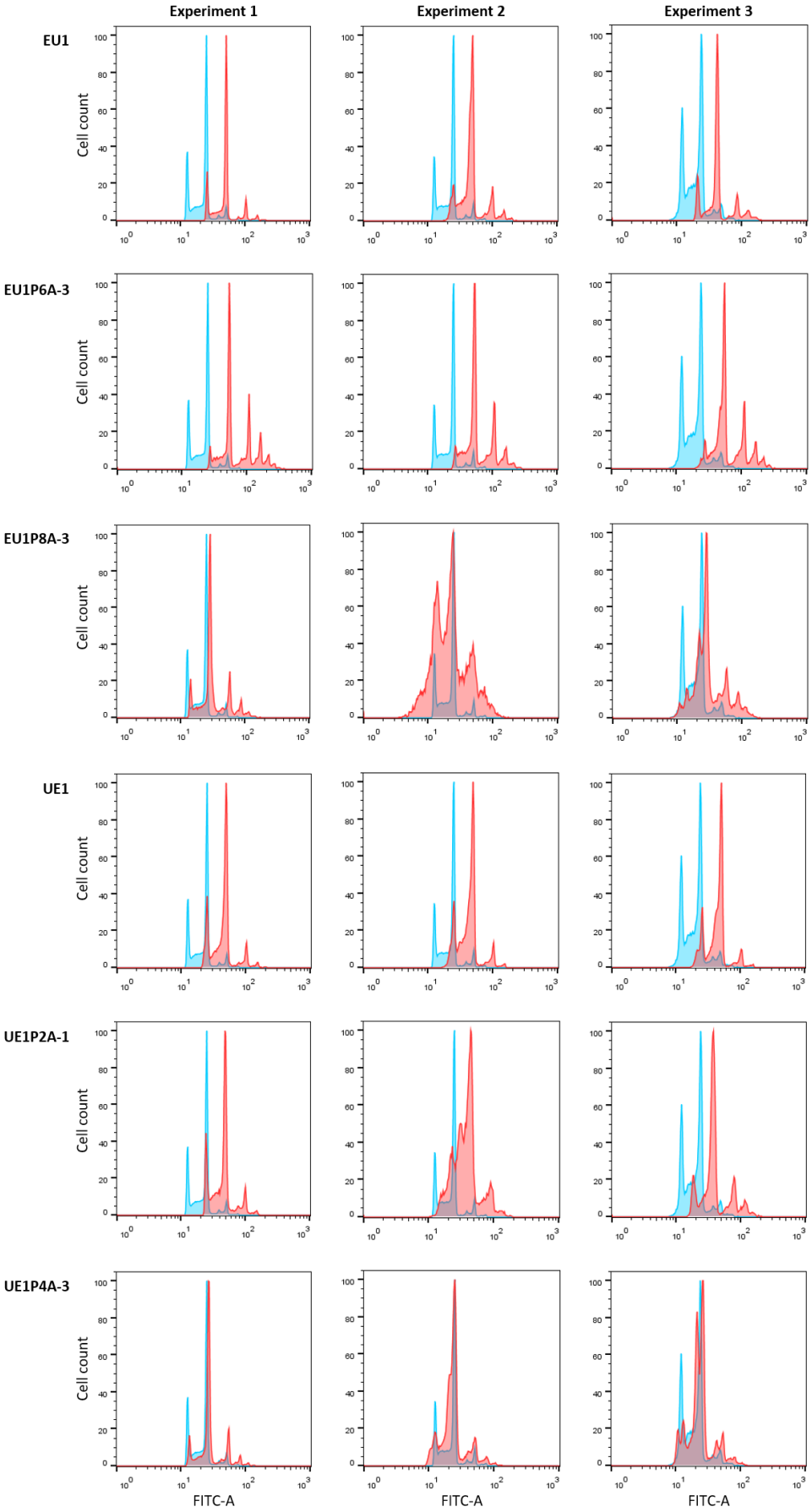

Appendix A5 (continued on the next page)

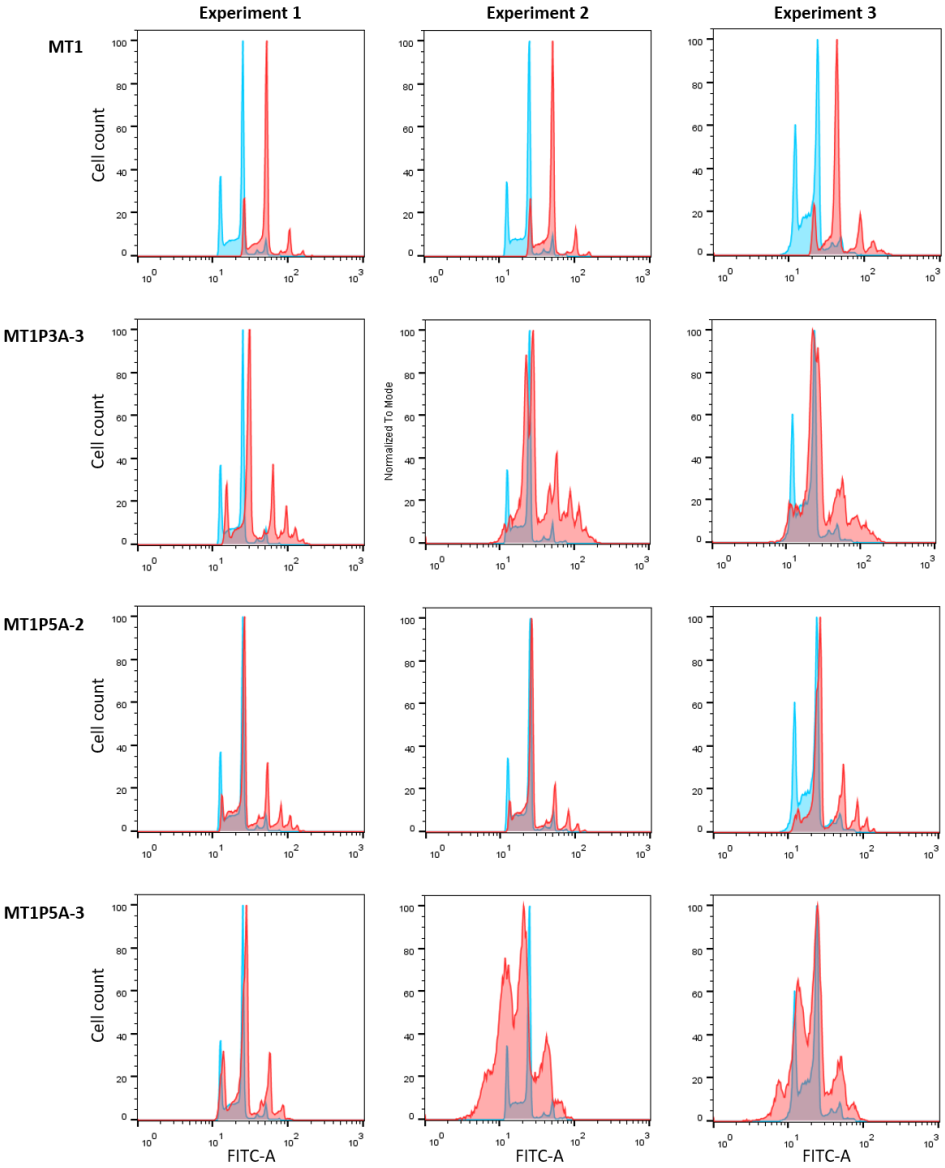

Appendix A5 (continued on the next page)

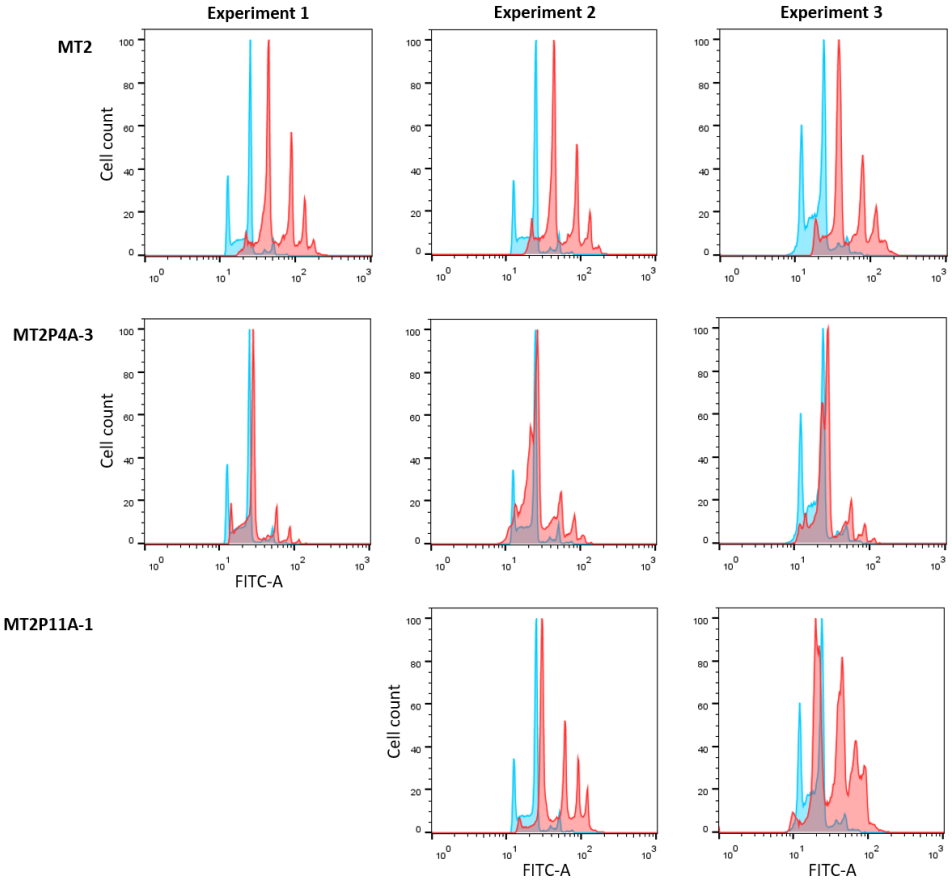

Appendix A5 (continued on the next page)

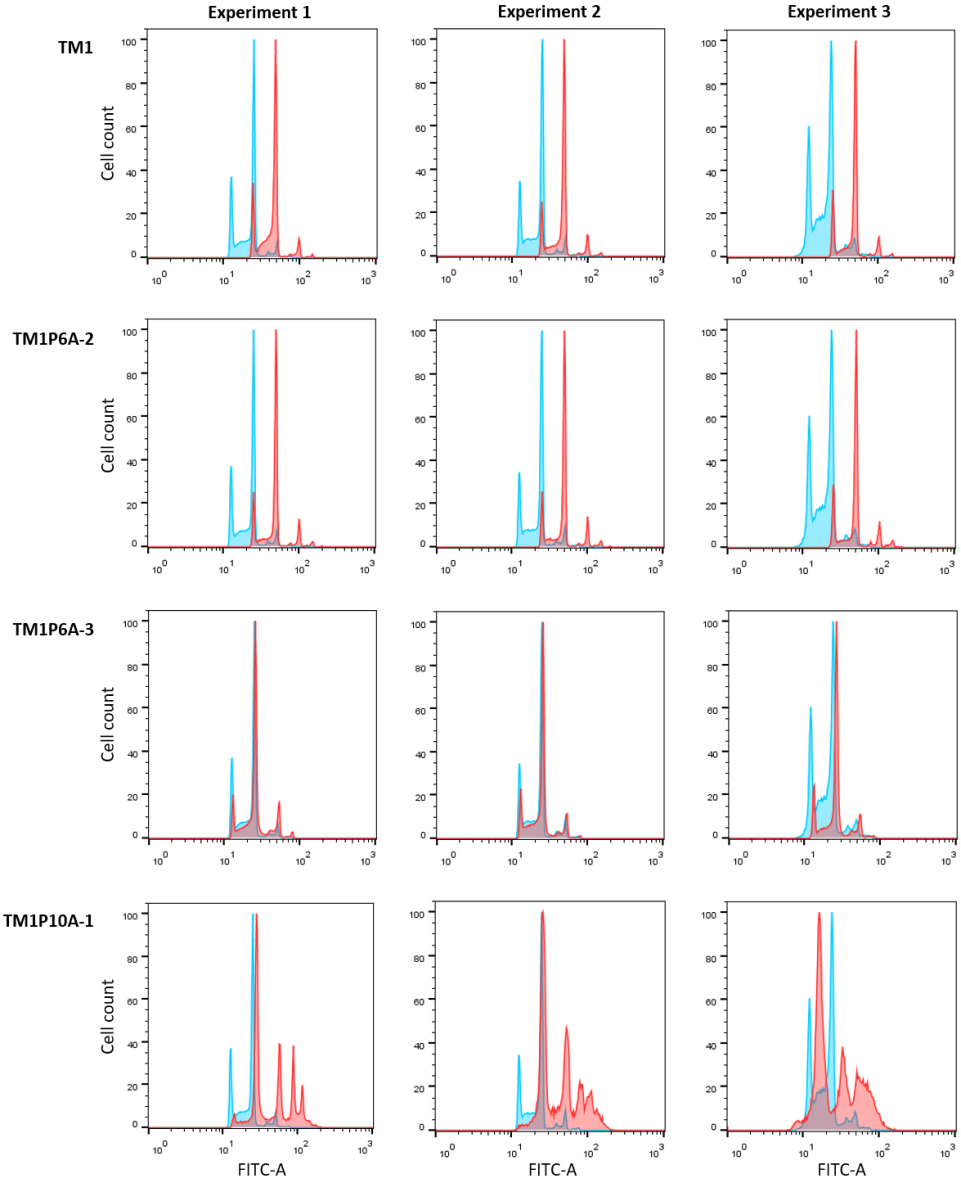

Appendix A5 (continued on the next page)

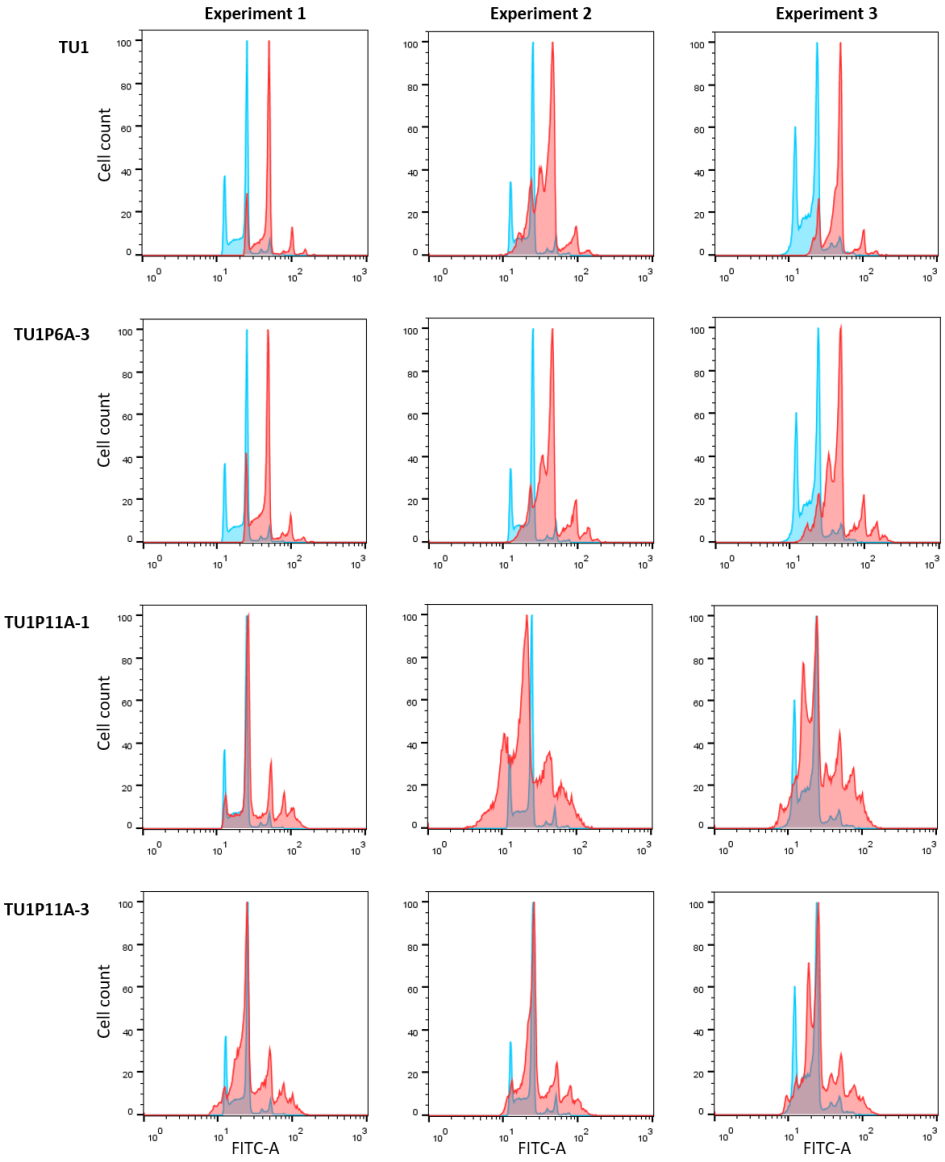

Appendix A5 (continued on the next page)

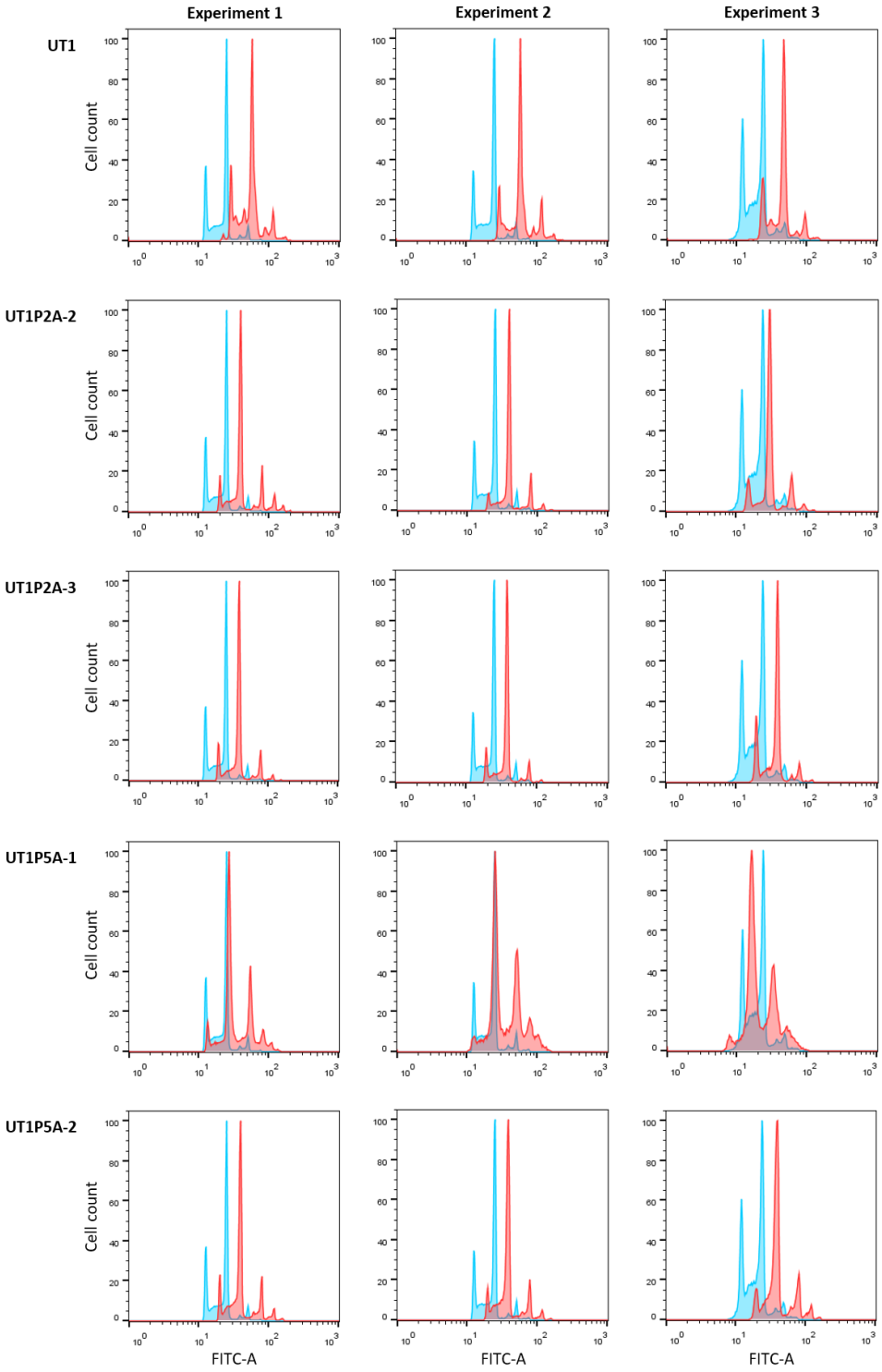

Appendix A5 (continued on the next page)

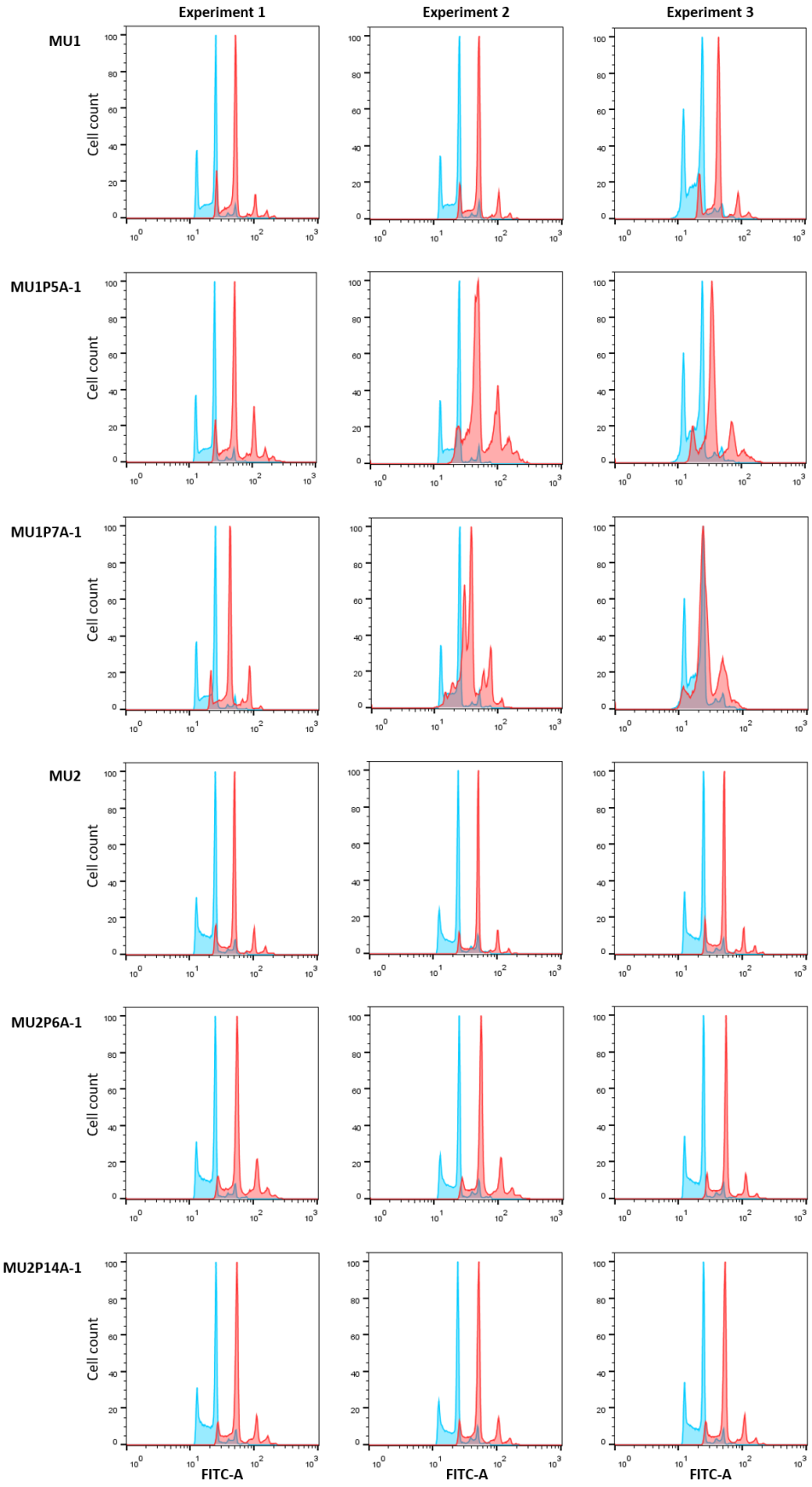

Appendix A5 (continued on the next page)

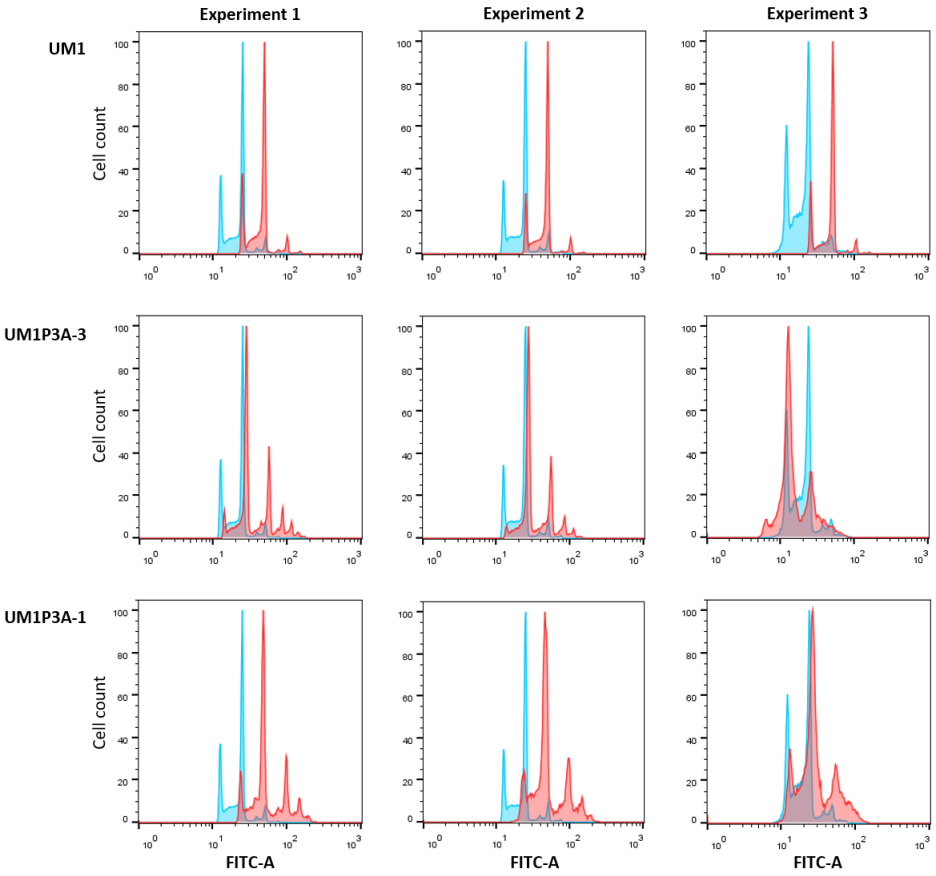
Experiment 1
Experiment 2
Experiment 3
UM1
UM1P3A-3
UM1P3A-1
Cell count
FITC-A

Appendix A6

Overview of ET1 mating product progeny with intermediate fluconazole resistance and high fluconazole resistance from two experiments. Given are relevant genomic changes of each strain in comparison to the parental strain ET1 (MIC 8µg/ml) and the passage in which the strains were isolated, including the fluconazole concentration in the respective passage. Parts published by Popp *et al.* [274].

Strain name	Experiment	MIC [µg/ml]	Genomic changes in comparison to the parental mating product[(a)]	Passage (fluconazole concentration in the passage)
ET1P2A-2	Experiment 1	16		2 (4µg/ml)
ET1P7A-3		32	Loss of wild-type *TAC1-1,* decrease in *ERG11** and *MTL***a**	7 (32µg/ml)
ET1P6B-1	Experiment 2	32	Decrease of *ERG11**, wild-type *TAC1-1* and *MTL***a**	6 (16µg/ml)
ET1P6B-3		32	Loss of wild-type *TAC1-1*	
ET1P8B-3		64		8 (32µg/ml)

[(a)] In relation to the other allele(s) (see Southern blots in Figure 28).

Appendix A7

Genetic analysis of fluconazole resistance-associated genes and the *MTL* locus of ET1 progeny of two different experiments. The *MTL* locus and the resistance-associated genes *ERG11* and *TAC1* were analyzed by Southern hybridization. Used restriction enzymes, probes and a schematic showing the expected fragment sizes after hybridization are given in chapter 4.2.5.2. Parts published by Popp *et al.* [274].

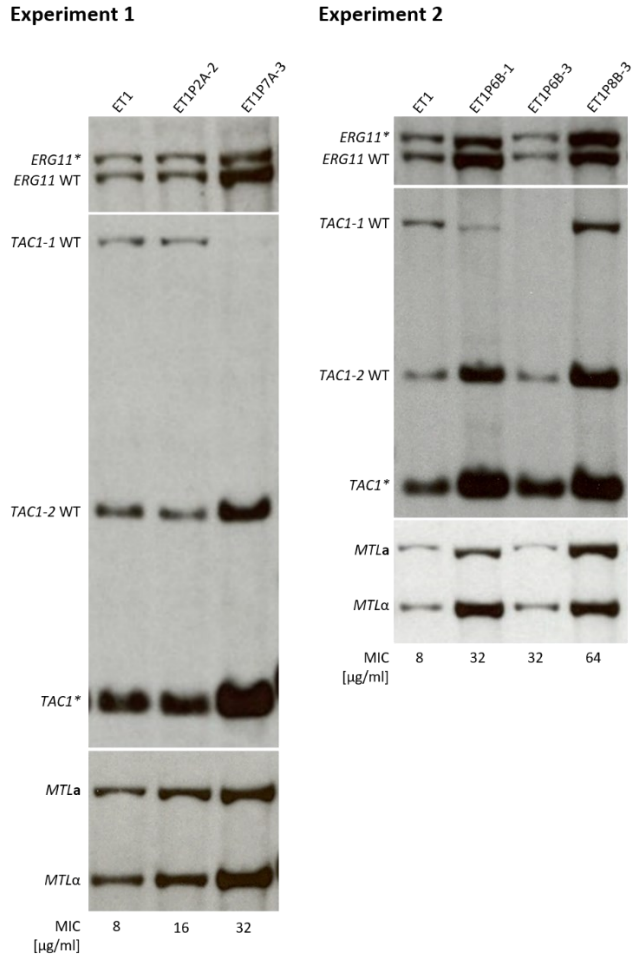

Appendix A8

Ploidy of ET1 mating product progeny of two different experiments. Flow cytometry profiles of the reference strain SC5314 is shown in blue and of the mating product ET1 and its progeny of two different experiments with intermediate and high resistance levels in red. For comparison, MIC values are indicated. Parts published by Popp *et al.* [274].

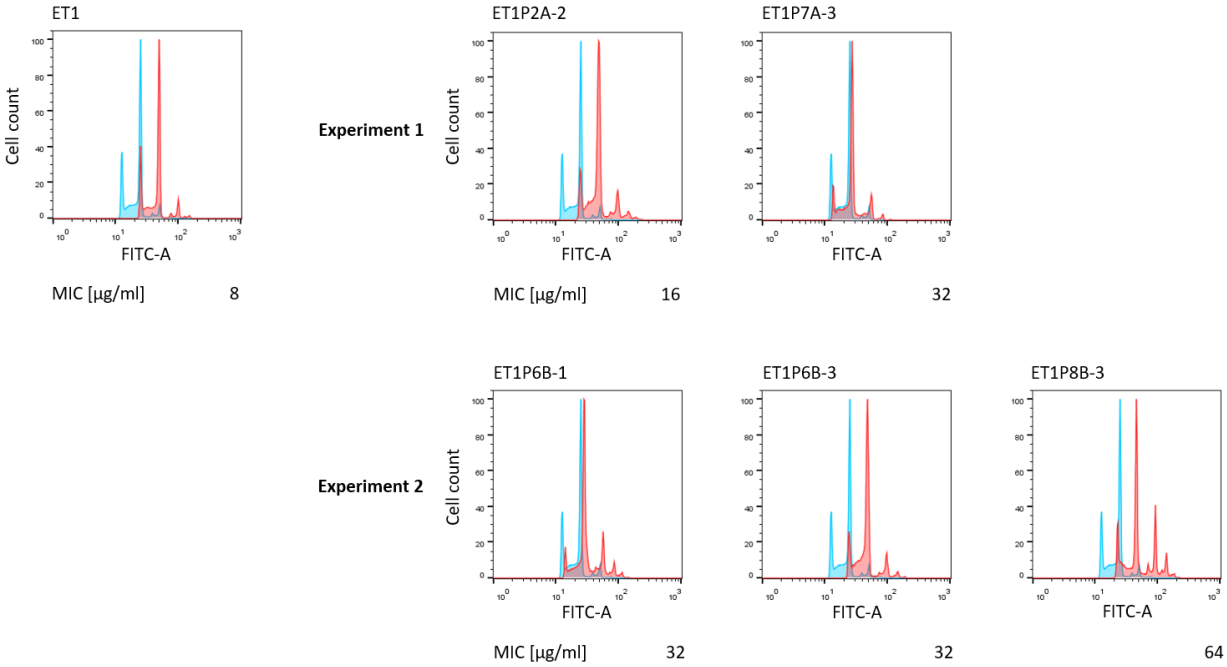

7. Curriculium Vitae

8. Publikationsliste

Publikationen aus der Promotion

02/2019 **Popp C.**, Ramirez-Zavala B., Schwanfelder S., Krüger I, and Morschhäuser J., Evolution of Fluconazole-Resistant *Candida albicans* Strains by Drug-Induced Mating Competence and Parasexual Recombination. MBio, 2019. 10(1).

07/2017 **Popp C.**, Hampe I. A. I., Hertlein T., Ohlsen K., Rogers P. D., Morschhäuser J., Competitive Fitness of Fluconazole-Resistant Clinical *Candida albicans* Strains. Antimicrob Agents Chemother, 2017. 61(7).

Weitere Publikationen

03/2014 Jung J., **Popp C.**, Sparbier K., Lange C., Kostrzewa M., Schubert S., Evaluation of Matrix-Assisted Laser Desorption Ionization-Time of Flight Mass Spectrometry for rapid detection of β-Lactam resistance in Enterobacteriaceae derived from blood cultures. Journal of Clinical Microbiology, 2014. 52(3): p. 924-930.

03/2013 Jung J., **Popp C.**, Schubert S., Anwendungsmöglichkeiten der MALDI-TOF MS Massenspektrometrie zur Resistenztestung im klinisch-mikrobiologischen Labor. Der Mikrobiologe, 2013. 23: p. 36.

08/2011 Schubert S., **Popp C.**, Rogers P.D., Morschhäuser J., Functional dissection of a *Candida albicans* zinc cluster transcription factor, the multidrug resistance regulator Mrr1. Eukaryotic Cell, 2011. 10(8): p. 1110-21.

9. Affidavit/Eidesstattliche Erklärung

Affidavit

I hereby confirm that my thesis entitled “Evolution of antifungal drug resistance of the human-pathogenic fungus *Candida albicans*” is the result of my own work. I did not receive any help or support from commercial consultants. All sources and/or materials applied are listed and specified in the thesis.

Furthermore, I confirm that this thesis has not yet been submitted as part of another examination process neither in identical nor in similar form.

_____ _____

Place, Date Signature

Eidesstattliche Erklärung

Hiermit erkläre ich an Eides statt, die Dissertation „Evolution der Antimykotikaresistenz im humanpathogenen Pilz *Candida albicans*” eigenständig, d.h. insbesondere selbstständig und ohne Hilfe eines kommerziellen Promotionsberaters, angefertigt und keine anderen als die von mir angegebenen Quellen und Hilfsmittel verwendet zu haben.

Ich erkläre außerdem, dass die Dissertation weder in gleicher noch in ähnlicher Form bereits in einem anderen Prüfungsverfahren vorgelegen hat.

_____ _____

Ort, Datum Unterschrift